AN ABSTRACT OF THE THESIS OF

Kendra L. Hatcher for the degree of Master of Science in Geography presented on March 17, 2011.

Title: Interacting Effects of Climate, Forest Dynamics, Landforms, and River Regulation on Streamflow Trends since 1950: Examples from the Willamette Basin and Forested Headwater Sites in the US

Abstract approved:

_____

Julia A. Jones

Streamflow patterns are a result of the interaction of many factors, including climate, vegetation, geology, and topography. Analyses indicate that streamflow patterns have changed around the United States over the past century, raising questions about the possible role of climate variability as a driver of water yield. This thesis examines streamflow trends in two separate analyses: a study of streamflow trends and the physical characteristics of large basins in the Willamette River Basin, and a study of streamflow trends in small headwater basins around the United States.

In the Willamette River basin, as in much of the western US where summer precipitation is low, declining streamflow will exacerbate the task of water

management to meet varying demands for water. Although regional climate warming over the past half-century in the Pacific Northwest is a plausible cause of declining streamflow, climate is only one of several factors that determine the hydrologic regime of the Willamette River basin. This study quantified trends in streamflow from 1950 to 2010 in ten sub-basins of the Willamette, including seven 60-600 km^2 predominantly forested sub-basins above dams in the Willamette National Forest, and three gages downstream of dams in urban areas of the Willamette valley (Albany, Salem, and Portland). Trends at the annual, seasonal, and daily time scales were estimated using linear regression with appropriate transformation of variables and the Mann-Kendall non-parametric test.

Trends in streamflow and runoff ratios in the Willamette Basin were compared to geology, topography, and changes in forest cover above dams. Data on forest cover by age class were obtained from Willamette National Forest. Up to 29% of area in sub-basins above dams was clearcut since the 1930s. From 1 to 51% of basin area above dams is on young (<7 ma) volcanic rocks of the High Cascades, which have longer water residence times than the older (7-25 ma) volcanic rocks of the western Cascades, which make up the remainder of basin area above dams. From 71 to 93% of basin area above dams is above 800 m elevation, where seasonal snowpacks are controlled by winter temperature and precipitation.

Over the study period (1950-2010), precipitation in the Willamette River basin did not change significantly at the seasonal or annual time scale. Declining

streamflows in spring and summer were found in low elevation basins above dams. These trends may be attributed to climate-warming-induced increases in the rain:snow ratio and earlier snowmelt, or changes in water use by vegetation in response to climate warming, or both. More rapid declines in summer and fall discharge and runoff ratios occurred in basins which experienced relatively rapid conversion of old to young forest in the past half-century and have relatively large proportions of young forest today. Declining flows can be attributed to increasing evapotranspiration in young forests and shallow flow paths in Western Cascades-dominated basins that intersect the rooting zone. High-elevation basins with greater percentages of High Cascades geology are less susceptible to declining discharge, even if they have substantial areas in young forest.

In contrast to the trends in streamflow above dams, trends over time in streamflow downstream of dams in the Willamette basin have been largely influenced by management of reservoirs and flow. Flow downstream of the dams has become more homogenized throughout the year, with higher flows in the fall and declines in the later winter/early spring. However, discharge has declined at the annual time scale, and in the spring and summer. These trends may be a result of flow management, decreasing spring streamflow upstream of the dams, or a recent trend of relatively dry years.

Although historical water yields may not be representative of future water yields, long term historical climate and discharge records from instrumented sites

provide the basis for understanding the effects of climate variability on water yield from headwater systems. This study quantified trends in climate and streamflow data from eight predominantly forested headwater basins in the US to understand the complex relationships between climate change, basin geography, vegetation, history, and hydrology. Data were obtained for up to 70-year periods from the Long Term Ecological Research (LTER) network and US Forest Service system of Experimental Forests and Ranges (EFR). Trends in precipitation, temperature, discharge, and runoff ratios were calculated for annual, seasonal, and daily data using linear regression of appropriately transformed data and Mann-Kendall non-parametric tests. Linear regression with appropriate transformation of variables produced similar results to the Mann-Kendall analysis.

The first day of spring (defined as the last day of freezing temperature) has moved earlier by 0.31 to 1.98 days/year at all sites, except the alpine site. Most sites experienced significant increases in spring minimum air temperature, but only a few sites experienced an associated change in spring runoff ratios. Spring runoff ratios decreased in sites with snowpacks and near-zero mean spring air temperature (AND). Fall baseflow increased at the alpine, non-forested site (NWT), apparently as a result of increased permafrost melt. Earlier snowmelt and decreases in spring discharge and runoff ratios are expected to lead to increases in winter streamflow and reductions in summer streamflow. However, despite increases in summer minimum air temperature at most sites, summer runoff ratios did not change at most sites, and some sites (HBR, FER) experienced increases in summer and fall runoff ratios. The expected reduction

in summer runoff ratios in response to warmer temperature at these sites may have been mitigated by reductions in leaf area due to disturbance or forest succession after logging in the early 1900s. These findings indicate that both climate change and hydrologic response to climate change varies across the US. The lack of expected streamflow responses apparently is the result of ecosystem processes that produce counteracting trends in vegetation water use in response to climate trends; these processes deserve further study.

Interacting Effects of Climate, Forest Dynamics, Landforms, and River Regulation on Streamflow Trends since 1950: Examples from the Willamette Basin and Forested Headwater Sites in the US

by
Kendra L. Hatcher

A THESIS

submitted to

Oregon State University

in partial fulfillment of
the requirements for the
degree of

Master of Science

Presented March 17, 2011
Commencement June 2011

Master of Science thesis of Kendra L. Hatcher presented on March 17, 2011.

APRROVED:

_____

Major Professor, representing Geography

_____

Chair of the Department of Geosciences

_____

Dean of the Graduate School

I understand that my thesis will become part of the permanent collection of Oregon State University libraries. My signature below authorizes release of my thesis to any reader upon request.

_____

Kendra L. Hatcher, Author

ACKNOWLEDGMENTS

I would like to express my gratitude to my major adviser, Dr. Julia Jones, for all her encouragement and helpful feedback throughout my entire time as a student at Oregon State. I would like to thank Evan Miles for helping me learn MATLAB, and for patiently answering any questions I had. I appreciated help from Alexis Smoluk in getting me started using the R statistical program. My gratitude also goes to Lynette de Silva and Dr. Aaron Wolf for my RA funding, with work on interesting and challenging projects, and an office with a window. And finally, to Adam, my partner for eight wonderful years, I thank you for your endless support and encouragement.

TABLE OF CONTENTS

TABLE OF CONTENTS (Continued)

Page

TABLE OF CONTENTS (Continued)

Page

LIST OF FIGURES

LIST OF FIGURES (Continued)

Figure Page

LIST OF TABLES

LIST OF APPENDICES

LIST OF APPENDIX FIGURES

LIST OF APPENDIX FIGURES (Continued)

Figure Page

LIST OF APPENDIX FIGURES (Continued)

Figure Page

1. Introduction

Climate change results in varied trends in different parts of the U.S. as described in *Global Climate Change Impacts in the United States*, a report provided to the U.S. Congress on the impact of climate change around the country (Karl, Melillo, and Peterson 2009). Water resources were a major focus of the study. Whether a result of climate change or climate variability, water resources reflect temperature and precipitation patterns. The study found stream discharge has declined in the Southwest and the Pacific Northwest, but has increased in the east due to increased precipitation (Karl, Melillo, and Peterson 2009). Snowmelt is occurring one to four weeks earlier due to increased temperature (Karl, Melillo, and Peterson 2009). The frequency of intense precipitation events has increased, and further changes in precipitation patterns will result in more intense flooding and drought periods (Karl, Melillo, and Peterson 2009).

Climate change is expected to continue, with most models predicting temperature will continue to rise. Areas in the north and east of the US are expected to become wetter, while areas in the west and southwest are expected to become drier. Areas reliant on winter snowpacks are expected to experience increasingly earlier runoff periods and decreases in summer flow. These changes imply that historical water yield may no longer provide an adequate basis for water management plans in the future (Milly et al 2008). At the same time, water yield is changing due to ongoing

changes in forests, which provide the source for nearly two-thirds of freshwater in the US (NRC 2008, Jones et al 2009).

Research has shown declining trends in annual discharge and summer and fall discharge from 1948-1988 in the Pacific Northwest (Lettenmair, Wood, and Wallis 1994). Significant declines in annual discharge were found in the Columbia basin from 1948-2004 (Dai et al. 2009). Decreases were also observed in median and minimum daily flow in the Pacific Northwest across varying time periods in the 20th century (Lins and Slack 1999). Luce and Holden (2009) found a decline in the 25th percentile of annual flow throughout the Pacific Northwest, as well as declines in the 50th percentile and mean annual flow in the Cascade region. Significant cumulative discharge from 1951 to 2000 also showed declines in the Pacific Northwest (Milliman et al. 2008).

These trends have generally been attributed to increased temperature. Increases in temperature are expected to reduce winter snow pack in the western US, contributing to earlier spring snowmelt and reduced summer flow. Many mountainous areas of the western US have experienced a decrease in the snow water equivalent (SWE), which is a measure of both snow pack depth and the quantity of water it contains, and this decline is particularly pronounced in the Cascade Mountains (Mote et al. 2003; Mote 2003). SWE is an important factor in summer flow conditions, when little precipitation is occurring (Mote et al. 2005). In many areas, increased cool season temperature are believed to have resulted in more precipitation falling as rain

than snow, particularly in areas of transient snow pack, where the temperature remain close to the freezing point (Karl, Melillo, and Peterson 2009; Knowles et al. 2006; Mote et al. 2005; Regonda et al. 2005; Stewart et al. 2005). Winter warming trends in areas with snowpack would be expected to increase streamflow in the late fall, winter, and early spring, but decrease streamflow in late spring, summer, and fall (Karl, Melillo, and Peterson 2009).

Many studies have also shown that spring snowmelt runoff is occurring earlier in the spring (Cayan et al. 2001; Hamlet et al. 2005; Regonda et al. 2005; Stewart et al. 2005; Barnett et al. 2008).Warming temperature in the spring are expected to accelerate vegetation phenology. Cayan et al. (2001) showed that lilacs and honeysuckles, which are responsive to changes in temperature, are now blooming 5 to 10 days earlier than in the 1970s. Earlier leafout and associated earlier onset of evapotranspiration (ET) may reduce streamflow, particularly in the summer growing season when water quantities are lowest (Hamlet and Lettenmaier 1999).

Summer low flow deficits have also been attributed to the rapid growth of young vegetation (Hicks et al. 1991; Hornbeck et al. 1997; Jones and Post 2004; Perry 2007). A study in the HJ Andrews showed that riparian forests consisting of 40 year old stands had much higher rates of transpiration and water use than stands with 450 year old trees (Moore et al. 2004). Increased water use in younger Douglas fir trees can be attributed to greater water use per sapwood area than older trees as measured by the sap flux density, and a greater percentage of sapwood basal area (Moore et al. 2004).

The type of vegetation that initially grows following harvest also impacts water use. Angiosperms (broadleaf trees) use more water than gymnosperms (needleleaf trees) (Jarvis 1975).

In undisturbed, unregulated headwater watersheds, both abiotic and biotic factors might delay or counteract the expression of a climate warming effect on streamflow. Abiotic effects include: (1) increased precipitation that could mitigate increased temperature effects on ET and (2) cold snowpacks that could mitigate or delay expression of a warming effect on snow. Biotic effects include: (1) climate/vegetation systems with low precipitation (high PET/P) might not respond and (2) changes over time in leaf area and/or species composition that could counteract effects. Runoff ratios (discharge/precipitation) can be used to separate effects of precipitation trends from streamflow trends, revealing changes in ET and water storage.

In watersheds that have experienced disturbance or flow regulation, additional factors might mitigate, obscure, or overwhelm climate effects on streamflow. A principal abiotic factor is flood control dams and reservoir operations, which alter flow regimes (Poff et al 2007). A biotic factor is changes in land use and land cover that influence ET. Conversion of old to young has been shown to increase winter streamflow and, by a couple of decades after harvest, decrease summer streamflow.

For all these reasons, streamflow response to climate trends would be expected to vary by region of the US, by season, and by location within a large watershed. Ch 2, "Effects of forest cover change, geology, and dams on streamflow trends since 1950 in the Willamette Basin, Oregon," examines how streamflow trends vary from the headwaters to the outlet of a

large river basin experiencing climate change and forest cover change. This analysis combined historical forest cover data with analysis of trends in streamflow and precipitation in large (60-600 km^2) basins above dams in the Willamette River basin.

Ch 3, "Effects of regional climate and forest dynamics on streamflow: an analysis of records from eight Long-term Ecological Research and Forest Service Experimental Forest sites in the US," addresses the effects of differing regional climates on streamflow response to climate trends. To examine the effects of climate trends on hydrology at headwater sites, long-term records from eight LTER/USFS EFR sites were examined to quantify and compare trends among predominantly forested sites distributed across the US but differing in abiotic and biotic contexts.

2. Effects of forest cover change, geology, and dams on streamflow trends since 1950 in the Willamette Basin, Oregon

2.1 Introduction

Understanding streamflow patterns is important for water management in areas where surface water is the primary water source, such as the Willamette River basin in the Pacific Northwest. Streamflow patterns vary throughout the year in often predictable patterns. These seasonal trends provide water managers with the basis for the annual water allocation and, in the case of the Willamette River, dam operation. While these plans do account for the natural variability expected in streamflow, long term trends in streamflow have shown declines throughout the region (Lettenmaier et al. 1994; Lins and Slack 1999; Zhang et al. 2008; Milliman et al. 2008; Dai et al. 2009; Luce and Holden 2009) and further declines are predicted in the future, particularly for summer and fall flow (Mote et al. 2003; Karl, Melillos, and Peterson 2009). In the Pacific Northwest region with minimal summer precipitation and streamflow, fulfilling environmental regulations and meeting the needs of water users may become more difficult.

Many factors control the hydrologic regime of a basin, including climate, vegetation, geology, topography, and soils. Changes in any one of the factors is likely to result in changes to the hydrology. Changes in both climate and vegetation have been observed since at least the last half of the 20th century and the impacts of both on streamflow have been studied in a variety of settings.

Studies in the Pacific Northwest have examined temperature trends since at least the last half of the 20th century (Cayan et al. 2001; Mote 2003b; Hamlet et al. 2005; Barnett et al. 2008). Increasing temperature will affect snowpack, with more precipitation falling as rain (Karl et al. 2009; Knowles et al. 2006; Mote et al. 2005; Regonda et al. 2005; Stewart et al. 2005), and less snow water equivalent (SWE) (Mote et al. 2003; Mote 2003a). These studies have attributed earlier timing of spring snow melt, higher winter/early spring flow, and decreased summer flow to increases in temperature (Cayan et al. 2001; Hamlet et al. 2005; Regonda et al. 2005; Stewart et al. 2005; Barnett et al. 2008).

In the same time period, forests of the Oregon Cascades changed dramatically. Beginning in the 1930s and accelerating after World War II, widespread logging on federal forest lands in the Oregon Cascade Range and in the headwaters of the Willamette Basin altered contiguous old growth, primarily Douglas fir (*Pseudotsuga menziesii)* forests to a patchwork of old forests, clearcuts, and stands at varying stages of regrowth. Small headwater basin studies have found vegetation removal and regrowth to substantially influence discharge (Hicks et al. 1991; Hornbeck, Martin, and Eagar 1997; Jones 2000; Jones and Post 2004; Perry 2007). Initial removal of forest stands leads to increases in discharge (Rothacher 1970; Harr and McCorison 1979; Harr et al. 1982; Wright et al 1990; Hicks et al. 1991; Jones and Grant 1996; Hornbeck et al. 1997; Thomas and Megahan 1998; Jones 2000). In paired headwater basins experiments in US research forests (H.J. Andrews, Coweeta, Hubbard Brook),

forest harvest showed summer low flows declined below preharvest levels after removal of mature native vegetation, when vegetation began to regenerate (Hornbeck et al. 1997; Jones and Post 2004). In the Pacific Northwest, replacing old Douglas-fir or mixed-conifer forest with young Douglas-fir plantations produced declining summer flow that persisted 25-40 years after the initial harvest (Perry 2007). These declines in summer and fall flow were attributed to the rapid growth and high water use by young forests (Moore et al. 2004). In addition, replacement of native forests by young plantations, including of non-native species, led to declining dry season flow (Smith and Scott 1992; Scott and Lesch 1997). Grass and shrub land basins in South Africa that were afforested with *Eucalyptus grandis* and *Pinus patula* were found to have significant declines in low flow values (Smith and Scott 1992; Scott and Lesch 1997).

Although recent studies of regional trends in streamflow in the Pacific Northwest have focused on climate change as the mechanism for declining trends in spring and summer discharge, some of this effect may be attributable to increased area of young forest in these large basins. There is some evidence that increasing area of young forest has led to declines in streamflow in large watersheds (Trimble et al. 1987; Little et al. 2009). Work in the southern Piedmont region of Georgia and South Carolina found significant declines in water yield with the afforestation of agricultural lands in large (2,820 to 19,450 km^2) basins (Trimble et al. 1987). Trends in residuals from summer discharge were found to be significantly negative when native deciduous

Nothofagus obliqua and *Nothofagus glauca* forests were replaced with fast growing *Pinus radiata* plantations in large basins (250 and 700 km^2) in south central Chile (Little et al. 2009). However, this hypothesis has not been explored in the Pacific Northwest, and it is a major motivation for this study.

The influence of changes in vegetation and climate on hydrology in large basins may be moderated by basin physical characteristics, especially elevation, hydrogeology, and topography. The distribution of elevation in a basin influences the spatial distribution of area in seasonal snowpack vs. transient snow or rain zones, which in turn influences the seasonal timing of streamflow: more area that is in the seasonal snowpack zone, the higher the spring and summer flow. High-elevation seasonal snowpacks are colder than those at lower elevations and less susceptible to warming above the threshold of melt at 0°C. Temperature increases and corresponding changes to the snowpack are expected to be most pronounced in elevation ranges where the winter temperature remain close to the freezing point (Knowles et al. 2006; Mote et al. 2005; Regonda et al. 2005; Stewart et al. 2005; Nolin and Daly 2006).

The underlying geology, especially the volume of recent, porous lava flow, influences the hydrogeology (the flowpath distributions, or the mean residence times of water) in a basin, such that basins with a larger volume of recent lava flow have longer average water residence times, relatively high spring and summer flow, and little interannual variation in discharge (Manga 1997; Tague and Grant 2004; Jefferson

et al. 2008). Predicted increases in the ratio of rain to snow are moderated by hydrogeology to produce different effects in basins dominated by so-called "High Cascades geology," compared to "western Cascades geology." The term "High Cascades geology" refers to areas in the Cascade Range of Oregon of younger, high-porosity, high-permeability rocks on little-eroded landforms with low drainage density (Callaghan and Buddington 1938; Ingebritzen et al 1992), where mean residence times of water are 3-14 years (Jefferson et al. 2006). The term "western Cascades geology refers to areas of older volcaniclastic materials on highly eroded landforms with high drainage density (Callaghan and Buddington 1938; Ingebritzen et al 1992), where mean residence times of water are 0.8 to 3.3 yrs (McGuire et al 2005). Under increased warming scenarios basins in the Cascade Range of Oregon that are dominated by High Cascades geology are predicted to experience the greatest declines in late summer and fall streamflow (Tague and Grant 2009; Tague et al. 2008). This finding is the result of two mechanisms. First, if climate warming causes precipitation to shift from snow to rain, recharge to the deep groundwater system will occur earlier in the water year, and over multiple decades, despite the long residence times of water, these basins will shift to hydrologic regimes with lower streamflow in summer and fall than at present. Second, the hydrogeology of basins draining recent, porous lava flow produces relatively high streamflow in summer and fall, so these basins can experience larger absolute changes in summer and fall streamflow, compared to basins draining highly weathered, eroded, steep western Cascades, where summer and fall discharges are very low.

Topography influences soil depth and thereby controls the relationship between vegetation rooting depth and subsurface flowpaths of water. In areas where most water flowpaths are below the rooting zone, changes in climate and associated evapotranspiration would be expected to have relatively little effect on discharge. At a small paired basin study in the HJ Andrews Experimental Forest, WS 1 experienced significant summer declines 8 years following logging relative to the control, whereas WS 3 had continued increased summer flow during the same time period (Hicks et al. 1991). The authors attributed the difference in trends to accumulated sediment in the WS 1 channel that allowed for rapid reestablishment of riparian vegetation, and a narrow, debris flow-prone valley with limited opportunity for riparian regrowth in WS 3 (Hicks et al. 1991). The sediment wedges in WS1 fostered surface-subsurface water exchange and a well-developed hyporheic zone in which tree roots are direct contact with subsurface flow (Bond et al. 2002; Wondzell et al. 2007). In contrast, the lack of riparian vegetation in the WS 3 channel limits vegetation influence on stored soil moisture. In large basins with relatively large areas of High Cascades geology, high-permeability rocks, and low drainage density, water flowpaths may be out of contact with tree roots for most of the distance between infiltration and emergence in springs.

This study seeks to understand the impact of forest age structure and climate variation on hydrology in seven large basins (64-650 km^2) with varied geology and elevation, and three gages below dams in the Willamette River basin. Streamflow and precipitation of seven sub-basins above dams and three gages on the mainstem of the

Willamette River below dams were analyzed for trends at annual, seasonal, and daily time scales over the period 1950 to 2009. Using spatial analysis, the area of vegetation change, dominant geologic substrates, and the distribution of elevation ("hypsometry") were determined for each basin. Trends in discharge and runoff ratios were compared to the physical characteristics of each basin to test relationships with changes in temperature and forest stand age. Trends above and below dams were compared to explore if upstream trends propagate downstream and how upstream trends are mitigated by reservoir operations.

2.2 Hypothesis

Based on trends in streamflow at seven large (64-650 km^2) basins above dams in the Willamette basin, we evaluated the following hypotheses (which are not mutually exclusive):

1) Trends in streamflow are explained by the proportion of area in the seasonal snow zone (above 800 m). The seasonal snowpack zone (above 800 m) is less susceptible to climate warming than snowpacks in the transient zone (below 800 m). Earlier snowpack melting may be accompanied by increased rates of ET at lower elevations. We expect larger declining trends in spring and summer discharge at basins with relatively small proportions of area above 800 m.

2) Trends in streamflow are explained by basin geology, particularly the proportion of basin area underlain by High Cascades recent volcanics, which have large aquifers and relatively long water residence time distributions, compared to Western Cascades volcanics, which are highly weathered and eroded, with relatively small aquifers and relatively short residence times. We expect larger declining trends in spring and summer discharge at basins with relatively large proportions of area in High Cascades geology.

3) Trends in streamflow are explained by forest cover and forest age structure and its effects on evapotranspiration. Young forests (<40 yrs) have higher rates of ET in summer, but lower rates of ET in winter, than old growth forests. We expect larger declining trends in spring and summer discharge in basins where a relatively large proportion of area was converted from oldgrowth to young forest.

Comparing trends at seven basins above dams to trends at three gages on the main stem of the Willamette River, we evaluated this hypothesis:

4) Trends in streamflow below dams are explained by reservoir operation for flood control and water releases, and hence interannual trends in streamflow above dams associated with climate change and forest cover change have limited effects on hydrologic regimes in downstream, urban areas.

2.3 Study Sites

The study was conducted in seven sub-basins and three gages on the mainstem of the Willamette River basin (WRB) (Fig.2.1, Table 2.1). The WRB occupies 29,000 km^2 in western Oregon with headwaters near Cottage Grove, Oregon, draining into the Columbia River near Portland, Oregon. The WRB basin spans elevations from 3 to 3,197 m, and is bordered on the west by the Coast Range Mountains and to the east by the Cascade Mountains. The main stem of the Willamette River flows 230 km though the wide, low gradient Willamette Valley (Stanford et al. 2005, 615). The Willamette River is fed by tributaries from both the Coast Range and the Cascades, but seven of the study sub-basins are located in a 6,700 km^2 portion of the Willamette National Forest (WNF) in the Cascade Range (Fig. 2.1).

The seven sub-basins ranged in size from 64 to 29,000 km^2 (Table 2.1). From north to south, they are the Breitenbush River, North Santiam River, Blue River, Lookout Creek, South Fork McKenzie River, North Fork Middle Fork Willamette River, and Salmon Creek. The mainstem gages used were Albany, Salem and Portland.

Geology of the study basins consists of Tertiary and Quaternary volcanics (Fig. 2.2). The most significant difference occurs between the High Cascades geology in the eastern reaches of the forest and extending to the crest of the Cascades, and the older Western Cascades, located in the western lower elevation portions of the forest.

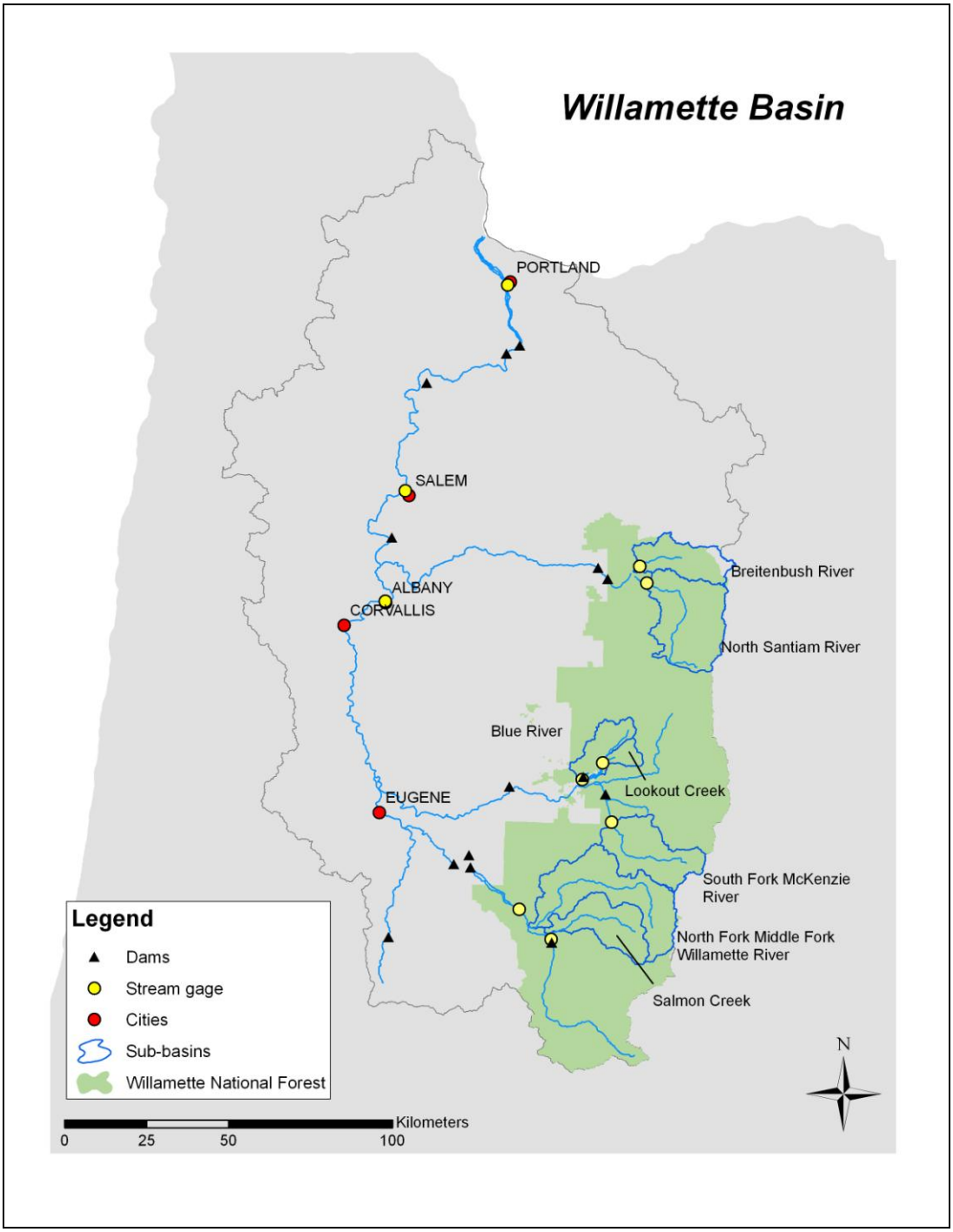

Figure 2.1 Map of Willamette River Basin, showing seven upstream study basins, and three gages downstream of dams.

Table 2.1 Basin data sources

	Name of Stream Gage	Basin Area (km^2)	Gage Number	Record Length	Data Source	Precip Record Length	Precip Data Source	Temp. Record Length	Temp. Data Souce
Blue River	BLUE RIVER NR BLUE RIVER, OREG.	130	14162000	1935-1964	USGS	1950-2009/1957-2009	4km PRISM Precipitation Grids/CS2MET	1958-2010	CS2MET
	BLUE RIVER BELOW TIDBITS CREEK, NR BLUE RIVER, OR		14161100	1963-2003	USGS				
Lookout Creek	GSLOOK	64		1949-2008	HJA Andrews				
Breitenbush River	BREITENBUSH R ABV FRENCH CR NR DETROIT, OR.	280	14179000	1932-2009	USGS/USACE				
North Santiam River	NO SANTIAM R BLW BOULDER CRK, NR DETROIT, OR	559	14178000	1907-2009	USGS				
South Fork McKenzie River	SO FK MCKENZIE RIVER ABV COUGAR LAKE NR RAINBOW OR	405	14159200	1957-2009	USGS				
North Fork Middle Fork Willamette	N FK OF M FK WILLAMETTE R NR OAKRIDGE,OREG.	646	14147500	1910-1994	USGS				
Salmon Creek	SALMON CREEK NEAR OAKRIDGE,OREG.	299	14146500	1913-1993	USGS/USACE				
Albany	WILLAMETTE RIVER AT ALBANY, OR	12,500	14174000	1893-2009	USGS				
Salem	WILLAMETTE RIVER AT SALEM, OR	19,000	14191000	1909-2009	USGS				
Portland	WILLAMETTE RIVER AT WILSONVILLE, OREG.	29,000	14198000	1948-1973	USGS				
	WILLAMETTE RIVER AT PORTLAND, OR		14211720	1972-2009	USGS				

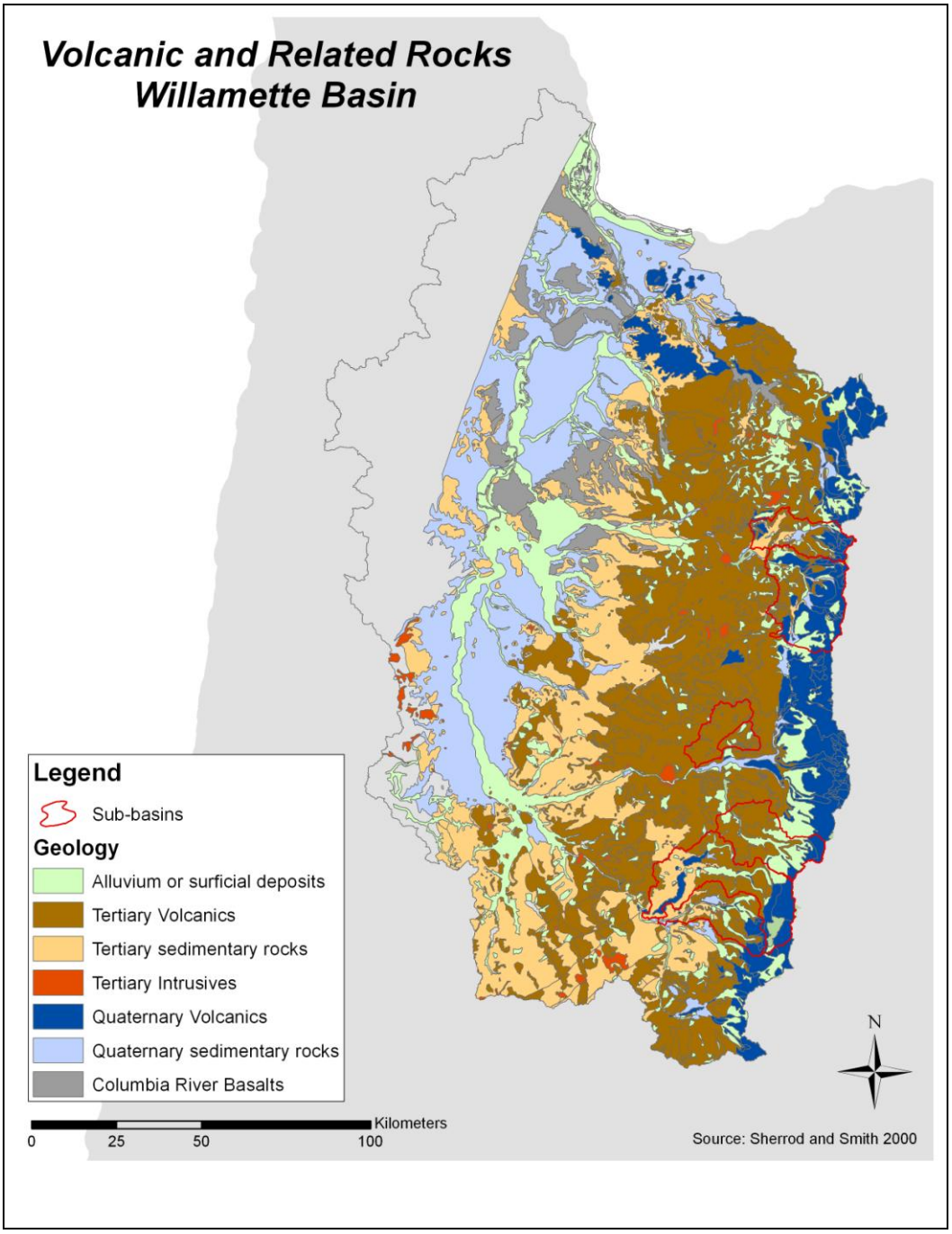

Figure 2.2 Geology of the Willamette River basin Cascades region showing High Cascades and Western Cascades geology.

The formation of the Western Cascades began in the Miocene with eruptions from a volcanic arc, with volcanism slowing considerably by 10 million years ago (Orr, Orr, and Baldwin 1992; 144-145). Further uplift, folding, and faulting occurred in the Western Cascades 4 to 5 million years ago, around the same time as the depression of the Cascades graben (145). These events resulted in the eruption of the High Cascades volcanics (145), which continued into human history (147). The younger High Cascades geology has relatively shallow slopes, and the young volcanics are much more porous, resulting in high groundwater storage and many springs (Tague and Grant 2004; Manga 1997). The older Western Cascades, however, have very steep, highly dissected slopes and limited groundwater storage (Tague and Grant 2004).

The Willamette basin experiences a Mediterranean climate, with warm, dry summers and wet, cool winters. In the valley most of the precipitation falls as rain, but moving up in elevation, the proportion of precipitation that falls as snow increases. The elevation range of the basins encompasses the mostly rain zone (<600 meters), the rain and snow, or transient zone, and the snow dominant zone (>800 meters). As a result, rivers often have the highest flow in later winter and spring due to melting of snow, and the lowest flow during the summer period of very little precipitation. Annual precipitation is 1,600 mm, of which 80% occurs between November and April. Mean monthly temperature ranges from 3° in January to 18° in July. Temperature and precipitation are closely correlated with elevation. Annual precipitation ranges from 1,100 mm at 200 m elevation near Portland to 2,600 mm at 3000 m elevation in the

High Cascades. Mean annual temperature ranges from 12°C at 200 m elevation near Portland to 1°C at 3,000 m elevation in the High Cascades.

The seven sub-basins (Fig. 2.1) were unregulated, and three mainstem gages (Albany, Salem, Portland) are downstream of flow regulation dams. Streamflow records range from 52 to 116 years (Table 2.1).

The WRB is predominantly conifer forest above 600 m elevation, and agriculture and urban land uses below 300 m. Forests are dominated by Douglas fir (*Pseudotsuga menziesii*), western hemlock (*Tsuga heterophylla*), and western red cedar (*Thuja plicata*) (Spies 1991; Franklin and Dyrness 1973). At higher elevations mountain hemlock (*Tsuga mertensiana*) and Pacific silver fir (*Abies amabilis*) are also prevalent (Franklin and Dyrness 1973).

The study area consists of stands of old-growth (>200 yr-old), mature (80-200-yr-old) and young (<80-yr-old) forests (Fig.2.3). Because wildfire has been effectively suppressed since 1920, most young forest stands were created by clearcut harvests. Logging of old growth Douglas fir in study basins in the WNF began as early as the 1930s and steadily increased until the 1980s (Jones and Grant 1996). In 1990, old-growth logging on federal lands effectively ended (Northwest Forest Plan 1994). Forest stand history information is only available for the seven sub-basins within the Willamette National Forest.

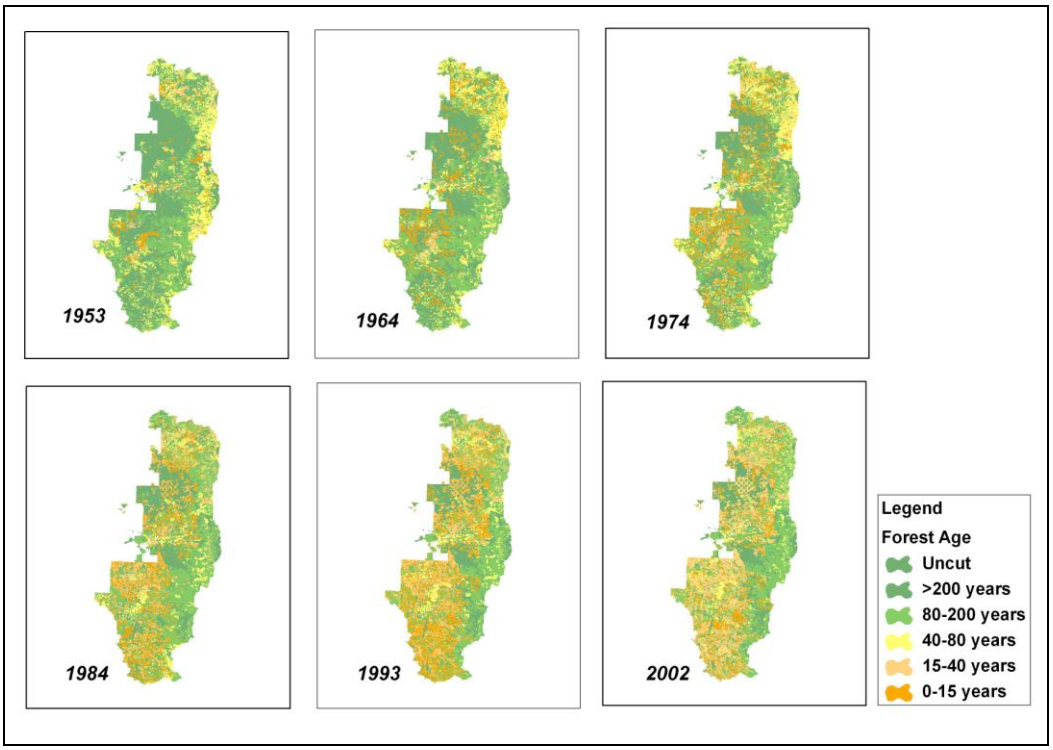

Figure 2.3 Vegetation stand age in the Willamette National Forest from 1953-2002. Darker green areas indicate old growth; orange areas indicate the youngest stands.

2.4 Methods

2.4.1 Temporal data sources

Temperature data was only obtained from one meteorological station, CS2MET, located at the HJ Andrews site. Data from this station was downloaded from the HJ Andrews Experimental Forest's Forest Science Data Bank. Precipitation data came from the PRISM Climate Group (PRISM Climate Group, Oregon State University, http://prism.oregonstate.edu, created 11 July 2002-12 February 2010). PRISM data sets are 4 km gridded GIS layers that provide precipitation estimates for the conterminous United States on a monthly data from 1895 to present (Daly 1994, Daly 2008). Daily precipitation data from CS2MET, the same meteorological station used for temperature analysis was used for this analysis. Discharge data was mostly from the United States Geological Survey (USGS) historical streamflow records (USGS Surface-Waterdata for the Nation, http:// waterdata.usgs.gov/nwis/sw, last accessed 19 February 2011), but a few sites, Breitenbush and South Fork McKenzie, were supplemented with data from the United States Army Corp of Engineers (USACE) (US Army Corp of Engineers, Northwest Division, dataquery, http://www.nwd-wc.usace.army.mil/perl/dataquery.pl, last accessed 19 February 2011). Blue River and Portland data were a combination of two USGS gages (Table 2.1). Discharge records for Lookout Creek were provided by the HJ Andrews Experimental Forest research program, funded by the National Science Foundation's Long-Term Ecological Research Program (DEB 08-23380), US Forest Service Pacific

Northwest Research Station, and Oregon State University (http://andrewsforest.oregonstate.edu/data.cfm?topnav=8, last accessed 19 February 2011). Discharge values were downloaded in units of cubic feet per second (cfs), and converted to a depth value of millimeters per month based on calculations in Table 2.2.

Discharge data for Blue River and the Portland gage involved combination of two gages. Discharge data for these gages was normalized by the drainage area for each gage before the data was combined.

2.4.2 Spatial data sources

Watershed boundaries for the individual basins were extracted from the Oregon Hydrologic Unit Boundaries from the Oregon Spatial Data Library. All basins, except for Lookout Creek, came from the *Hydrologic Unit Boundaries (5^{th}) for Oregon (Geographic Nad 83)* (Oregon Spatial Data Library, http://spatialdata.oregonexplorer.info/GPT9/catalog/main/home.page, last accessed 19 February 2011). Lookout Creek came from *Hydrologic Unit Boundaries (6^{th}) for Oregon (Geographic Nad 83)* (Oregon Spatial Data Library, http://spatialdata.oregonexplorer.info/GPT9/catalog/main/home.page, last accessed 19 February 2011).

Table 2.2 Conversion of flow data from cubic feet per second(cfs) to millimeters per month (mm/month)

cubic feet per second (cfs) to cubic meters per second (cms)	cms=cfs*0.02832
cubic meters per second (cms) to cubic meters per month (cm/month)	cmm=cms*2629743.83
cubic meters per month (cm/month) to meters per month (m/month)	m/month=cmm/drainage area
meters per month (m/month) to millimeters per month (mm/month)	mm/month=m/month*1000

Stand age was determined using the "VegetationStand" spatial dataset from the Willamette National Forest. The dataset contains information about vegetation type, owner information, harvest history, and year of establishment for both managed and unmanaged stands (Willamette National Forest Data Library, http://www.fs.fed.us/r6/data-library/gis/willamette/, last accessed 19 February 2011).

The geology spatial layer, created by Sherrod and Smith (2000), encompasses an area of western Oregon from the northern and southern borders of the state, and from the base of the Coast Range Mountains to east of the Cascade Mountains (Fig. 2.2). The dataset contains high resolution mapping of Western and High Cascades geology.

Elevation data came from 10 meter Oregon state wide digital elevation models (DEMs). DEMs were created with data from the USGS, United States Forest Service, and Bureau of Land Management.

2.4.3 Temporal analysis

This study tested for trends in runoff ratios, as well as precipitation and discharge, to control for effects of interannual variation in precipitation on runoff. Trends in seasonal and daily flow were also analyzed to separate changes associated with flooding (winter), snowmelt (spring) and ET (summer, fall).

Streamflow, precipitation, runoff ratios, and temperature were tabulated by water year and by season. The water year extends from October 1 to September 30 of

the following year. Seasons were: Fall-September, October, November; Winter-December, January, February; Spring-March, April, May; Summer-June, July, August. While stream gages had varied lengths of records, to standardize the data, only data from 1950 to the end of the record (Table 2.1) was used.

Linear regression and the Mann-Kendall trend test were used to quantify trends in temperature, precipitation, streamflow and runoff ratios. Annual and seasonal temperature, precipitation, discharge, and runoff ratio data were tested for autocorrelation prior to analysis, using the autocorrelation function in the statistical software R. The residuals from regression analyses of data that were autocorrelated and had significant trends over time were also tested for autocorrelation (Table 2.3).

Another issue in statistical analysis is the distribution of the data. Parametric statistics, such as linear regression, assumes that the data is not only independent (not autocorrelated), but comes from a Gaussian distribution. Streamflow and precipitation values do not follow a Gaussian distribution. The distribution does not affect the trend, only whether the trend is significant (Helsel and Hirsh 1992). Therefore, these data were also analyzed with a nonparametric test, the Mann-Kendall, to explore possible trends. The Mann-Kendall test ranks results and determines if the values are changing more or less in relation to the dependant variable, in this case time (Helsel and Hirsch, 2002). This type of analysis is supported by USGS, which developed the software used to perform this analysis (Helsel et al., 2005).

Analysis of trends in seasonal and annual temperature

Temperature trends were estimated for one site, CS2MET at the HJ Andrews Forest (Lookout Creek). Maximum and minimum daily mean temperature were averaged on an annual and seasonal basis from 1959-2009. While temperature values were not a focus of this analysis, data was analyzed for trends though time. Simple linear regression and the Mann-Kendall test were used to look at trends in temperature of the time period of this study.

Analysis of trends in seasonal and annual precipitation using PRISM data

Monthly PRISM datasets were obtained from the PRISM website from 1950 to 2009. Data were downloaded as an ASCII text file, which contains spatial location information as well as the data. The data were brought into a GIS by converting the ASCII file to a raster file. The raster data must be converted to integer format, and then divided by 100 to provide the correct value in millimeters. Data were registered to World Geodetic Spheroid 1972 (WGS72) coordinate system. The files downloaded from the PRISM are for the conterminous United States, and therefore have to be clipped to the project extent. In this project data were clipped to the extent of the entire Willamette basin and to each of the seven upstream basins. The basin extents were projected to the coordinate system of the PRISM data. Mean monthly precipitation in millimeters was determined for all months and years using zonal statistics to determine the average values within each of the basins.

Analysis of trends in seasonal and annual discharge and runoff ratios

Discharge data was analyzed at a seasonal and annual time scale from 1950 to 2009 with linear regression and the Mann-Kendall trend test. The baseflow component of flow, which is the continuous flow not effected by direct input or runoff from precipitation events, was also analyzed. Baseflow was determined from a baseflow separation program (Appendix A) following Post and Jones (2001). The baseflow separation program applies a moving five day window to daily discharge values to determine the minimum for each 5-day period. The subset of local minimum values were then compared to adjacent minima, and values that were less than 90% of the surrounding minima were connected to define baseflow. Daily baseflow was aggregated to the monthly, annual and seasonal time frames for analysis.

Runoff ratios (Q/P) were calculated at the seasonal and annual time scale, from the water balance equation

$$Q=P-ET-\Delta S$$

where P is precipitation, ET is evapotranspiration, and ΔS is change in storage. The runoff ratio (Q/P) reflects changes in evapotranspiration or storage potential. Simple linear regression and the Mann-Kendall test were also used to evaluate trends in runoff ratios.

Trends in temperature, precipitation, discharge, baseflow, and runoff ratios were estimated for 1950 to the end of the period of record (Table 2.1) for each study

sub-basin. The 1950 date was chosen to allow a long period to analyze, and have a consistent time period between basins.

Analysis of trends in daily temperature, precipitation, and discharge data

Trends in daily data were calculated using a program written by E. Miles in MATLAB (Appendix B). The program formats data by day of water year for each year using a parsing code. Data were log transformed to produce a near-normal distribution, and values for each day were tested for trends using linear regression. Trends were considered significant if the slope of the regression was significant at $p<0.05$. The program outputs trend analysis for each day of the water year over the period of record.

Trends in daily data were estimated for maximum and minimum daily temperature and precipitation (from CS2MET, 1959-2009) and discharge (from seven basins and three downstream gages, Table 2.1). Data from the entire record (Table 2.1) was used for the daily analysis. Salmon Creek and North Fork Middle Fork Willmette only had part of the entire record evaluated (1949-2003 and 1936-1994, respectively) due to excessive missing values in the early part of the record. Blue River and Portland were evaluated by the depth value (mm/day) to account for using two different gages with different drainage areas for both.

2.4.4 Spatial analysis

Spatial analysis was used to explore how forest stand age, geology, and area of seasonal snowpack were related to trends in streamflow. GIS layers of vegetation stand age, geology, and elevation were created and analyzed using ESRI ArcMap Geographic Information System (GIS) v 9.3.1.

Basin boundaries for each of the seven basins were extracted from the Oregon Hydrologic Unit State Boundaries. After gaging stations were located, Blue River and Salmon Creek had to be resized to account for the part of the basin upstream of the dam on Blue River, and upstream of the gage on Salmon Creek. All further analysis was based on these extents for each basin.

Stand age

The area in young forest plantations was compared to mature and old forest to account for forest management effects on runoff trends over time.

Vegetation stand age classes were calculated though time for each of the basins. The Willamette National Forest "VegetationStand" layer (Fig. 2.3) was first clipped to the extent of each watershed. The "year of origin" attribute was primarily used to determine age classes for every decade from 1950 to 2000, as the metadata lists this as the primary focus for the creation of the dataset (USDA Forest Service, Willamette National Forest, Supervisors Office 2007). The number of years for each age class was subtracted from the year of interest to determine the year of origin. Any

areas that were not classified as forest were removed from the total. For each basin, the total area of forest aged 0-10, 10-20, 20-30, 30-40, 40-50,50-60, 60-70, 70-80, 80-200, and greater than 200 years was calculated for each decade. Areas of forest ranging from 0 to 40 years old were then grouped to create a "young forest" category.

This analysis was repeated for each basin within a 10 meter buffer around all the stream channels. The National Hydrography Dataset was clipped to each of the watershed boundaries. Then a 10 meter buffer was placed around all the stream channels. This buffer was then used to clip the VegetationStand layer, and the percentage of 0-40 year old stands was determined in the buffers for each of the watersheds.

Geology

This analysis also tested for area underlain by recent compared to old volcanic rock to account for effect of springs on runoff trends over time

The basins lie in the region that straddles both Western and High Cascades geology. Since the two create distinctive hydrologic regimes, the percentage of each type of geology was determined for each basin. Using the Sherrod and Smith (2000) dataset (Fig. 2.2), the separation of the two types of geology was based on age, as was the method used in other research in the Cascades (Jefferson et al. 2008; Tague and Grant 2004). The Western Cascades are composed of Tertiary lavas, and the High

Cascades are composed of Quaternary lava flow. From this dataset, these were the only geologic units distinguished within each of the basins.

Elevation

To account for effect of possible changes in seasonal snowpack on runoff trends over time, this analysis tested for area above 800 meters.

The hypsometry dataset was used to calculate the cumulative percentages of area within 100 meter increments from 400 meters to 3,200 meters for each of the study basins (Fig 2.4). The elevation of concern is around 800 meters, which is the elevation at which precipitation begins to change from a mixture of snow and rain, creating a transient snowpack, to mostly snow, where a seasonal snowpack develops. The cumulative percentage of area above this elevation was determined for each basin.

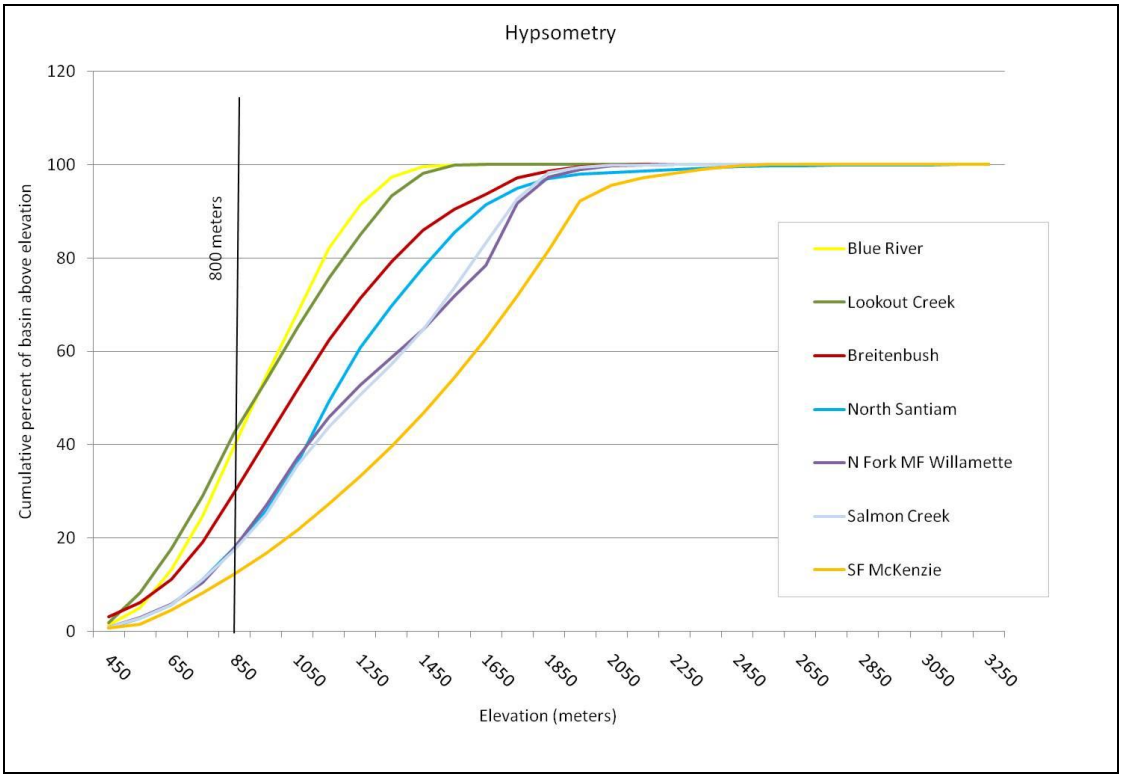

Figure 2.4 Hypsometry of seven sub-basins upstream of dams, showing the cumulative percent of area above an elevation. 800 meters is marked as the elevation of interest in this study.

2.5 Temporal Results

2.5.1 Temperature

Annual minimum temperature was found to be autocorrelated (Table 2.3a). However the residuals of annual minimum temperature were not autocorrelated. Summer maximum temperature showed a slight correlation at a lag of 1 year. Fall minimum temperature showed a slight negative correlation at a lag of 6 years. Winter minimum temperature showed autocorrelation at a lag of 1 year.

Annual minimum temperature increased significantly with linear regression at the CS2MET site in the HJ Andrews Forest over the period 1959 to 2009 (Table 2.3a). Decreasing temperature was observed in maximum temperature data.

Results from the Mann-Kendall test also showed significant increases in annual minimum temperature (Table 2.3a). Maximum temperature showed increases, but the trend was not significant.

Linear regression showed minimum temperature increased in all seasons, and spring maximum temperature also increased at CS2MET from 1959 to 2009 (Table 2.3a-e). Significant increases in temperature occurred for spring and annual minimum temperature.

Increasing trends were found in all seasons with the Mann-Kendall test (Table 2.3a-e). Spring minimum temperature was the only data to show significant increases.

Analysis of daily data from 1958-2006 showed significant increases in maximum daily temperature in January, March and April (Appendix C). Significant increases were found for minimum daily temperature in winter, spring, and summer.

Table 2.3A-E Results from linear regression analysis and the Mann-Kendall test for each basin, annual (A) and for each season (Spring-B, Summer-C, Fall-D, and Winter E).

A	Linear Regression						Mann-Kendall					Auto-	Residual
	N	Intercept	Slope	R2	P	Sig	Intercept	Slope	Tau	P	Sig	correlation	Autocorrelation
Annual Q/P													
Blue River	54	1.0020	-0.0014	0.04	0.04	*	3.8766	-0.0015	-0.150	0.11			
Breitenbush	60	0.8903	0.0000	0.00	0.98		0.8900	0.0000	0.005	0.96			
Lookout Creek	60	0.8508	-0.0023	0.14	0.00	*	5.1839	-0.0022	-0.282	0.00	*		
North Santiam	60	0.7807	-0.0002	0.00	0.12		1.2314	-0.0002	-0.051	0.57		x	
NFMF	44	0.7959	-0.0035	0.23	0.00	*	5.6388	-0.0025	-0.282	0.01	*		
Salmon	43	0.9512	-0.0048	0.29	0.00	*	9.6000	-0.0044	-0.398	0.00	*	x	x
SF Mckenzie	52	0.8032	-0.0006	0.02	0.34		0.7700	0.0000	-0.032	0.74			
Albany	59	0.7295	-0.0029	0.32	0.00	*	6.3071	-0.0029	-0.428	0.00	*	x	
Salem	59	0.7807	-0.0024	0.25	0.00	*	5.6600	-0.0025	-0.369	0.00	*	x	
Portland	59	0.7449	-0.0023	0.25	0.00	*	5.3695	-0.0024	-0.365	0.00	*	x	
Annual Base Q/P													
Blue River	54	0.4944	-0.0013	0.07	0.01	*	4.0536	-0.0018	-0.215	0.02	*		
Breitenbush	60	0.5574	0.0002	0.00	0.63		0.5600	0.0000	0.001	1.00			
Lookout Creek	60	0.4562	-0.0013	0.10	0.00	*	2.9470	-0.0013	-0.220	0.01	*		
North Santiam	59	0.5956	-0.0003	0.01	0.55		1.5700	-0.0005	-0.078	0.39		x	
NFMF	44	0.6306	-0.0023	0.15	0.01	*	3.3864	-0.0014	-0.167	0.12			
Salmon	43	0.6806	-0.0034	0.23	0.00	*	6.2414	-0.0029	-0.339	0.00	*	x	x
SF Mckenzie	52	0.5920	-0.0015	0.06	0.07		2.5535	-0.0010	-0.125	0.19		x	
Albany	59	0.6128	-0.0018	0.18	0.00	*	4.0135	-0.0017	-0.292	0.00	*		
Salem	59	0.6391	-0.0010	0.06	0.01	*	2.2136	-0.0008	-0.149	0.10			
Portland	59	0.6107	-0.0011	0.08	0.01	*	2.3113	-0.0009	-0.166	0.07			
Annual Q													
Blue River	53	1991.2000	-3.0527	0.01	0.49		7300.4000	-2.7420	-0.073	0.44			
Breitenbush	59	1954.3000	-2.9962	0.01	0.42		6697.8000	-2.4620	-0.071	0.43		x	
Lookout Creek	59	1907.0000	-7.1016	0.06	0.06		13157.0000	-5.7830	-0.143	0.11		x	
North Santiam	60	1741.7000	-3.0983	0.03	0.22		8255.7000	-3.3480	-0.116	0.20			
NFMF	44	1254.3000	-6.1892	0.08	0.06		14112.0000	-6.5710	-0.171	0.11			
Salmon	43	1439.9000	-5.9300	0.06	0.11		14632.0000	-6.7780	-0.195	0.07			
SF Mckenzie	52	1399.0000	0.0084	0.00	1.00		735.8300	0.3333	0.013	0.90		x	
Albany	59	1191.2000	-5.3295	0.11	0.01	*	11462.0000	-5.2810	-0.242	0.01	*		
Salem	59	1275.4000	-4.6952	0.08	0.04	*	10621.0000	-4.8000	-0.189	0.04	*		
Portland	59	1216.6000	-4.4699	0.07	0.04	*	10281.0000	-4.6540	-0.206	0.02	*		
Annual Base Q													
Blue River	53	984.3300	-3.1920	0.04	0.13		7221.9000	-3.2070	-0.148	0.12			
Breitenbush	59	1218.2000	-1.7297	0.01	0.41		4722.8000	-1.8060	-0.096	0.29		x	
Lookout Creek	59	1018.8000	-4.0124	0.07	0.04	*	7258.4000	-3.2000	-0.147	0.10			
North Santiam	59	1324.5000	-2.8324	0.05	0.10		7289.0000	-3.0560	-0.137	0.13			
NFMF	44	988.3300	-4.0744	0.06	0.09		7668.2000	-3.4350	-0.136	0.21			
Salmon	43	1021.5000	-4.0587	0.06	0.10		9307.3000	-4.2380	-0.193	0.07			
SF Mckenzie	52	1023.6000	-1.9649	0.02	0.32		4439.3000	-1.7310	-0.082	0.39			
Albany	59	1000.8000	-3.4947	0.06	0.05	*	7692.4000	-3.4390	-0.192	0.03	*		
Salem	58	1044.7000	-2.2529	0.02	0.24		5395.9000	-2.2390	-0.102	0.26			
Portland	58	997.8700	-2.3959	0.03	0.20		5280.4000	-2.2000	-0.110	0.22			
Annual Precipitation													
Willamette	60	1578.6000	-0.2056	0.00	0.93		2523.6000	-0.4853	-0.024	0.79		x	
Annual Max Temperature													
CS2MET	49	14.2910	-0.0010	0.00	0.99		14.0000	0.0000	-0.017	0.86			
Annual Min Temperature													
CS2MET	49	4.1062	0.0139	0.09	0.04	*	4.0000	0.0000	0.221	0.01	*	x	

Table 2.3 cont.

B		Linear Regression					Mann-Kendall					Auto-	Residual
	N	Intercept	Slope	R2	P	Sig	Intercept	Slope	Tau	P	Sig	correlation	Autocorrelation
Spring Q/P													
Blue River	54	1.5188	-0.0064	0.06	0.06		10.5060	-0.0047	-0.166	0.08			
Breitenbush	59	1.3645	-0.0027	0.02	0.27		4.1104	-0.0015	-0.050	0.59			
Lookout Creek	59	1.2748	-0.0066	0.15	0.00	*	11.1550	-0.0051	-0.224	0.01	*		
North Santiam	60	1.1657	-0.0021	0.02	0.33		4.3283	-0.0017	-0.072	0.42			
NFMF	44	1.1677	-0.0072	0.14	0.01	*	11.3540	-0.0053	-0.164	0.12			
Salmon	43	1.3466	-0.0091	0.17	0.01	*	16.8790	-0.0080	-0.207	0.06			
SF Mckenzie	52	1.1420	-0.0018	0.01	0.43		3.6187	-0.0013	-0.059	0.55			
Albany	50	0.8924	-0.0059	0.30	0.00	*	11.6190	-0.0055	-0.350	0.00	*	x	
Salem	60	0.9673	-0.0056	0.25	0.00	*	10.6950	-0.0050	-0.316	0.00	*	x	
Portland	60	0.9263	-0.0047	0.20	0.00	*	9.2414	-0.0043	-0.281	0.00	*		
Spring Base Q/P													
Blue River	54	0.9877	-0.0064	0.14	0.01	*	11.3560	-0.0054	-0.252	0.01	*	x	
Breitenbush	59	0.9854	-0.0020	0.02	0.27		3.7896	-0.1471	-0.068	0.46			
Lookout Creek	59	0.8628	-0.0051	0.17	0.00	*	8.3761	-0.0039	-0.238	0.01	*		
North Santiam	60	0.8696	-0.0002	0.00	0.90		2.2336	-0.0007	-0.026	0.77			
NFMF	44	1.0388	-0.0064	0.14	0.01	*	10.7050	-0.0050	-0.204	0.06			
Salmon	43	1.0528	-0.0076	0.20	0.00	*	14.1950	-0.0068	-0.256	0.02	*		
SF Mckenzie	52	0.9205	-0.0037	0.06	0.07		7.2268	-0.0032	-0.145	0.13			
Albany	59	0.7864	-0.0051	0.27	0.00	*	10.1590	-0.4815	-0.328	0.00	*	x	
Salem	59	0.8477	-0.0046	0.21	0.00	*	8.7989	-0.0041	-0.269	0.00	*		
Portland	59	0.8133	-0.0036	0.14	0.00	*	7.0312	-0.0032	-0.213	0.02	*		
Spring Q													
Blue River	54	663.6300	-1.0408	0.01	0.56		2596.0000	-1.0000	-0.051	0.59			
Breitenbush	59	617.7800	-0.3795	0.00	0.74		2477.6000	-0.9500	-0.057	0.53			
Lookout Creek	59	616.4000	-1.7174	0.03	0.21		4158.8000	-1.8240	-0.113	0.21			
North Santiam	60	544.8200	-0.3589	0.00	0.68		2044.8000	-0.7619	-0.077	0.40			
NFMF	44	420.4300	-1.2935	0.02	0.35		1421.9000	-0.5200	-0.051	0.64			
Salmon	43	464.2600	-0.9377	0.01	0.54		3531.0000	-1.5710	-0.107	0.32			
SF Mckenzie	52	457.1900	0.7947	0.01	0.47		579.1700	-0.0556	-0.004	0.97			
Albany	59	325.1100	-1.9322	0.13	0.00	*	4110.1000	-1.9500	-0.220	0.01	*		
Salem	60	350.2500	-1.7236	0.10	0.02	*	3805.2000	-1.7780	-0.184	0.04	*		
Portland	60	336.2400	-1.4013	0.07	0.04	*	3062.6000	-1.4000	-0.154	0.09			
Spring Base Q													
Blue River	54	430.1800	-1.8450	0.06	0.08		3953.9000	-1.8080	-0.163	0.08			
Breitenbush	59	447.5300	-0.4070	0.01	0.58		1691.4000	-0.6429	-0.102	0.26			
Lookout Creek	59	418.8100	-1.6860	0.06	0.06		4174.8000	-1.9230	-0.183	0.04	*		
North Santiam	59	435.5700	-0.4168	0.01	0.51		1854.1000	-0.7222	-0.096	0.29			
NFMF	44	373.2300	-1.1841	0.03	0.30		1534.6000	-0.6000	-0.064	0.55			
Salmon	43	364.1500	-1.0099	0.02	0.37		3753.4000	-1.7350	-0.125	0.25			
SF Mckenzie	52	372.0400	-0.6755	0.01	0.42		1410.7000	-0.5238	-0.051	0.60			
Albany	59	284.6900	-1.6504	0.14	0.00	*	3393.4000	-1.6000	-0.239	0.01	*		
Salem	59	305.3300	-1.4147	0.09	0.02	*	2892.0000	-1.3330	-0.168	0.06			
Portland	59	294.0500	-1.0631	0.05	0.08		2136.1000	-0.9500	-0.132	0.14			
Spring Precipitation													
Willamette	59	363.9900	0.3971	0.01	0.58		-589.4200	0.4737	0.071	0.43			
Spring Max Temperature													
CS2MET	47	12.7150	0.0194	0.04	0.17		13.0000	0.0000	0.155	0.11			
Spring Min Temperature													
CS2MET	47	2.3688	0.0290	0.16	0.01	*	3.0000	0.0000	0.253	0.01	*	x	

Table 2.3 cont.

C	Linear Regression						Mann-Kendall					Auto-	Residual
	N	Intercept	Slope	R2	P	Sig	Intercept	Slope	Tau	P	Sig	correlation	Autocorrelation
Summer Q/P													
Blue River	54	1.3280	-0.0095	0.08	0.04	*	13.2930	-0.0063	-0.159	0.09			
Breitenbush	60	2.7413	-0.0079	0.01	0.47		21.8800	-0.0100	-0.123	0.17			
Lookout Creek	59	1.2801	-0.0080	0.06	0.06		9.9555	-0.0045	-0.116	0.20		x	
North Santiam	60	2.9735	-0.0069	0.00	0.61		27.0290	-0.0126	-0.130	0.15			
NFMF	44	1.8122	-0.0204	0.13	0.02	*	29.4430	-0.0143	-0.249	0.02	*		
Salmon	43	2.6815	-0.0370	0.19	0.00	*	43.1810	-0.0211	-0.273	0.01	*		
SF Mckenzie	52	2.2276	-0.0062	0.01	0.52		25.9080	-0.0122	-0.126	0.19			
Albany	60	1.4066	-0.0013	0.00	0.81		5.8371	-0.0024	-0.070	0.44			
Salem	60	1.3040	0.0002	0.00	0.97		4.1046	-0.0015	-0.039	0.67			
Portland	60	1.1846	-0.0012	0.00	0.79		6.2273	-0.0027	-0.070	0.44			
Summer Base Q/P													
Blue River	54	1.2505	-0.0112	0.09	0.03	*	15.5640	-0.0075	-0.180	0.06		x	
Breitenbush	60	2.3297	-0.0059	0.01	0.54		19.9450	-0.0092	-0.144	0.11			
Lookout Creek	59	1.1871	-0.0084	0.07	0.05	*	13.0510	-0.0062	-0.179	0.05	*	x	x
North Santiam	59	2.7545	-0.0052	0.00	0.69		23.4150	-0.0108	-0.121	0.18			
NFMF	44	1.7165	-0.0194	0.13	0.01	*	27.9870	-0.0136	-0.237	0.03	*		
Salmon	43	2.4918	-0.0355	0.19	0.00	*	38.4020	-0.0188	-0.258	0.02	*		
SF Mckenzie	52	2.1254	-0.0096	0.02	0.32		28.5290	-0.0136	-0.140	0.15		x	
Albany	59	1.3713	-0.0018	0.00	0.75		6.0575	-0.0025	-0.061	0.50			
Salem	60	1.2425	0.0005	0.00	0.92		3.9203	-0.1471	-0.042	0.64			
Portland	60	1.1323	-0.0012	0.00	0.79		5.4569	-0.0023	-0.065	0.47			
Summer Q													
Blue River	54	139.6800	-0.8071	0.05	0.11		1045.7000	-0.4800	-0.110	0.24			
Breitenbush	60	305.0900	-1.2185	0.05	0.09		2570.2000	-1.1740	-0.154	0.09			
Lookout Creek	59	148.2300	-0.6236	0.03	0.16		906.6000	-0.4000	-0.098	0.28			
North Santiam	60	338.0600	-1.4548	0.08	0.03	*	3295.0000	-1.5250	-0.201	0.02	*		
NFMF	44	152.9700	-0.8433	0.05	0.14		895.9700	-0.3871	-0.063	0.56			
Salmon	43	238.4100	-1.3976	0.07	0.08		2815.8000	-1.3330	-0.116	0.28			
SF Mckenzie	52	214.5500	-0.2635	0.00	0.67		1226.7000	-0.5172	-0.100	0.30			
Albany	59	120.3200	-0.1880	0.01	0.36		470.8200	-0.1818	-0.094	0.30			
Salem	60	114.6900	-0.1150	0.00	0.59		304.9000	-0.1000	-0.041	0.65			
Portland	60	103.3300	-0.2018	0.02	0.30		531.7800	-0.2222	-0.088	0.33			
Summer Base Q													
Blue River	54	124.3500	-0.9639	0.09	0.02	*	1316.8000	-0.6250	-0.189	0.04	*		
Breitenbush	60	257.9400	-0.9884	0.06	0.07		2438.4000	-1.1250	-0.191	0.03	*		
Lookout Creek	59	130.9700	-0.6425	0.05	0.08		1089.5000	-0.5000	-0.181	0.04	*		
North Santiam	59	299.0500	-0.9420	0.05	0.09		3195.0000	-1.4860	-0.219	0.02	*		
NFMF	44	143.1900	-0.7601	0.05	0.13		802.2900	-0.3421	-0.055	0.61			
Salmon	43	215.2900	-1.2867	0.09	0.05	*	2580.4000	-1.2220	-0.179	0.10			
SF Mckenzie	52	201.0000	-0.5900	0.02	0.28		1600.4000	-0.7143	-0.135	0.16			
Albany	59	115.0600	-0.1628	0.01	0.36		385.0600	-0.1400	-0.087	0.33			
Salem	60	108.2300	-0.0796	0.00	0.67		226.6900	-0.0625	-0.027	0.77			
Portland	60	97.7920	-0.1935	0.02	0.28		518.2200	-0.2174	-0.093	0.30			
Summer Precipitation													
Willamette	59	101.7600	-0.0237	0.00	0.94		201.9700	-0.0541	-0.015	0.87			
Summer Max Temperature													
CS2MET	47	26.6050	-0.0169	0.02	0.55		26.0000	0.0000	-0.083	0.41		x	
Summer Min Temperature													
CS2MET	47	9.8945	0.0085	0.03	0.21		10.0000	0.0000	0.093	0.30			

Table 2.3 cont.

D	Linear Regression						Mann-Kendall					Auto-	Residual
	N	Intercept	Slope	R2	P	Sig	Intercept	Slope	Tau	P	Sig	correlation	Autocorrelation
Fall Q/P													
Blue River	54	0.5301	-0.0021	0.05	0.12		4.1552	-0.0019	-0.126	0.18			
Breitenbush	60	0.5424	-0.0005	0.01	0.58		2.1492	-0.0008	-0.102	0.25			
Lookout Creek	59	0.4460	-0.0020	0.08	0.03	*	4.3580	-0.0020	-0.176	0.05	*		
North Santiam	60	0.5080	0.0006	0.00	0.69		2.2691	-0.0009	-0.094	0.30			
NFMF	45	0.4012	-0.0020	0.09	0.05	*	4.5696	-0.0021	-0.208	0.05	*		
Salmon	43	0.6206	-0.0051	0.15	0.01	*	7.2277	-0.0034	-0.299	0.00	*		
SF Mckenzie	53	0.4344	0.0016	0.03	0.23		0.4450	0.0000	-0.017	0.87			
Albany	60	0.4542	0.0006	0.01	0.57		0.4400	0.0000	-0.018	0.85			
Salem	60	0.4845	0.0007	0.01	0.47		0.4900	0.0000	0.004	0.97			
Portland	60	0.4397	-0.0001	0.00	0.88		1.9824	-0.0008	-0.127	0.16			
Fall Base Q/P													
Blue River	54	0.1820	-0.0003	0.01	0.46		0.8076	-0.0003	-0.080	0.40		x	
Breitenbush	60	0.3255	-0.0002	0.00	0.78		0.3000	0.0000	0.029	0.75			
Lookout Creek	59	0.2003	-0.0009	0.09	0.02	*	1.9691	-0.0009	-0.204	0.02	*		
North Santiam	60	0.4053	0.0005	0.00	0.69		0.8212	-0.0002	-0.033	0.71			
NFMF	45	0.2811	-0.0006	0.01	0.54		1.1888	-0.0005	-0.084	0.43			
Salmon	43	0.4591	-0.0037	0.06	0.11		4.1304	-0.0019	-0.174	0.10			
SF Mckenzie	53	0.3450	-0.0002	0.00	0.85		0.8848	-0.0003	-0.041	0.67		x	
Albany	59	0.4048	0.0006	0.00	0.60		-0.9193	0.0007	0.071	0.43			
Salem	60	0.3927	0.0019	0.06	0.07		-2.1513	0.0013	0.166	0.06			
Portland	60	0.3575	0.0008	0.02	0.29		-0.0602	0.0002	0.049	0.59			
Fall Q													
Blue River	54	312.9200	-1.6103	0.03	0.23		3482.8000	-1.6250	-0.115	0.22			
Breitenbush	60	329.0100	-1.4529	0.04	0.13		1040.1000	-0.4483	-0.124	0.17			
Lookout Creek	59	281.5700	-1.4668	0.04	0.14		3033.9000	-1.4190	-0.113	0.21			
North Santiam	60	295.4900	-1.0605	0.06	0.02	*	2307.3000	-1.0370	-0.152	0.09			
NFMF	45	177.4400	-1.6288	0.09	0.05	*	2784.6000	-1.3420	-0.149	0.16			
Salmon	44	228.2600	-1.6598	0.09	0.02	*	3378.4000	-1.6210	-0.195	0.07			
SF Mckenzie	53	218.6300	-0.6564	0.02	0.26		952.0500	-0.3826	-0.068	0.48			
Albany	59	200.6700	-0.5572	0.02	0.25		1082.5000	-0.4545	-0.094	0.30			
Salem	60	221.9200	-0.7724	0.03	0.16		1181.5000	-0.5000	-0.082	0.36			
Portland	60	200.5600	-0.9003	0.06	0.07		1432.4000	-0.6364	-0.129	0.15			
Fall Base Q													
Blue River	54	101.2200	-0.3126	0.01	0.46		870.1200	-0.3939	-0.067	0.48			
Breitenbush	60	175.7200	-0.5324	0.03	0.16		1040.1000	-0.4483	-0.124	0.17			
Lookout Creek	59	116.5800	-0.5787	0.04	0.12		1205.2000	-0.5676	-0.144	0.11			
North Santiam	60	217.6100	-0.6652	0.11	0.00	*	1664.9000	-0.7407	-0.243	0.01	*	x	x
NFMF	45	120.4400	-0.8988	0.07	0.08		1165.5000	-0.5420	-0.109	0.30			
Salmon	44	152.4200	-0.9128	0.13	0.00	*	1488.5000	-0.6923	-0.264	0.01	*		
SF Mckenzie	53	154.6500	-0.4889	0.04	0.16		479.6300	-0.1716	-0.074	0.44		x	
Albany	59	167.2500	-0.1119	0.00	0.78		153.0000	0.0000	-0.011	0.91			
Salem	60	175.5700	-0.0882	0.00	0.85		-152.4700	0.1579	0.041	0.65			
Portland	60	157.5900	-0.3053	0.01	0.44		537.8000	-0.2000	-0.046	0.61		x	
Fall Precipitation													
Willamette	59	439.6200	-0.7693	0.01	0.48		2010.2000	-0.8000	-0.056	0.54		x	
Fall Max Temperature													
CS2MET	47	13.5730	-0.0181	0.03	0.25		13.0000	0.0000	-0.079	0.42			
Fall Min Temperature													
CS2MET	47	4.7503	0.0004	0.00	0.88		5.0000	0.0000	-0.043	0.65		x	

Table 2.3 cont.

E	Linear Regression						Mann-Kendall					Auto-correlation	Residual Autocorrelation
	N	Intercept	Slope	R2	P	Sig	Intercept	Slope	Tau	P	Sig		
Winter Q/P													
Blue River	54	1.0496	0.0011	0.01	0.43		-1.2818	0.0012	0.083	0.38			
Breitenbush	50	0.7463	0.0015	0.02	0.24		-1.4289	0.0011	0.072	0.42			
Lookout Creek	59	0.9134	-0.0015	0.02	0.24		3.8018	-0.0015	-0.099	0.27			
North Santiam	60	0.5986	0.0005	0.00	0.62		0.6100	0.0000	-0.010	0.92			
NFMF	45	0.7205	-0.0003	0.00	0.86		-0.7915	0.0008	0.045	0.67			
Salmon	44	0.7652	0.0007	0.00	0.72		-2.9643	0.0019	0.073	0.50			
SF Mckenzie	53	0.7027	-0.0001	0.00	0.95		3.1831	-0.0013	-0.087	0.37			
Albany	60	0.7893	-0.0034	0.20	0.00	*	8.5960	-0.0040	-0.350	0.00	*		
Salem	60	0.8571	-0.0028	0.13	0.01	*	8.1813	-0.0038	-0.303	0.00	*		
Portland	60	0.8384	-0.0026	0.12	0.01	*	7.9464	-0.0036	-0.326	0.00	*		
Winter Base Q/P													
Blue River	54	0.4107	0.0003	0.00	0.09		-0.1540	0.0003	0.035	0.71			
Breitenbush	50	0.3867	0.0005	0.01	0.58		-1.5252	0.9677	0.105	0.24			
Lookout Creek	59	0.3899	-0.0003	0.00	0.72		0.3800	0.0000	-0.029	0.75			
North Santiam	60	0.3731	0.0004	0.00	0.61		-0.0598	0.0002	0.037	0.68			
NFMF	45	0.5074	0.0010	0.01	0.50		-1.6706	0.0011	0.094	0.37			
Salmon	44	0.4385	0.0017	0.02	0.32		-1.3418	0.0009	0.068	0.53			
SF Mckenzie	53	0.4286	-0.0008	0.01	0.46		1.8111	-0.7143	-0.080	0.41			
Albany	59	0.6409	-0.0025	0.12	0.01	*	5.6128	-0.0026	-0.240	0.01	*		
Salem	59	0.6662	-0.0010	0.02	0.33		4.0759	-0.0017	-0.135	0.14			
Portland	59	0.6547	-0.0012	0.03	0.20		4.1512	-0.0018	-0.150	0.10			
Winter Q													
Blue River	54	932.5200	-1.6559	0.01	0.51		4743.0000	-1.9800	-0.070	0.46			
Breitenbush	60	750.0600	-1.1328	0.01	0.56		3349.7000	-1.3500	-0.068	0.45			
Lookout Creek	59	868.9800	-2.4679	0.02	0.26		6085.1000	-2.6920	-0.121	0.18			
North Santiam	60	597.7500	-1.1808	0.01	0.36		3031.8000	-1.2630	-0.100	0.27			
NFMF	45	551.2800	-4.9660	0.17	0.01	*	8435.4000	-4.0670	-0.206	0.05	*		
Salmon	44	561.2900	-4.7094	0.15	0.01	*	7876.0000	-3.7730	-0.210	0.05	*	x	
SF Mckenzie	53	492.3700	0.2460	0.00	0.87		809.4200	-0.1667	-0.007	0.95		x	
Albany	59	564.6600	-3.0601	0.11	0.01	*	8091.4000	-3.8540	-0.272	0.00	*		
Salem	60	620.4400	-3.0405	0.09	0.02	*	7445.5000	-3.5000	-0.234	0.01	*		
Portland	60	605.5100	-2.8381	0.08	0.03	*	7256.6000	-3.4170	-0.208	0.02	*	x	
Winter Base Q													
Blue River	54	357.6900	-0.9714	0.03	0.23		1634.7000	-0.6667	-0.077	0.42			
Breitenbush	60	364.7300	-0.4117	0.00	0.62		1256.4000	-0.4615	-0.051	0.57			
Lookout Creek	59	356.4000	-0.5951	0.01	0.44		2195.8000	-0.9524	-0.098	0.27			
North Santiam	60	356.8300	-0.4609	0.01	0.45		1152.6000	-0.4091	-0.063	0.48			
NFMF	45	384.5900	-3.0196	0.17	0.01	*	5686.0000	-2.7260	-0.262	0.01	*		
Salmon	44	319.8400	-2.4662	0.22	0.00	*	4317.5000	-2.0560	-0.302	0.00	*	x	
SF Mckenzie	53	285.0000	-0.0942	0.00	0.89		807.1400	-0.2553	-0.050	0.61			
Albany	59	448.8400	-1.9076	0.06	0.07		5732.7000	-2.6980	-0.214	0.02	*		
Salem	59	480.7300	-1.5653	0.03	0.16		3606.3000	-1.6090	-0.122	0.18		x	
Portland	59	471.1500	-1.6389	0.04	0.12		3215.4000	-1.4170	-0.121	0.18		x	
Winter Precipitation													
Willamette	59	710.8200	-0.6216	0.00	0.66		2837.6000	2837.6000	-0.064	0.48			
Winter Max Temperature													
CS2MET	47	4.3657	-0.0006	0.00	0.92		4.0000	0.0000	-0.052	0.60			
Winter Min Temperature													
CS2MET	47	-0.5372	0.0073	0.01	0.49		0.0000	0.0000	0.002	0.99		x	

2.5.2 Precipitation

Precipitation values between all the basins and the entire Willamette basin were found to be highly correlated (correlation coefficient > 0.96). Therefore, analysis was performed on the precipitation data from the entire Willamette basin.

The annual data was not autocorrelated (Table 2.3a). Spring, summer, and winter data were not autocorrelated, although fall data did show a slight negative correlation at a lag of 3 years.

Precipitation declined at the annual time scale from 1950 to 2009, although the declines were not significant from linear regression analysis or the Mann-Kendall test (Table 2.3a).

Declining trends were observed in fall, winter, and summer for seasonal precipitation from 1950 to 2009 (Table 2.3b-e). Spring precipitation increased. The trends were not significant from linear regression analysis or the Mann-Kendall test.

Monthly precipitation data from CS2MET was found to be highly correlated (correlation coefficient of 0.98) with the monthly PRISM datasets, so it was assumed that the results would be applicable to this analysis. The log transformed daily precipitation data showed significant increases for one day in October and one day in May, and a significant decrease for one day in April.

2.5.3 Discharge data

Annual discharge data showed slight negative correlation at a lag of 5 years for Breitenbush River total flow, and positive correlation at a lag of 2 years for baseflow. Lookout Creek and South Fork McKenzie River total flow annual data showed negative correlation at a lag of 5 years. Spring and summer discharge data did not show autocorrelation at any site. North Fork Middle Fork showed slightly negative correlation for fall total flow at a lag of 1 year. Fall baseflow showed a slight correlation at a lag of 1 year at North Santiam River, and the residuals showed a negative correlation at a lag of 3 years. Portland and South Fork McKenzie River showed a slight negative correlation at a lag of 3 years for fall baseflow (Table 2.3a-e).

Linear regression of annual data showed negative trends in all basins for total flow and baseflow, except for South Fork McKenzie River total discharge. Lookout Creek showed significant declines in total discharge. Significant declines were found for total discharge at Albany, Salem, and Portland, and in baseflow discharge at Albany (Table 2.3a-e).

The Mann-Kendal test also found declining trends in the annual discharge data at all locations except total flow at South Fork McKenzie River. Significant declines were not found in any of the basins. Significant declines were found in total flow at Salem and Portland, and in total flow and baseflow discharge at Albany

(Table 2.3a-e).

Linear regression showed declines in all basins and at Albany, Salem, and Portland for summer and fall. Spring and winter data showed declines in all basins and at Albany, Salem, and Portland except for total discharge at South Fork McKenzie River. Significant declines were found in the spring for total discharge at Albany, Salem, and Portland, and for baseflow at Albany and Salem. North Santiam showed significant declines in summer total discharge, and Blue River and Salmon Creek showed significant declines in summer baseflow. Significant declines were found in fall total and baseflow discharge at North Santiam River and Salmon Creek, and for total discharge only at North Fork Middle Fork Willamette. North Fork Middle Fork Willamette and Salmon showed significant declines in winter total and baseflow discharge. Significant declines were found for total winter discharge at Albany, Salem, and Portland (Table 2.3a-e).

The Mann-Kendall test found all discharge trends to be negative at all locations in the spring and summer. Albany, Salem, and Portland discharges also declined. Lookout Creek was the only basin to show significant declines in spring baseflow. The trends of summer baseflow were significantly negative at Blue River, Breitenbush River, Lookout Creek, and for total flow and baseflow at North Santiam River. Fall discharges were all negative. Fall baseflow showed significant declining trends only at North Santiam and Salmon Creek. Salem baseflow increased, but discharges decreased for Albany, Salem total flow, and Portland. Winter discharges decreased at all sites. North Fork Middle Fork Willamette and Salmon showed

significant declines in winter total and baseflow. Albany, Salem, and Portland winter discharges also declined. Albany and Salem total flow both declined significantly (Table 2.3a-e).

Daily discharge results and change estimates from 1950 to 2010

Analysis of the daily data showed fine scale changes in the hydrograph that were not necessarily apparent in the seasonal grouping. Figure 2.5a-j shows the estimated changes in the hydrographs based on the long term daily streamflow mean values for each day of the water year at each site. Data output from the MATLAB program is found in Appendix C.

Daily data trends at Blue River (total discharge and baseflow) showed significant declines in August, September, and October, and also in May. Declines occurred from May until the fall. Increases occurred November and December, February, and March, but they were not significant. Breitenbush River total discharge had significant increases in December and January, and baseflow had significant increases in January, February, and March. There was little change in discharge in Breitenbush River the rest of the year. Lookout Creek daily data (total discharge and baseflow) showed significant declines in April and May, and then in August, September, and October. Declines were observed in June and July also. North Fork Middle Fork Willamette showed significant increases in December for both total discharge and baseflow, but there was little change throughout the rest of the year. North Santiam River showed significant increases January for total discharge and

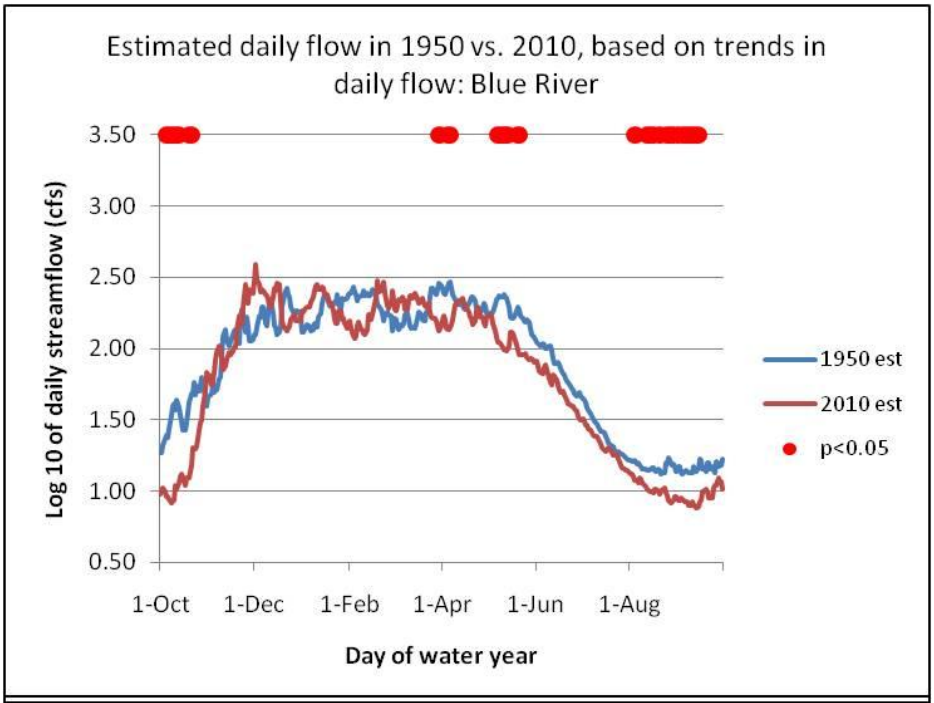

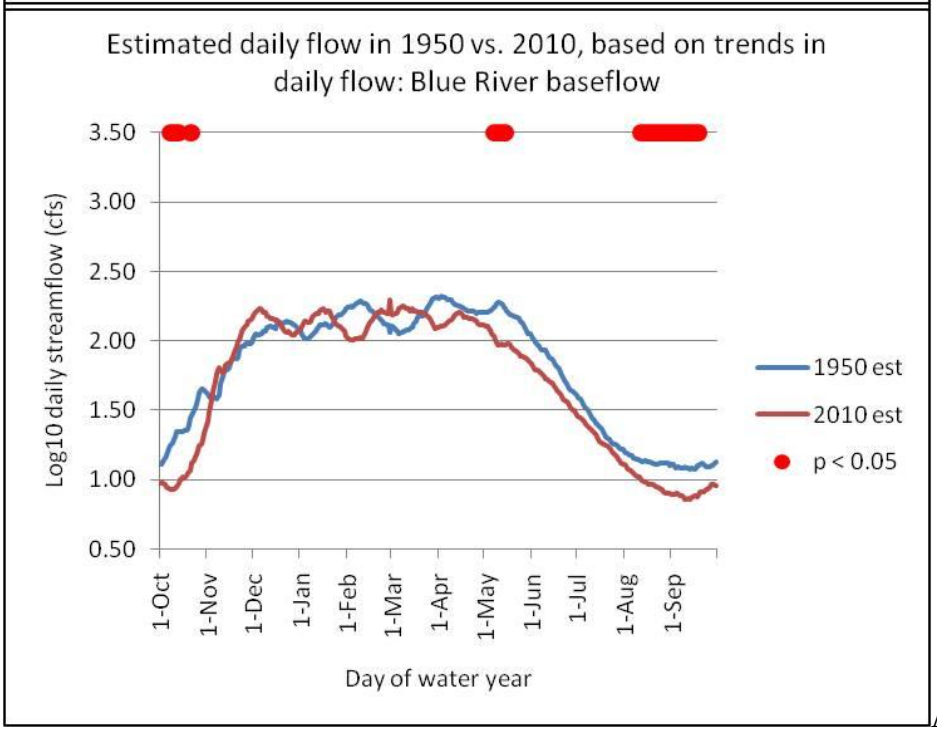

A.

Figure 2.5a-j Estimated daily flow change 1950 to 2010. Graphs were created using output from MATLAB daily analysis. Significant changes occurred in areas below the red dots.

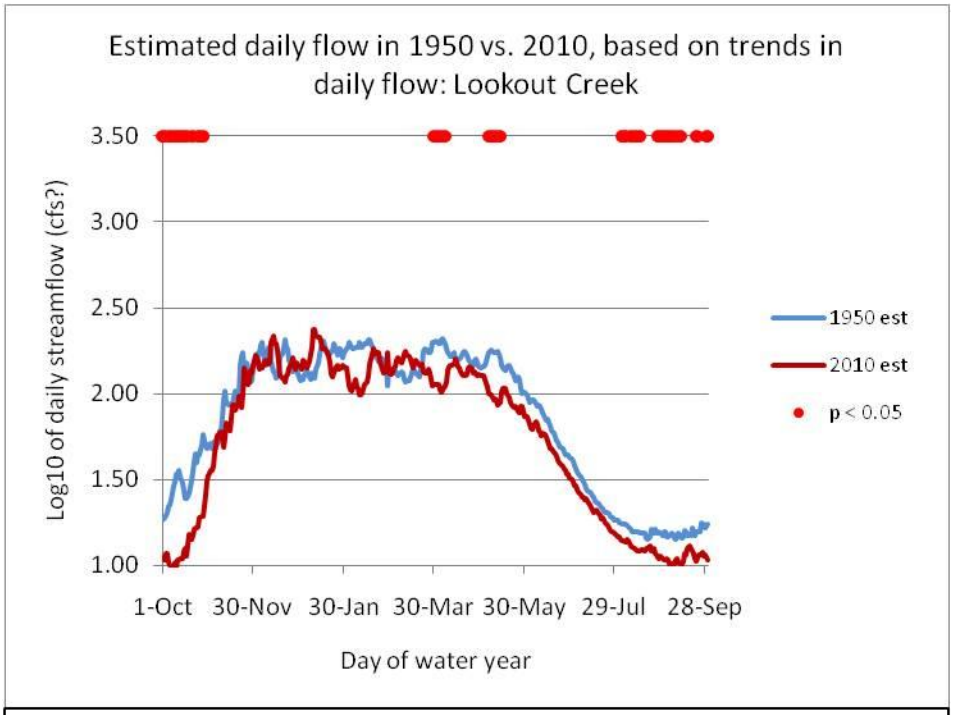

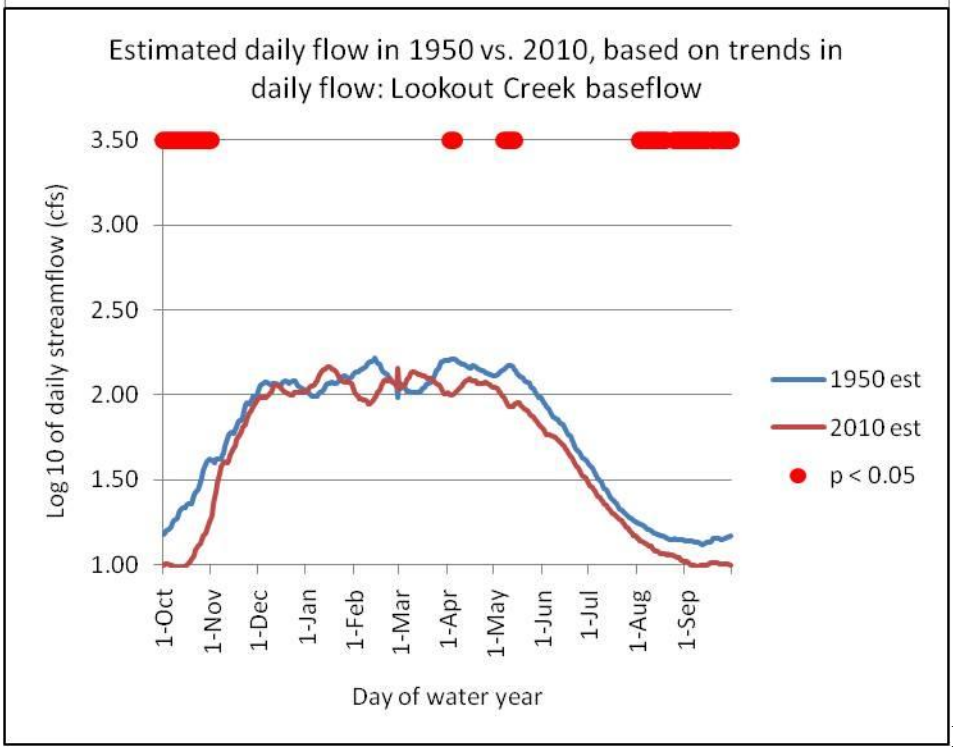

B.

Figure 2.5 cont.

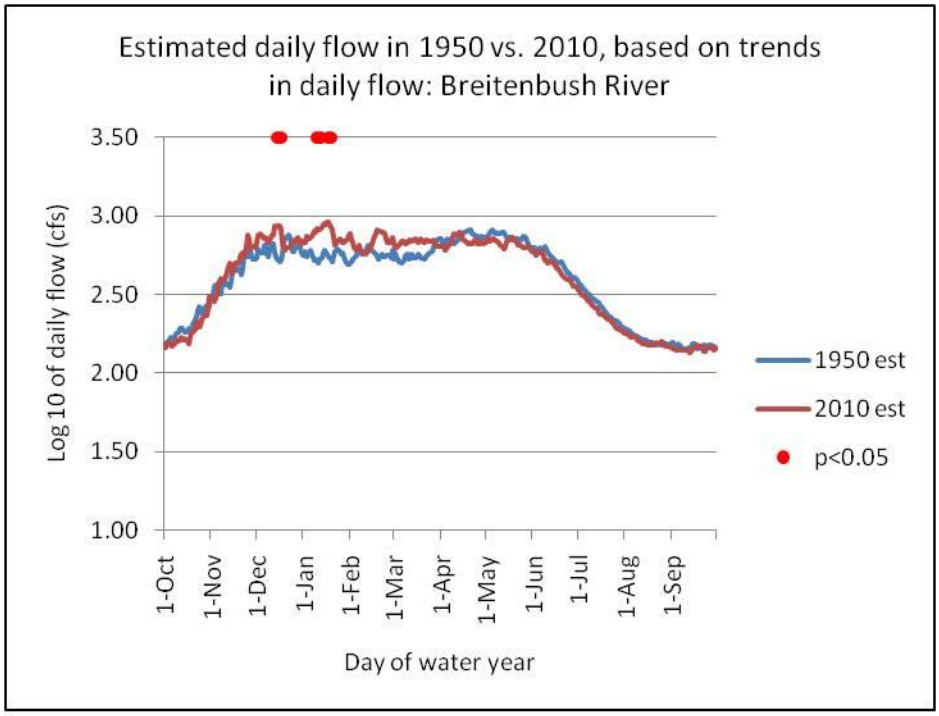

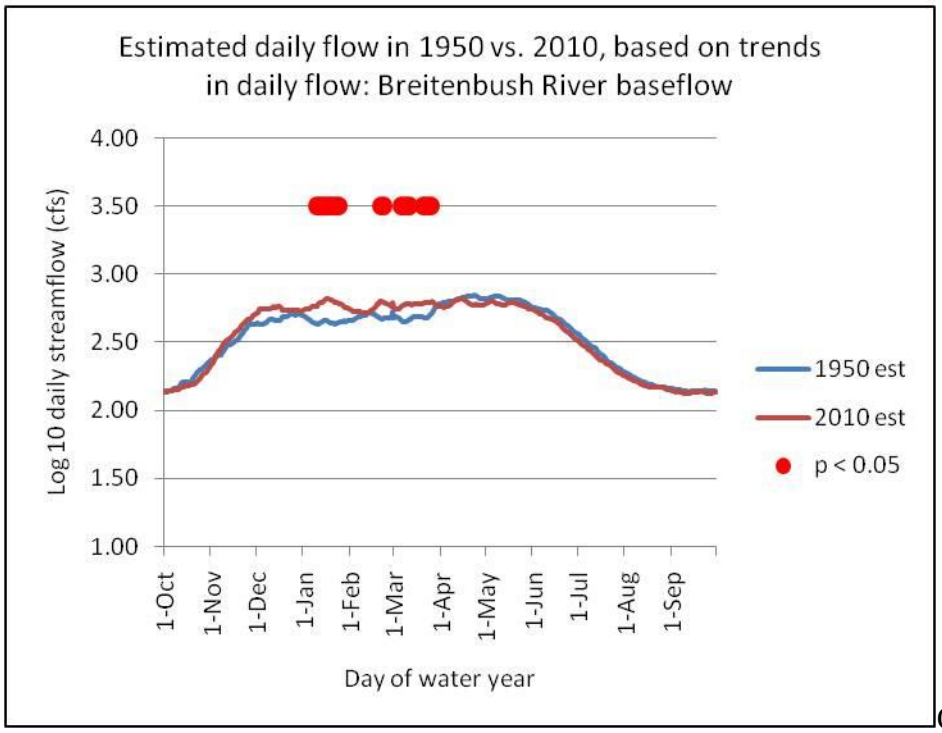

C.

Figure 2.5 cont.

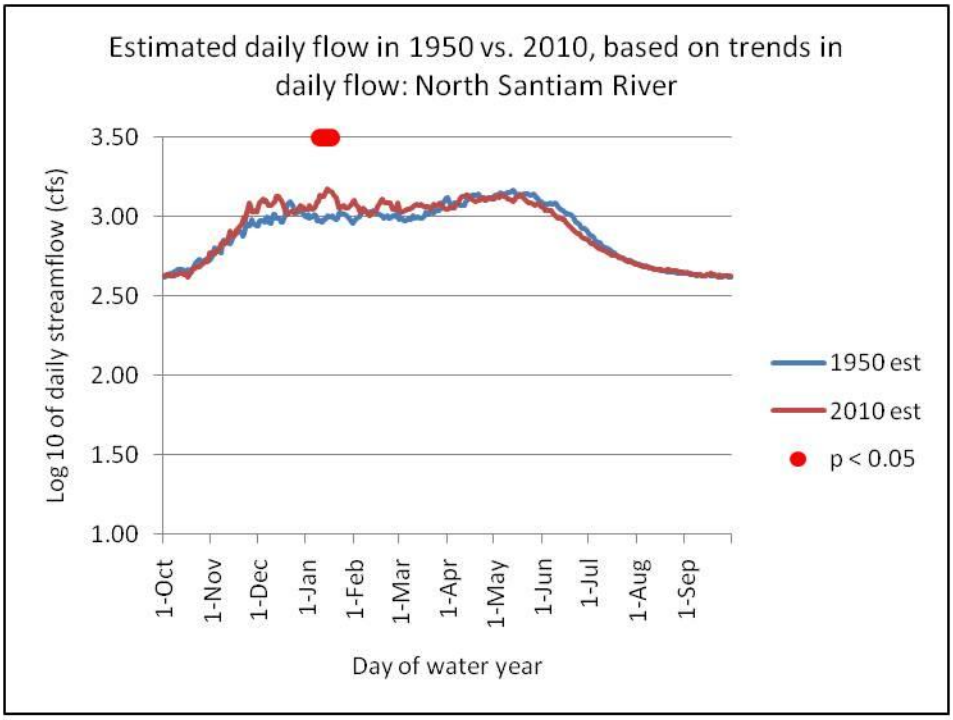

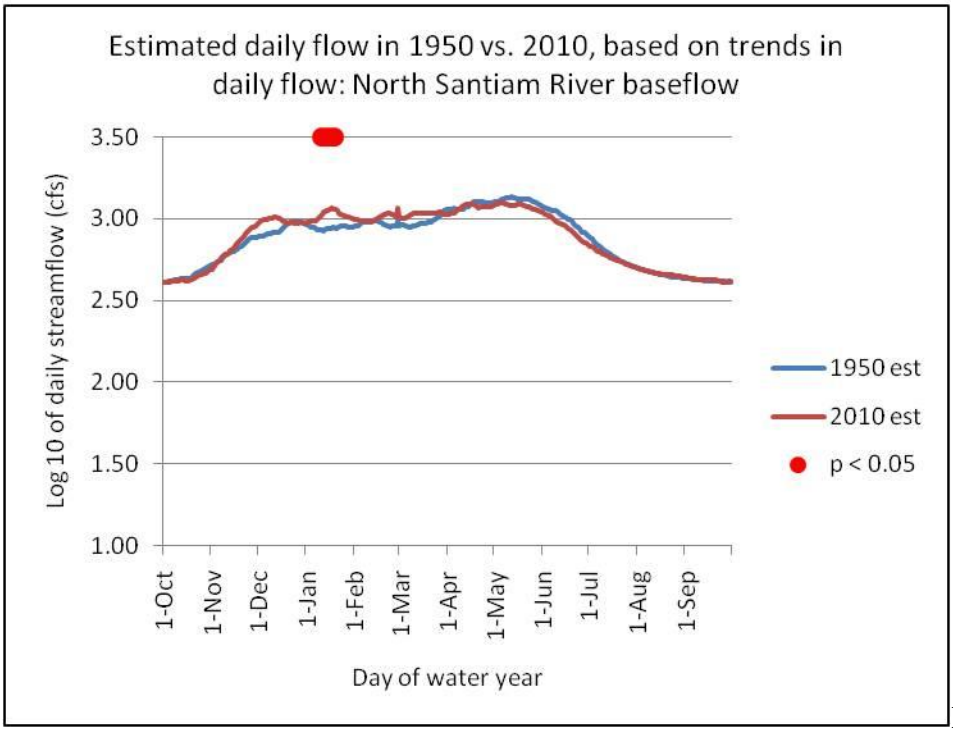

D.

Figure 2.5 cont.

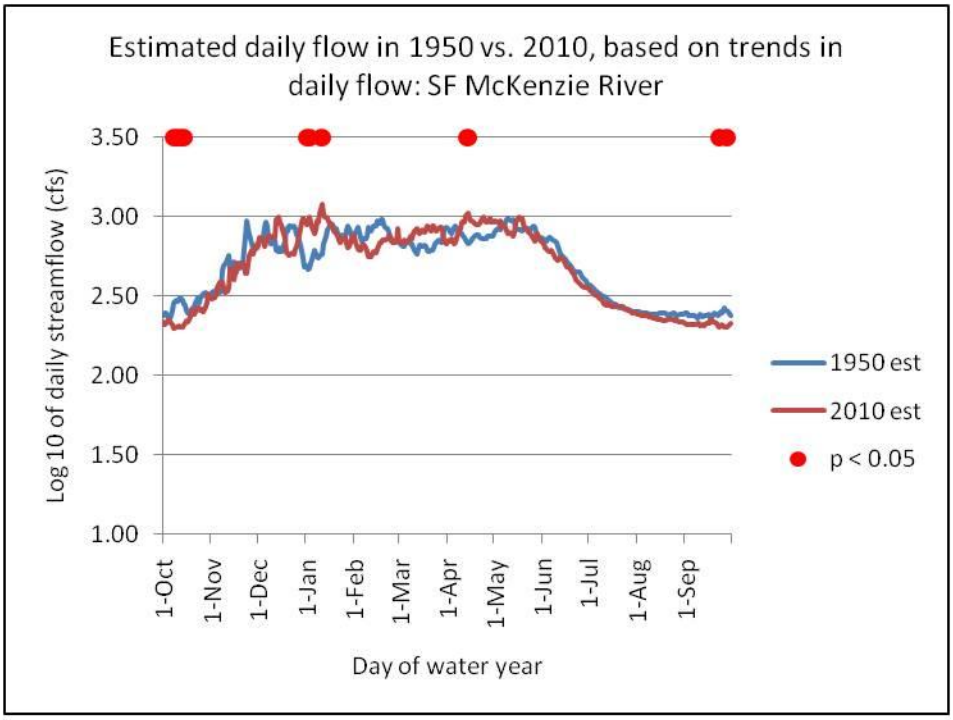

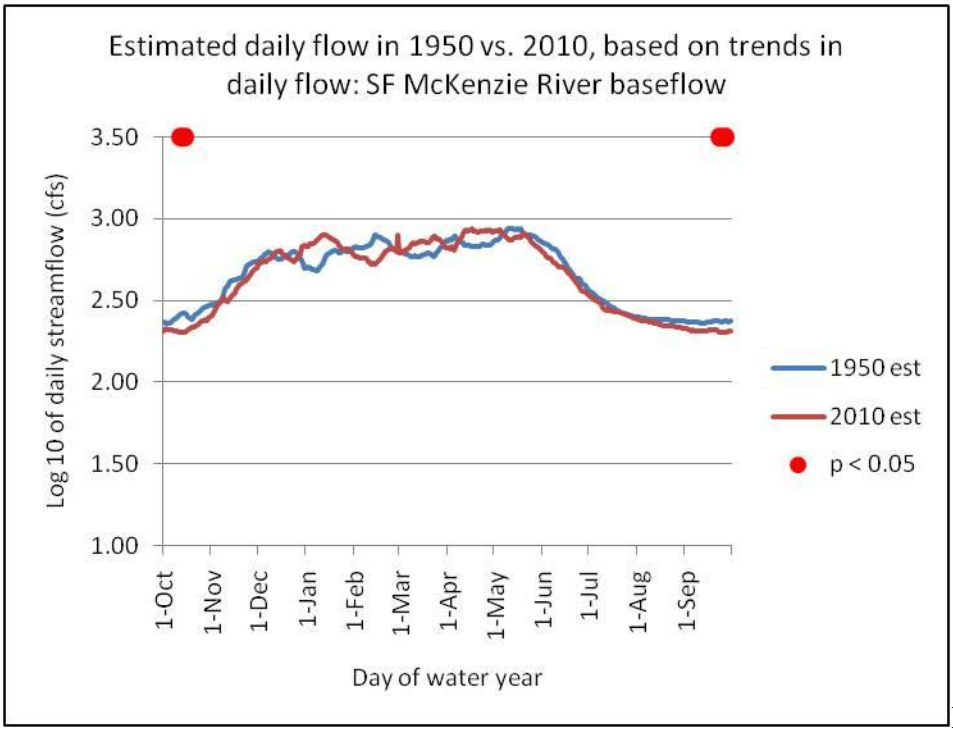

E.

Figure 2.5 cont.

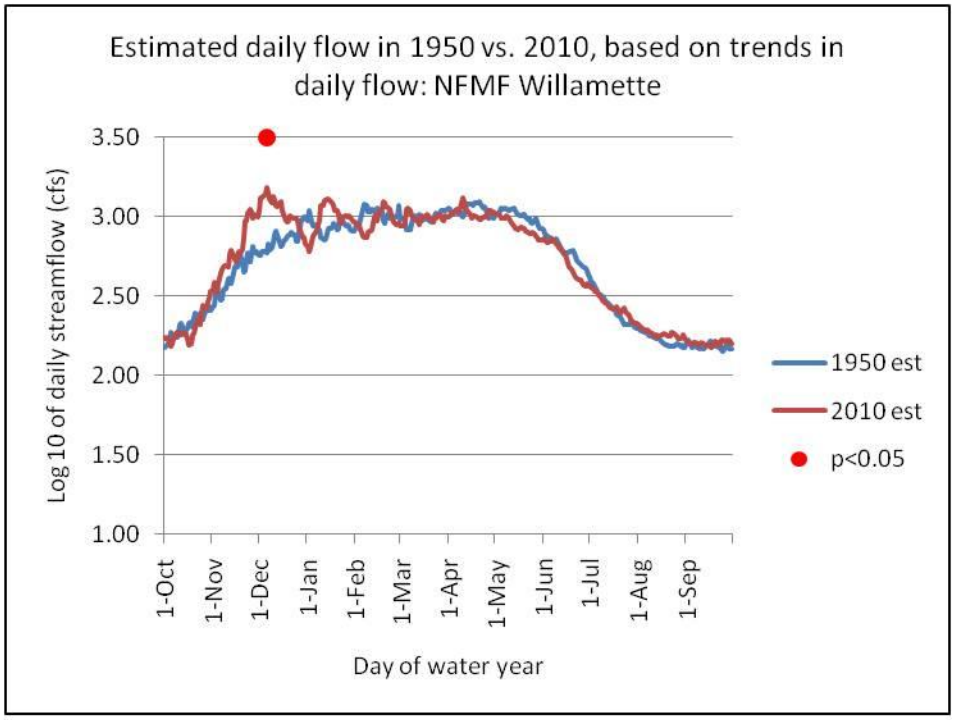

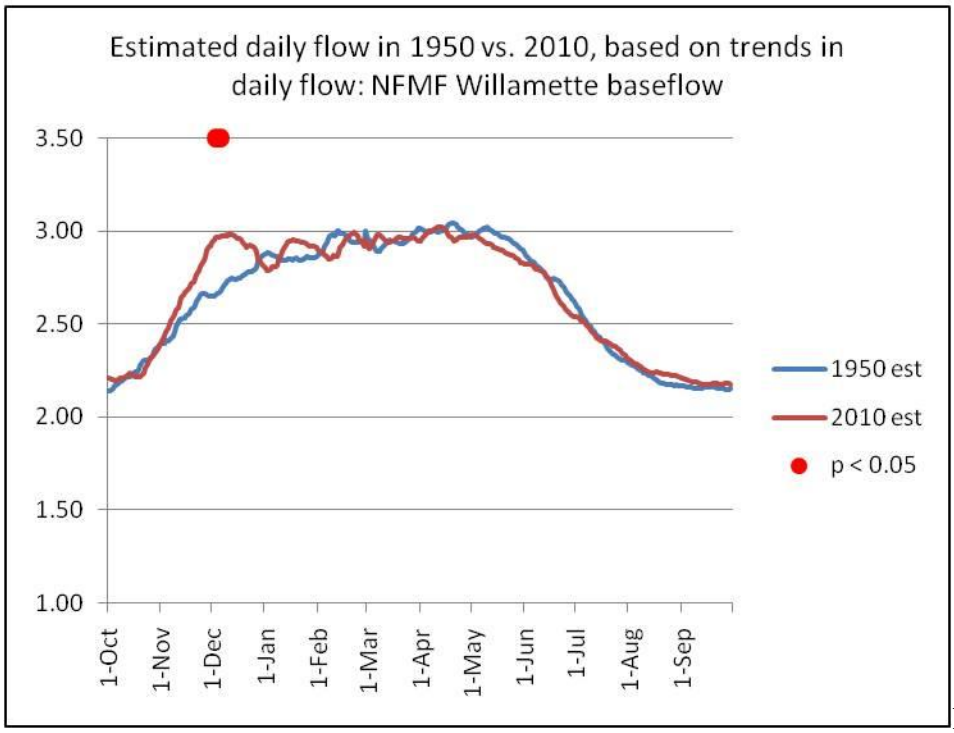

F.

Figure 2.5 cont.

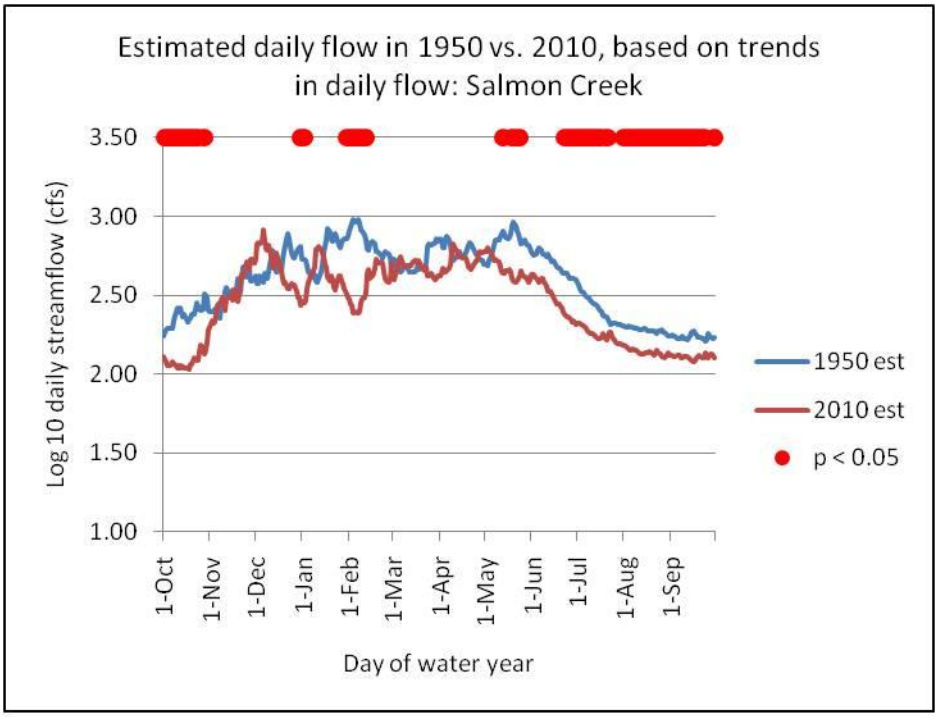

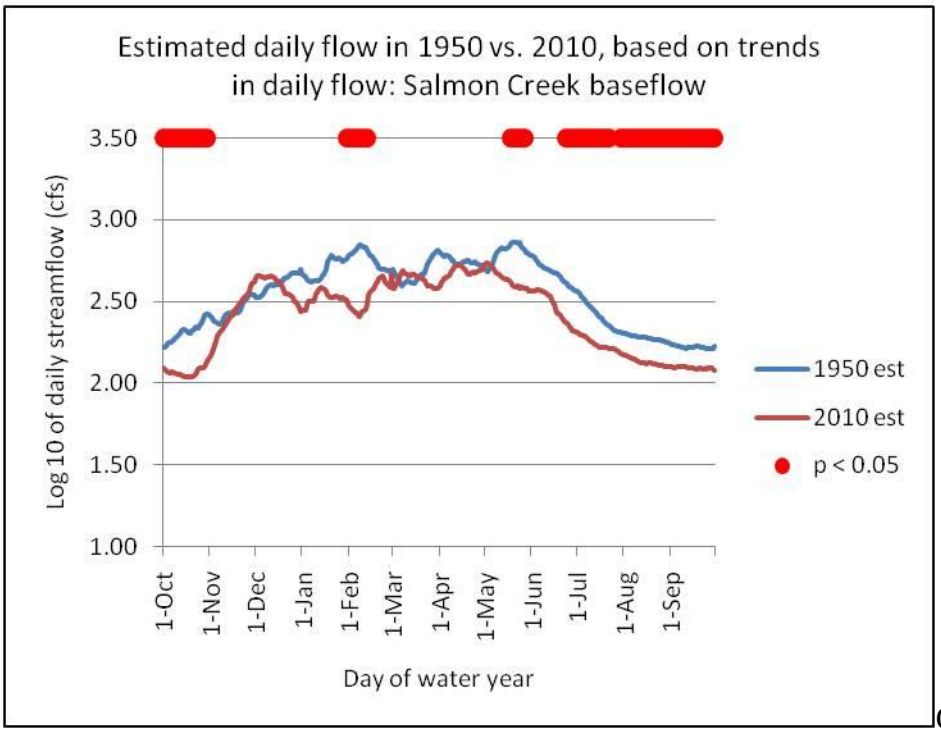

G.

Figure 2.5 cont.

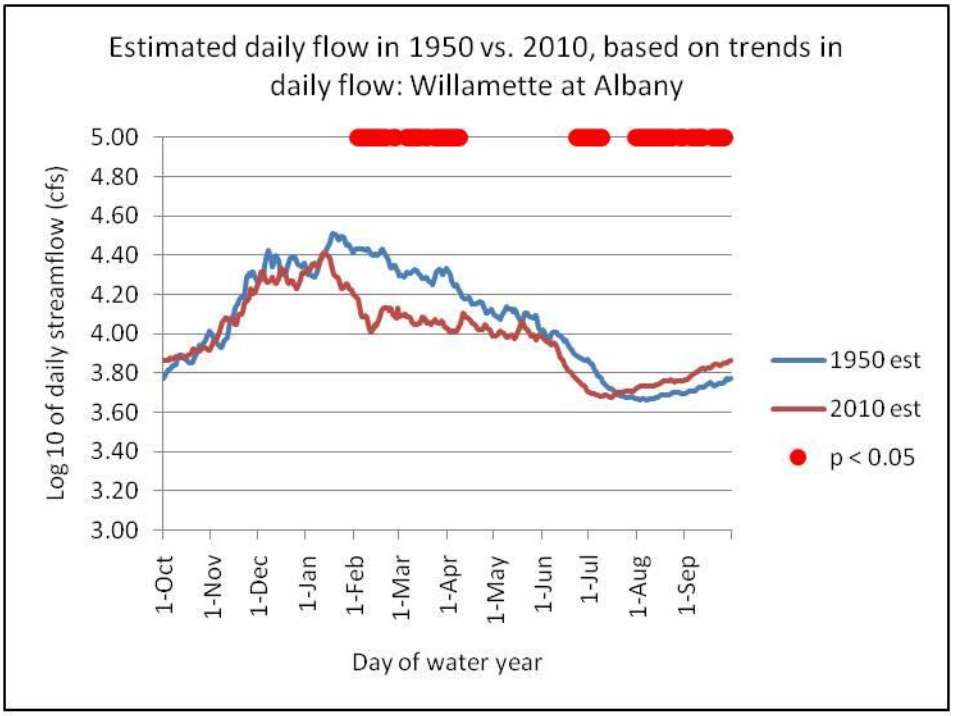

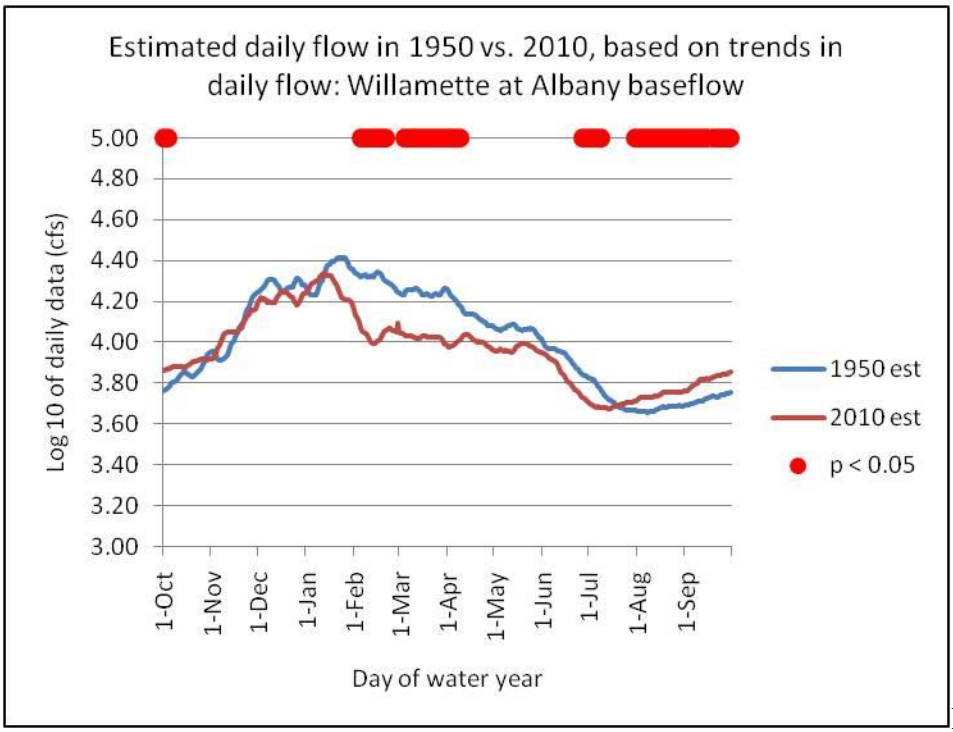

H.

Figure 2.5 cont.

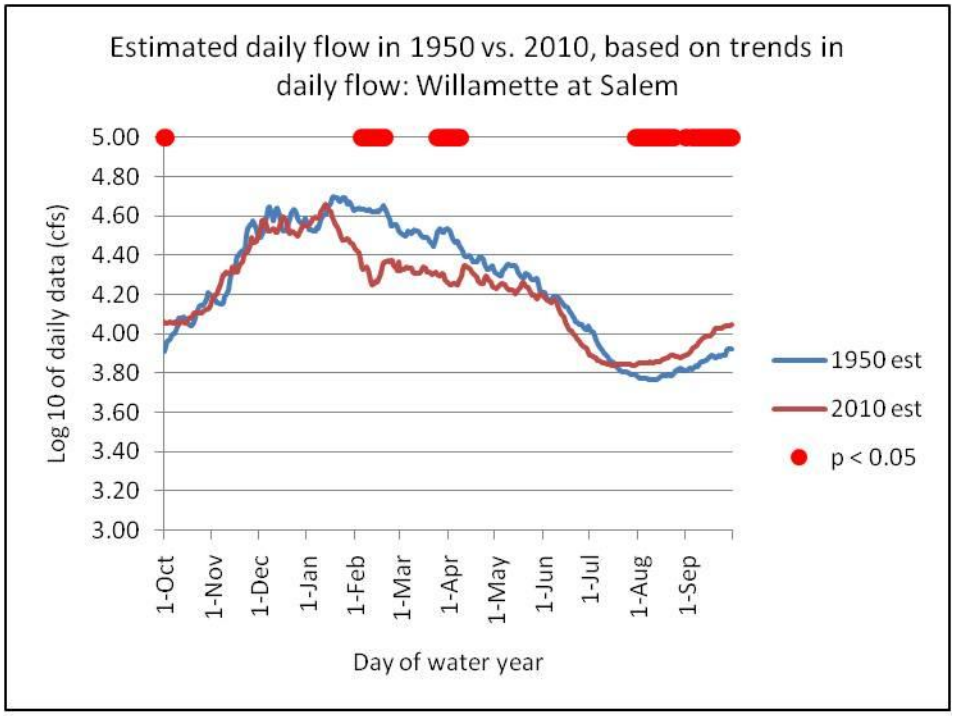

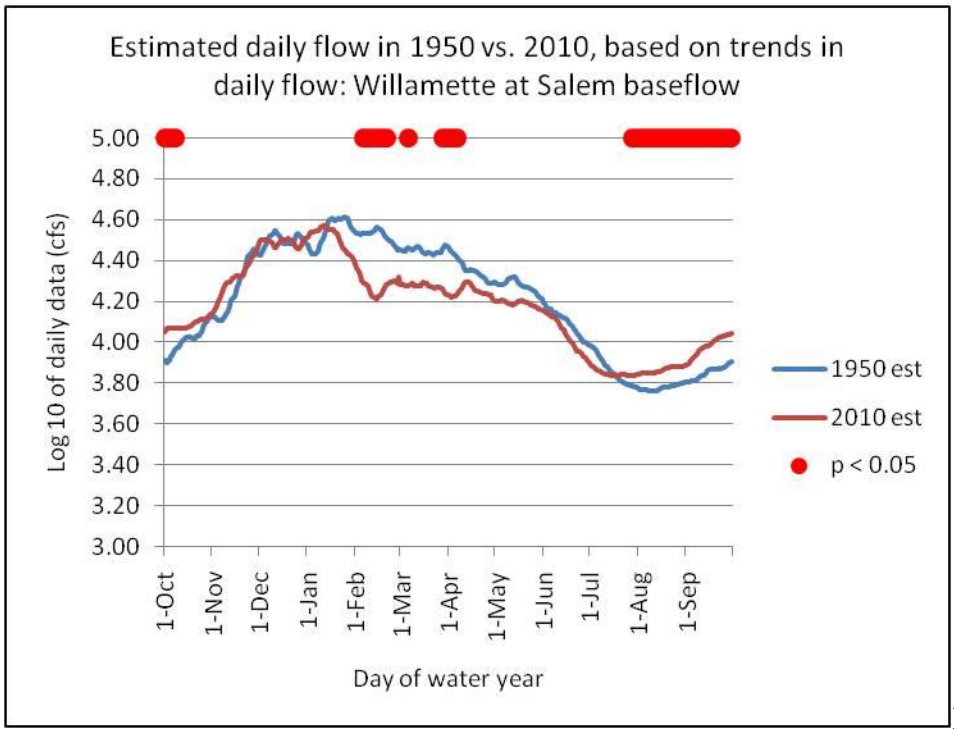

I.

Figure 2.5 cont.

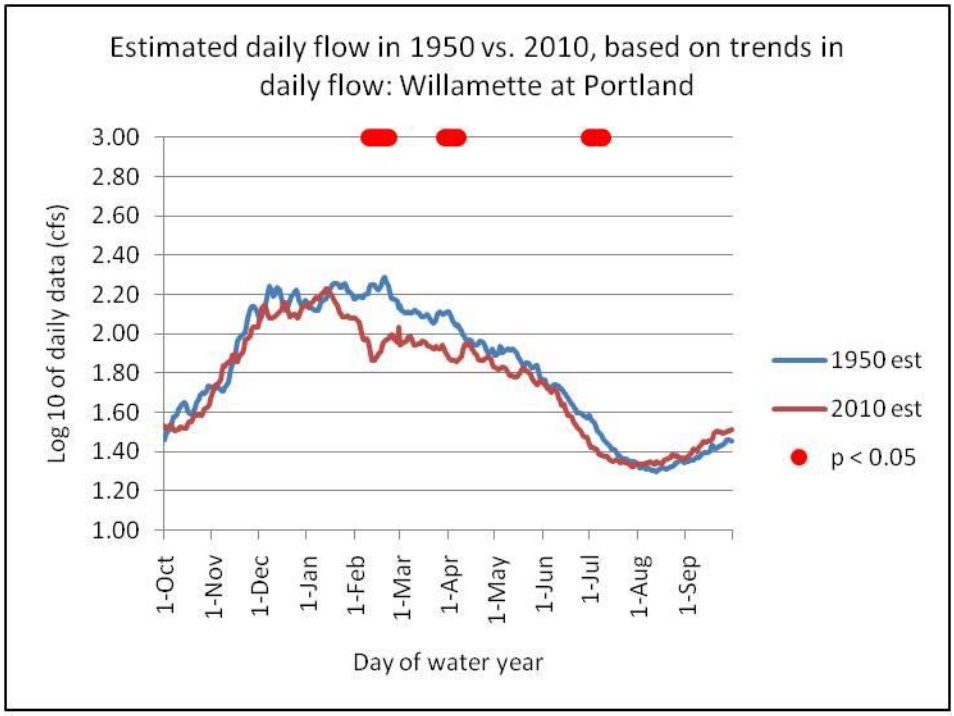

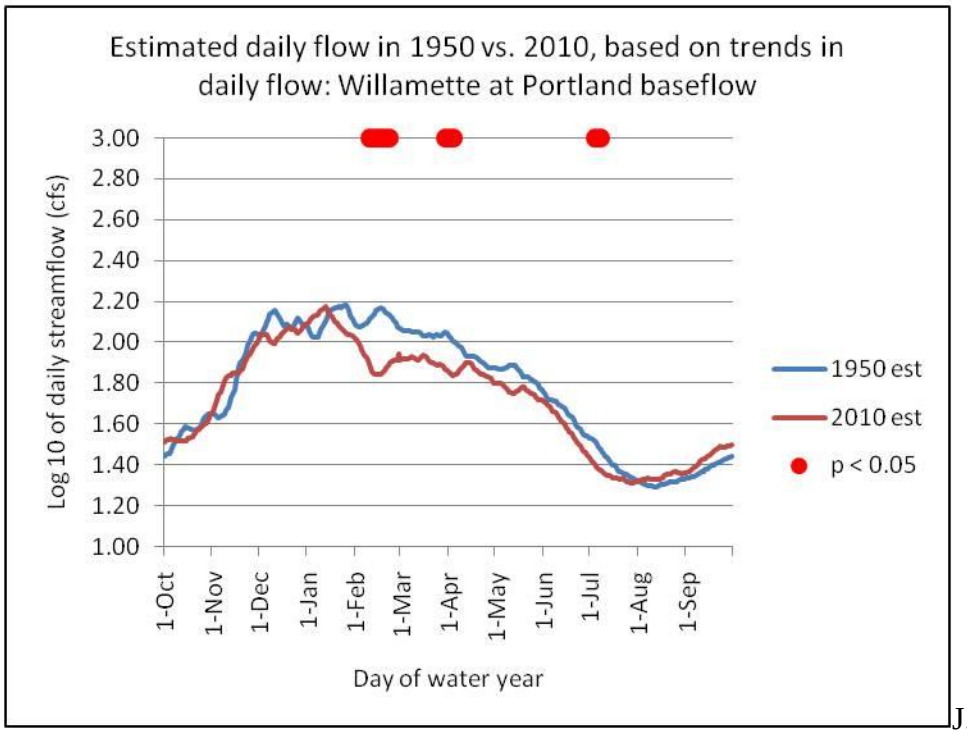

J.

Figure 2.5 cont.

baseflow. There was a slight decline in May and June, but there was no change in later summer flow. Salmon Creek (total discharge and baseflow) declined significantly from May through October, and in January. There were slight increases in December, but they were not significant. South Fork McKenzie River showed significant declines in September and October (total discharge and baseflow). Increases were observed in January and April, but they were only significant in total discharge streamflow.

Albany daily data showed significant declines in February through April, and in July. Significant increases occurred in August and September (total discharge and baseflow), and October (baseflow). Declines were also observed in May and June. Salem daily data showed significant decreases in February and April (total discharge and baseflow), and in March (baseflow). Significant increases were found in total discharge and baseflow in August through October. Significant decreases were observed in February, April, and July for Portland daily data (total discharge and baseflow), with declines also observed in March, May, and June. Increases occurred in August and September, but they were not significant.

2.5.4 Runoff Ratios

North Santiam annual total flow and base flow ratios both showed strong autocorrelation at 1 year. Salmon Creek showed slight correlation at a lag of 2 years for both total flow and baseflow annual ratios, and the residuals for both showed negative correlation at a lag of 6 years. South Fork McKenzie River baseflow annual

ratios showed correlation at a lag of 1 year. Albany annual ratios showed autocorrelation at a lag of 1 year, but residuals did not show any correlation. Salem annual total flow ratios showed slight correlation at a lag of 4 years, but the residuals did not show any correlation. Portland annual total flow ratios showed autocorrelation at a lag of 1 year, but the residuals did not show any correlation (Table 2.3a).

Spring baseflow ratios at Blue River showed slight correlation at a lag of 3 years, but the residuals did not show autocorrelation. Albany spring ratios showed autocorrelation at a lag of 1 year for both total flow and baseflow, but the residuals did not show autocorrelation. Salem spring ratios showed slight correlation at a lag of 1 year for spring data. Summer ratios for baseflow at Blue River showed slight correlation for a lag of 5 years, but the residuals did not show autocorrelation. Lookout Creek summer baseflow ratios showed correlation at a lag of 5 years, and the residuals also showed correlation at a lag of 5 years. South Fork McKenzie River showed a slight correlation for a lag of 5 years for summer baseflow ratios. Fall baseflow ratios showed negative correlation at a lag of 4 years at Blue River. South Fork McKenzie River showed a slight negative correlation at a lag of 5 years for fall baseflow ratios. There winter ratios were not autocorrelated (Table 2.3b-e).

Linear regression analysis found annual runoff ratios for both total flow and baseflow decreased at all basins except for Breitenbush River. Significant declines occurred in the three downstream gages at Albany, Portland, and Salem. Significant

declines were also observed for both total flow and baseflow for North Fork Middle Fork Willamette, Salmon Creek, Lookout Creek, and Blue River (Table 2.3a).

Mann-Kendall tests also showed declines at all sites except for Breitenbush River for the annual runoff ratio data. Albany, Salem, and Portland runoff ratios also declined. Significant declines were observed in the annual runoff ratios for total flow for North Fork Middle Fork Willamette, for baseflow at Blue River, and for both at Lookout Creek and Salmon Creek. Albany, Salem and Portland all declined significantly in total flow ratios, but baseflow ratios only declined significantly at Albany (Table 2.3a).

Linear regression analysis of seasonal data showed a declining trend in spring and summer runoff ratios in all basins. A significant decreasing trend in spring and summer runoff ratio was observed for both total flow and baseflow for North Fork Middle Fork Willamette, Salmon Creek, Lookout Creek, and Blue River. Runoff ratios declined significantly in the spring at Albany, Salem, and Portland. Summer ratios declined at Albany and Portland, but increased at Salem. Fall ratios declined at Lookout Creek, Blue River, Breitenbush River, North Fork Middle Fork Willamette, and Salmon Creek. Fall ratio declines were only significant for total flow at North Fork Middle Fork Willamette. North Santiam and total flow ratios for South Fork McKenzie River increased. Albany, Salem, and baseflow ratios at Portland also increased. Winter ratios declined at South Fork McKenzie River, Lookout Creek, and total flow ratios for North Fork Middle Fork Willamette. Significant trends were not

observed in any basin. Winter ratios all declined for Albany, Salem, and Portland. Albany showed significant declining trends in the winter for total flow and baseflow ratios, but Portland and Salem only showed significant declines in the winter for total flow runoff ratios (Table 2.3b-e).

Results from the Mann-Kendall test showed declines in runoff ratios at all sites in the spring and summer. For the spring season, significant declines were found in total flow and baseflow runoff ratios for Lookout Creek and Salmon Creek, and for baseflow in North Fork Middle Fork Willamette and Blue River. Albany, Salem, and Portland runoff ratios also declined significantly in the spring. Summer runoff ratios showed significant declines in North Fork Middle Fork Willamette and Salmon Creek, and for baseflow ratios at Lookout Creek. Albany, Salem, and Portland ratios also declined in the summer. Fall ratios declined at all sites except for the baseflow ratio at Breitenbush River. Significant declines were observed in fall runoff ratios of total flow and base for Lookout Creek, but only for total discharge at North Fork Middle Fork Willamette and Salmon Creek. Salem fall ratios increased for total flow and baseflow, but only for baseflow at Albany and Portland. Winter ratios increased at most sites, except for Lookout Creek, South Fork McKenzie, and total flow ratio for North Santiam River. Declines were occurred at Albany, Salem and Portland ratios. Significant declines were observed in the winter for total flow and baseflow ratios at Albany, but only for total flow at Salem and Portland (Table 2.3b-e).

2.6 Spatial Results

2.6.1 Stand age

In all basins the percent of young forest, age 0 to 40 years, increased from 1950 to 2002 (Table 2.4). The greatest percentage increases occurred in Lookout Creek (2700%), Salmon Creek (500%), Blue River (165%), and Breitenbush (148%). The smallest increases occurred in North Santiam River (89%), North Fork Middle Fork Willamette (65%), and South Fork McKenzie River (23%).

As of 2002, the basins with the highest percentage of area in young forest were Salmon River (29%), Blue River (23%), and Breitenbush River (23%) (Table 2.4). South Fork McKenzie River (8%) had the lowest portion of young forest. Lookout Creek, North Fork Middle Fork Willamette, and North Santiam were in the middle with similar results at 17%, 18%, and 18%, respectively.

Salmon River also had the greatest absolute area in young forest, with over 8,500 ha (Table 2.4). North Santiam River had more than 6,700 ha in young forest. North Fork Middle Fork Willamette was third with more than 5,400 ha. Lookout Creek had the lowest absolute area, with more than 1,150 ha.

In the 10 meter buffer around all stream channels, the percent of 0 to 40 year old forest also increased, but the percent increases were slightly different than in the entire basin, although the basins were in almost the order as the entire basin (Table

Table 2.4 Table of forest age changes from 1950 to 2002.

	% Forested	% Forest Cover, Old Growth (>200) 1950	% Forest Cover, Old Growth (>200) 2002	% Forest Cover, Young (<40 yrs) Growth 1950	% Forest Cover, Young (<40 yrs) Growth 2002	% Increase in Young Forest 1950-2002	Rate of Change (ha/year)	Total Area in Young Forest 2002 (ha)
Blue River	92	30	32	8	22	165%	78	3,893
Lookout Creek	96	55	59	0.6	16	2700%	23	1,158
Breitenbush River	90	33	35	9	23	148%	97	4,860
North Santiam River	90	17	19	10	18	89%	135	6,768
South Fork McKenzie River	74	16	25	7	8	23%	36	1,794
North Fork Middle Fork Willamette	90	22	37	11	18	65%	109	5,438
Salmon Creek	94	24	36	5	29	500%	171	8,539

Table 2.5 Table showing forest age changes from 1950-2002 in a 10 meter buffer around all streams within each basin.

	% Forest Cover, Young (<40 yrs) Growth 1950	% Forest Cover, Young (<40 yrs) Growth 2002	% Increase in Young Forest 1950-2002	Rate of Change (ha/year)	Total Area in Young Forest 2002 (ha)
Blue River	9	27	191%	43	269
Lookout Creek	0.34	17	4860%	11	48
Breitenbush River	8	22	165%	60	440
North Santiam River	9	16	75%	57	610
South Fork McKenzie River	7	10	51%	43	361
North Fork Middle Fork Willamette	11	23	120%	76	608
Salmon Creek	2	32	1890%	78	377

2.5). The greatest increases occurred in Lookout Creek (4900%), Salmon Creek (1500%), Blue River (200%), and Breitenbush (175%). The smallest increases occurred in North Fork Middle Fork Willamette (109%), North Santiam (78%), and South Fork McKenzie River (43%).

Area (percent) of the basin as a whole covered by <40-yr-old forest is very strongly correlated with area within 10 m of streams covered by <40-yr-old forest (R^2 > 0.92 for all basins except for North Santiam, which has a R^2 of 0.7).

2.6.2 Geology

All basins had a higher percentage of Western Cascades geology then High Cascades geology except for North Santiam River (Table 2.5).

Blue River was almost exclusively Western Cascades geology (>99%), with Lookout Creek the next highest percentage of Western Cascades geology (84%). North Fork Middle Fork Willamette, South Fork McKenzie River, Breitenbush River, and Salmon Creek all had similar percentages of Western and High Cascades geology. North Santiam River had a much greater proportion of High Cascades geology (51%) than Western Cascades geology (27%).

Table 2.6 Table showing the area of High Cascades geology versus Western Cascades geology in each basin.

	% Western Cascades Geology	% High Cascades Geology	Geologic Substrate
Blue River	>99	0	~99% Tertiary basalts and andesites
Lookout Creek	84	0	84% Tertiary basalts and andesites; 17% landslide deposits
Breitenbush River	58	31	58% Tertiary basalts and andesites; 31% Quaternary basalts and andesites; 17% Tertiary sedimentary rocks
North Santiam River	27	51	51% Quaternary basalts and andesites; 27% Tertiary basalts and andesites; 22% Alluvium and landslide deposits
South Fork McKenzie River	55	14	55% Tertiary basalts and andesites; 31% Glacial and landslide deposits; 14% Quaternary basalts and andesites
North Fork Middle Fork Willamette	57	26	57% Tertiary basalts and andesites; 26% Quaternary basalts and andesites; 23% Tertiary sedimentary rocks
Salmon Creek	60	21	60% Tertiary basalts and andesites; 21% Quaternary basalts and andesites; 18% Glacial and landslide deposits

2.6.3 Elevation

A hypsometric curve was created for each of the study basins (Fig 2.4). The elevation data was used to find the percentage of each basin that is above the transient snow zone, where a seasonal snowpack develops in the winter. The cumulative percentage of each basin that is above 800 meters was calculated (Table 2.7). Blue River and Lookout Creek had the lowest percentage of area greater than 800 meters at 75% and 71%, respectively. South Fork McKenzie River and North Santiam River had the highest percentage, at 93% and 89%, respectively. Breitenbush River, North Fork Middle Fork Willamette and Salmon Creek all had values around 80%.

2.7 Discussion

2.7.1 Summary of trends above dams

Annual runoff ratios ranged from 0.72 to 0.90, indicating that about 20% of precipitation is lost to evapotranspiration. Annual runoff ratios declined at all seven basins from 1950-2009. However, annual runoff ratios declined significantly only at Lookout Creek and North Fork Middle Fork Willamette (total and baseflow ratios), and Blue River (baseflow ratios). Annual discharge (both total flow and baseflow) declined at all sites except South Fork McKenzie River (total flow), but none of these trends was significant.

Runoff ratios in spring ranged from 0.99 to 1.24, indicating that spring discharge experiences a pulse from snowmelt, whereas summer runoff ratios ranged

Table 2.7 Elevation range and percentage of each basin greater than 800 meters in elevation.

	Elevation Range (m)	% Area with Elevation >800 m
Blue River	412-1,625	75
Lookout Creek	412-1,626	71
Breitenbush River	477-2,136	81
North Santiam River	484-3,197	89
South Fork McKenzie River	543-2,075	93
North Fork Middle Fork Willamette	312-2,221	82
Salmon Creek	349-2,175	83

from 0.91 to 2.25, indicating that water is being released from groundwater storage. Spring and summer runoff ratios and discharge declined at all sites. Spring runoff ratios declined significantly at Lookout Creek (total flow and baseflow ratios), Blue River and Salmon Creek (baseflow ratio). Spring discharge declined significantly at Lookout Creek (baseflow only). Summer runoff ratios declined significantly at North Fork Middle Fork Willamette and Salmon Creek (total flow and baseflow). Total summer discharge declined significantly only at North Santiam River, but summer baseflow declined significantly at Blue River, Breitenbush River, Lookout Creek, and North Santiam River.

Fall runoff ratios ranged from 0.36 to 0.52, indicating that soil water storage reservoirs are refilling after depletion during dry summers. Winter runoff ratios ranged from 0.60 to 0.87, indicating build-up of snowpack during this period of the year. Fall runoff ratios declined at most sites. Fall runoff ratios declined significantly at Lookout Creek (total flow and baseflow) and at North Fork Middle Fork Willamette and Salmon Creek (total flow ratios). Fall discharge declined at all sites, but significant declines occurred only at Salmon Creek (baseflow). Winter runoff ratios increased at most sites, but there are no significant trends. In contrast, winter discharge declined at all sites, and declined significantly at North Fork Middle Fork Willamette and Salmon Creek.

Daily discharge declined in the spring, summer, and fall at five sites: Blue River (1935-2003), Breitenbush River (1932-2009), Lookout Creek (1949-2008),

North Fork Middle Fork Willamette (1936-1994), and Salmon Creek (1949-1993). Daily baseflow declined in spring and summer at five sites: Blue River (1935-2003), Breitenbush River (1932-2009), Lookout Creek (1949-2008), North Santiam (1907-2009), and Salmon Creek (1949-1993). Fall daily baseflow declined at three sites: Blue River (1935-2003), Lookout Creek (1949-2008), and Salmon Creek (1949-1993). Winter daily discharge and baseflow increased at five sites: Blue River (1935-2003), Breitenbush River (1932-2009), North Fork Middle Fork Willamette (1936-1994), North Santiam River (1907-2009), and South Fork McKenzie River (1957-2009).

The results of this analysis were consistent with regional studies of streamflow trends. Research has shown declining trends in annual discharge and summer and fall discharge from 1948-1988 in the Pacific Northwest (Lettenmair, Wood, and Wallis 1994). Zhang et al. (2008) also found declines in the annual streamflow and in summer and fall months in the Pacific Northwest at Canadian sites. However, Zhang et al. (2008) did find increases in spring discharge. Significant declines in annual discharge were found in the Columbia basin from 1948-2004 (Dai et al. 2009). Decreases were also observed in median and minimum daily flow in the Pacific Northwest across varying time periods in the 20th century (Lins and Slack 1999). Luce and Holden (2009) found a decline in the 25th percentile of annual flow throughout the Pacific Northwest, as well as declines in the 50th percentile and mean annual flow in the Cascade region. Significant cumulative discharge from 1951 to 2000 also showed declines in the Pacific Northwest (Milliman et al. 2008).

Although the trends from the study basins generally follow broad regional trends, trends among the basins varied. The possible reasons for this variation will be discussed in subsequent sections.

2.7.2 Effects of dams on trends in discharge and runoff ratios

Annual runoff ratios and annual discharge declined at Albany, Salem and Portland from 1950 to 2009. Annual discharge and annual runoff ratio (total flow) declined significantly at all three sites, but baseflow ratios and baseflow discharge declined significantly only at Albany.

Spring runoff ratios and spring discharge declined at Albany, Salem, and Portland. Spring runoff ratios (total flow and baseflow) declined significantly at all three sites. Spring discharge declined significantly at Albany and Salem, and spring baseflow discharge declined significantly at Albany. Summer runoff ratios and summer discharge declined at all three sites, but the trends were not significant. Fall runoff ratios increased at Albany and Salem but decreased at Portland. Fall discharge declined at all three sites, but fall baseflow increased at Albany and Salem. None of the trends in fall ratios or discharge were significant. Winter runoff ratios and winter discharge declined at all three sites. Winter runoff ratio and winter discharge declined significantly at all sites (total flow), but winter baseflow ratios and winter baseflow discharge declined significantly only at Albany.

Daily discharge (total and baseflow) increased in the summer and fall and declined in the winter at Albany (1893-2009), Salem (1909-2009), and Portland (1948-2009).

These trends are consistent with well-known and intended effects of flood control dams on downstream flow regimes. Dams reduce variability of flow by increasing low flow, decreasing high flow or floods, and limiting interannual variablilty (Poff et al. 2007). Poff et al. (2007) found the Pacific Northwest to have a high degree of "hydrologic homogenization."

The Flood Control Acts of 1938, 1950, and 1960 authorized 13 United States Army Corp of Engineers (USACE) large dam projects to minimize flooding hazards in the Willamette basin (USACE 2010a). To control floods, reservoirs above flood control dams on the McKenzie River (Blue River and Cougar), North Santiam River (Detroit and Big Cliff), and Middle Fork Willamette (Lookout Point, Hills Creek, Dexter) are emptied at the end of the summer (September), and filled during the winter high flow period (November-March). Flood control dam operations would be expected to contribute to a reduction in winter and early spring flow at gages downstream of dams. From April to November, the Willamette dams release water from reservoir storage for hydroelectric power generation and irrigation purposes (USACE 2010b). USACE must also release water to control temperature values for federally threatened and endangered species, such as spring Chinook salmon, Oregon

chub, and bull trout (USACE 2010a). Releases of water stored in flood control dams would be expected to increase summer and fall flow at downstream gages.

Statistically significant declines in winter discharge at gages downstream of dams (Albany, Salem, and Portland) are consistent with dam operations for flood control to decrease winter and spring flooding on the Willamette. The increases in daily discharge in summer and fall observed in this study are also consistent with expected effects of later summer releases of water stored in reservoirs to supplement municipal and agricultural water use and maintain stream temperature. The observed decreases in spring discharge, baseflow, and runoff ratios may also be the result of dam operations to reduce spring flooding from snowmelt, or they may reflect the declines in spring discharge, baseflow, and runoff ratios at three of the seven basins upstream of dams during the same period.

2.7.3 Climate effects on trends in discharge and runoff ratios

Results from this analysis confirm other studies showing increases in minimum temperature, especially spring temperature at the HJ Andrews Forest. Greenland (1994) found a trend of increasing annual mean temperature from 1973-1991. Moore (2010) found increases of 1.4°C and 1.7°C in daily minimum temperature in spring (March-May) over 55-year (Watershed 2) and 44-year (Watershed 8) periods of record.

Regional studies also have shown that temperature has been increasing in the Pacific Northwest since at least the middle 20th century (Cayan et al. 2001; Mote 2003b; Hamlet et al. 2005). Mote (2003b) found that average annual temperature in the Pacific Northwest had increased by 0.9°C from 1930 to 1995, with the largest increases occurring in the winter months.

Large scale periodic climatic patterns, such as ENSO (El Niño/El Niña-Sothern Oscillation) or PDO (Pacific Decadal Oscillation), may explain some of the trends in air temperature in the Pacific Northwest. Although these indices influence temperature and precipitation in the Pacific Northwest, researchers agree that they cannot explain all the warming observed for a variety of time periods based both on actual data and model outputs (Barnett et al. 2008; Hamlet et al. 2005; McCabe and Wolock 2009; Mote 2003a; Stewart et al. 2005).

This analysis does not show any significant trends in precipitation from the PRISM dataset or from CS2MET data, although trends are negative except for spring precipitation. Moore (2010) also did not find changes in precipitation from CS2MET from 1958 to 2007. Mote (2003b) found an increase in spring precipitation in the maritime Pacific Northwest from 1930 to 1995. Other studies have not shown clear trends in precipitation in the Pacific Northwest, and when they occur, precipitation trends are spatially variable (Mote et al. 2005, Stewart et al 2005).

Some of the trends observed in this study could be attributed to changes in rain:snow fractions in precipitation, because the study basins have large areas of

transient and seasonal snowpack. In many areas, increased cool season temperature are believed to have resulted in more precipitation falling as rain than snow, particularly in areas of transient snow pack, where the temperature remain close to the freezing point (Karl, Melillo, and Peterson 2009; Knowles et al. 2006; Mote et al. 2005; Regonda et al. 2005; Stewart et al. 2005). Winter warming trends in areas with snowpack would be expected to increase streamflow in the late fall, winter, and early spring, but decrease streamflow in late spring, summer, and fall (Karl, Melillo, and Peterson 2009). Findings from this study are consistent with this prediction, in that we found evidence of declining streamflow in spring and summer above dams. We did not find evidence of increasing trends in fall and winter streamflow above dams; however, daily analysis found early winter (December, January) increases at some of the basins, which may be an indication that more precipitation is falling as rain as opposed to snow.

On the other hand, some of the trends in this study may be explained by changes in water use by vegetation in response to climate warming. Warming temperature in the spring is expected to accelerate vegetation phenology. Cayan et al. (2001) showed that lilacs and honeysuckles, which are responsive to changes in temperature, are now blooming 5 to 10 days earlier than in the 1970s. Earlier leafout and associated earlier onset of evapotranspiration (ET) may reduce streamflow, particularly in the summer growing season when water quantities are lowest (Hamlet and Lettenmaier 1999). However, there is limited research on the effect of climate

change on ET. Using the Regional Hydro-Ecological Simulation System (RHESSys) model applied to the Upper Merced basin on the west side of the Sierra Nevada Mountains, Christensen et al. (2008) found that, under a warming environment, ET rates are most sensitive to precipitation at lower elevations, but more sensitive to changes in temperature at higher elevations. Increased temperature leads to higher ET, but actual ET depends on other factors, including season and soil conditions (Hamlet and Lettenmaier 1999). Findings from this study suggest that the effects of climate warming on ET may depend on elevation, particularly on the amount of basin area in transient and seasonal snowpack zones, as well as on the type and age of vegetation. These factors are discussed below.

2.7.4 Effects of snowpack on trends in discharge and runoff ratios

In the Cascade Mountains, elevation controls whether precipitation falls mostly as rain, mostly as snow, or some combination. Long-term snowpack observations at the Andrews Forest indicate that seasonal snowpacks form above 800 m elevation, whereas transient snowpacks and rain dominate below 800 m (Jones and Perkins 2010). The ratio of snow to rain, which is determined by the proportion of the basin above 800 m, influences the shape of the annual hydrograph (Fig 2.6). Of the seven study basins above dams, Lookout Creek and Blue River have the greatest proportion of area in lower, rain- and transient-snow-dominated elevations, the highest streamflow in November and December, and the most rapid recession in April and May. They also show the greatest range of flow values (Fig 2.7). In contrast, North

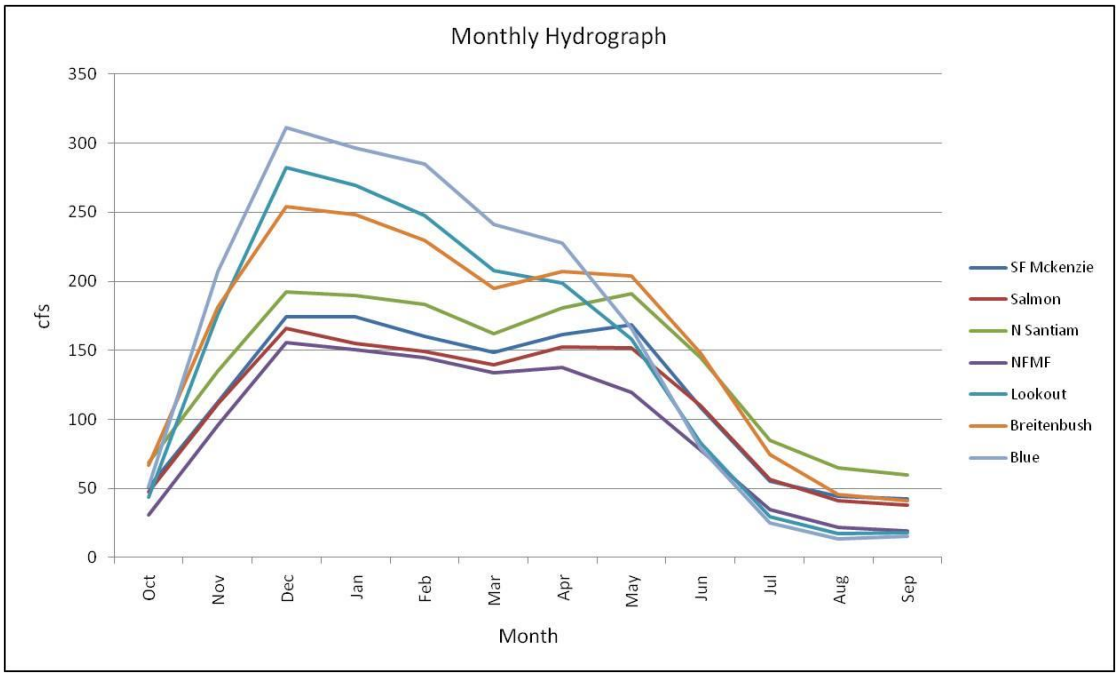

Figure 2.6 Hydrograph showing monthly average flow for seven basins upstream of dams.

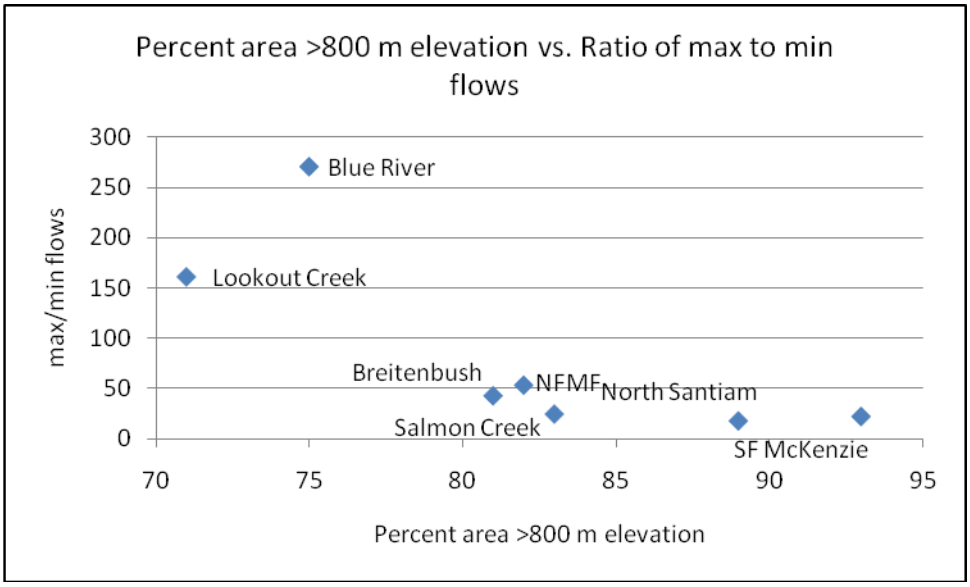

Figure 2.7 Area of each basin greater than 800 meter in elevation vs the ratio of average maximum to minum values for each basin.

Santiam and South Fork McKenzie River have a much higher proportion of basin area above 800 m, high flow in November and December, and flow increase through March and April. In these basins large areas of seasonal snowpack contribute to higher summer and fall flow compared to the basins with a small proportion of area in the seasonal snow zone.

Increases in temperature are expected to reduce winter snow pack in the western US, contributing to earlier spring snowmelt and reduced summer flow. Many mountainous areas of the western US have experienced a decrease in the snow water equivalent (SWE), which is a measure of both snow pack depth and the quantity of water it contains, and this decline is particularly pronounced in the Cascade Mountains (Mote et al. 2003; Mote 2003a). SWE is an important factor in summer flow conditions, when little precipitation is occurring (Mote et al. 2005). Many studies have also shown that spring snowmelt runoff is occurring earlier in the spring (Cayan et al. 2001; Hamlet et al. 2005; Regonda et al. 2005; Stewart et al. 2005; Barnett et al. 2008). Regonda et al. (2005) found that flow were much higher earlier in the spring (March and April) due to earlier melt, but this led to a decrease in flow later in the spring (May and June). The center of mass of annual stream flow, the date at which time half of the annual flow has already passed, has also been found to occur earlier (Stewart et al. 2005).

April 1st SWE anomalies from SNOTEL and meteorological stations in the Cascade region near the study basins show a declining trend from 1928 to 2007, but

there is considerable variability (Fig 2.8). Snowpacks were low from 1977 to 1982, and again beginning in 2005, which were among the lowest-precipitation years since the early 1950s, contributing to downward trends in regression analysis of snowpacks.

Elevations with a transient snowpack that experience winter average temperature close to the freezing point are more susceptible to temperature increases than those with winter average temperature well below freezing (Knowles et al. 2006; Mote et al. 2005; Regonda et al. 2005; Stewart et al. 2005; Nolin and Daly 2006). If so, basins with a lower proportion of area above 800 meters elevation would be expected to experience greater changes to the hydrograph, with increases in the winter and declines in the spring runoff period, compared to basins with high proportions of basin area above 800 meters. This analysis does show significant discharge declines in basins at the lowest elevations, but these basins do not show significant increases in winter discharge. Spring declines could be occurring at lower elevations due to increases in ET with warmer temperature and an increased growing season. Daily analysis shows significant increases in the early winter (December, January) but this is occurring in basins with greater areas of high elevations. This may indicate that some early storms are occurring as rainfall instead of snowfall. These trends do not influence the seasonal data, however.

2.7.5 Geologic effects on trends in discharge and runoff ratios

Cascade Mountains geology also affects the annual hydrograph. Quaternary High Cascades geology has relatively shallow slopes, and the young volcanics are

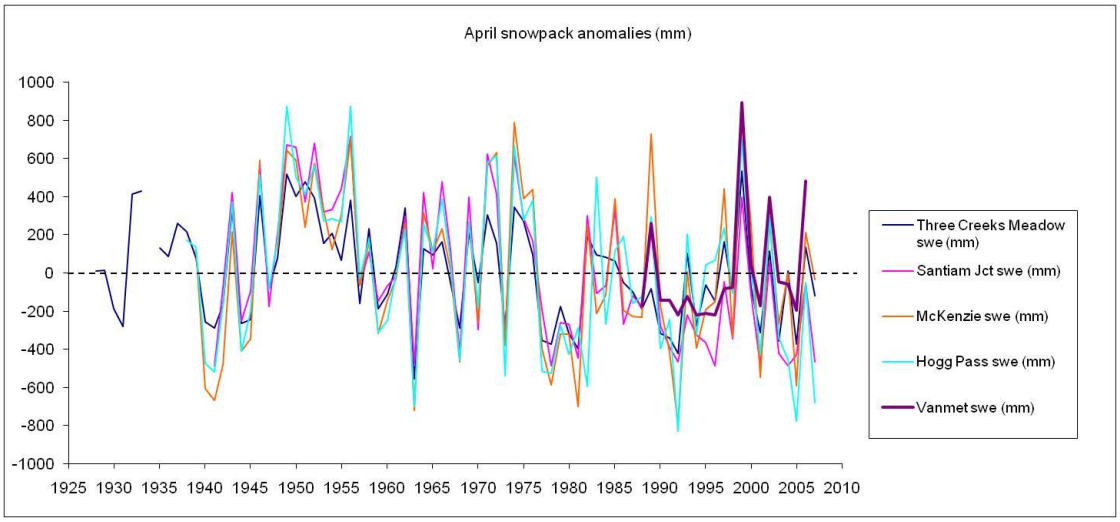

Figure 2.8 April snowpack anomalies form SNOTEL stations in the western Cascades region

much more porous, resulting in high groundwater storage and many springs (Tague and Grant 2004; Manga 1997). The Tertiary Western Cascades, however, have very steep, highly dissected slopes and limited groundwater storage (Tague and Grant 2004). Studies from small basins have shown that basins in predominantly High Cascades geology have a moderated hydrograph, as opposed to basins in predominantly Western Cascades geology are much flashier, with higher peaks and lower base flow (Jefferson et al 2008, Tague and Grant 2004) (Fig 2.6,2.9). High Cascades geology has substantial groundwater storage potential, and is characterized by natural springs. Jefferson et al. (2008) found that while annual flows are comparable between Smith River, a Western Cascades dominated basin, and the McKenzie River at Clear Lake, a High Cascades dominated basin, the September flows on the McKenzie were six times higher than the flow at Smith River. Tague and Grant (2004) found a strong correlation between the flow regime and geology, with the timing and magnitude of flow being linearly related the percentage of High Cascades geology in a basin.

In this study, Lookout Creek and Blue River, which are overwhelmingly in the Western Cascades geology region, show the highest and lowest monthly flow. North Santiam River is the only basin that has a greater percentage of High Cascades geology than Western Cascades. The other basins, despite being dominated by Western Cascades geology, have substantial portions of High Cascades geology within their boundaries (Table 2.6).

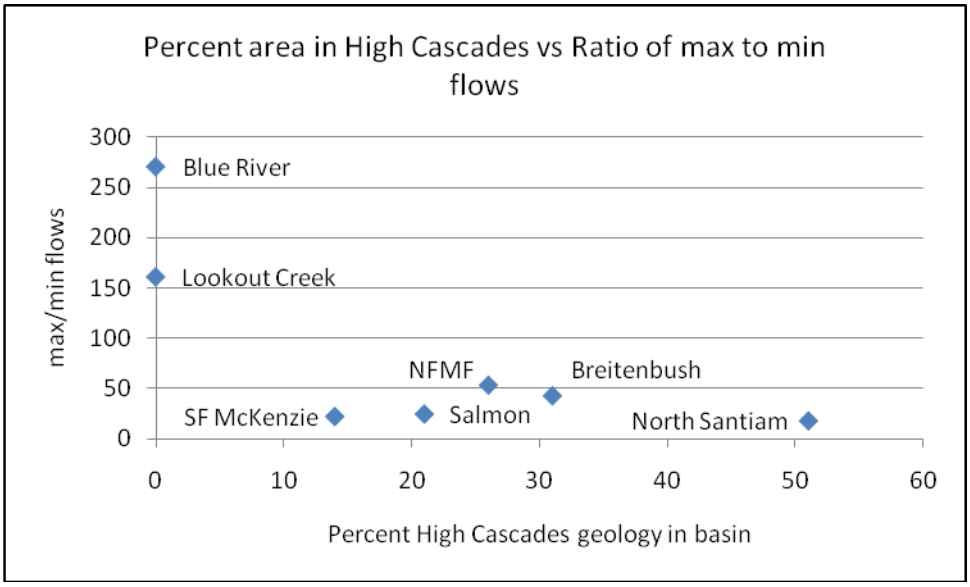

Figure 2.9 Percent of each basin with High Cascades geology versus the ratio of average maximum to minimum flow. Basins with almost no High Cascades geology have a much greater change in maximum and minimum values than basins with any percentage of High Cascades geology.

Running the RHESSys (Regional hydro-ecologic simulation system) model using 1.5° and 2.8° increases to climate data from 1960-1999 predicts that summer streamflow will decrease more in basins dominated by High Cascades geology than in those dominated by Western Cascades geology (Tague and Grant 2009, Tague et al. 2008). These temperature increases are two to three times greater than the increase (0.9°) that was found in annual temperature from 1930 to 1995 (Mote 2003b). August streamflow in High Cascade regions will show the greatest absolute declines because peak recharge will occur earlier in the winter as rain, and although there will be delay in discharge due to groundwater storage, it will occur much earlier in the spring, allowing for a longer recession period (Tague et al. 2008).

Research on historical records has shown a significant decline in summer streamflow in basins dominated by High Cascades geology, but not in basins dominated by Western Cascades geology (Jefferson et al. 2008). Summer discharge did decline significantly at North Santiam River, which is dominated by High Cascades geology. However, Lookout Creek and Blue River baseflow discharge, which have virtually no High Cascades geology, also showed significant declines. These basins had the greatest percent of area less than 800 m in elevation, which in this study has found to correspond to increases in ET and declines in spring and summer flow. These basins also have shallow groundwater paths due to the Western Cascades geology. The rooting zone of vegetation is within the groundwater flowpaths (Fig. 2.10), making ET and changes in ET a larger influence in discharge

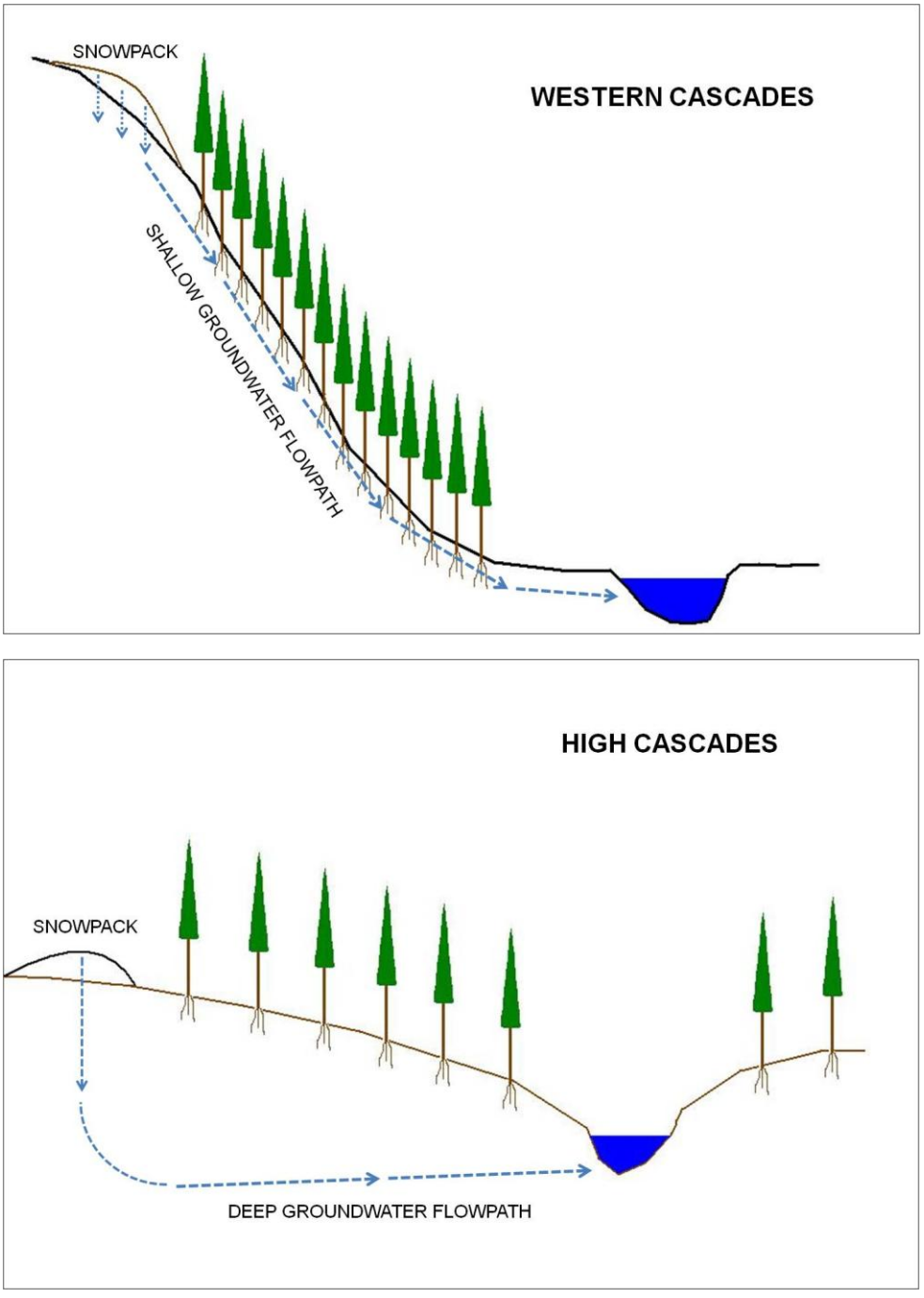

Figure 2.10 Conceptual diagram between the groundwater flowpaths in the Western Cascades versus the High Cascades. In Western Cascades, shallow groundwater flowpaths are within the rooting zone of plants, and ET is a greater factor in discharge and runoff ratios.

and runoff ratios than in basins with more High Cascades geology and deeper flowpaths. Other influences of vegetation on discharge and runoff ratios are discussed in the next section.

2.7.6 Forest harvest effects on trends in discharge and runoff ratios

Vegetation change and succession may also influence trends in discharge and runoff ratios. Many studies in small basins have shown that streamflow increases initially after forest removal (Rothacher 1970; Harr and McCorsion 1979; Harr et al. 1982; Wright et al 1990; Hicks et al. 1991; Jones and Grant 1996; Hornbeck et al. 1997; Thomas and Megahan 1998; Jones 2000). Research from large basins has been conflicting, but some studies have shown increases in peak flow following harvest (Ruprecht and Schofield 1989; Jones and Grant 1996; Thomas and Megahan 1998; Hubbart et al 2007; Lin and Wei 2008). Studies have also shown that during forest regrowth after harvest, baseflow actually declined below preharvest levels (Trimble et al. 1987; Smith and Scott 1992; Hornbeck et al. 1997; Scott and Lesch 1997; Jones and Post 2004). Research in the HJ Andrews (Lookout Creek) found summer low flow deficits 4 to 18 years after clearcutting: summer streamflow in the clearcut watershed (WS 1) was 25% lower than in the control basin (WS 2) (Hicks et al. 1991). Perry (2007) found that streamflow deficits were greatest 25 to 40 years after logging in basins in small paired basins in the HJ Andrews and in the drier South Umpqua Experimental Forest, Oregon.

Summer low flow deficits were attributed to the rapid growth of young vegetation in these studies (Hicks et al. 1991; Hornbeck et al. 1997; Jones and Post 2004; Perry 2007). A study in the HJ Andrews showed that riparian forests consisting of 40 year old stands had much higher rates of transpiration and water use than stands with 450 year old trees (Moore et al. 2004). Increased water used in younger Douglas fir trees can be attributed to greater water use per sapwood area than older trees as measured by the sap flux density, and a greater percentage of sapwood basal area (Moore et al. 2004).

The type of vegetation that initially grows following harvest also impacts water use. Within the Cascade region of this study, old growth forests are dominated by Douglas fir (*Pseudotsuga menziesii*), western hemlock (*Tsuga heterophylla*), and western red cedar (*Thuja plicata*) (Hicks et al. 1991; Spies 1991; Franklin and Dyrness 1973), and before harvest the riparian area was dominated by large conifers and shade tolerant herbaceous plants (Hicks et al. 1991). Following forest harvest, Douglas fir was planted on hillslopes, but angiosperms such as red alder (*Alnus rubra*) and willow (*Salix* spp.) colonized the riparian area (Hicks, Beschta, and Harr 1991). Angiosperms (broadleaf trees) use more water than gymnosperms (needleleaf trees) (Jarvis 1975). Moore et al. (2004) found sap flux density to be 1.41 times higher in red alder than young Douglas fir from July to September, with greater declines in water use by Douglas fir compared to red alder late in the summer. Red alder also had greater sapwood area (Moore et al. 2004).

The seven sub-basins in this study are all mostly forested. Forest cover exceeded 90% in six basins, and was 74% of South Fork McKenzie River (Table 2.4). All sub-basins experienced cumulative patch clearcutting starting as early as the 1930s and continuing into the early 1990s (Jones and Grant 1996). However, basins in this study were harvested at different rates, and as a result they have different percentages of young forest (forest < 40 yrs old) today (Table 2.4). Salmon Creek, Breitenbush River, and Blue River have the greatest proportion of area in young forest (29%, 23%, and 22%, respectively), and South Fork McKenzie River has the lowest proportion of area in young forest (8%). The rate at which old growth forest was converted to young forest differs between the basins. Since 1970, Salmon Creek, North Santiam River, and North Fork Middle Fork Willlamette had the highest rates of harvesting, and today they have the largest proportion of area in young forest. Lookout Creek experienced rapid rates of harvest in the 1950s and 1960s (Jones and Grant 1996), but since 1970 it had the lowest rate of harvest and has the lowest proportion of area in young forest.

2.7.7 Correlation between variables

Figure 2.11shows the correlation between the variables (elevation, geology, and vegetation). The proportion of High Cascades has a strong positive correlation with the proportion of elevation greater than 800 meters in the basin. The eruption of Quaternary volcanics created the high peaks of the Cascades, so the young porous lavas are more likely to be found at higher elevations. Elevation is also correlated,

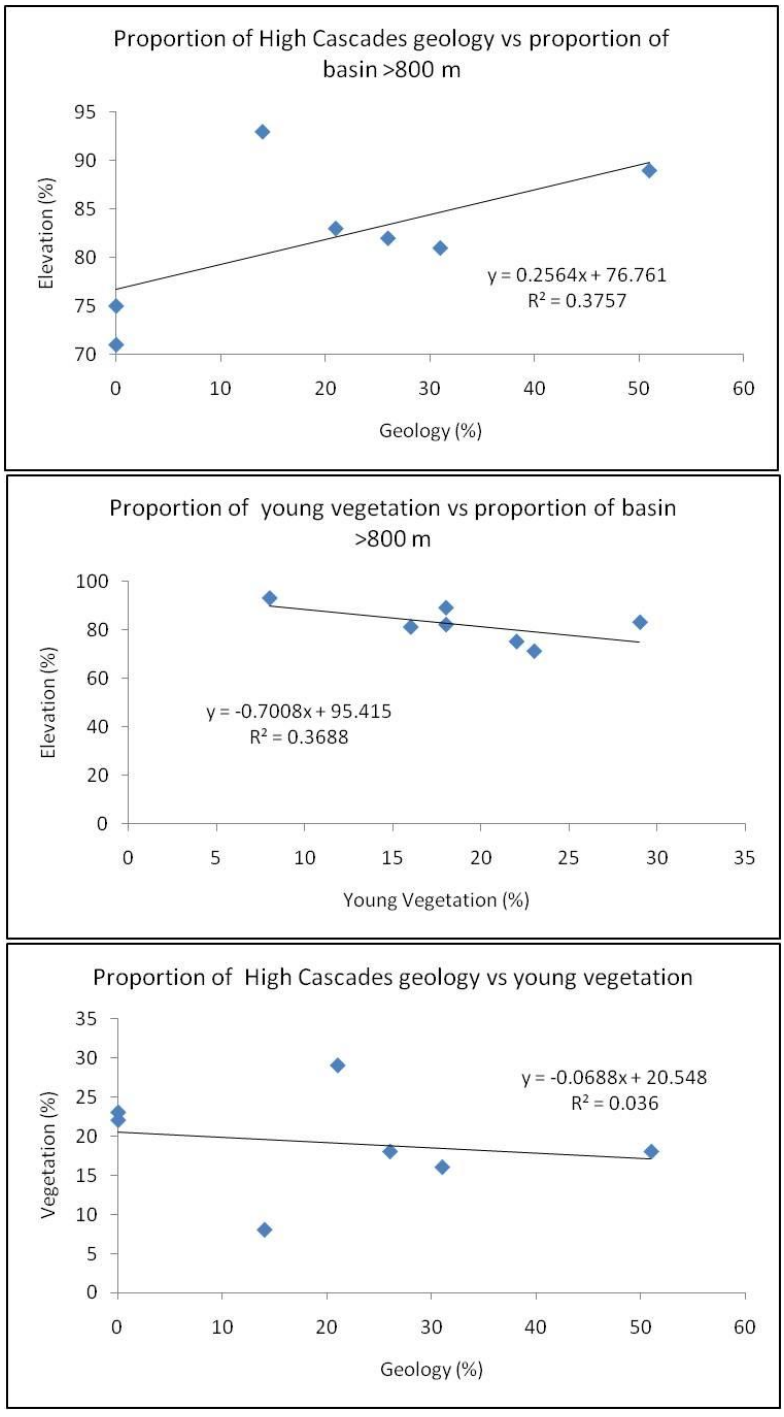

Figure 2.11 Correlation between variables of this study: geology vs elevation (top), vegetation vs elevation (center), and geology vs vegetation (bottom).

although negatively, with the proportion of young forest in each basin. Lower elevations were harvested first, as they were closer to transportation ways and processing facilities. Much of the higher elevations of the Cascades are also protected as wilderness, prohibiting forest harvest.

It is difficult to isolate any one of these features, particularly at the size of basins that were of interest in this study. The hypotheses of this research are not mutually exclusive, so correlation among the variables does not make the findings of any hypothesis invalid. This study does not attempt to determine any one causal factor; rather, it explores streamflow patterns as a result of the combination of characteristics of each basin.

2.7.8 Effects of snowpack area, basin geology, and young forest cover on trends in streamflow above dams

Based on trends in streamflow at seven basins above dams in the Willamette basin, we evaluated the following hypotheses (which are not mutually exclusive):

1) Trends in streamflow are explained by the proportion of area in the seasonal snow zone (above 800 m). The seasonal snowpack zone (above 800 m) is less susceptible to climate warming than snowpacks in the transient zone (below 800 m). Earlier snowpack melting may be accompanied by increased rates of ET at lower elevations. We expect larger declining trends in spring and

summer discharge at basins with relatively small proportions of area above 800 m.

2) Trends in streamflow are explained by basin geology, particularly the proportion of basin area underlain by High Cascades recent volcanics, which have large aquifers and relatively long water residence time distributions, compared to Western Cascades volcanics, which are highly weathered and eroded, with relatively small aquifers and relatively short residence times. We expect larger declining trends in spring and summer discharge at basins with relatively large proportions of area in High Cascades geology.

3) Trends in streamflow are explained by forest cover and forest age structure and its effects on evapotranspiration. Young forests (<40 yrs) have higher rates of ET in summer, but lower rates of ET in winter, than old growth forests. We expect larger declining trends in spring and summer discharge in basins where a relatively large proportion of area was converted from old growth to young forest.

Annual

Declines in annual discharge are greater in areas of low elevations, but these trends were not significant (Figure 2.12). South Fork McKenzie River, which has the most area greater than 800 meters, was the only site at which annual discharge

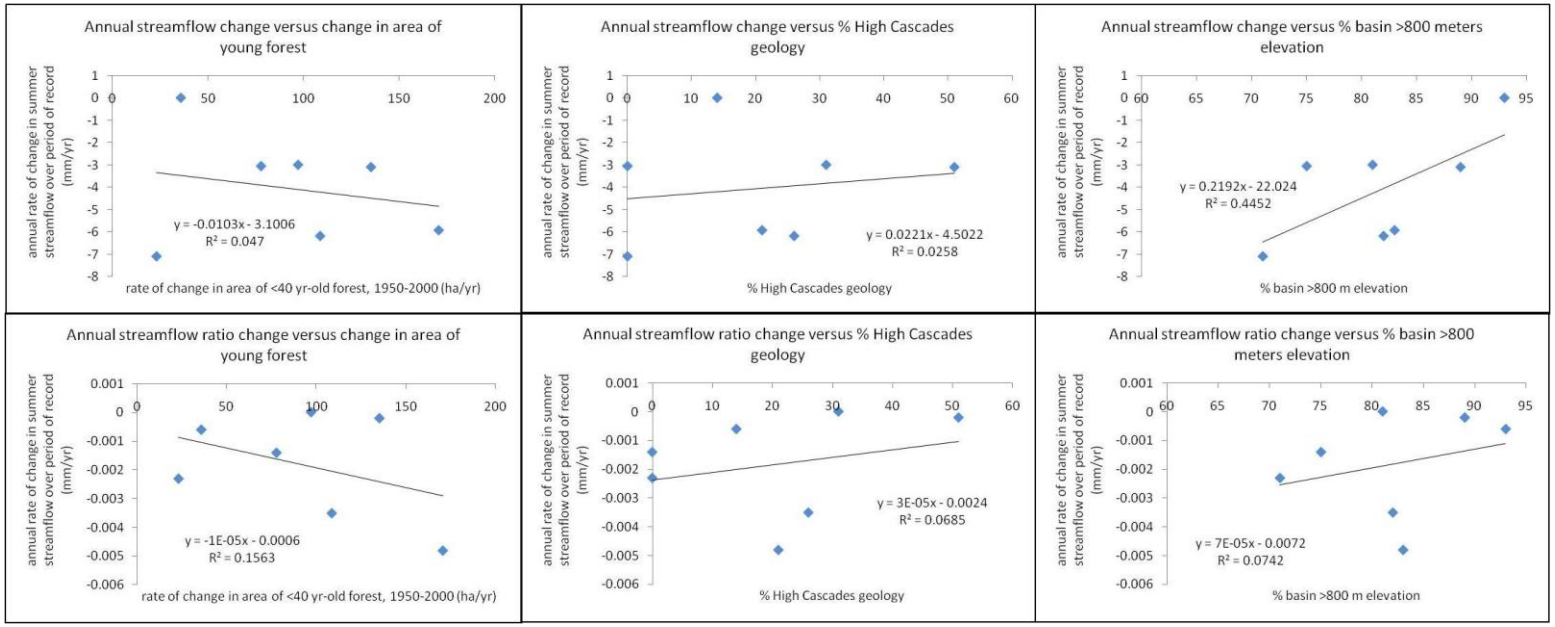

Figure 2.12 Annual streamflow and runoff ratio changes in relation to percent forest cover (right), percent High Cascades geology (center), and percent of basin greater than 800 meters in elevation.

increased over the study period. This finding provides weak support for Hypothesis #1.

Annual runoff ratios declined with increasing proportion of area converted to young forest, but the relationship is not very strong (Fig 2.12). Basins with higher rates of change in vegetation showed greater change in runoff ratios. Significant declines in annual runoff ratios were found at Lookout Creek, North Fork Middle Fork Willamette, and Blue River. Lookout Creek has the greatest percent increase in young forest, North Fork Middle Fork Willamette had one of the highest rates of change and greatest absolute area in young forest, and Blue River has one of the highest percentages of basin area in young forest. This finding provides weak support for Hypothesis #3.

Spring

Spring discharge and runoff ratios declined faster in basins at lower elevations than those at high elevations (Fig 2.13). Lower elevations have greater rates of ET and conditions are more favorable for it to begin earlier in the season. Lookout Creek, which has the smallest area greater than 800 meters elevation, was the only basin at which spring discharge declined significantly. Significant declines were found in runoff ratios at Lookout Creek, Blue River, and Salmon Creek. Increased ET was found in response to increased spring temperature, which led to declines in spring runoff ratios at small watersheds at the HJ Andrews (Moore 2010). Lookout Creek and Blue River have the lowest elevations, and Salmon Creek has moderate

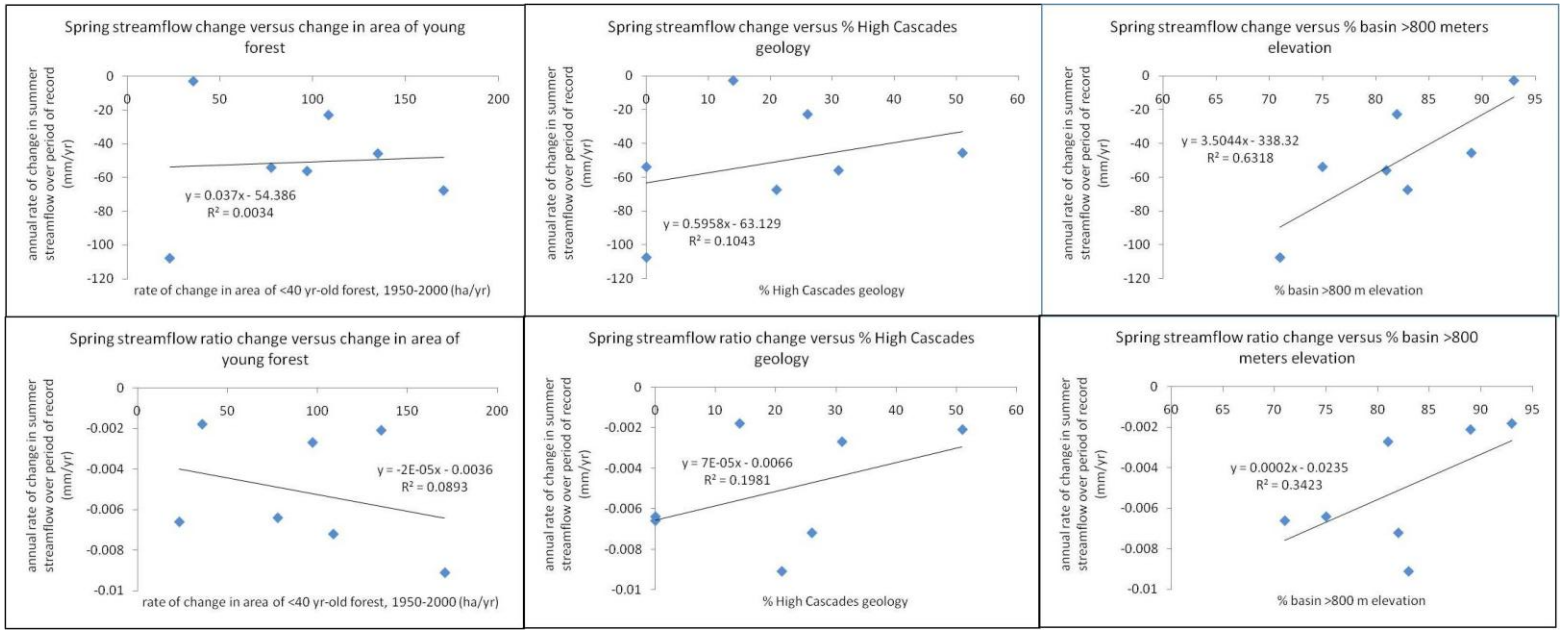

Figure 2.13 Spring streamflow and runoff ratio changes in relation to percent forest cover (right), percent High Cascades geology (center), and percent of basin greater than 800 meters in elevation.

elevations, which would be susceptible to influence by changes in temperature. This finding is consistent with Hypothesis #1.

The three basins that experienced the most rapid declines in spring discharge and runoff ratios also have the highest percentage of Western Cascades geology. The percentage of High Cascades geology has a negative relationship with streamflow changes, and explains a small (~20%) portion of the variance in spring runoff ratios. Western Cascades geology is more influenced by ET, as illustrated by Fig 2.13. High Cascades geology and higher elevation areas with greater portions High Cascade geology have much deeper flow paths, and flow that reaches the stream may bypass the root zone of the forest. Western Cascades geology has little groundwater storage and flow paths intersect the root zone of the forest. This finding is contrary to Hypothesis #2.

The shallow flowpaths are another factor in the significant declines in spring runoff ratios at Salmon Creek (Fig 2.10). Although forest change explains just a small portion of the variance in spring runoff ratios, Salmon Creek, which has the highest rates of forest change and greatest absolute area in young forest, showed declines even though it had higher elevations and greater area in High Cascades geology.

Forest age does not seem to explain declines in spring discharge. Trends in spring discharge and runoff ratios do not seem to support Hypothesis #3.

Summer

Summer discharge declined more basins with greater area in the High Cascades than in the Western Cascades (Fig 2.14). North Santiam River is the only basin to have predominantly High Cascades geology, and was the only basin to show significant declines in summer discharge. Breitenbush River also has a high percentage of High Cascades geology, and showed significant declines in baseflow discharge. Both of these basins are also at moderate elevations, and daily data showed shifts in runoff to earlier in the winter, possibly explaining the observed declines in summer flow as predicted by Tague et al. (2008). This finding is contrary to Hypothesis #1.

Summer discharge declines, and particularly declines in summer runoff ratios, can also be explained by the rate of change in young forest area (Fig 2.3). Higher ET in young forests was found to create greater declines in summer runoff ratios (Perry 2007). North Fork Middle Fork Willamette and Salmon Creek, which had the highest rates of conversion of old forest to young forest and the highest area of young forest, were the only basins in which summer runoff ratios declined significantly, although summer discharge did not change significantly. North Santiam also had one of the highest rates of vegetation change and highest absolute areas of young forest. Breitenbush River had the 4th highest rate of vegetation change and absolute area in young forest, and it also showed significant declines in baseflow discharge. This finding is consistent with Hypothesis #3.

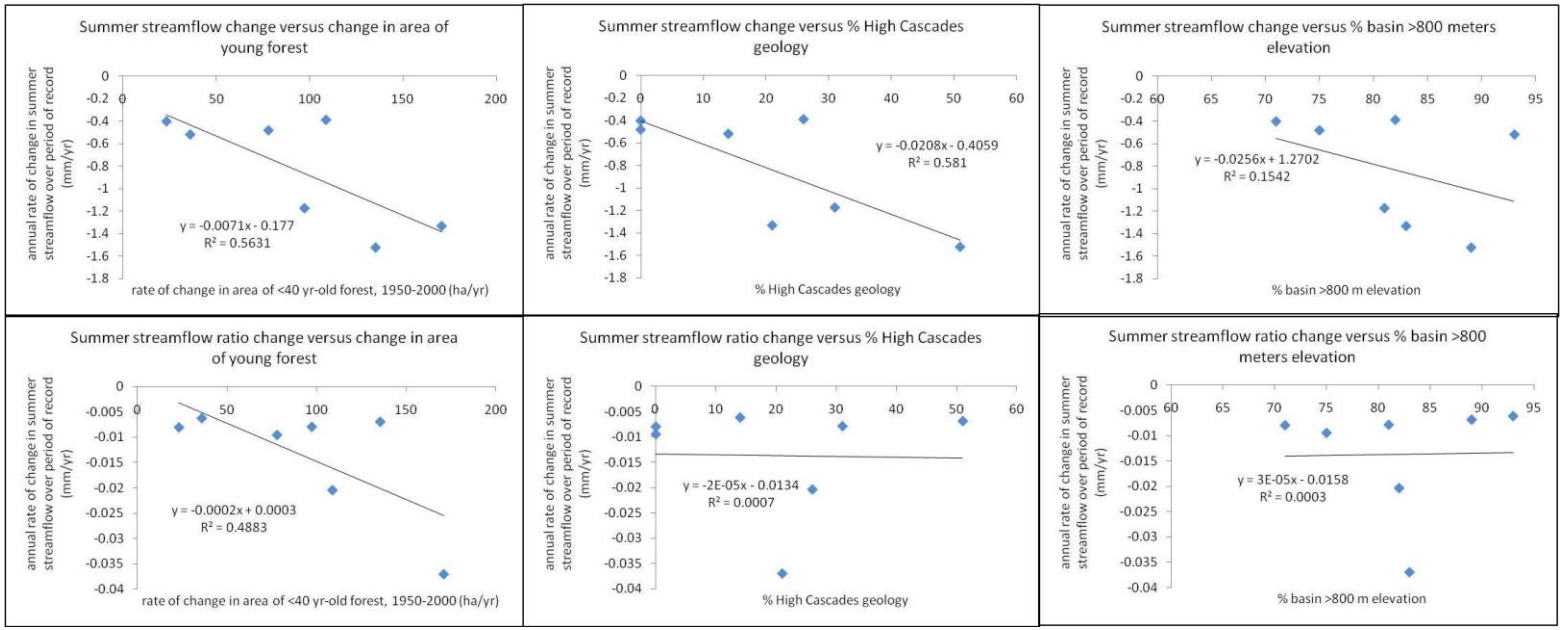

Figure 2.14 Summer streamflow and runoff ratio changes in relation to percent forest cover (right), percent High Cascades geology (center), and percent of basin greater than 800 meters in elevation.

The proportion of area in young forest also may explain trends in summer baseflow in Blue River and Lookout Creek. Blue River had a moderate rate of change and absolute area in young forest, but Lookout Creek had a low rate of change and absolute area in young forest and a moderate percentage of young forest in the basin. However, these basins have the lowest percentage of area greater than 800 m, and have very little High Cascades geology. With little groundwater storage in these basins, and flow paths directly in the rooting zones, these basins would be impacted by higher rates of ET (Fig 2.10). This is consistent with Hypothesis #1, although it is contrary to #2.

Fall

Fall discharge declined in basins with less area above 800 meters perhaps because ET is higher at lower elevations (Fig 2.15). Some of the variation in discharge can also be explained by young forest, with more declines in basins with greater rates of vegetation change. Fall baseflow discharge declined significantly only at Salmon Creek, which has intermediate elevations, but the highest rates of vegetation change and the greatest absolute area in young forest. ET is greater at lower elevations than higher elevations, and weather conditions are conducive to ET later into the fall. In the Western Cascades, flow paths are in the rooting zones and baseflow would be susceptible to decline in areas of greater ET (Fig 2.10). It would seem that this would create significant declines in discharge at many of the basins, but

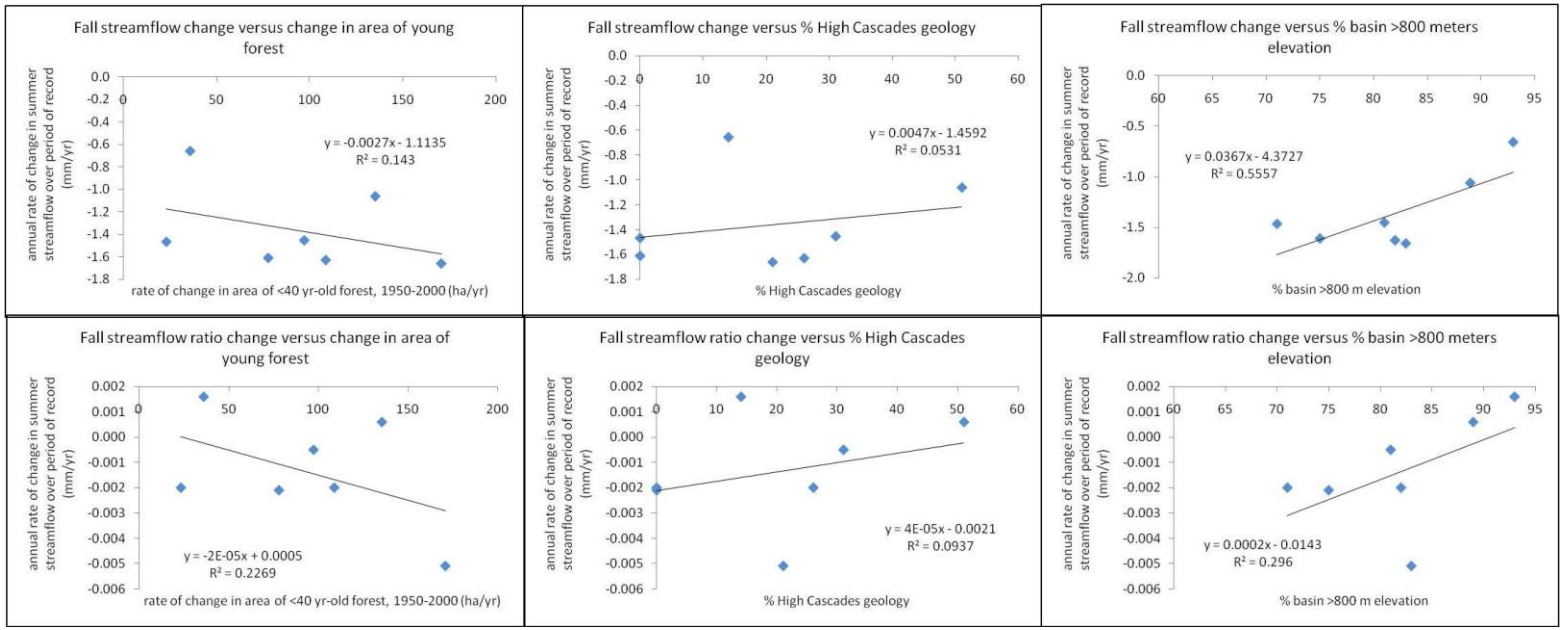

Figure 2.15 Fall streamflow and runoff ratio changes in relation to percent forest cover (right), percent High Cascades geology (center), and percent of basin greater than 800 meters in elevation.

the grouping of fall months and the variability in the arrival of fall storms may alter the trends.

Rates of decline of fall runoff ratios can also be explained by conversion of old to young forest (Fig 2.15). Basins at lower elevation and basins with higher rates of forest change have greater declines in runoff ratios. Lookout Creek has the lowest percent of area greater than 800 meters, and had the largest percentage gain in young forest. North Fork Middle Fork Willamette and Salmon Creek, where fall discharge declined significantly, had the highest rates of change in vegetation and highest absolute areas in young forest. Moore et al. (2004) also found that increases in ET in young forest became more pronounced in the fall, which would further reduce runoff ratios.

North Santiam River also had one of the highest rates of vegetation change and young forest, but it is also had a much higher elevation and is mostly in High Cascades geology. Geology has a weak negative relationship with declines in discharge and runoff ratios (Fig 2.15).

Winter

Winter discharge showed greater changes in basins with greater rates of change in vegetation (Fig 2.16). Significant declines in winter discharge were found in North Fork Middle Fork Willamette and Salmon Creek, which have the highest rates of change in vegetation and the greatest absolute area in young forest. The area of the

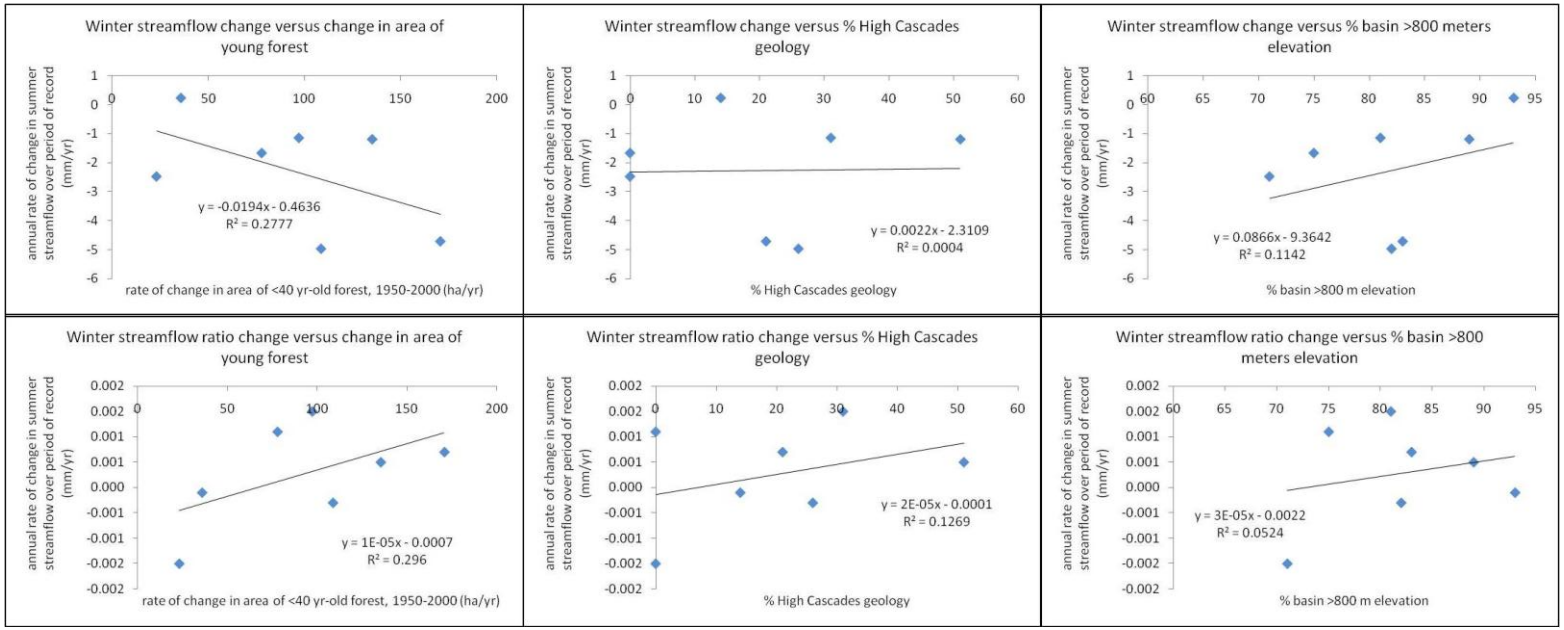

Figure 2.16 Winter streamflow and runoff ratio changes in relation to percent forest cover (right), percent High Cascades geology (center), and percent of basin greater than 800 meters in elevation.

basin greater than 800 meters has some influence on the trends in discharge, with lower elevations showing greater declines in discharge. This may explain why North Santiam, which also had one of the highest rates of change in vegetation and the greatest absolute area in young forest but has one of the highest percentages of area greater than 800 meters, does not show declines in discharge.

Winter runoff ratios can also be explained by forest change, but the impact is the opposite of discharge values (Fig 2.16). Basins with higher rates of change in vegetation have smaller changes in runoff ratios. However, trends in runoff ratios are also opposite of discharge trends with the study basins generally showing increases in runoff ratios, although these trends are not significant.

2.8 Conclusions

The combination of elevation, geology, forest age, and human alteration determine the hydrologic regime of each basin. The particular combination will influence the response in each of the basins to climate variability. Current research claims that increases in temperature will alter snowpacks, with the timing of snowmelt occurring earlier in the winter, and overall summer and fall deficits will increase. These changes will be most pronounced at elevations with temperature that are consistently near the freezing point, and in basins dominated by High Cascades geology due to groundwater recharge occurring earlier in the winter.

More rapid declines in summer and fall discharge and runoff ratios occurred in basins which experienced relatively rapid conversion of old to young forest in the past half-century and have relatively large proportions of young forest today. These changes can be attributed to increasing ET in young forests and shallow flow paths in Western Cascades-dominated basins that intersect the rooting zone. Increasing ET due to increases in spring temperature has also caused declines in spring discharges and runoff ratios at lower elevations. High elevation basins with greater percentages of High Cascades geology are less susceptible to declining discharge, even if they have substantial areas in young forest.

Compared to the trends upstream of dams, which have responded to changes in forest structure and climate, trends over time in streamflow downstream of dams in the Willamette basin have been largely influenced by management of reservoirs and flow. Flow downstream of the dams has become more homogenized throughout the year, with higher flow in the fall and declines in the later winter/early spring. However, discharge has shown declining trends at the annual time scale, and in the spring and summer. These trends may be a result of the decreases upstream of the dams caused by increased young vegetation, or they may result from a recent trend of relatively dry years (Luce et al 2009).

If temperature continues to rise, greater changes in snowpack may alter the hydrology in higher elevation and High Cascades basins. Higher temperature may also further increase ET in young forest, making streamflow declines more prominent

in all basins. Understanding the trends of the past and the factors that influenced those trends will be important for water management in the future in light of continued changes in climate and vegetation.

3. Effects of regional climate and forest dynamics on streamflow: an analysis of records from eight Long-term Ecological Research and Forest Service Experimental Forest sites in the US

3.1 Introduction

Annual temperature has already increased by 2° over the entire United States in the past 50 years (Karl, Melillo, and Peterson 2009). Most climate predictions expect temperature to continue to increase, along with increased storm intensity.

Climate trends have altered hydrology in different areas of the country. The proportion of precipitation as snow has decreased (Karl, Melillo, and Peterson 2009; Knowles et al. 2006; Mote et al. 2005; Regonda et al. 2005; Stewart et al. 2005), and snowmelt is occurring early in the spring in the west and northeast (Karl, Melillo, and Peterson 2009; Cayan et al. 2001; Hamlet et al. 2005; Regonda et al. 2005; Stewart et al. 2005; Barnett et al. 2008) due to increased spring temperature (Cayan et al. 2001; Mote2003b; Hamlet et al. 2005). Stream discharge has declined in the Southwest and the Pacific Northwest, but has increased in the east due to increased precipitation (Karl, Melillo, and Peterson 2009).

Areas in the north and east of the US are expected to become wetter, while areas in the west and southwest are expected to become drier. Areas reliant on winter snowpacks are expected to experience increasingly earlier runoff periods and decreases in summer flow. At the same time, water yield is changing due to ongoing

changes in forests, which provide the source for nearly two-thirds of freshwater in the US (NRC 2008, Jones et al 2009). These changes imply that historical water yield may no longer provide an adequate basis for water management plans in the future (Milly et al 2008).

Although historical water yield may not be representative of future water yield, long term historical climate and discharge records from instrumented sites provide the basis for understanding the nature and magnitude of climate change and other effects on water yield from headwater systems. The network of Long Term Ecological Sites (LTER) and US Forest Service system of Experimental Forests and Ranges (EFR) provide these records for headwater streams in various parts of the US. These data can be used to understand the complex relationships between climate, basin geography, vegetation, history, and hydrology, and to predict future hydrologic changes under climate variability.

Instrumented watersheds at LTER and EFR sites are generally protected areas, with minimal human impact outside of controlled experimental areas. The sites are not pristine untouched areas, however. Many were established as forest management experimental sites, with different logging techniques tested prior to establishment in the research forest network. Other sites experienced forest disturbances before their establishment as experimental sites. This history of disturbances and vegetation succession allows for analysis of not only climate change trends in control basins, but also the impact of vegetation change and climate change on discharge.

Trends in these small headwater basins are important to downstream areas. In many cases these basins serve as source water areas for downstream communities. Niwot Ridge encompasses the headwaters of Boulder Creek, which is used for drinking water in Boulder, Colorado. Discharge from the HJ Andrews flows into the Blue River and then the Mckenzie River, which is utilized by the city of Eugene, Oregon. Many other sites can be traced back as the headwaters to metropolitan areas around the country.

This study examined trends in climate and streamflow at eight sites from the LTER and EFR networks. Long-term trends in temperature, precipitation, discharge, and runoff ratio data were estimated and evaluated with respect to these hypotheses:

H1: Climate change has altered the hydrologic cycle; increased temperature is associated with changes in streamflow throughout the US.

H2: Both temperature and precipitation have increased in the eastern US, resulting in increased streamflow.

H3: Temperature has increased, but precipitation has decreased in the western US, resulting in decreased streamflow.

H4: Increased temperature has led to decreases in snowpack, earlier melts runoff, increased streamflow in winter and early spring, and reduced streamflow in late spring and summer.

3.2 Study Sites

Study sites are located at Long Term Ecological Research (LTER) and Forest Service Experimental Forest (EF) sites located in the continental United States. Four of the sites have both the LTER and EF designation. Data from eight sites were analyzed in this study: Coweeta LTER and EF, Fernow EF, Fraser EF, Hubbard Brook LTER and EF, HJ Andrews LTER and EF, Luquillo LTER and EF, Marcell EF, and Niwot Ridge LTER (Fig 3.1). The sites were chosen to encompass a range of climate and vegetation types. Study sites also had temperature, precipitation, and streamflow records available at an online harvester (CLIMDB/HYDRODB), and they had at least a 20 year record (Table 3.1, Table 3.1, Table 3.2).

Coweeta Experimental Forest/Long Term Ecological Research site

Coweeta EF covers 2,200 hectares in the Blue Ridge Province in southern North Carolina. The climate is marine, with cool summers and mild winters. Precipitation is evenly distributed throughout the year, and is mostly rain. The forest is predominantly deciduous oak canopy, with a thick evergreen understory of rhododendron and mountain laurel. The forest has been undisturbed since 1927, with forest management prescriptions occurring in some experimental catchments since then.

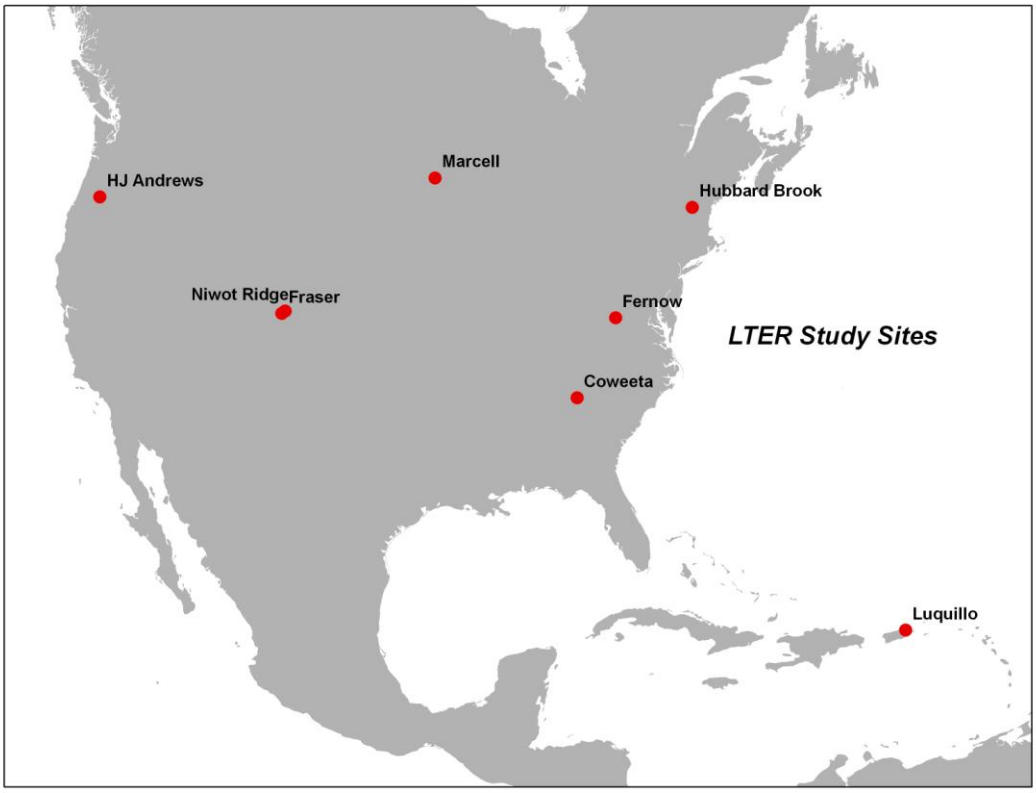

Figure 3.1 Map showing locations of LTER/EF study sites.

Table 3.1 Study basin data sources.

Site	Name of Stream or Stream Gage	Record Length	Basin area (hectares)	Precip Record Length	Precip Data Site	Temp. Record Length	Temp. Data Site	Data Source
Coweeta	Watershed 18	1937-2009	12	1937-2009	Climate Station 01	1937-2009	Climate Station 01	Climb/HydroDB
	Watershed 27	1946-2009	39					
Fernow	Watershed 4	1951-2007	39	1951-2007	Camp Hollow B	1951-2007	Camp Hollow B	
Fraser	East Lewis Creek	1943-1985	803	1976-2001	Headquarters 3	1976-2001	Headquarters 3	
Hubbard Brook	GS Watershed 3	1957-2007	42	1956-2007	Watershed 1	1955-2007	Weather Station 1	
Luquillo	ES50063800	1966-2010	2233	1975-2010	El Verde Log	1975-2010	El Verde Log	
Marcell	Watershed 2	1961-2007	10	1961-2008	South Unit, Upland, WS2	1961-2008	South Unit, Upland, WS2	
Niwot Ridge	GL4	1981-2002	225	1952-2006	D1 Met Station	1952-2006	D1 Met Station	
HJA	WS2	1953-2007	60	1958-2007	CS2MET	1958-2007	CS2MET	Forest Science Data Bank
HJA	WS8	1964-2007	21					
HJA	WS8	1969-2007	9					

Table 3.2 Site characteristics

Site name	Station name	Elevation range	MAP (mm)	Mean ppt (mm) Jan	Mean ppt (mm) July	MAT(°C)	Mean max T(°C) January	Mean min T (°C) January	Mean max T (°C) July	Mean min T (°C) July	Vegetation type
Coweeta	CS01	679-1592	1793	171	137	13	10	-3	29	15	Deciduous broadleaf hardwoods
Fernow	WS4/Camp Hollow B	1,750-3,650	1450	120	148	9	2	-7	25	14	Deciduous broadleaf hardwoods
Fraser	HQ 3	2,680-2,900	603	45	57	1	-2	-17	22	2	Subalpine needle-leaf forest and alpine tundra
Hubbard Brook	WS3/Weather Station1	222-1,015	1329	102	112	6	-4	-13	24	14	Deciduous broadleaf northern hardwoods
Luquillo	El Verde Log	200-1,075	3669	252	318	24	24	19	27	22	Evergreen broadleaf
Marcell	S2-UP-MS	422-433	775	30	113	3	-9	-21	26	12	Black sprurce bog-aspen and paper birch
Niwot Ridge	D-1	3,380-4,084	1047	127	68	-3	-9	-16	13	4	Abover timberline
HJ Andrews	CS2MET	410-1,630	2200	362	16	10	4	0	28	11	Evergreen needle-leaf conifers

Fraser Experimental Forest

Fraser EF is located in 9,300 hectares of the Arapahoe National Forest, about 40 kilometers west of Denver and on the west slope of the continental divide. The climate is long, cold winters and short, cool summers. Almost two-thirds of precipitation falls between October and May as snow. About one-third of the forest is above timberline. The rest of the forest is alpine tundra and subalpine forest, with Engelmann spruce and subalpine fir in the higher, wetter elevations and lodgepole pine at lower, drier elevations. Most of the of the forest is a result of natural revegetation after a stand replacing fire in 1685, but experiments have included forest harvest in some areas.

Hubbard Brook Experimental Forest/Long Term Ecological Research site

Hubbard Brook EF is located in the southern part of White Mountain National Park in central New Hampshire. The climate is predominantly continental, with long cold, winters, and short, cool summers. Precipitation is evenly distributed throughout the year, with about one-third to one-quarter falling as snow. The forest is predominantly deciduous northern hardwood, including sugar maple, beech, and yellow birch. Conifers were removed prior to the end of logging around 1915. Harvest has occurred in experimental catchments since then.

HJ Andrews Experimental Forest/Long Term Ecological Research Site

The HJ Andrews EF is located in the western Cascades Mountains of Oregon. The 6,400 hectares site encompasses all of the Lookout Creek drainage, which is sub-basin of the Willamette River. The climate has wet, cool winters and dry, warm summers. About 80% of the precipitation falls between April and November, with mostly rain at the lower elevations and mostly snow at the higher elevations. Douglas fir, western hemlock, and western red cedar are the dominant vegetation at lower elevations, and noble fir, Pacific silver fir, Douglas-fir, and western hemlock are prominent at higher elevations. Wildfire disturbance and logging experiments have led to patches of various aged forest stands, but areas of old growth, with trees 400 years and older, still exist within the site.

Luquillo Experimental Forest/Long Term Ecological Research site

Luqillo EF is located in the Luquillo Mountains of Puerto Rico. The 11,330 hectare forest has a warm and humid subtropical marine climate. Precipitation occurs year round, but February through April is generally a drier period, and September through December is the wettest. Cloud drip is also a factor in the water budget, with values up to 10% of annual rainfall totals. The vegetation is evergreen broadleaf forest, made up of four major forest types: Tabonuco forest at lower elevations, colorado and palm forests at higher elevations, and the dwarf forest at the highest elevations. The forest has been undisturbed since about 1940, but there was a

hurricane that affected the forest in 1989. Past disturbance included logging and clearing for agriculture.

Marcell Experimental Forest

Marcell EF is located about 40 kilometers north of Grand Rapids, Minnesota. The 890 hectare forest is on property owned by Chippewa National Forest, State of Minnesota, Itasca County, and a private individual. The climate is continental with dry, cold winters and moist, warm summers. About one-third of precipitation falls as snow, and the rest as rain. Forested bogs and fens are composed of black spruce and tamarack, with northern white cedar and black ash also in the fens. The uplands forests contain red and jack pine as a result of fire or plantations. Aspen, white birch, balsam fir, and white spruce are also found in the uplands. The forest is mostly undisturbed, with possible logging in the early 1900s. Watershed studies have included forest harvest in experimental catchments.

Niwot Ridge Long Term Ecological Site

Niwot Ridge LTER is located about 35 kilometers west of Boulder, Colorado, with most of the site located above treeline. The Continental Divide provides the western boundary of the site. The site has low temperature throughout the year, high levels of solar radiation, and a short growing season. Most precipitation falls as snow in the winter and spring months. The site contains the Arikaree Glacier and various glacial landforms, including glacial lakes and moraines. Alpine tundra is also found at

the site. The lowest elevations of the site do contain subalpine forest and meadows. The site is relatively undisturbed.

3.3 Methods

3.3.1 Data sources

Data were obtained from the Climate and Hydrology Database Projects (CLIMDB/HYDRODB, http://www.fsl.orst.edu/climhy/), a partnership between the Long-Term Ecological Research program and the U.S. Forest Service Pacific Northwest Research Station, Corvallis, Oregon. Significant funding for these data was provided by the National Science Foundation Long-Term Ecological Research program and the USDA Forest Service. Data are uploaded directly to the website by the individual research site, and are publicly available for download. Precipitation data was obtained for Fraser from the PRISM Data Explorer (PRISM Climate Group, Oregon State University, http://prismmap.nacse.org/nn/index.phtml) for the period 1943-1985. This data was only used for the creation of runoff ratios due to the short precipitation record at the site.

This study uses results from Moore (2010) for seasonal and annual analysis of data from WS2, WS8, and WS9 in the HJ Andrews Forest.

3.3.2 Data analysis

This study tested for trends in runoff ratios, as well as precipitation and discharge, to control for effects of interannual variation in precipitation on runoff. Trends in seasonal and daily flow were also analyzed to separate changes associated with flooding (winter), snowmelt (spring) and ET (summer, fall).

Streamflow, precipitation, runoff ratios, and temperature were tabulated by water year and by season. The water year extends from October 1 to September 30 of the following year. Seasons were: Fall-September, October, November; Winter-December, January, February; Spring-March, April, May; Summer-June, July, August.

Linear regression and the Mann-Kendall trend test were used to quantify trends in climate, streamflow and runoff ratios. Annual and seasonal climate, discharge, and runoff ratio data were tested for autocorrelation prior to analysis, using the autocorrelation function in the statistical software R. The residuals from regression analyses of data that were autocorrelated and had significant trends over time were also tested for autocorrelation.

Another issue in statistical analysis is the distribution of the data. Parametric statistics, such as linear regression, assume that the data is not only independent (not autocorrelated), but comes from a Gaussian distribution. Streamflow and precipitation values do not follow a Gaussian distribution. The distribution does not affect the trend, only whether the trend is significant (Helsel and Hirsh 1992). Therefore, these

data were also analyzed with a nonparametric test, the Mann-Kendall, to explore possible trends. The Mann-Kendall test ranks results and determines if the values are changing more or less in relation to the dependant variable, in this case time (Helsel and Hirsch, 2002). This type of analysis is supported by USGS, which developed the software used to perform this analysis (Helsel et al., 2005).

Analysis of trends in seasonal and annual temperature

Temperature trends were estimated for one meteorological station from each site, generally the one with the longest record. Maximum and minimum daily mean temperature was averaged on an annual and seasonal basis for the extent of record. Simple linear regression and the Mann-Kendall test were used to look at trends in temperature of the period of record.

Analysis of trends in seasonal and annual precipitation

Precipitation trends were estimated for one meteorological station from each site, generally the one with the longest record. Daily precipitation values were averaged on an annual and seasonal basis for the extent of record. Simple linear regression and the Mann-Kendall test were used to look at trends in precipitation for the period of record.

Analysis of trends in seasonal and annual discharge and runoff ratios

Discharge values were downloaded in units of liters per second (lps), and converted to a depth value of millimeters per month based on calculations in Table 3.3.

Discharge data was analyzed at a seasonal and annual time scale with linear regression and the Mann-Kendall trend test. The baseflow component of flow, which is the continuous flow not changed by direct input or runoff from a precipitation event, was also analyzed. Baseflow was determined from a baseflow separation program (see Appendix A) following Post and Jones (2001). The baseflow separation program applies a moving five day window to daily discharge values to determine the minimum for each 5-day period. The subset of local minimum values then are compared to adjacent minima, and values that are less than 90% of the surrounding minima are connected to define baseflow. Daily baseflow were aggregated to the monthly, annual and seasonal time frames for analysis.

Runoff ratios (Q/P) were calculated at the seasonal and annual time scale, from the water balance equation

$$Q=P-ET-\Delta S$$

where P is precipitation, ET is evapotranspiration, and ΔS is change in storage. The runoff ratio (Q/P) reflects changes in evapotranspiration or storage potential.

Table 3.3 Conversion of liters per second (lps) to millimeters per month (mm/month)

liters per second (lps) to cubic meters per second (cms)	cms=lps*0.001
cubic meters per second (cms) to cubic meters per month (cm/month)	cmm=cms*2629743.83
cubic meters per month (cm/month) to meters per month (m/month)	m/month=cmm/drainage area
meters per month (m/month) to millimeters per month (mm/month)	mm/month=m/month*1000

Trends in discharge, baseflow, and runoff ratios were estimated for the period of record for each site. Simple linear regression and the Mann-Kendall test were used to evaluate trends in discharge and runoff ratios.

Analysis of trends in daily temperature, precipitation, and discharge data

Trends in daily data were calculated using a program written by E. Miles in MATLAB (Appendix B). The program formats data by day of water year for each year using a parsing code. Data were log transformed to produce a near-normal distribution, and values for each day are tested for trends using linear regression. Trends were considered significant if the slope of the regression was significant at $p<0.05$. The program outputs trend analysis for each day of the water year over the period of record.

3.4 Results

3.4.1 Overview of climate trends at all sites

Change in annual temperature, precipitation, discharge, runoff ratios

The sites span a range of climates from cool dry to moist humid (Fig. 3.1). Most sites experienced significant increases in minimum annual temperature, but only two sites (Niwot Ridge, Hubbard Brook) experienced significant increases in annual precipitation.

Annual precipitation decreased at Coweeta, Fernow, and HJ Andrews. Mean annual precipitation increased at Fraser, Hubbard Brook, Niwot Ridge, Luquillo, and Marcell, but the increases were statistically significant only at Hubbard Brook and Niwot Ridge (Table 3.4a, Fig. 3.2). The Mann-Kendall test showed increases in annual precipitation at all sites except for Fernow and Marcell.

Annual maximum temperature has increased at all sites except for Niwot Ridge and HJ Andrews. The Mann-Kendall test showed increases at all sites. Significant increases occurred at Hubbard Brook, Luquillo, and Marcell (linear regression and Mann-Kendall). (Table 3.4a, Fig. 3.3).

Annual minimum daily temperature increased significantly at Coweeta, Fernow, Fraser, Hubbard Brook, Luquillo, HJ Andrews and Marcell (Table 3.4a, Fig. 3.4). Declines were observed at Niwot Ridge, but they were not significant.

Table 3.4 Results from linear regression analysis and the Mann-Kendall test for each basin, annual (A) and for each season (Spring-B, Summer-C, Fall-D, and Winter E).

A.

		Linear Regression					Mann-Kendall					Auto-	Residual
	N	Intercept	Slope	R2	P	Sig	Intercept	Slope	Tau	P	Sig	correlation	Autocorrelation
Annual Q/P													
Coweeta WS 18	71	0.5416	0.0001	0.00	0.85		-0.2978	0.0004	0.054	0.51		x	
Coweeta WS 27	60	0.9271	0.0001	0.00	0.86		0.9300	0.0000	0.008	0.93			
Fernow	56	0.4109	0.0010	0.09	0.02	*	-1.6448	0.0011	0.201	0.03	*	x	
Fraser	42	0.7395	-0.0024	0.04	0.22		5.4419	-0.0024	-0.141	0.19			
Hubbard Brook	50	0.5849	0.0015	0.09	0.03	*	-1.8531	0.0013	0.178	0.07			
Luquillo	35	0.6828	-0.0013	0.02	0.43		3.9617	-0.0017	-0.138	0.25			
Marcell	45	0.1995	0.0005	0.01	0.49		-0.9824	0.0006	0.068	0.52		x	
Niwot Ridge	21	0.7355	0.0063	0.13	0.10		-9.1800	0.0050	0.238	0.14			
WS2	55	2.9170	-0.0010	0.04	0.13								
WS8	44	5.9210	-0.0030	0.14	0.01	*							
WS9	39	5.8320	-0.0030	0.08	0.08								
Annual Base Q/P													
Coweeta WS 18	71	0.4624	0.0010	0.00	0.81		-0.2346	0.0004	0.046	0.57		x	
Coweeta WS 27	60	0.5830	0.0002	0.00	0.73		0.5800	0.0000	0.001	0.99			
Fernow	56	0.1792	0.0005	0.09	0.03	*	-0.8251	0.0005	0.225	0.01	*		
Fraser	42	0.6960	-0.0023	0.04	0.23		5.8247	-0.2632	-0.132	0.22			
Hubbard Brook	50	0.2892	0.0000	0.00	1.00		0.2900	0.0000	0.006	0.96			
Luquillo	35	0.2600	0.0000	0.00	0.98		0.2500	0.0000	-0.005	0.98			
Marcell	45	0.1232	-0.0009	0.07	0.07		2.0740	-0.0010	-0.185	0.07			
Niwot Ridge	21	0.6125	0.0067	0.23	0.03	*	-12.2980	0.0065	0.290	0.07			
Annual Q													
Coweeta WS 18	71	0.5414	0.0001	0.00	0.87		-1876.6000	1.4780	0.049	0.55		x	
Coweeta WS 27	60	1785.7000	-3.0221	0.02	0.28		3840.1000	-1.0810	-0.029	0.75		x	
Fernow	56	603.6900	1.4647	0.02	0.25		-1343.0000	1.0000	0.079	0.40			
Fraser	42	383.6700	-0.1965	0.00	0.89		1655.6000	-0.6471	-0.055	0.62		x	
Hubbard Brook	50	738.8300	3.9549	0.09	0.04	*	-7178.1000	4.0420	0.219	0.03	*		
Luquillo	35	2378.8000	2.9127	0.00	0.79		-12693.0000	7.6000	0.059	0.63		x	
Marcell	45	156.9300	0.4912	0.01	0.52		-1256.8000	0.7171	0.081	0.44			
Niwot Ridge	21	962.9800	1.4106	0.00	0.81		-14217.0000	7.6250	0.176	0.28			
WS2	55	11062.5550	-4.9210	0.04	0.15								
WS8	44	15644.3000	-7.2940	0.06	0.12								
WS9	39	18745.1510	-8.7990	0.06	0.15								
Annual Base Q													
Coweeta WS 18	71	0.4624	0.0001	0.00	0.84		-1741.7000	1.3300	0.050	0.54		x	
Coweeta WS 27	60	1118.0000	-1.6011	0.02	0.34		3130.5000	-1.0400	-0.050	0.57		x	
Fernow	56	263.4100	0.5919	0.03	0.20		-801.6800	0.5467	0.104	0.26			
Fraser	42	360.4200	-0.1563	0.00	0.90		1496.4000	-0.5769	-0.065	0.55		x	
Hubbard Brook	50	359.8000	1.0265	0.04	0.17		-1381.9000	0.8966	0.124	0.21			
Luquillo	35	891.5200	3.0931	0.02	0.41		-8811.6000	4.8890	0.150	0.21			
Marcell	45	96.5090	-0.6750	0.01	0.52		1394.7000	-0.6667	-0.144	0.16			
Niwot Ridge	21	799.9400	3.0482	0.02	0.51		-11754.0000	6.3260	0.171	0.29			
WS2	55	6005.0000	-2.7460	0.07	0.06								
WS8	44	9588.6000	-4.5840	0.11	0.03	*							
WS9	39	10090.6000	-4.8330	0.10	0.05	*							

Table 3.4 cont.

A cont.

		Linear Regression					Mann-Kendall						
	N	Intercept	Slope	R2	P	Sig	Intercept	Slope	Tau	P	Sig	Auto-correlation	Residual Autocorrelation
Annual Precipitation													
Coweeta WS 18													
Coweeta WS 27	71	1805.6000	-0.3369	0.00	0.78		985.7100	0.4286	0.027	0.74			
Fernow	56	1457.4000	-0.2560	0.00	0.88		2442.8000	-0.5109	-0.033	0.72			
Fraser	25	580.4100	1.7652	0.02	0.49		-5166.6000	2.8950	0.127	0.39			
Hubbard Brook	51	1226.5000	3.9474	0.09	0.03	*	-8820.2000	5.1110	0.247	0.01	*		
Luquillo	35	3451.8000	12.0750	0.03	0.36		-11387.0000	7.6000	0.116	0.33			
Marcell	46	780.0900	0.1967	0.00	0.88		1215.2000	-0.2143	-0.020	0.85			
Niwot Ridge	54	758.8400	10.4700	0.32	0.00	*	-21685.0000	11.480 0	0.423	0.00	*	x	x
CS2MET	50	6840.1200	-2.3120	0.01	0.60								
Annual Max Temperature													
Coweeta WS 18												x	
Coweeta WS 27	72	19.7120	0.0059	0.03	0.13		20.0000	0.0000	0.106	0.14			
Fernow	53	14.4400	0.0040	0.00	0.63		15.0000	0.0000	0.054	0.54		x	
Fraser	24	8.8977	0.0416	0.13	0.08		10.0000	0.0000	0.217	0.10			
Hubbard Brook	52	9.9457	0.0181	0.14	0.01	*	10.0000	0.0000	0.190	0.03	*		
Luquillo	35	24.7740	0.0693	0.62	0.00	*	-84.7220	0.0556	0.523	0.00	*	x	x
Marcell	46	8.7518	0.0428	0.23	0.00	*	-69.3800	0.0400	0.310	0.00	*		
Niwot Ridge	54	0.5154	-0.0121	0.02	0.32		0.0000	0.0000	-0.014	0.88		x	
CS2MET	49	14.2910	-0.0010	0.00	0.99		14.0000	0.0000	-0.017	0.86			
Annual Min Temperature													
Coweeta WS 18													
Coweeta WS 27	72	4.8281	0.0264	0.38	0.00	*	-33.4700	0.0200	0.374	0.00	*	x	x
Fernow	53	3.0310	0.0199	0.13	0.01	*	3.0000	0.0000	0.163	0.07		x	x
Fraser	24	-8.2732	0.0632	0.39	0.00	*	-8.0000	0.0000	0.272	0.04	*		
Hubbard Brook	52	0.3393	0.0226	0.18	0.00	*	1.0000	0.0000	0.244	0.01	*		
Luquillo	35	20.0720	0.0392	0.52	0.00	*	21.0000	0.0000	0.385	0.00	*	x	x
Marcell	46	-4.1472	0.0522	0.33	0.00	*	-95.3020	0.0465	0.358	0.00	*	x	
Niwot Ridge	54	-6.6743	-0.0133	0.03	0.19		-7.0000	0.0000	-0.064	0.45		x	
CS2MET	49	4.1062	0.0139	0.09	0.04	*	4.0000	0.0000	0.221	0.01	*		

Table 3.4 cont.

B.

		Linear Regression					Mann-Kendall					Auto-correlation	Residual Autocorrelation
	N	Intercept	Slope	R2	P	Sig	Intercept	Slope	Tau	P	Sig		
SpringQ/P													
Coweeta WS 18	72	0.8463	-0.0005	0.00	0.56		0.8300	0.0000	0.013	0.87		x	
Coweeta WS 27	61	1.1176	-0.0002	0.00	0.79		0.3930	0.0004	0.027	0.76			
Fernow	56	0.6409	0.0007	0.02	0.35		-1.0713	0.0009	0.123	0.18			
Fraser	43	0.4158	-0.0039	0.07	0.08		9.1180	-0.0045	-0.218	0.04	*	x	x
Hubbard Brook	50	1.5362	-0.0084	0.21	0.00	*	16.2790	-0.0076	-0.320	0.00	*	x	x
Luquillo	35	0.6244	-0.0001	0.00	0.95		-0.9223	0.0008	0.042	0.73			
Marcell	45	0.4537	0.0007	0.00	0.78		-0.0698	0.0003	0.017	0.88			
Niwot Ridge													
WS2	55	7.5230	-0.0030	0.11	0.02	*							
WS8	44	18.0250	-0.0090	0.16	0.01	*							
WS9	39	11.8470	-0.0060	0.19	0.01	*							
Spring Base Q/P													
Coweeta WS 18	72	0.7597	-0.0004	0.00	0.63		0.7400	0.0000	0.008	0.92		x	
Coweeta WS 27	61	0.7580	0.0006	0.01	0.52		-0.4106	0.0006	0.064	0.47			
Fernow	56	0.3200	0.0003	0.01	0.48		-0.4132	0.0004	0.088	0.34			
Fraser	43	0.3736	-0.0036	0.07	0.08		7.7694	-0.0038	-0.208	0.05	*	x	x
Hubbard Brook	50	0.8382	-0.0055	0.14	0.01	*	8.5600	-0.0040	-0.224	0.02	*	x	x
Luquillo	35	0.2029	0.0015	0.05	0.20		-2.5064	0.0014	0.188	0.11			
Marcell	45	0.3104	-0.0009	0.00	0.67		2.2340	-0.0010	-0.062	0.56			
Niwot Ridge													
Spring Q													
Coweeta WS 18	72	404.3500	-0.3838	0.00	0.60		1077.2000	-0.3550	-0.029	0.72			
Coweeta WS 27	61	571.9600	-1.4463	0.02	0.20		2779.3000	-1.1480	-0.080	0.37			
Fernow	56	254.9400	0.1478	0.00	0.77		-138.4000	0.2010	0.040	0.67			
Fraser	43	63.0290	-0.5703	0.09	0.05	*	1192.7000	-0.5833	-0.218	0.04	*		
Hubbard Brook	50	436.0200	-0.9117	0.02	0.29		2524.4000	-1.0620	-0.117	0.23			
Luquillo	35	540.4600	-1.0502	0.00	0.81		50.6320	0.2105	0.013	0.92			
Marcell	45	88.0590	-0.2322	0.01	0.62		483.8000	-0.2000	-0.036	0.73		x	
Niwot Ridge													
WS2	55	5401.0810	-2.5450	0.08	0.03	*							
WS8	44	6121.1500	-2.8930	0.05	0.13								
WS9	39	5197.8220	-2.4600	0.05	0.18								
Spring Base Q													
Coweeta WS 18	72	359.3000	-0.3271	0.00	0.58		528.7800	-0.0955	-0.008	0.92			
Coweeta WS 27	61	377.5700	-0.6107	0.02	0.28		1276.9000	-0.4623	-0.069	0.43			
Fernow	56	126.9900	0.0110	0.00	0.96		-214.1500	0.1711	0.066	0.48		x	
Fraser	43	56.4420	-0.5281	0.09	0.05	*	1094.1000	-0.5357	-0.220	0.04	*	x	
Hubbard Brook	50	229.4600	-0.6170	0.03	0.21		1767.2000	-0.7857	-0.140	0.15			
Luquillo	35	166.2200	1.0150	0.02	0.44		-2320.0000	1.2500	0.114	0.34			
Marcell	45	58.0800	-0.3560	0.02	0.32		811.8000	-0.3875	-0.112	0.28			
Niwot Ridge													
WS2	55	3691.4000	-1.7640	0.15	0.00	*							
WS8	44	5533.1000	-2.6850	0.13	0.02	*							
WS9	39	2641.0000	-1.2490	0.06	0.15								

Table 3.4 cont.

B cont.

		Linear Regression					Mann-Kendall						
	N	Intercept	Slope	R2	P	Sig	Intercept	Slope	Tau	P	Sig	Auto-correlation	Residual Autocorrelation
Spring Precipitation													
Coweeta WS 18													
Coweeta WS 27	73	488.9100	-0.4505	0.00	0.57		1493.1000	-0.5343	-0.059	0.47			
Fernow	56	395.2900	-0.1430	0.00	0.82		912.4700	-0.2629	-0.038	0.69		x	
Fraser	26	188.4600	0.2083	0.00	0.85		186.0000	0.0000	0.006	0.98			
Hubbard Brook	52	289.9400	1.0958	0.05	0.13		-2144.8000	1.2400	0.147	0.13			
Luquillo	35	809.1700	0.2978	0.00	0.95		4842.4000	-2.0330	-0.044	0.72			
Marcell	47	201.7300	-0.9328	0.06	0.09		2216.6000	-1.0270	-0.203	0.05	*		
Niwot Ridge	54	224.4300	3.8590	0.25	0.00	*	-7275.5000	3.8460	0.324	0.00	*	x	x
CS2MET	50	382.5920	0.0750	0.00	0.96								
Spring Max Temperature													
Coweeta WS 18													
Coweeta WS 27	73	19.7430	0.0105	0.05	0.05	*	20.0000	0.0000	0.149	0.05	*		
Fernow	53	15.0880	-0.0029	0.00	0.82		15.0000	0.0000	-0.014	0.89		x	
Fraser	25	7.7007	0.0652	0.14	0.07		-32.4170	0.0208	0.223	0.11			
Hubbard Brook	52	9.1927	0.0184	0.05	0.12		10.0000	0.0000	0.099	0.29			
Luquillo	35	24.6580	0.0764	0.55	0.00	*	-106.8000	0.0667	0.519	0.00	*	x	
Marcell	47	9.6652	0.0550	0.14	0.01	*	-105.7100	0.0588	0.264	0.01	*	x	x
Niwot Ridge	54	-2.0565	-0.0017	0.00	0.92		-2.0000	0.0000	0.112	0.22			
CS2MET	47	12.7150	0.0194	0.04	0.17		13.0000	0.0000	0.155	0.11			
Spring Min Temperature													
Coweeta WS 18													
Coweeta WS 27	73	4.0933	0.0285	0.25	0.00	*	-41.4300	0.0235	0.300	0.00	*	x	
Fernow	53	2.1797	0.0165	0.05	0.11		3.0000	0.0000	0.127	0.16			
Fraser	25	-8.7480	0.0658	0.26	0.01	*	-8.0000	0.0000	0.203	0.13			
Hubbard Brook	52	-0.8554	0.0199	0.07	0.06		0.0000	0.0000	0.133	0.15			
Luquillo	35	19.4040	0.0298	0.20	0.01	*	20.0000	0.0000	0.240	0.02	*	x	x
Marcell	47	-4.1119	0.0396	0.10	0.03	*	-93.1820	0.0455	0.228	0.02	*		
Niwot Ridge	54	-9.5549	0.0037	0.00	0.78		-9.0000	0.0000	0.094	0.31			
CS2MET	47	2.3688	0.0290	0.16	0.01	*	3.0000	0.0000	0.253	0.01	*		

Table 3.4 cont.

C.

		Linear Regression					Mann-Kendall					Auto-correlation	Residual Autocorrelation
	N	Intercept	Slope	R2	P	Sig	Intercept	Slope	Tau	P	Sig		
Summer Q/P													
Coweeta WS 18	73	0.3853	0.0006	0.01	0.42		-0.7806	0.0006	0.066	0.41			
Coweeta WS 27	61	0.6069	-0.0004	0.00	0.79		2.1541	-0.0008	-0.043	0.63			
Fernow	56	0.1473	0.0008	0.02	0.36		-1.5540	0.0009	0.074	0.42			
Fraser	43	2.3609	0.0005	0.00	0.97		-0.2850	0.0013	0.011	0.92			
Hubbard Brook	50	0.1404	0.0030	0.10	0.03	*	-5.5806	0.0029	0.274	0.01	*	x	x
Luquillo	35	0.5766	-0.0014	0.01	0.53		5.2071	-0.0024	-0.096	0.43			
Marcell	45	0.1224	0.0011	0.04	0.21		-2.1068	0.0011	0.129	0.21			
Niwot Ridge	21	4.0490	-0.0204	0.02	0.59		72.8270	-0.0348	-0.152	0.35			
WS2	55	-2.8540	0.0020	0.01	0.44								
WS8	44	-1.4720	0.0010	0.01	0.64								
WS9	39	1.8520	-0.0010	0.00	0.84								
Summer Base Q/P													
Coweeta WS 18	73	0.3424	0.0006	0.01	0.43		-0.8558	0.0006	0.066	0.41		x	
Coweeta WS 27	61	0.3961	-0.0003	0.00	0.72		0.3900	0.0000	-0.017	0.85			
Fernow	56	0.0440	0.0003	0.02	0.31		-0.5499	0.0003	0.125	0.17			
Fraser	43	2.2342	0.0009	0.00	0.95		2.0100	0.0000	0.007	0.96			
Hubbard Brook	50	0.0515	0.0007	0.04	0.15		-1.2967	0.0007	0.204	0.04	*	x	x
Luquillo	35	0.2155	0.0001	0.00	0.88		0.2100	0.0000	0.034	0.79			
Marcell	45	0.0576	-0.0004	0.02	0.31		1.0320	-0.0005	-0.153	0.14			
Niwot Ridge	21	3.3504	-0.0028	0.00	0.93		26.8230	-0.0119	-0.038	0.83			
Summer Q													
Coweeta WS 18	73	158.6500	0.2130	0.00	0.65		551.8500	-0.2062	-0.056	0.49			
Coweeta WS 27	61	271.7600	-0.3722	0.00	0.99		1610.5000	-0.6998	-0.054	0.55			
Fernow	56	64.9210	0.5481	0.02	0.31		-917.7500	0.5000	0.091	0.33			
Fraser	43	295.7900	-0.0070	0.00	1.00		565.5700	-0.1429	-0.014	0.90		x	
Hubbard Brook	50	49.7190	1.3805	0.07	0.10		-2319.0000	1.2000	0.281	0.00	*		
Luquillo	35	560.1400	-2.4734	0.01	0.49		-66.0000	0.1250	0.007	0.97			
Marcell	45	39.0440	0.5513	0.04	0.20		-653.0700	0.3498	0.094	0.37			
Niwot Ridge	21	799.4500	-7.2677	0.09	0.18		11993.0000	-5.6830	-0.152	0.35			
WS2	55	-274.1930	0.1640	0.01	0.39								
WS8	44	105.8030	-0.0270	0.00	0.94								
WS9	39	640.5080	-0.2960	0.01	0.52								
Summer Base Q													
Coweeta WS 18	73	139.5700	0.1841	0.00	0.64		307.2900	-0.0939	-0.028	0.73			
Coweeta WS 27	61	170.8800	-0.2664	0.00	0.98		946.1600	-0.4062	-0.064	0.47			
Fernow	56	19.5570	0.1447	0.02	0.35		-385.1500	0.2042	0.124	0.18			
Fraser	43	279.2300	0.0312	0.00	0.98		800.8100	-0.2703	-0.039	0.72			
Hubbard Brook	50	16.7710	0.3421	0.06	0.10		-548.4300	0.2857	0.238	0.02	*		
Luquillo	35	205.9600	-0.2702	0.00	0.83		-66.0000	0.1250	0.007	0.97			
Marcell	45	18.7140	-0.1090	0.01	0.47		254.2200	-0.1216	-0.135	0.19			
Niwot Ridge	21	655.3800	-3.1596	0.04	0.40		3849.9000	-1.6410	-0.086	0.61			
WS2	55	-123.8000	0.0830	0.01	0.49								
WS8	44	241.7000	-0.1030	0.01	0.62								
WS9	39	659.5000	-0.3120	0.03	0.34								

Table 3.4 cont.

C cont

		Linear Regression					Mann-Kendall					Auto-	Residual
	N	Intercept	Slope	R2	P	Sig	Intercept	Slope	Tau	P	Sig	correlation	Autocorrelation
Summer Precipitation													
Coweeta WS 18													
Coweeta WS 27	73	434.1100	-0.6088	0.01	0.46		2301.8000	-0.9756	-0.118	0.14			
Fernow	56	398.1300	0.4997	0.01	0.57		-1561.0000	1.0000	0.071	0.44			
Fraser	26	128.4200	0.7952	0.02	0.52		-1196.7000	0.6667	0.098	0.49			
Hubbard Brook	52	316.3200	1.3510	0.06	0.09		-2626.2000	1.4940	0.179	0.06			
Luquillo	35	926.5200	-0.3941	0.00	0.92		762.4400	0.0741	0.002	1.00		x	
Marcell	47	311.6100	0.1131	0.00	0.90		-341.3300	0.3333	0.031	0.76			
Niwot Ridge	54	204.1600	0.0044	-0.28	0.63		22.4080	0.0816	0.010	0.92		x	
CS2MET	50	-328.6970	0.2230	0.00	0.66								
Summer Max Temperature													
Coweeta WS 18													
Coweeta WS 27	73	27.8750	0.0066	0.03	0.17		28.0000	0.0000	0.090	0.23			
Fernow	53	24.0070	0.0228	0.06	0.07		25.0000	0.0000	0.112	0.22			
Fraser	25	21.3230	-0.0194	0.02	0.56		21.0000	0.0000	-0.050	0.73		x	
Hubbard Brook	52	22.4530	0.0097	0.02	0.35		23.0000	0.0000	0.029	0.76			
Luquillo	35	26.4970	0.0559	0.60	0.00	*	-56.0000	0.0417	0.484	0.00	*	x	
Marcell	47	23.8690	0.0253	0.06	0.09		-36.1210	0.0303	0.217	0.03	*		
Niwot Ridge	54	10.4140	0.0214	0.06	0.09		11.0000	0.0000	0.168	0.07		x	
CS2MET	47	26.6050	-0.0169	0.02	0.55		26.0000	0.0000	-0.083	0.41			
Summer Min Temperature													
Coweeta WS 18													
Coweeta WS 27	73	13.5150	0.0212	0.28	0.00	*	-21.8730	0.0182	0.333	0.00	*	x	x
Fernow	53	12.3180	0.0355	0.35	0.00	*	-34.6700	0.0241	0.338	0.00	*	x	x
Fraser	25	0.4097	0.0759	0.33	0.00	*	-150.9200	0.0769	0.403	0.00	*		
Hubbard Brook	52	12.1270	0.0124	0.04	0.15		13.0000	0.0000	0.093	0.31		x	
Luquillo	35	21.4500	0.0355	0.46	0.00	*	-44.4000	0.0333	0.413	0.00	*	x	
Marcell	47	9.6478	0.0443	0.28	0.00	*	-71.6670	0.4167	0.381	0.00	*	x	x
Niwot Ridge	54	2.5686	0.0130	0.03	0.20		3.0000	0.0000	0.126	0.16		x	
CS2MET	47	9.8945	0.0085	0.03	0.21		10.0000	0.0000	0.093	0.30			

Table 3.4 cont.

D.

		Linear Regression					Mann-Kendall					Auto-correlation	Residual Autocorrelation
	N	Intercept	Slope	R2	P	Sig	Intercept	Slope	Tau	P	Sig		
Fall Q/P													
Coweeta WS 18	73	0.3352	-0.0005	0.01	0.51		1.1986	-0.0005	-0.061	0.45			
Coweeta WS 27	61	0.7489	0.0002	0.00	0.88		-0.9424	0.0009	0.043	0.63		x	
Fernow	56	0.1340	0.0021	0.06	0.06		-4.7788	0.0025	0.196	0.03	*	x	
Fraser	43	0.3619	-0.0008	0.00	0.74		-0.1736	0.0003	0.020	0.86			
Hubbard Brook	50	0.3598	0.0041	0.10	0.02	*	-7.4300	0.0040	0.229	0.02	*		
Luquillo	35	0.7240	-0.0010	0.00	0.80		2.7407	-0.0010	-0.066	0.59		x	
Marcell	45	0.1424	-0.0017	0.05	0.14		1.8444	-0.0009	-0.101	0.33			
Niwot Ridge	21	0.4066	0.0233	0.31	0.01	*	-48.9970	0.0249	0.395	0.01	*		
WS2	54	2.4630	-0.0010	0.03	0.21								
WS8	43	1.1130	0.0000	0.00	0.72								
WS9	38	3.1530	-0.0010	0.03	0.32								
Fall Base Q/P													
Coweeta WS 18	73	0.2865	-0.0009	0.02	0.25		1.6637	-0.0007	-0.096	0.23			
Coweeta WS 27	61	0.4512	-0.0009	0.01	0.39		1.9637	-0.0008	-0.055	0.53		x	
Fernow	56	0.0505	0.0010	0.08	0.04	*	-2.1394	0.0011	0.205	0.03	*	x	x
Fraser	43	0.3555	-0.0010	0.00	0.70		-0.1968	0.0003	0.019	0.87			
Hubbard Brook	50	0.1446	0.0014	0.07	0.06		-2.6371	0.0014	0.162	0.10			
Luquillo	35	0.2813	-0.0007	0.01	0.66		1.1555	-0.0005	-0.044	0.72		x	
Marcell	45	0.0836	-0.0016	0.15	0.01	*	1.7429	-0.0009	-0.202	0.05	*		
Niwot Ridge	21	0.3979	0.0204	0.27	0.02	*	-37.5190	0.0191	0.443	0.01	*		
Fall Q													
Coweeta WS 18	73	106.4600	0.5388	0.02	0.26		-317.9400	0.2113	0.049	0.55			
Coweeta WS 27	61	303.4100	0.6130	0.00	0.64		-123.9000	0.2205	0.020	0.83			
Fernow	56	45.7120	0.7681	0.05	0.11		-1435.1000	0.7500	0.171	0.06			
Fraser	41	30.7230	0.2033	0.04	0.24		-199.2700	0.1177	0.066	0.55			
Hubbard Brook	50	125.2400	2.1361	0.09	0.03	*	-2.6371	0.0014	0.162	0.10			
Luquillo	35	735.8000	0.0875	0.00	0.99		450.6700	0.1111	0.005	0.98			
Marcell	45	31.6190	0.0347	0.00	0.91		142.8000	-0.0564	-0.031	0.77		x	
Niwot Ridge	21	136.4000	2.7085	0.16	0.07		-6311.0000	3.2500	0.324	0.04	*	x	
WS2	54	1974.3040	-0.9120	0.02	0.34								
WS8	43	1070.0820	-0.4740	0.00	0.69								
WS9	38	2402.5550	-1.1220	0.01	0.49								
Fall Base Q													
Coweeta WS 18	73	89.3430	0.2701	0.01	0.46		-24.5110	0.0520	0.013	0.88			
Coweeta WS 27	61	180.2500	-0.1303	0.00	0.84		595.2300	-0.2196	-0.022	0.80		x	
Fernow	56	16.5180	0.3416	0.07	0.05	*	-586.2700	0.3060	0.194	0.04	*	x	x
Fraser	41	29.9820	0.1832	0.03	0.27		-159.9300	0.0972	0.052	0.64			
Hubbard Brook	50	50.0390	0.7101	0.09	0.04	*	-1338.1000	0.7105	0.203	0.04	*		
Luquillo	35	281.5100	-0.4979	0.00	0.79		377.6700	-0.0556	-0.008	0.95			
Marcell	45	20.0160	-0.2565	0.07	0.08		539.0700	-0.2667	-0.191	0.07		x	
Niwot Ridge	21	132.3400	2.1424	0.12	0.12		-2794.7000	1.4770	0.233	0.15		x	
WS2	54	585.4000	-0.2680	0.01	0.42								
WS8	43	430.2000	-0.1960	0.01	0.01								
WS9	38	1187.2000	-0.5740	0.04	0.21								

Table 3.4 cont.

D cont.

	Linear Regression						Mann-Kendall					Auto-correlation	Residual Autocorrelation
	N	Intercept	Slope	R2	P	Sig	Intercept	Slope	Tau	P	Sig		
Fall Precipitation													
Coweeta WS 18													
Coweeta WS 27	73	321.99	2.0025	0.08	0.02	*	-3346.10	1.8820	0.185	0.02	*		
Fernow	56	280.46	0.7169	0.02	0.31		-1431.60	0.8763	0.112	0.23			
Fraser	26	124.79	0.4776	0.01	0.65		-1200.70	0.6667	0.095	0.51		x	
Hubbard Brook	52	325.14	1.3245	0.05	0.12		-2217.90	1.3020	0.135	0.16			
Luquillo	35	1023.60	1.2950	0.00	0.82		-117.67	0.5556	0.015	0.91		x	
Marcell	47	179.79	0.8861	0.03	0.21		-1392.90	0.8049	0.092	0.37			
Niwot Ridge	54	143.16	2.8614	0.22	0.00	*	-5644.90	2.9610	0.350	0.00	*	x	x
CS2MET	49	4321.35	-1.8750	0.02	0.38								
Fall Max Temperature													
Coweeta WS 18													
Coweeta WS 27	73	20.6670	-0.0006	0.00	0.92		21.00	0.0000	-0.046	0.55			
Fernow	53	15.4170	0.0034	0.00	0.78		16.00	0.0000	0.029	0.76			
Fraser	25	8.7753	0.0431	0.07	0.20		9.00	0.0000	0.190	0.18		x	
Hubbard Brook	52	11.5200	0.0071	0.01	0.51		12.00	0.0000	0.053	0.57			
Luquillo	35	25.0740	0.0729	0.59	0.00	*	-91.18	0.0588	0.437	0.00	*	x	x
Marcell	47	10.2100	0.0003	0.00	0.98		10.00	0.0000	0.031	0.76			
Niwot Ridge	54	1.8396	-0.0381	0.10	0.02	*	64.86	-0.0323	-0.219	0.02	*	x	x
CS2MET	47	13.5730	-0.0181	0.03	0.25		13.00	0.0000	-0.079	0.42			
Fall Min Temperature													
Coweeta WS 18													
Coweeta WS 27	73	4.6428	0.0363	0.33	0.00	*	-59.7670	0.0333	0.389	0.00	*	x	
Fernow	53	4.0838	0.0188	0.06	0.09		4.0000	0.0000	0.145	0.11			
Fraser	25	-7.3157	0.0432	0.09	0.13		-7.0000	0.0000	0.120	0.39			
Hubbard Brook	52	2.6221	0.0106	0.02	0.31		3.0000	0.0000	0.123	0.19			
Luquillo	35	20.7460	0.0425	0.62	0.00	*	-44.4000	0.0333	0.445	0.00	*	x	x
Marcell	47	-0.9548	0.0174	0.03	0.26		-1.0000	0.0000	0.125	0.21			
Niwot Ridge	54	-5.0092	-0.0444	0.17	0.00	*	59.9830	-0.0333	-0.244	0.01	*	x	x
CS2MET	47	4.7503	0.0004	0.00	0.88		5.0000	0.0000	-0.043	0.65			

Table 3.4 cont.

E.

	Linear Regression						Mann-Kendall					Auto-correlation	Residual Autocorrelation
	N	Intercept	Slope	R2	P	Sig	Intercept	Slope	Tau	P	Sig		
Winter Q/P													
Coweeta WS 18	73	0.6087	0.0000	0.00	0.97		0.6200	0.0000	-0.011	0.89			
Coweeta WS 27	61	1.1190	0.0009	0.01	0.35		-0.4423	0.0008	0.061	0.49			
Fernow	56	0.6250	0.0025	0.15	0.00	*	-4.0333	0.0024	0.242	0.01	*	x	
Fraser													
Hubbard Brook	50	0.3675	0.0056	0.18	0.00	*	-10.1600	0.0054	0.302	0.00	*		
Luquillo	35	0.7076	0.0016	0.02	0.37		-2.1157	0.0014	0.081	0.50		x	
Marcell	45	0.0103	0.0002	0.01	0.59		0.0000	0.0000	-0.093	0.33			
Niwot Ridge													
WS2	55	1.1440	0.0000	0.00	0.85								
WS8	44	2.5530	-0.0010	0.01	0.62								
WS9	39	4.0140	-0.0020	0.01	0.47								
Winter Base Q/P													
Coweeta WS 18	73	0.4985	0.0003	0.00	0.80		0.5100	0.0000	0.008	0.92			
Coweeta WS 27	61	0.7143	0.0008	0.01	0.40		-0.5667	0.0007	0.056	0.53			
Fernow	56	0.2663	0.0014	0.14	0.00	*	-2.1594	0.0013	0.229	0.01	*		
Fraser													
Hubbard Brook	50	0.2078	0.0023	0.24	0.00	*	-4.2357	0.0023	0.336	0.00	*		
Luquilo	35	0.3280	0.0011	0.02	0.48		-0.5455	0.0005	0.047	0.70			
Marcell	45	0.0115	-0.0001	0.02	0.39		0.0000	0.0000	-0.122	0.18			
Niwot Ridge													
Winter Q													
Coweeta WS 18	73	330.2400	-0.5268	0.01	0.43		1489.6000	-0.5969	-0.069	0.39		x	
Coweeta WS 27	61	623.1800	-1.0785	0.02	0.33		3159.0000	-1.3060	-0.102	0.25		x	
Fernow	56	238.6200	0.0216	0.00	0.97		-35.4330	0.1333	0.027	0.77			
Fraser													
Hubbard Brook	50	116.0900	1.7563	0.07	0.06		-2712.3000	1.4380	0.242	0.01	*		
Luquillo	35	524.9900	4.2560	0.05	0.20		-8304.6000	4.4670	0.145	0.23		x	
Marcell	45	0.7988	0.0217	0.01	0.51		7.9080	-0.0039	-0.092	0.38			
Niwot Ridge													
WS2	55	4631.6510	-1.9660	0.01	0.44								
WS8	44	7927.1080	-3.6880	0.03	0.26								
WS9	39	9793.9570	-4.5650	0.03	0.30								
Winter Base Q													
Coweeta WS 18	73	265.9000	-0.2539	0.00	0.64		671.9400	-0.2017	-0.027	0.74		x	
Coweeta WS 27	61	389.2200	-0.5395	0.01	0.37		1621.7000	-0.6306	-0.092	0.30			
Fernow	56	100.8900	0.1025	0.01	0.58		-9.2067	0.0572	0.030	0.75		x	
Fraser													
Hubbard Brook	50	62.9410	0.6274	0.16	0.00	*	-1157.4000	0.6216	0.300	0.00	*		
Luquillo	35	224.4100	2.6322	0.14	0.03	*	-6376.9000	3.3450	0.279	0.02	*		
Marcell	45	0.9520	-0.0095	0.01	0.48		6.7933	-0.0033	-0.100	0.34			
Niwot Ridge													
WS2	55	2040.3000	-0.8920	0.02	0.35								
WS8	44	3458.4000	-1.6370	0.04	0.19								
WS9	39	5259.1000	-2.5260	0.06	0.12								

Table 3.4 cont.

E cont.

		Linear Regression					Mann-Kendall					Auto-	Residual
	N	Intercept	Slope	R2	P	Sig	Intercept	Slope	Tau	P	Sig	correlation	Autocorrelation
Winter Precipitation													
Coweeta WS 18													
Coweeta WS 27	73	544.27	-0.7571	0.01	0.31		2333.3000	-0.9181	-0.097	0.23			
Fernow	56	378.66	-1.1495	0.06	0.08		2570.2000	-1.1210	-0.149	0.11			
Fraser	26	125.66	0.8138	0.02	0.50		-1414.6000	0.7778	0.098	0.49			
Hubbard Brook	52	309.99	-0.2226	0.00	0.75		792.3800	-0.2500	-0.038	0.70			
Luquillo	35	738.94	4.3206	0.03	0.29		-9692.2000	5.2670	0.109	0.36		x	
Marcell	47	86.77	-0.2224	0.01	0.46		260.3600	-0.0909	-0.034	0.74			
Niwot Ridge	54	197.88	3.7982	0.23	0.00	*	-7613.0000	4.0000	0.379	0.00	*	x	
CS2MET	50	3318.55	-1.1640	0.00	0.72								
Winter Max Temperature													
Coweeta WS 18													
Coweeta WS 27	73	10.6220	0.0050	0.01	0.53		11.0000	0.0000	0.059	0.46			
Fernow	53	3.2573	-0.0032	0.00	0.84		4.0000	0.0000	0.001	0.99			
Fraser	25	-2.0653	0.0545	0.12	0.09		-125.2500	0.0625	0.297	0.03	*		
Hubbard Brook	52	-3.1261	0.0304	0.11	0.02	*	-43.7570	0.0211	0.219	0.02	*		
Luquillo	35	22.6970	0.0738	0.55	0.00	*	-113.3800	0.0690	0.551	0.00	*	x	x
Marcell	47	-8.3070	0.0722	0.21	0.00	*	-123.7100	0.0588	0.276	0.01	*		
Niwot Ridge	54	-8.1785	-0.0298	0.07	0.06		-9.0000	0.0000	-0.159	0.08			
CS2MET	47	4.3657	-0.0006	0.00	0.92		4.0000	0.0000	-0.052	0.60			
Winter Min Temperature													
Coweeta WS 18													
Coweeta WS 27	73	-2.7035	0.0129	0.03	0.18		-2.0000	0.0000	0.129	0.10		x	
Fernow	53	-6.4868	0.0132	0.01	0.44		-6.0000	0.0000	0.072	0.45		x	
Fraser	25	-17.4290	0.0463	0.06	0.24		-141.2500	0.0625	0.240	0.09			
Hubbard Brook	52	-12.3900	0.0443	0.14	0.01	*	-83.0780	0.0364	0.205	0.03	*		
Luquillo	35	18.6370	0.0416	0.51	0.00	*	19.0000	0.0000	0.400	0.00	*	x	
Marcell	47	-21.0800	0.0995	0.25	0.00	*	-212.5600	0.0976	0.335	0.00	*	x	x
Niwot Ridge	54	-14.7560	-0.0249	0.05	0.10		-15.0000	0.0000	-0.122	0.18		x	
CS2MET	47	-0.5372	0.0073	0.01	0.49		0.0000	0.0000	0.002	0.99			

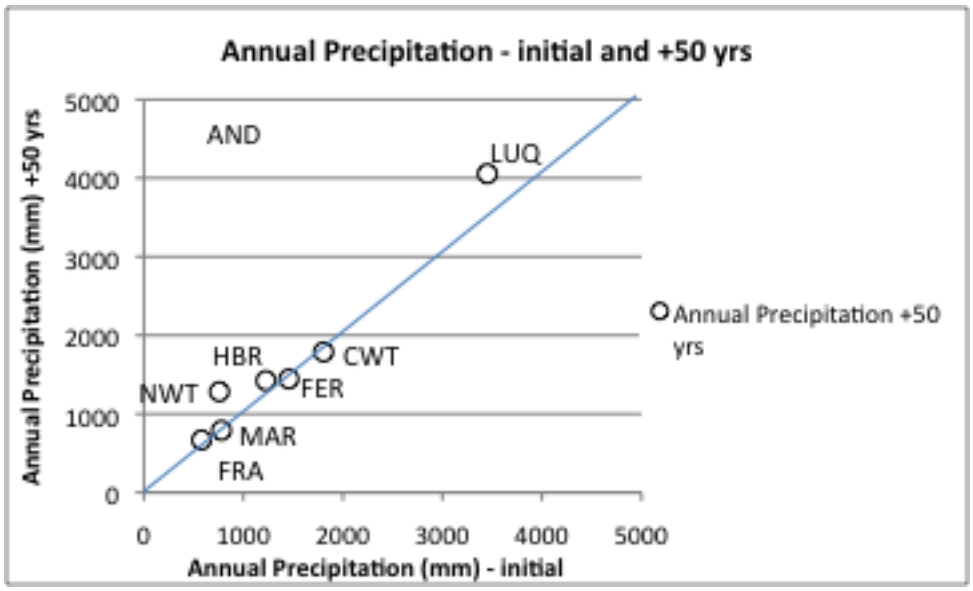

Figure 3.2 Changes in annual precipitation at study sites from the initial year of record to 50 years later (Table 3.1).

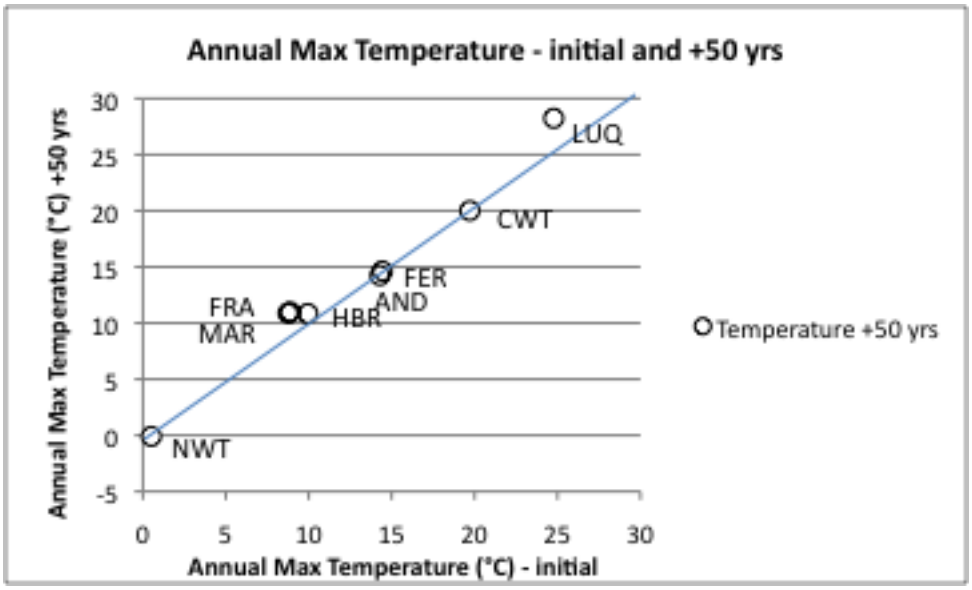

Figure 3.3 Changes in annual maximum temperature at study sites from the initial year of record to 50 years later (Table 3.1).

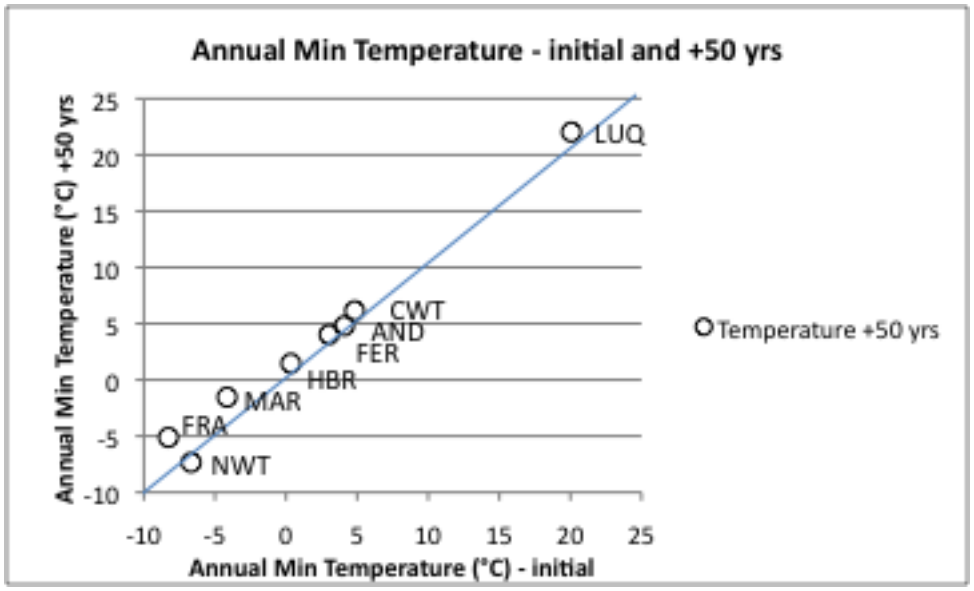

Figure 3.4 Changes in annual minimum temperature at study sites from the initial year of record to 50 years later (Table 3.4).

Annual total streamflow increased significantly at Hubbard Brook (Table 3.4a, Fig. 3.5). Annual increases occurred at Coweeta WS18, Fernow, Hubbard Brook, Luquillo, Marcell, and Niwot Ridge.

Annual baseflow increased at Coweeta WS18, Fernow, Hubbard Brook, Luquillo, and Niwot Ridge and decreased at Fraser, HJ Andrews WS2 , HJ Andrews WS8, HJ Andrews WS9, Coweeta WS27 and Marcell; the decreases at HJ Andrews WS8 and HJ Andrews WS9 were statistically significant (linear regression only) (Table 3.4a, Fig. 3.6).

Significant declines in annual runoff ratios occurred at Fernow, HJ Andrews WS8 (linear regression only), and Hubbard Brook (linear regression only). Annual runoff ratios also declined at HJ Andrews WS2, HJ Andrews WS9, Luquillo and Fraser. Increases occurred at Coweeta WS18 and WS27, Fernow, Niwot Ridge, Marcell and Hubbard Brook (Table 3.4a, Fig. 3.7).

Annual baseflow runoff ratios increased significantly at Fernow and Niwot Ridge (linear regression only) (Table 3.4a, Fig. 3.5). Annual baseflow runoff ratios decreased at Fraser and Marcell, but the decreases were not significant (Table 3.4a, 3.8).

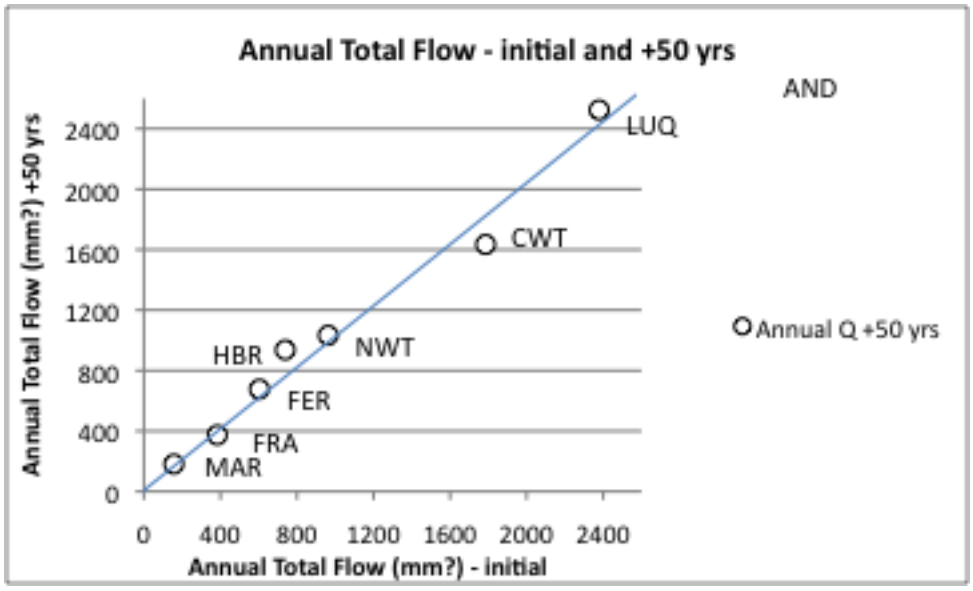

Figure 3.5 Changes in annual discharge at study sites from the initial year of record to 50 years later (Table 3.1).

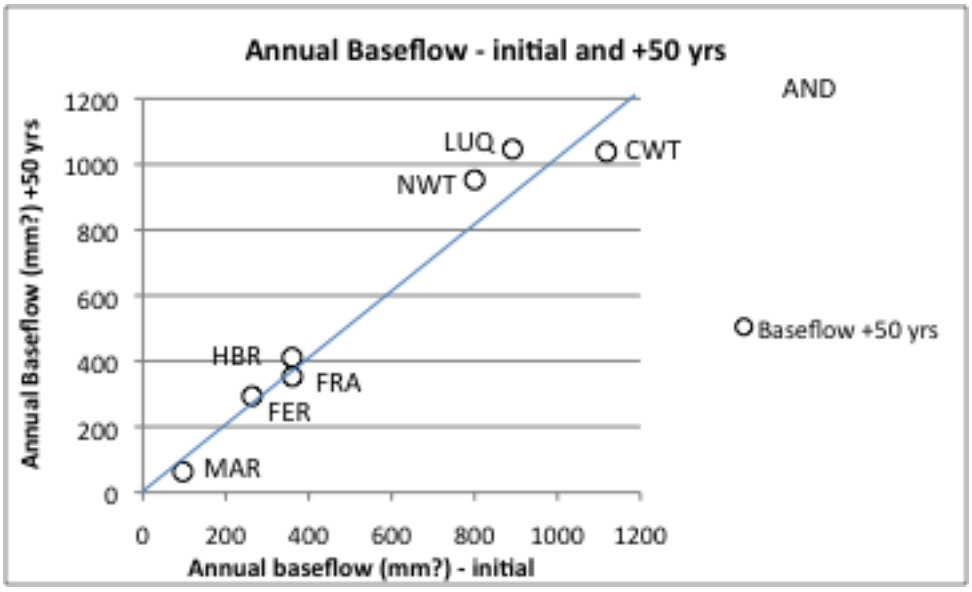

Figure 3.6 Changes in annual baseflow at study sites from the initial year of record to 50 years later (Table 3.1).

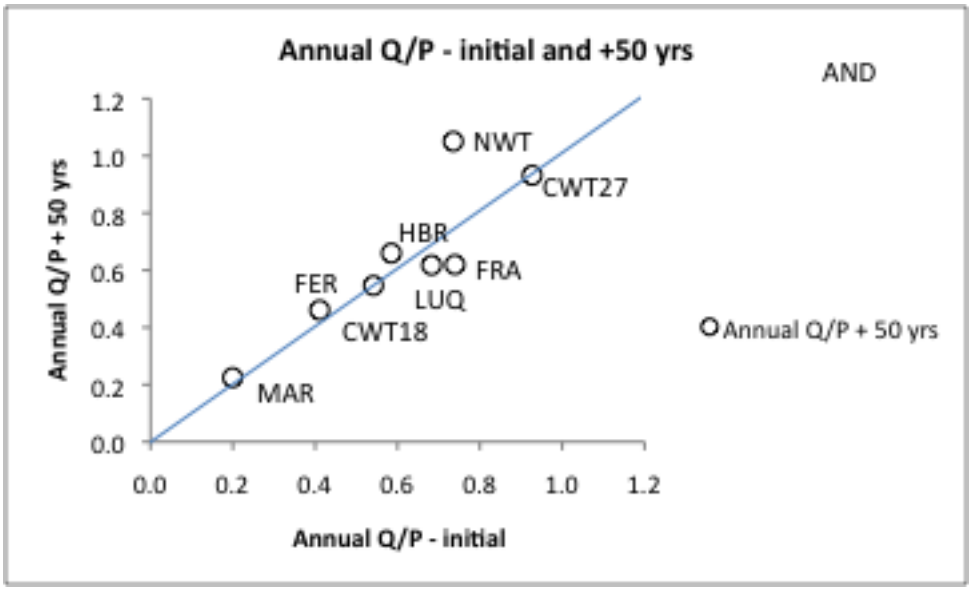

Figure 3.7 Changes in annual runoff ratios at study sites from the initial year of record to 50 years later (Table 3.1)

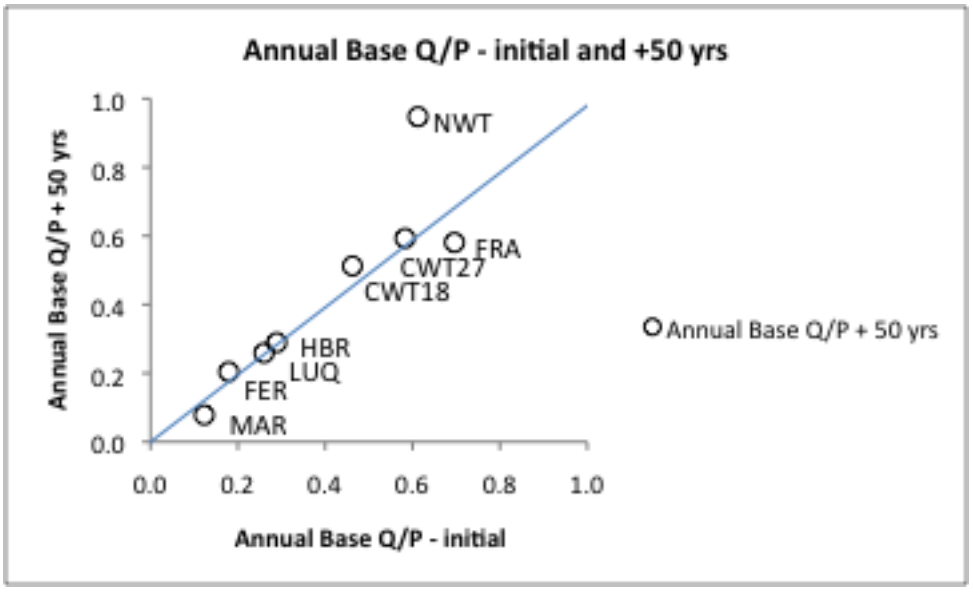

Figure 3.8 Changes in annual baseflow runoff ratios at study sites from the initial year of record to 50 years later (Table 3.1).

Change in spring temperature, precipitation, discharge, runoff ratios

Spring precipitation decreased at Coweeta, Fernow, and Marcell, and increased at Hubbard Brook, Fraser, Niwot Ridge, HJ Andrews, and Luquillo (Table 3.4b). Increases were significant at Niwot Ridge.

Maximum spring temperature increased significantly at Coweeta, Luquillo, and Marcell. Spring maximum temperature increased at all sites based on the Mann-Kendall test. Spring maximum temperature decreased at Fernow and Niwot Ridge based on linear regression analysis, but the trends were not significant (Table 3.4b).

Spring minimum temperature increased at all sites. Spring minimum temperature increased significantly at Coweeta, Luquillo, Marcell, HJ Andrews and Fraser (linear regression only) (Table 3.4b).

Spring discharge declined at Coweeta WS18 and WS27, Fraser, Hubbard Brook, and Marcell, HJ Andrews WS2, HJ Andrews, WS8, and HJ Andrews WS9. Decreases were significant at Fraser and HJ Andrews WS2 (linear regression only). Increases occurred at Fernow. Luqillo discharge decreased with linear regression analysis, but increased with the Mann-Kendall test; the trends were not significant (Table 3.4b).

Spring baseflow discharge declined at Coweeta WS18 and WS27, Fraser, Hubbard Brook, and Marcell, HJ Andrews WS2, HJ Andrews WS8, and HJ Andrews WS9. Decreases were significant at Fraser, HJ Andrews WS2 (linear regression only)

and HJ Andrews WS8 (linear regression only). Baseflow discharge increased at Luquillo and Fernow (Table 3.4b).

Spring runoff ratios decreased at Coweeta WS18 and WS27, Hubbard Brook, Fraser, Luquillo, HJ Andrews WS2 (linear regression only), HJ Andrews WS8 (linear regression only), HJ Andrews WS9 (linear regression only). Runoff ratios were not available for Niwot Ridge in the spring. From the Mann-Kendall test, spring runoff ratios were positive at all sites except for Fraser and Hubbard Brook. The declines at Hubbard Brook, Fraser (Mann-Kendall only), HJ Andrews WS2 (linear regression only), HJ Andrews WS8 (linear regression only), and HJ Andrews WS9 (linear regression only) were significant (Table 3.4b).

Spring baseflow runoff ratios decreased at Fraser, Hubbard Brook, and Marcell. Declines were significant at Hubbard Brook and Fraser (Mann-Kendall only). Coweeta WS 18 showed declines with linear regression analysis, but the Mann-Kendall test trend increased. The trends were not significant (Table 3.4b).

Change in summer temperature, precipitation, discharge, runoff ratios

Summer precipitation increased at all sites except for Coweeta. Luqillo precipitation increased with the Mann-Kendall test, but decreased with linear regression analysis. There were no significant trends in summer precipitation at any site (Table 3.4c).

Summer maximum temperature increased at all sites with the Mann-Kendall test, but Fraser and HJ Andrews showed declines with linear regression analysis. The declines were significant at Luquillo and Marcell (Mann-Kendall only) (Table 3.4c).

Summer minimum temperature increased at all sites. Significant increasing summer minimum trends occurred at Coweeta, Fernow, Luquillo, Marcell, and Fraser (Table 3.4c).

Summer discharge decreased at Coweeta WS27, Fraser, Niwot Ridge. Increases occurred at Fernow, Hubbard Brook, and Marcell. Hubbard Brook showed significant increases in summer flow (Mann-Kendall only). Coweeta WS18 increased with linear regression analysis, but declined with the Mann-Kendall test. Luquillo decreased with linear regression analysis, but increased with the Mann-Kendall test. Trends at Coweeta WS18 and Luquillo were not significant (Table 3.4c).

Summer baseflow discharge decreased at Coweeta WS27, Fraser, Niwot Ridge, and Marcell. Increases occurred at Fernow, and Hubbard Brook. Hubbard Brook showed significant increases in summer flow (Mann-Kendall only). Coweeta WS18 increased with linear regression analysis, but declined with the Mann-Kendall test. Luquillo decreased with linear regression analysis, but increased with the Mann-Kendall test. Trends at Coweeta WS18 and Luquillo were not significant (Table 3.4c).

Summer runoff ratios decreased at Coweeta WS27, Niwot Ridge, Luquillo,

and HJ Andrews WS9. Summer runoff ratios increased at Coweeta WS18, Fernow, Fraser, Hubbard Brook, Marcell, HJ Andrews WS2 (linear regression only) and HJ Andrews WS8 (linear regression only). Increases were significant for total flow runoff ratios at Hubbard Brook (Table 3.4c).

Summer baseflow ratios decreased at Marcell and Niwot Ridge. Summer baseflow runoff ratios at Coweeta WS27 declined with linear regression analysis, but increased with Mann-Kendall; the trends were not significant. Summer baseflow runoff ratios increased at Coweeta WS18, Fernow, Fraser, Hubbard Brook, and Luquillo. Increasing trends were significant at Hubbard Brook (Mann-Kendall only) (Table 3.4c).

Change in fall temperature, precipitation, discharge, runoff ratios

Fall precipitation increased at all sites except HJ Andrews (linear regression only). Increases were significant at Coweeta and Niwot Ridge (Table 3.4d).

Fall maximum temperature increased at all sites except Coweeta and Niwot Ridge. Increases were significant at Luquillo, and decreases at Niwot Ridge were significant. Fall maximum temperature at HJ Andrews decreased with linear regression analysis, but increased with Mann-Kendall analysis; the trends were not significant (Table 3.4d).

Fall minimum temperature increased at all sites except Niwot Ridge. Fall minimum temperature increased significantly at Coweeta and Luquillo, and decreased significantly at Niwot Ridge (Table 3.4d).

Fall discharge increased at all sites except HJ Andrews WS2, WS8, and WS9 (linear regression only). Increases were significant at Hubbard Brook (linear regression only) and Niwot Ridge (Mann-Kendall only). Fall discharge at Marcell increased with linear regression analysis, but decreased with the Mann-Kendall test; the trends were not significant (Table 3.4d).

Baseflow declined at Coweeta WS27, Luquillo, Marcell and HJ Andrews WS2, WS8, and WS9 (linear regression only) . Fall baseflow increased significantly at Hubbard Brook and Fernow (Table 3.4d).

Fall runoff ratios decreased at Coweeta WS18, Luquillo, Marcell, and HJ Andrews WS2 and WS9 (linear regression only). Fall runoff ratios increased at Coweeta WS27, Fernow, Hubbard Brook, Niwot Ridge, and HJ Andrews WS8. Increases were significant at Fernow (Mann-Kendall only), Hubbard Brook, and Niwot Ridge. Fall runoff ratios at Fraser decreased with linear regression analysis, but increased with the Mann-Kendall test; the trends were not significant (Table 3.4d).

Fall baseflow runoff ratios declined at all sites except Fernow, Hubbard Brook, and Niwot Ridge. The increases at Fernow and Niwot Ridge were significant. Declines at Marcell were significant. Fall baseflow runoff ratios at Fraser decreased

with linear regression analysis, but increased with the Mann-Kendall test; the trends were not significant (Table 3.4d).

Change in winter temperature, precipitation, discharge, runoff ratios

Winter precipitation increased at Luquillo, Niwot Ridge, and Fraser, and decreased at Coweeta, Fernow, Hubbard Brook, and Marcell. Increases were significant at Niwot Ridge (Table 3.4e).

Winter maximum temperature increased at all sites with the Mann-Kendall test, but linear regression showed declines at Fernow, Niwot Ridge, and HJ Andrews. Increases were significant at Hubbard Brook, Luquillo, Marcell, and Fraser (Mann-Kendall only) (Table 3.4e).

Winter minimum temperature increased at all sites. The increase was statistically significant at Hubbard Brook, Luquillo, and Marcell. Winter minimum temperature at Niwot Ridge decreased with linear regression analysis, but increased with the Mann-Kendall test; the trends were not significant (Table 3.4e).

Winter discharge decreased at Coweeta WS18 and WS27 and HJ Andrews WS2, WS8, and WS9. Winter discharge increased at Fernow, Hubbard Brook, and Luquillo. Winter discharge at Hubbard Brook increased significantly (Mann-Kendall only). Fraser and Niwot Ridge had no winter discharge data due to frozen conditions. Winter discharge at Marcell increased with linear regression analysis, but decreased with the Mann-Kendall test; the trends were not significant (Table 3.4e).

Winter baseflow decreased at Coweeta WS18 and WS27, Marcell, and HJ Andrews WS2, WS8, and WS9. Winter discharge increased at Fernow, Hubbard Brook, and Luquillo. Winter baeflow at Hubbard Brook and Luquillo increased significantly. Fraser and Niwot Ridge had no winter baseflow data due to frozen conditions (Table 3.4e).

Winter runoff ratios increased at all sites except HJ Andrews WS8 and WS9. Increases were significant at Fernow and Hubbard Brook. Winter runoff ratios were not available for Niwot Ridge and Fraser (Table 3.4e).

Winter baseflow runoff ratios increased at all sites. Increases were significant at Fernow and Hubbard Brook. Winter baseflow ratios were not available for Niwot Ridge and Fraser. Winter baseflow ratios at Marcell decreased with linear regression analysis, but increased with the Mann-Kendall test; the trends were not significant (Table 3.4e).

3.4.2 Trends by site

Each of the study sites experienced distinct trends in temperature, precipitation, discharge, and runoff ratios. Trends are described by site, from warm moist climates to cool dry climates. All changes in discharge and runoff ratios are from "reference" watersheds which were not disturbed during the study period, although they experienced disturbances prior to the study period.

Warm moist: Luquillo

Luquillo, which has a warm, moist climate, has experienced a strong warming signal in all seasons, but no change in precipitation or discharge over the period from 1975 to 2010 (temperature, precipitation) and 1966-2010 (discharge).

Mesic temperate, little or no seasonal snow: Coweeta

Coweeta, which has a mesic temperate climate, experienced a strong climate warming signal (1937-2009) and increasing precipitation (1937-2009), but no response in discharge over the period 1937 to 2009.

Mesic temperate, little or no seasonal snow: Fernow

Fernow, which has a mesic temperate climate, experienced a climate warming signal in minimum temperature, no change in precipitation or discharge (except fall baseflow), but a strong increase in runoff ratios (total flow and baseflow) over the period 1951 to 2007.

Mesic temperate with seasonal snow: Hubbard Brook

Hubbard Brook, which has a mesic temperate climate with a seasonal snowpack, has experienced a climate warming signal in annual and winter temperature, and an increase in annual precipitation, accompanied by increases in annual discharge and baseflow; fall baseflow; winter discharge, baseflow, runoff ratios

and baseflow runoff ratios; and summer discharge, baseflow, runoff ratios and baseflow runoff ratios, over the period 1957 to 2007.

Mesic temperate with seasonal snow: Marcell

Marcell, which has a mesic temperate climate with seasonal snow, experienced a strong warming signal in winter, spring, and summer, no trend in precipitation, and no trends in annual discharge, baseflow, runoff ratios, or baseflow runoff ratios over the period 1961 to 2008.

Xeric temperate, seasonal snow: Fraser

Fraser, which has a xeric temperate climate and seasonal snow, has experienced a strong warming signal in minimum temperature (1976-2001), no trend in precipitation (1976-2001), and declines in spring discharge, baseflow, and baseflow runoff ratios over the period 1943 to 1985.

Xeric temperate, seasonal to permanent snow: Niwot Ridge

Niwot Ridge, which has a xeric temperate climate with seasonal and permanent snow, has experienced no trend in temperature (1952-2006) except cooler fall, a strong increase in precipitation (1952-2006) year-round, and an increase in fall baseflow runoff ratio but not baseflow over the period 1981 to 2002.

Xeric temperate, seasonal and transient snow: HJ Andrews

HJ Andrews, which as a xeric temperate climate with seasonal and transient snow, has experienced strong warming signal in spring temperature (1958-2007), no change in precipitation (1958-2007), and a decline in spring discharge, baseflow, and runoff ratios over the period 1953-2007 (Moore 2010).

3.4.3 Autocorrelation tests

Autocorrelation in seasonal and annual precipitation

Annual precipitation data was autocorrelated at a lag of 1 year at Niwot Ridge only. The residuals from linear regression of precipitation over time at Niwot Ridge were autocorrelated at a lag of 2 years. Spring precipitation data at Fernow were autocorrelated at a lag of 4 years. Spring data at Niwot Ridge were autocorrelated at a lag of 1 year, and the residuals of regressions were autocorrelated at a lag of 2 years. Summer data at Luquillo were slightly negatively autocorrelated at a lag of 4 years. Niwot Ridge summer data were autocorrelated at a lag of 2 years. Fall precipitation data at Fraser were slightly autocorrelated at a lag of 1 year. Luqillo fall and winter data were slightly negatively autocorrelated at a lag of 4 years, and Niwot Ridge fall and winter data were autocorrelated at 1 year. The residuals from linear regression of fall precipitation at Niwot Ridge also were autocorrelated at a lag of 1 year, but the residuals of the winter data were not autocorrelated (Table 3.4).

Autocorrelation in seasonal and annual temperature

Annual minimum temperature at Coweeta and the residuals of regressions of temperature over time at Coweeta were autocorrelated at a lag of 1 year. Maximum annual temperature at Fernow was autocorrelated. Minimum temperature at Fernow was autocorrelated at a lag of 1 year, as were the residuals from linear regressions of minimum temperature over time. Maximum and minimum annual temperature at Luquillo was autocorrelated at a lag of 1 year, as were the residuals of regressions of temperature over time. Annual minimum temperature at Marcell was slightly autocorrelated at a lag of 1 year, but the residuals were not autocorrelated. Maximum and minimum annual temperature at Niwot Ridge was autocorrelated at a lag of 1 year (Table 3.4a).

Spring minimum temperature at Coweeta was autocorrelated at a lag of 1 year, but the residuals were not autocorrelated. Spring maximum temperature at Fernow was slightly negatively autocorrelated at a lag of 7 years. Spring maximum and minimum temperature at Luquillo was autocorrelated at a lag of 1 year, and the residuals of linear regressions of minimum temperature over time were negatively autocorrelated at a lag of 10 years. Spring maximum temperature at Marcell was autocorrelated at a lag of 1 year, and the residuals were slightly autocorrelated at a lag of 1 year (Table 3.4b).

Summer minimum temperature at Coweeta was autocorrelated at a lag of 1 year, and the residuals were autocorrelated at a lag of 2 years. Summer minimum

temperature at Fernow was autocorrelated at a lag of 1 year, and the residuals were autocorrelated at a lag of 2 years. Summer maximum temperature at Fraser was slightly negatively autocorrelated at a lag of 4 years. Summer minimum temperature at Hubbard Brook was autocorrelated at a lag of 1 year. Both maximum and minimum summer temperature at Luquillo were autocorrelated at a lag of 1 year, but the residuals were not autocorrelated. Summer minimum temperature at Marcell was autocorrelated at lag of 4 years, and the residuals were slightly negatively autocorrelated at a lag of 9 years. Summer maximum temperature at Niwot Ridge was autocorrelated at a lag of 3 years, and summer minimum temperature was autocorrelated at a lag of 4 years (Table 3.4c).

Fall minimum temperature at Coweeta was autocorrelated at 1 year, but the residuals were not autocorrelated. Fraser maximum temperature was slightly negatively correlated at 5 years. Fall maximum and minimum temperature was autocorrelated at a lag of 1 year at Luquillo and Niwot Ridge. The residuals from regression over time for Luquillo fall maximum and minimum temperature were correlated at a lag of 1 year. The residuals from regression over time from Niwot Ridge fall maximum temperature were correlated at a lag of 2 years, while the residuals from regression over time from minimum data were correlated at a lag of 1 year (Table 3.4c).

Winter minimum temperature was autocorrelated at a lag of 1 year at Coweeta. Winter minimum temperature at Fernow was autocorrelated at a lag of 1 year.

Minimum and maximum temperature at Luquillo was autocorrelated at 1 year. The residuals of Luquillo winter maximum temperature were negatively autocorrelated at a lag of 7 years, but the residuals were not autocorrelated. Winter minimum temperature at Marcell and Niwot Ridge was slightly autocorrelated at a lag of 1 year. The residuals from Marcell winter minimum temperature were negatively autocorrelated at a lag of 2 years (Table 3.4e).

Autocorrelation in annual and seasonal discharge

Annual total flow and baseflow at Coweeta WS18 and WS27 were autocorrelated at a lag of 1 year. Fraser annual total flow and baseflow data were negatively correlated at a lag of 6 years. Luquillo total flow was very slightly negatively correlated at a lag of 5 years (Table 3.4a).

Spring baseflow at Fernow was negatively correlated at a lag of 4 years. Fraser spring baseflow was slightly correlated at a lag of 4 years, but the residuals of regressions of baseflow over time were not correlated. Marcell spring total flow was negatively correlated at a lag of 2 years. Summer total flow at Fraser was slightly negatively correlated at a lag of 7 years. Coweeta fall baseflow was negatively correlated at a lag of 4 years. Fall baseflow at Fraser, as well as the residuals of regression through time were negatively autocorrelated at a lag of 7 years. Fall total flow at Marcell was negatively correlated at a lag of 2 years, and baseflow was autocorrelated at a lag of 4 years. Fall total flow and baseflow at Niwot Ridge were autocorrelated at a lag of 1 year, but the residuals of regressions of total flow were not

autocorrelated. Winter total flow and baseflow were correlated at a lag of 1 year for Coweeta WS18. Winter total flow at Coweeta WS27 was slightly negatively correlated at a lag of 6 years. Winter baseflow at Fernow was autocorrelated at a lag of 7 years. Winter total flow at Luquillo was autocorrelated at a lag of 1 year, and negatively autocorrelated at a lag of 4 years. Fraser and Niwot Ridge winter flow were not tested due to the lack of winter data (Table 3.4).

Autocorrelation in annual and seasonal runoff ratios

Annual total flow and baseflow runoff ratios at Coweeta WS18 were autocorrelated at a lag of 1 year. Fernow annual total flow runoff ratios were correlated at a lag of 7 years, but the residuals of regression through time were not autocorrelated. Marcell annual total flow runoff ratios were negatively autocorrelated at a lag of 2 years (Table 3.4a).

Spring total flow and baseflow runoff ratios at Coweeta WS18 were both negatively autocorrelated at a lag of 6 years. Fraser spring total flow and baseflow runoff ratios were autocorrelated at a lag of 8 years, and the residuals of regression through time from both datasets were also autocorrelated a lag of 8 years. Spring total flow and baseflow runoff ratios from Hubbard Brook were autocorrelated at a lag of 4 years. The residuals of regression from both datasets were negatively autocorrelated at a lag of 5 years, but baseflow runoff ratios also were autocorrelated at a lag of 6 years. Coweeta summer baseflow runoff ratios were autocorrelated at a lag of 7 years. Summer total flow runoff ratios at Hubbard Brook were negatively autocorrelated at a

lag of 10 years, and the residuals were negatively autocorrelated at a lag of 4 years. Summer baseflow runoff ratios from Hubbard Brook were autocorrelated at a lag of 6 years, and the residuals of regression were autocorrelated at a lag of 4 years. Both fall total flow and baseflow runoff ratios from Coweeta WS27 were autocorrelated at a lag of 1 year and negatively autocorrelated at a lag of 4 years. Fall total flow runoff ratios at Fernow were slightly autocorrelated at a lag of 1 year, but the residuals of regression were not autocorrelated. Fall baseflow runoff ratios at Fernow were autocorrelated at a lag of 7 years, and the residuals of regression were also autocorrelated at a lag of 7 years. Both fall total flow and baseflow runoff ratios at Luquillo were autocorrelated at a lag of 5 years. Winter total flow runoff ratios were autocorrelated at a lag of 2 years at Fernow, but the residuals of regression were not autocorrelated. Luquillo winter total flow ratios were autocorrelated at a lag of 1 year (Table 3.4).

3.4.4 Trends in climate and discharge by day of water year

Climate and hydrologic variables may have changed over periods of only a few days, rather than for seasonal or annual averages. Significant trends by day of water year are described below for each of the climate variables (precipitation, maximum and minimum temperature), by site. The mention of a month indicates that one or more days in that month experienced the trend described (Appendices D-F).

Precipitation by day

Results presented are from the log-transformed data. Precipitation at Coweeta increased significantly in December, April, and May, and decreased significantly in February and March. Precipitation at Fernow increased significantly in October, November, March, and July, and decreased significantly in October, December, April, and August. Precipitation at Fraser increased significantly in October, April, and July. Precipitation at Luquillo increased significantly in November, December, March, April, June, and July. Precipitation at Marcell increased significantly in October, December, March, June, July, and September. Precipitation at Niwot Ridge increased significantly in November to January, and April, and decreased significantly in February and May through September. Precipitation at HJ Andrews increased significantly in May and October, and decreased significantly in April (Appendix D).

Maxmimum and minimum temperature by day

Maximum daily temperature at Coweeta increased significantly in December, March, July, and August. Minimum temperature increased significantly throughout the year, except in January (Appendix E, Fig E.1). The last day of freezing has moved significantly earlier (0.54 days/year), but the first day also has moved significantly earlier in the water year (0.05 days/year).

Maximum daily temperature at Fernow increased significantly in December, March, July, and August, and decreased significantly in October and February.

Minimum daily temperature increased significantly in November, December, February, March, July, and August, and decreased significantly in March (Appendix E, Fig. E.2). The last day of freezing has moved significantly earlier (1.05 days/year), and the first day of freezing in the water year also has moved significantly earlier (0.59 days/year).

Maximum daily temperature at Fraser increased significantly in November, January, and March. Minimum daily temperature at Fraser increased significantly throughout the year. The last day of freezing has moved significantly earlier (1.98 days/year), and the first day of freezing in the water year also has moved significantly earlier (0.78 days/year) (Appendix E, Fig. E.3).

Maximum daily temperature at Hubbard Brook increased significantly in December, February-April, and June-August. Minimum daily temperature at Hubbard Brook increased significantly in December-August (Appendix E, Fig. E.4) The last day of freezing has moved significantly earlier (1.14 days/year), but the first day of freezing temperature has not changed (0.01 days/year).

Maximum and minumum daily temperature at Luquillo increased significantly throughout the year (Appendix E, Fig. E.6).

Maximum and minimum daily temperature at Marcell increased significantly from December-September. Maximum and minimum daily temperature decreased significantly in October (Appendix E, Fig. E.7). The last day of freezing has moved

earlier in the water year (0.31 days/year), and the first day of freezing in the water year also has moved earlier (0.27 days/year).

Maximum daily temperature at Niwot Ridge increased significantly in July and August, and decreased significantly in December, February, and March. Minimum daily temperature increased significantly in March, July, and August, and decreased significantly in December, February, and March (Appendix E, Fig. E.8). Neither the last day of freezing (0 days/yr) nor the first day of freezing (0.02 days/year) have changed.

Maximum daily temperature at HJ Andrews increased significantly in January, March, and April, and decreased significantly in October. Minimum temperature increased in October-January, March-May, and July, and decreased significantly in June and September (Appendix E, Fig. E.5). The last day of freezing has moved earlier in the water year (0.71 days/year), and the first day of freezing in the water year also has moved earlier (0.33 days/year).

Discharge by day

Results presented are from the log-transformed data. Coweeta WS 18 did not show any significant trends by day in total flow or baseflow discharge (Appendix F, Fig. F.1-2). Total flow at Coweeta WS27 increased significantly in December, and decreased significantly in February and July (Appendix F, Fig. F.3). Baseflow at Coweeta WS27 decreased significantly in February and March (Appendix F, Fig. F.4).

Total flow at Fernow increased significantly in October, February, and July (Appendix F, Fig. F.5). Fernow baseflow increased significantly in July, September, and October-January (Appendix F, Fig. F.6). Total flow at Hubbard Brook increased significantly in June through January, and March, and decreased significantly in April (Appendix F, Fig. F.7). Baseflow at Hubbard Brook increased significantly in June-September, December, January, and March, and decreased significantly in April (Appendix F, Fig. F.8). Total flow at Luquillo increased significantly in October, January, April, and September (Appendix F, Fig. F.9). Baseflow at Luquillo increased significantly in April, May, and September (Appendix F, Fig. F.10). Total flow at Marcell increased significantly in April and declined significantly in June, August, and September (Appendix F, Fig. F.11). Baseflow at Marcell could not be analyzed with the MATLAB program due to prevalence of zero values in baseflow data. Total flow and baseflow at HJ Andrews WS2 decreased significantly in April (Appendix F, Fig. F.12-13). HJ Andrews WS8 had no significant trends in total flow or baseflow (Appendix F, Fig. F.14-15). Total flow at HJ Andrews WS9 declined significantly in June, August, and September (Appendix F, Fig. F.16). WS9 baseflow declined significantly in August and September (Appendix F, Fig. F.17). Daily discharge from Fraser and Niwot Ridge could not be analyzed with the MATLAB program due to missing values from the winter period.

3.5 Discussion

3.5.1 Methodological issues

Effects of autocorrelation on the results

The presence of autocorrelation in climate and streamflow data can bias the detection of trends. Autocorrelated data are not independent, so the true degrees of freedom are overestimated, leading to an overestimate of the significance of trends fitted with linear regression.

Some of the datasets were autocorrelated; in these cases, residuals of linear trends fitted over time were also tested for autocorrelation. Variables that were autocorrelated tended to have autocorrelated residuals. Luquillo temperature data and the residuals of regression were correlated for annual, spring, fall, and winter time periods. Niwot Ridge precipitation data and the residuals from regression were autocorrelated for annual, spring, and fall time periods. Niwot Ridge temperature data and the residuals from regression were autocorrelated in the fall. Marcell temperature data and the residuals from regression were autocorrelated in the winter and summer. Coweeta temperature data and the residuals from regression were autocorrelated at the annual and summer time periods. Fraser runoff ratios and the residuals from regression were autorcorrelated in the spring. Fernow baseflow and baseflow runoff ratios and the residuals from regression were autocorrelated in the fall. Hubbard

Brook runoff ratios and baseflow runoff ratios were autocorrelated in the spring and summer.

Hoffmuller plots of raw daily data were examined to make a qualitative assessment of trends in the autocorrelated data. At Niwot, both Mann-Kendall and linear regression analyses indicated a positive trend in annual, fall, and spring precipitation, but these data and residuals from trends over time were significantly autocorrelated. These trends are not visually apparent in raw precipitation data from Niwot, and analyses by day indicate that only four days experienced increasing precipitation. At Marcell, both Mann-Kendall and linear regression analyses indicated a positive trend in annual, winter, and summer minimum temperature, but these variables and residuals from regressions over time were significantly autocorrelated. A warming trend is visually apparent in winter and summer minimum and spring maximum values at Marcell, minimum temperature increased on 20 days of the year, and the last day of freezing temperature moved earlier (0.31 days/year). At Coweeta, annual and summer minimum temperature increased significantly, but these variables and the residuals from regressions over time were autocorrelated. Analysis of daily data at Coweeta indicates that minimum daily temperature increased on many days of the year, and the last data of freezing has moved significantly earlier (0.54 days/year). The runoff ratios were not assessed on a daily basis; therefore Hoffmuller plots were not available.

Examination of the trend analyses by day of year and the raw daily data displayed in Hoffmuller plots indicate that significant trends from both linear regression and Mann-Kendall tests were supported only in some cases when the data were autocorrelated. Hence, there is reason to be cautious of accepting trends from autocorrelated data.

Differences between linear regression and Mann-Kendall

This study applied linear regression and the Mann-Kendall test to 280 datasets (8 sites, 5 time periods, and 7 variables). In almost all of these cases linear regression (including appropriate transformation of variables) and the Mann-Kendall test produced similar results. Sites and seasons displaying significant trends from linear regression also show significant trends from Mann-Kendall tests. Also, for statistically significant tests, the slope of the trend is similar between the Mann-Kendall and linear regression. In instances where one test is significant but the other is not, the slope of the trend is also similar.

In a few cases trends from linear regression do not agree with trends from the Mann-Kendall test. This appears to occur where the slope of the trend line is close to zero; one test may show a slight increasing trend, where the other test shows a slight decline. In these cases the p-value is greater than 0.20. The two tests agree in all cases that found statistically significant trends.

Unequal sample sizes

For this analysis the entire period of record was used for each variable (precipitation, temperature, discharge) at each site. Record lengths varied from 21 to 72 years. However, of the 24 sets of records (discharge, precipitation, and temperature records from each of 8 sites), only five (Niwot discharge, Fraser precipitation and temperature, Luquillo precipitation and temperature) were less than 40 years in length. Therefore, comparisons between sites are based on >40 years of record in almost all cases.

The records also cover largely overlapping periods; of the 24 sets of records, only four (Niwot discharge, Fraser discharge, precipitation, and temperature) ended before 2005. Therefore, the collection of records permits generalizations of climate trends over the period of approximately 1960-2010. Underlying interannual climate cycles might produce trends that are really cycles in records that are less than 40 years, such as precipitation and temperature trends at Fraser and Luqillo, or streamflow trends from Niwot Ridge.

Summary

Although tests of trends over time in climate and discharge in the recent literature are almost exclusively conducted using the Mann-Kendall test, this study showed that linear regression with appropriate transformation of variables produced similar results to the Mann-Kendall analysis. The Mann-Kendall corrects for undue

influence of outliers, and log-transformation of discharge and precipitation prior to linear regression also corrected for undue influence of extreme values.

Neither linear regression nor Mann-Kendall tests account for autocorrelated data, requiring a separate test. While most of the data was not autocorrelated, data from some sites was more likely to be autocorrelated. Trends from these data should be interpreted carefully, and significant trends may need to be discarded to err on the side of caution. Analysis of trends by day corroborated trends in the seasonal and annual data, and enabled detection of spurious trends. Trends in short (less than ~40 years) should also be interpreted carefully, as these trends may be a result of climatic cycles.

Despite these limitations of the data sets and the types of tests performed, this analysis can provide some insight to the climatic patterns observed and the hydrologic outcomes.

3.5.2 Observed, expected hydrologic responses to climate trends

Earlier snowmelt runoff

Most sites experienced increases in spring minimum air temperature. However, only a few sites experienced an associated change in runoff ratios (Fig. 3.9). HJ Andrews has near-zero spring air temperature, warming air temperature, and no change in precipitation. Spring runoff ratios declined at the HJ Andrews (Moore 2010). The last day of freezing temperature moved earlier in the year (0.71 days/year),

but runoff ratios or discharge in the winter did not increase. This could suggest reduced snow water equivalent (SWE), which has been found in the Cascade Mountains (Mote et al. 2003; Mote 2003a). This may also be a result of increased ET by vegetation. Warming temperature in the spring is expected to accelerate vegetation phenology. Cayan et al. (2001) showed that lilacs and honeysuckles, which are responsive to changes in temperature, are now blooming 5 to 10 days earlier than in the 1970s. Earlier leafout and associated earlier onset of evapotranspiration (ET) may reduce streamflow.

Sites with air temperature below freezing (cold snowpack) and above freezing (no snowpack) did not experience changes in spring runoff ratios. Hubbard Brook has a seasonal cold snowpack, but spring temperature did not increase. Summer discharge and baseflow did increase however. The last day of freezing temperature does not occur until the summer, so snowpack does not melt until the summer. Lack of summer warming or change in summer precipitation, combined with increases in summer discharge, baseflow, runoff ratios, and baseflow runoff ratios could also suggest decreased ET possibly from succession in control watersheds which were logged in the early 1900s and damaged by the 1938 hurricane (Jones and Post 2004). Warmer winter temperature with no change in winter precipitation explain the increases in winter discharge, baseflow, runoff ratios, and baseflow runoff ratios and are consistent with predictions of shift from snow to rain resulting from climate warming.

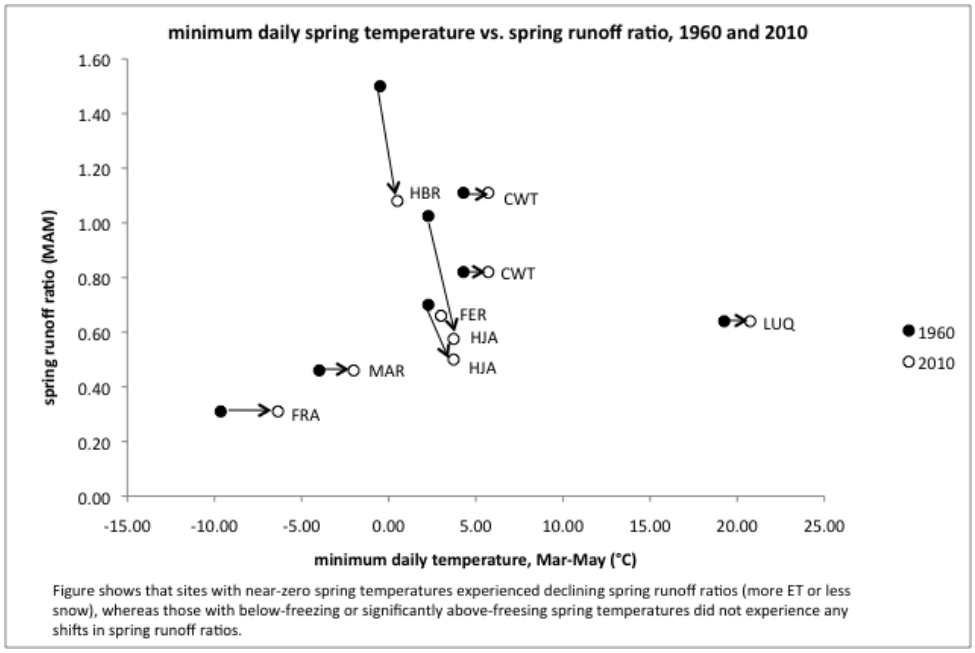

Figure 3.9 Changes in spring runoff ratio (Q/P) as a function of change in minimum daily spring temperature.

Fraser, which has a xeric temperate climate and seasonal snow, has experienced a strong warming signal in minimum temperature (1976-2001), no trend in precipitation (1976-2001), and declines in spring discharge, baseflow, and base runoff ratios over the period 1943 to 1985. This is the expected outcome for western mountain sites where spring warming is expected to decrease snowpacks and discharge. Contrary to predictions there is no increase in winter discharge or runoff ratios, nor any decline in summer discharge or runoff ratios at Fraser. This suggests that when the trees begin using water in late spring they compensate for drier soils by using less water.

Reduced spring discharge

The same mechanisms that have resulted in lower spring runoff ratios would result in lower spring discharge at HJ Andrews and Fraser. HJ Andrews has experienced strong warming signal in spring temperature (1958-2007), no change in precipitation (1958-2007), and declines in spring discharge, baseflow, and runoff ratios over the period 1953-2007. Decreased SWE and increased ET would lead to lower spring flow. Fraser has experienced a strong warming signal in minimum temperature (1976-2001), no trend in precipitation (1976-2001), and declines in spring discharge, baseflow, and base runoff ratios over the period 1943 to 1985. Reduced SWE and changes in water use by vegetation may cause a reduction in streamflow. Later in the summer ET may be reduced by decreases soil water content.

Increased fall baseflow

Niwot Ridge, which has a xeric temperate climate with seasonal and permanent snow, has experienced no trend in temperature (1952-2006) except cooler fall, no trend in precipitation (1952-2006), and an increase in fall baseflow runoff ratio but not baseflow over the period 1981 to 2002. The increase in fall baseflow runoff ratio is interpreted as a signal of permafrost melting (Mark Williams, pers. comm. 2010). This is the only nonforest site in the study.

3.5.3 Lack of expected hydrologic responses to climate warming

No reductions in summer discharge or baseflow despite summer warming

Most sites experienced increases in summer minimum air temperature. However, no sites experienced an associated change in summer runoff ratios (Fig. 3.10). Hubbard Brook did not experience significant increases in summer minimum temperature, although the trend was positive, and no change in precipitation, but summer discharge and baseflow increased significantly. Lack of summer warming or change in summer precipitation, combined with increases in summer discharge, baseflow, runoff ratios, and baseflow runoff ratios could also suggest decreased ET possibly from succession in control watersheds which were logged in the early 1900s and damaged by the 1938 hurricane (Jones and Post 2004).

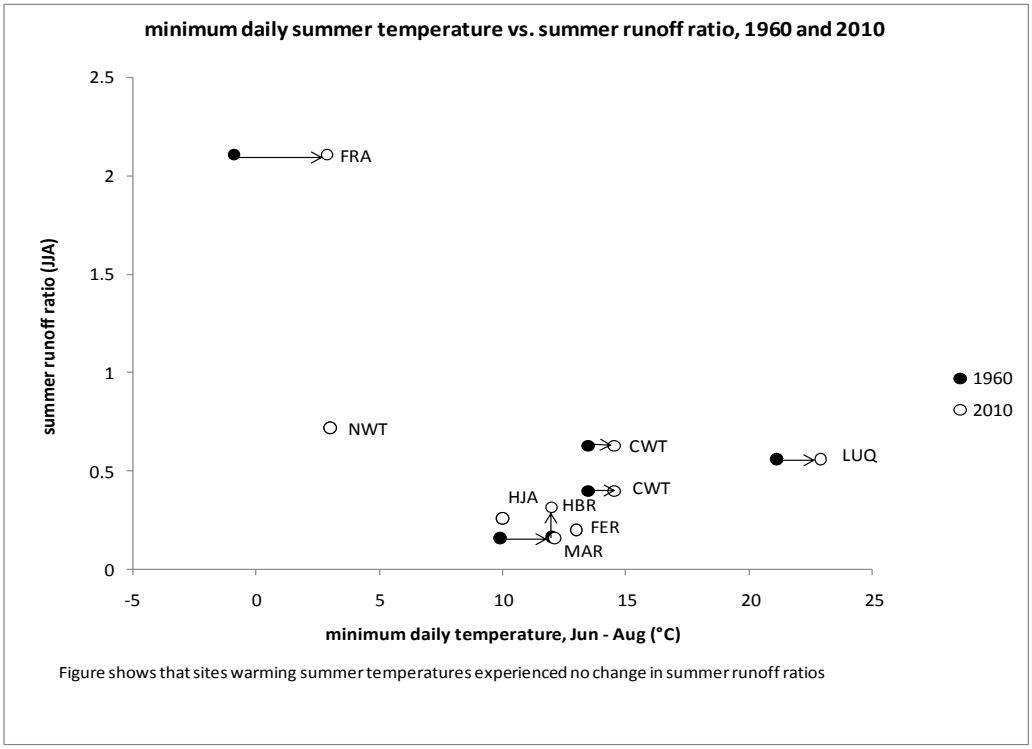

Figure 3.10 Changes in summer runoff ratios (Q/P) as a function of change in minimum daily spring temperature (Table 3.1).

Luquillo, which has a warm, moist climate, has experienced a warming signal in all seasons, but no change in precipitation or discharge over the period from 1975 to 2010 (temperature, precipitation) and 1966-2010 (discharge). A very strong hurricane (Hugo) removed significant amounts of leaf area in September 1989. The lack of response of discharge despite warming temperature over the study period may have been due to reduced leaf area and associated reduced ET. This site is already so warm and wet that increases in temperature do not significantly change runoff values.

No increases in winter discharge or baseflow despite winter warming

Fraser and Marcell both experienced significant increases in winter minimum temperature but discharge and baseflow did not increase. These sites both have long, cold winters with temperature well below freezing for most of the winter. While temperature may have increased, they did not significantly change the time above speeding, so no changes in discharge would be expected.

The HJ Andrews has a more moderate winter climate as compared to Fraser and Marcell. Temperature dip below freezing but they do not remain there for significant periods of time. Much of the forest is also below the seasonal snow elevation, with much of the forest receiving rain throughout the winter. Increased temperature would increase the elevation of seasonal snowpack, increasing the rain:snow fraction, and increasing winter soil moisture. In a coniferous forest, where trees can evapotranspire throughout the year whenever conditions are conducive,

increased temperature would allow vegetation to take advantage of increased soil moisture.

Increased flow and runoff ratios despite climate warming

Fernow, which has a mesic temperate climate, experienced a climate warming signal in minimum temperature (1951-2007), no change in precipitation (1951-2007) or discharge, but a strong increase runoff ratios (total flow and baseflow) over the period 1951 to 2007. This response is the opposite of what is expected from climate warming, which would increase ET and reduce runoff ratios. At Fernow, runoff ratio increases have occurred in fall and winter. These increases may be due to increased soil moisture storage carried over from spring and summer, resulting from decreased ET in summer due to succession and reduction in leaf area of the control watersheds. Logging has not occurred in the forest since 1905-1910, making the forests around 100 years old. These forests may be transpiring less due to decreased productivity.

3.6 Significance and implications

This study examined trends in climate and streamflow at eight sites from the LTER and EFR networks. This research found trends in temperature are generally positive, but did not find significant increased warming at all sites. Few sites show changes in precipitation, but significant trends were positive.

The impact of these trends has varied around the country. Expected changes in hydrology were occurring in few places, and mostly in the spring. This is mostly

related to changes in snowpack and changes in ET that take advantage of increased temperature and increased moisture. These trends, however, have not transferred from one season into others. Decreases in spring discharge and runoff ratios did not correspond to increases in winter discharge and runoff ratios, signaling a much earlier shift in snow melt. Spring decreases were also not carried into summer, which may be an indication that vegetation may be responding to reduced soil moisture, and evapotranspiring less.

Forest type and succession may also be mitigating climate changes. Coniferous forests may be taking advantage of longer time periods and higher elevations in which ET can occur. The study sites in the eastern U.S. experienced logging in the early part of the 20th century, but are now greater than 80 years old. Succession may be leading to less water use with the increasing age of trees.

The climate type also influenced how climate change impacted streamflow. Climate types at the extremes-either very cold or hot and humid-appeared to have minimal response from streamflow. The changes in temperature may not have been extreme enough to shift the hydrologic regime.

This research shows that while understanding broad scale patterns of climate are important, the type of impact of those changes may be localized. Trends in streamflow were influenced as much by the climate type, forest type, and forest history, as changes in temperature and precipitation. Future water management plans

must account for all these factors to accurately reflect the changes to the hydrologic regime.

4. Conclusions

Willamette River basin

Understanding streamflow patterns is important for water management in areas where surface water is the primary water source, such as the Willamette River basin in the Pacific Northwest. Analyses indicate that streamflow has declined in the region over the past century, raising questions about the possible role of climate as a driver of water yield. The Willamette River basin includes multiple flow-regulation dams constructed in the mid-1900s which are managed to reduce flood risk and augment summer low flows. In the Willamette River basin, as in much of the western US where summer precipitation is low, declining streamflow will exacerbate the task of water management to meet varying demands for water. Although regional climate warming over the past half-century in the Pacific Northwest is a plausible cause of declining streamflow, climate is only one of several factors that determine the hydrologic regime of the Willamette River basin. Other factors include vegetation, geology, topography, and river regulation. Ch 2 of this thesis, "Effects of forest cover change, geology, and dams on streamflow trends since 1950 in the Willamette Basin, Oregon," quantified trends in streamflow from 1950 to 2010 in ten sub-basins of the Willamette, including seven predominantly forested sub-basins of 60-600 km2 above dams in the Willamette National Forest, and three gages in urban areas of the Willamette valley (Albany, Salem, and Portland).

Over the study period, precipitation in the Willamette River basin did not change significantly at the seasonal or annual time scale. Annual discharge did not decline consistently at any basin above dams, but total flow or baseflow or both declined significantly below dams. Above dams, discharge, baseflow, or runoff ratios for total flow and baseflow, or all of these, declined in significantly in spring and summer in up to five of the seven-sub-basins. Four of the seven sub-basins above dams, which have most of their area in the western Cascades geologic province and slightly smaller areas of seasonal snowpack, experienced the most obvious declines in spring and summer discharge, baseflow, runoff ratios, and daily flows (Blue River, Lookout Creek, North Fork Middle Fork Willamette, and Salmon Creek).

Declining streamflows in spring and summer above dams may be attributed to increases in the rain:snow ratio and earlier snowmelt, but some of the spring trends also may be explained by changes in water use by vegetation in response to climate trends. More rapid declines in summer and fall discharge and runoff ratios occurred in basins which experienced relatively rapid conversion of old to young forest in the past half-century and have relatively large proportions of young forest today. These changes can be attributed to increasing ET in young forests and shallow flow paths in Western Cascades-dominated basins that intersect the rooting zone; high-elevation basins with greater percentages of High Cascades geology are less susceptible to declining discharge, even if they have substantial areas in young forest. In contrast to the trends in streamflow above dams, trends over time in streamflow downstream of

dams in the Willamette basin have been largely influenced by management of reservoirs and flow. Flow downstream of the dams has become more homogenized throughout the year, with higher flows in the fall and declines in the later winter/early spring. However, discharge has shown declining trends at the annual time scale, and in the spring and summer. These trends may be a result of the decreases upstream of the dams caused by increased young vegetation, or they may result from a recent trend of relatively dry years.

Long-term trends in streamflow from forested headwater sites in the US

From 1960 to 2010, annual average temperatures increased by 2°C over the entire United States. Climate variability affects the hydrology in different areas of the country. Although historical water yields may not be representative of future water yields, long term historical climate and discharge records from instrumented sites provide the basis for understanding the nature and magnitude of climate variability and other effects on water yield from headwater systems. Ch 3 of this thesis, "Effects of regional climate and forest dynamics on streamflow: an analysis of records from eight Long-term Ecological Research and Forest Service Experimental Forest sites in the US," quantified trends in climate and streamflow data from eight predominantly forested sites in the US to understand the complex relationships between climate, basin geography, vegetation, history, and hydrology, and to predict future hydrologic changes under predicted increased warming.

The first day of spring (defined as the last day of freezing temperature) has moved earlier by 0.31 to 1.98 days/year at all sites, except the alpine site. Most sites experienced significant increases in spring minimum air temperature, but only a few sites experienced an associated change in spring runoff ratios. Spring runoff ratios decreased in sites with snowpacks and near-zero mean spring air temperature (AND). Fall baseflow increased at the only alpine, non-forested site, apparently as a result of increased permafrost melt (NWT). Decreases in spring discharge and runoff ratios were not associated with predicted increases in winter discharge and runoff ratios, nor with reductions in summer runoff ratios. Although summer minimum air temperature increased at most sites, summer runoff ratios did not change at most sites, and some sites (HBR, FER) experienced increases in summer and fall runoff ratios, despite warming climate. The expected reduction in summer runoff ratio in response to climate warming at these sites may have been mitigated by reductions in leaf area due to disturbance (hurricane at LUQ), or forest succession after logging in the early 1900s (CWT, FER, HBR).

These findings indicate that both climate variability and hydrologic response to climate varies across the US. Moreover, hydrologic responses to climate variability are mostly confined to spring, and streamflow in summer or winter has not yet responded. The lack of expected streamflow responses is attributed to mechanisms that produce counteracting trends in vegetation water use in response to climate trends. These mechanisms merit further study, because they apparently have produced

ecological resilience of water yield to climate variability, and they will govern water yield responses under climate warming. Long-term ecological studies of dynamic ecosystems provide a rich basis for understanding climate trends.

Bibliography

Barnett, T.P., D.W. Pierce, H.G. Hidalgo, C. Bonfils, B.D Santer, T. Das, G. Bala, A.W. Wood, T. Nozawa, A.A. Mirin, D.R. Cayan, and M.D. Dettinger. 2008. Human-induced changes in the hydrology of the western United States. *Science* 319, 1080-1083.

Bond, B.J., J.A. Jones, G. Moore, N. Phillips, D. Post, and J. J. McDonnell. 2002. The zone of vegetation influence on baseflow revealed by diel patterns of streamflow and vegetation water use in a headwater basin. *Hydrological Processes* 16: 1671-1677.

Callaghan E., and A.F. Buddington. 1938. Metalliferous mineral deposits of the Cascade Range in Oregon. U.S. Geological Survey Bulletin 893.

Cayan, D.R., S.A. Kammerdiener, M.D. Dettinger, J.M. Caprio, and D.H. Peterson. 2001. Changes in the onset of spring in the western United States. *Bulletin of the American Meteorological Society* 82(3) 399-415.

Christensen, L., C.L. Tague, and J.S. Baron. 2008. Spatial patterns of simulated transpiration response to climate variability in a snow dominated mountain ecosystem. *Hydrological Processes* 22: 3576-3588.

CLIMDB/HYDRODB, http://www.fsl.orst.edu/climhy/ last accessed 08 March 2011.

Daly, C., R.P. Neilson, and D.L. Phillips. 1994. A statistical-topographic model for mapping climatological precipitation over mountainous terrain. *Journal of Applied Meteorology* 33: 140-158.

Daly, C., M. Halbleib, J.I. Smith, W.P. Gibson, M.K. Doggett, G.H. Taylor, J. Curtis, and P.P.Pasteris. 2008. Physiographically sensitive mapping of climatological temperature and precipitation across the conterminous United States. *International Journal of Climatology* doi: 10.1002/joc.1688.

Dai, A., T.T. Qian, K.E. Trenberth, and J.D. Milliman. 2009. Changes in continental freshwater discharge from 1948 to 2004. *Journal of Climate* 22(10): 2773-2792.

Franklin, Jerry F.; Dyrness, C.T. 1973. Natural vegetation of Oregon and Washington. Gen. Tech. Rep. PNW-GTR-008. Portland, OR: U.S. Department of Agriculture, Forest Service, Pacific Northwest Research Station.

Karl, T.R., J.M. Melillo, and T.C. Peterson, eds. 2009. Global Climate Change Impacts in the United States. New York: Cambridge University Press.

Greenland, D. 1994. The Pacific Northwest regional context of the climate of the H.J. Andrews Experimental Forest. *Northwest Science* 69(2): 81-96.

Hamlet, A.F., P.W. Mote, M.P. Clark, and D.P. Lettenmaier. 2005. Effects of temperature and precipitation variability on snowpack trends in the western United States. *Journal of Climate* 18(21): 4545-4561.

Hamlet, A.F. and D.P. Lettenmaier. 1999. Effects of climate change on hydrology and water resources in the Columbia River Basin. *Journal of the American Water Resources Association* 35(6): 1597-1623.

Harr, R.D., A. Levano, and R. Merserau. 1982. Streamflow changes after logging 130-year-old Douglas fir in 2 small watersheds. *Water Resources Research* 18(3): 637-644.

Harr,R.D. and F.M. McCorsion. 1979. Initial effects of clearcut logging on size and timing of peak flows in a small watershed in western Oregon. *Water Resources Research* 15(1):90-94.

Helsel, DR and RM Hirsch. 1992. Statistical Methods in Water Resources –part of Studies in Environmental Science 49. New York: Elsevier 522 p.

Helsel, D.R. and R.M. Hirsch. 2002. Statistical methods in water resources. In Techniques of Water-Resources Investigations of the United States Geological Survey, Book 4 Hydrological analysis and interpretation, Chapter A3. US Geological Survey.

Helsel, D.R., D.K. Mueller, and J.R. Slack. 2005. Computer program for the Kendall family of trend tests. Scientific Investigations Report 2005-5275. U.S. Geological Survey.

Hicks, B.J., R.L. Beschta, and R.D. Harr. 1991. Long-term changes in streamflow following logging in western Oregon and associated fisheries implications. *Water Resources Bulletin* 27(2): 217-226.

Hornbeck, J.W., C.W. Martin, and C. Eager. 1997. Summary of water yield experiments at Hubbard Brook Experimental Forest, New Hampshire. *Canadian Journal of Forest Research* 27(12): 2043–2052.

Hubbart, J.A., T.E. Link, J.A. Gravelle, and W.J. Elliot. 2007. Timber harvest impacts on water yield in the continental/maritime hydroclimatic region of the United States. *Forest Science* 43(2): 169-180.

Jarvis, P.G. 1975.Water transfer in plants. *In* Heat and Mass Transfer in the Biosphere: Part 1. Transfer Processes in the Plant Environment. Eds. D.A. deVries and N.H. Afgan, Scripta Book, Washington,DC, pp 369–394.

Jefferson, A., G. Grant, and T. Rose. 2006. Influence of volcanic history on groundwater patterns on the west slope of the Oregon High Cascades. *Water Resources Research* 42(W12411), doi:10.1029/2005WR004812.

Jefferson, A., A. Nolin, S. Lewis, C. Tague. 2008. Hydrogeologic controls on streamflow sensitivity to climate variation. *Hydrologic Processes* 22(22): 4371–4385.

Jones, J.A., G.L. Achterman, L.A. Augustine, I.F. Creed, P.F. Ffolliott, L. MacDonald, and B.C. Wemple. 2009. Hydrologic effects of a changing forested landscape—challenges for the hydrological sciences. *Hydrological Processes* 23:2699-2704.

Jones, J.A. 2000. Hydrologic processes and peak discharge response to forest removal, regrowth, and roads in 10 small experimental basins, western Cascades, Oregon. *Water Resources Research* 36(9): 2621-2642.

Jones, J.A. and G.E. Grant. 1996. Peak flow responses to clear-cutting and roads in small and large basins, western Cascades, Oregon. *Water Resources Research* 32(4): 959-974.

Jones, J. A., and D. A. Post. 2004. Seasonal and successional streamflow response to forest cutting and regrowth in the northwest and eastern United States. *Water Resources Research* 40(W05203).

Knowles N., M. Dettinger, and D. Cayan. 2006. Trends in snowfall versus rainfall for the Western United States. *Journal of Climate* 19: 4545–4559.

Lettenmair, D.P., E.F. Wood, and J.R. Wallis. 1994. Hydro-climatological trends the continental United States, 1948-88. *Journal of Climate* 7: 586-607.

Lins H.F. and J.R. Slack. 1999. Streamflow trends in the United States. *Geophysical Research Letters* 26: 227–230.

Little, C., A. Lara. J. McPhee, and R. Urrutia. 2009. Revealing the impact of forest exotic plantations on water yield in large scale watersheds in South-Central Chile. *Journal of Hydrology* 374(1-2): 162-170.

Luce, C.H. and Z.A. Holden. 2009. Declining annual streamflow distributions in the Pacific Northwest United States, 1948-2006. *Geophysical Research Letters* 36.

Manga, M. 1997. A model for discharge in spring-dominated streams and implications for the transmissivity and recharge of quaternary volcanic in the Oregon Cascades. *Water Resources Research* 33(8): 1813-1822.

McCabe, G.J. and D.M. Wolock. 2009. Recent declines in western U.S. snowpack in the context of twentieth-century climate variability. *Earth Interactions* 13(12).

McGuire, K. J., J. J. McDonnell, M. Weiler, C. Kendall, B. L. McGlynn, J. M. Welker, and J. Seibert. 2005. The role of topography on catchment-scale water residence time. Water Resources Reseach 41(W05002), doi:10.1029/2004WR003657.

Milliman, J.D., Farnsworth, K.L., Jones, P.D., Xu, K.H., Smith, L.C. 2008. Climatic and anthropogenic factors affecting river discharge to the global ocean, 1951-2000. Global and Planetary Change 62, 187-194.

Milly, P.C.D., J. Betancourt, M. Falkenmark, R.M. Hirsch, Z.W. Kundzewicz, D.P. Lettenmaier, and Ronald J. Stouffer. 2008. Stationarity Is Dead: Whither Water Management? *Science* 319: 574-574.

Mote, P.W. 2003a. Trends in snow water equivalent in the Pacific Northwest and their climatic causes. *Geophysical Research Letters* 30(12), 1601, doi:10.1029/2003GL017258.

Mote, P.W. 2003b. Trends in temperature and precipitation in the Pacific Northwest during the twentieth century. *Northwest Science* 77(4): 271-282.

Mote, P.W., E.A. Parson, A.F. Hamlet, W.S. Keeton, D. Lettenmaier, N. Mantua, E.L. Miles D.W. Peterson, D.L. Peterson, R. Slaughter, A.K. Snover. 2003. Preparing for climatic change: the water, salmon, and forests of the Pacific Northwest. *Climatic Change* 61: 45–88.

Mote, P.W., A.F. Hamlet, M.P. Clark, and D.P. Lettenmaier. 2005. Declining mountain snowpack in western North America. *Bulletin of the American Meteorological Society* 86(1):39-49.

Moore, K.M. 2010. Trends in streamflow from old growth forested watersheds in the western Cascades. Master's research project, Oregon State University.

Moore, G.W., B.J. Bond, J.A, Jones, N. Phillips, and F.C. Meinzer. 2004. Structural and compositional controls on transpiration in 40- and 450-year-old riparian forests in western Oregon, USA. *Tree Physiology* 24: 481-491.

National Research Council. 2008. Hydrologic Effects of a Changing Forest Landscape. Committee on Hydrologic Impacts of Forest Management, Water Science and Technology Board, Division on Earth and Life Studies 00 pp.; ISBN 0-309-12104-3.

Nolin, A.W. and C. Daly. 2006. Mapping "at risk" snow in the Pacific Northwest. *Journal of Hydrometeorology* 7: 1164-1171.

Northwest Forest Plan Record of Decision. 1994. http://www.reo.gov/library/reports/newroda.pdf, last accessed 7 March 2011.

Oregon Bureau of Land Management and U.S. Forest Service. Hydrologic Unit Boundaries (5th) for Oregon, Washington, and California (Geographic Nad 83). 2006. Oregon Spatial Data Library, http://spatialdata.oregonexplorer.info/GPT9/catalog/main/home.page, last accessed 19 February 2011.

Oregon Bureau of Land Management and U.S. Forest Service. Hydrologic Unit Boundaries (6th) for Oregon, Washington, and California (Geographic Nad 83). 2006. Oregon Spatial Data Library, http://spatialdata.oregonexplorer.info/GPT9/catalog/main/home.page, last accessed 19 February 2011.

Orr, E.L., W.N. Orr, and E.M. Baldwin. 1992. Geology of Oregon. 4th Edition. Kendall/Hunt Publishing Co, Dubuque, IA, 254 pg.

Perry, T.D. 2007. Do vigorous young forests reduce streamflow? Results from up to 54 years of streamflow records in eight paired-watershed experiments in the H.J. Andrews and South Umpqua Experimental Forests. Master's thesis, Oregon State University.

Poff, N.L., J.D. Olden, D.M. Merritt, and D.M. Pepin. 2007. Homogenization of regional river dynamics by dams and global biodiversity implications. *Proceedings of the National Academy of Sciences* 104(14): 5732–5737.

Post, D.A. and J.A. Jones. 2001. Hydrologic regimes of forested, mountainous, headwater basins in New Hampshire, North Carolina, Oregon, and Puerto Rico. *Advances in Water Resources* 24: 1195-1210.

PRISM Climate Group, Oregon State University, http://prism.oregonstate.edu, created 11 July 2002-12 February 2010

PRISM Climate Group, PRISM Data Explorer, Oregon State University, http://prismmap.nacse.org/nn/index.phtml, last accessed 10 March 2011.

Regonda, S.K., B. Rajagopalan, M. Clark, and J. Pitlick. 2005. Seasonal cycle shifts in hydroclimatology over the western United States. *Journal of Climate* 18: 372-384.

Rothacher, J. 1970. Increases in water yield following clear-cut logging in the Pacific Northwest. *Water Resources Research* 6(2): 653-658.

Ruprecht, J.K. and N.J. Schofield. 1989. Analysis of streamflow generation following deforestation in southwestern Western Australia. *Journal of Hydrology* 105(1-2): 1-17.

Sherrod, D. R., and J. G. Smith. 2000. Geologic Map of upper Eocene to Holocene volcanic and related rocks of the Cascade Range, Oregon, U.S. Geological Survey Geology Investigation Series, I-2569.

Scott, D.F. and W. Lesch. 1997. Streamflow response to afforestation with *Eucalyptus grandis* and *Pinus patula* and to felling in the Mokobulaan experimental catchments, South Africa. *Journal of Hydrology* 199(3-4): 360-377.

Smith, R.E. and D.F. Scott. 1992. The effects of afforestation on low flows in various regions of South Africa. *Water SA* 18(3):185-194.

Spies, T.A. 1991. Plant species diversity and occurrence in young, mature and old-growth Douglas-fir stands in western Oregon and Washington. In Wildlife and vegetation of unmanaged Douglas-fir forests. Gen. Tech. Rep. PNW-GTR-285. Portland, OR: U.S. Department of Agriculture, Forest Service, Pacific Northwest Research Station: 111–121.

Stanford, JA, FR Hauer, SV Gregory, and EB Snyder. 2005. Columbia River Basin. In *Rivers of North America*, ed Arthur C Benke and Colbert E Cushing, pages. Burlington, MA: Elsevier Academic Press.

Stewart, I., D.R. Cayan, M.D. Dettinger. 2005. Changes toward earlier streamflow timing across western North America. *Journal of Climate* 18:1136-1155.

Tague, C. and G.E. Grant. 2004. A geological framework for interpreting the low-flow regimes of Cascade streams, Willamette River Basin, Oregon. *Water Resources Research* 40(W04303).

Tague, C. and G.E. Grant. 2009. Groundwater dynamics mediate low-flow response to global warming in snow-dominated alpine regions. *Water Resources Research* 45(W07421).

Tague, C., G.E. Grant, M. Farrell, J. Choate, and A. Jefferson. 2008. Deep groundwater mediates streamflow response to climate warming in the Oregon Cascades. *Climatic Change* 86: 189-210.

Thomas, R.B. and W.F. Megahan. 1998. Peak flow responses to clear-cutting and roads in small and large basins, western Cascades, Oregon: A second opinion. *Water Resources Research* 34(12): 3393-3403.

Trimble, S.W., F.H. Weirich, and B.L. Hoag. 1987. Reforestation and the reduction of water yield on the southern Peidmont since circa 1940. *Water Resources Research* 23(3): 425- 437.

US Army Corp of Engineers , Northwest Division, dataquery, http://www.nwd-wc.usace.army.mil/perl/dataquery.pl, last accessed 19 February 2011

U.S. Army Corp Engineers (USACE). 2010a. Willamette Basin annual water quality report, 2009 water year. U.S. Army Corp of Engineers: Portland District 122 p.

U.S. Army Corp Engineers (USACE). 2010b. Supporting fish recovery in the Willamette Valley: An overview of the 2008 Biological Opinions. http://www.nwp.usace.army.mil/environment/wbiop_docs/WillametteBiOp_Overview_FS.pdf, last accessed 5 March 2011.

USGS Surface-Waterdata for the Nation, http:// waterdata.usgs.gov/nwis/sw, last accessed 19 February 2011.

Wright, K.A., K.H. Sendek, R.M. Rice, and R.B. Thomas. 1990. Logging effects on streamflow-storm runoff at Casper Creek in northwestern California. *Water Resources Research* 26(7): 1657-1667.

Wondzell, S. M., M. N. Gooseff, and B. L. McGlynn. 2007. Flow velocity and the hydrologic behavior of streams during baseflow. Geophysical Research Letters 34(L24404), doi:10.1029/2007GL031256.

U.S.D.A. Forest Service. 2007. VegetationStand. Willamette National Forest, Supervisors Office, OR, http://www.fs.fed.us/r6/data-library/gis/willamette/, last accessed 19 February 2011.

Zhang X., K.D. Harvey, W.D. Hogg, and T.R. Yuzyk. 2001. Trends in Canadian streamflow. *Water Resources Research* 37(4): 987–998.

APPENDIX A

Baseflow separation program code for MATLAB (Jones and Post 2001)

```
%<<<<input variables>>>>
%list of files to open - must be in same folder as m-file
Files = {}; %{'filename', 'data format'; ... }. data formats can be USGS or ClimDB
%Examples:  'brietenbush-raw.txt', 'USGS'; 'gsws01.txt', 'ClimDB'
%period N
N = 5;
O = N-1;
%sensitivity criteria for determining pivots. 0<L<1; increasing values more
%stringent
L = 0.9;
%-----------------------------------------------------------------%
for filenum = 1:size(Files,1)

   %open current file
   fid = fopen(Files{filenum,1},'r+');

   %write current filename to write to - output to contain [matlab
   %datenums, excel datenums, excel datenums for Mac, baseflow]
   fout = regexprep(Files{filenum,1}, '.txt', '-BF');
   %pivotout = [fout,'-pivots']; %will contain [pivotdates flowvalues]

   %specify file format based on source
```

```
switch Files{filenum,2}
    case 'USGS'
        fileform = '%*s %*d %d - %d - %d %d %*c';
        headerlines = 28;
        dateform = [1 2 3];
    case 'ClimDBMonth'
        fileform = '%*s %*s %d / %d / %d %f %*c';
        headerlines = 1;
        dateform = [3 1 2];
    case 'ClimDBYear'
        fileform = '%*s %*s %d - %d - %d %f %*c';
        headerlines = 1;
        dateform = [1 2 3];
end

%import file in RAW placeholder [agency site_no date dishargeCFS
%pub_status]
RAW = textscan(fid, fileform, 'HeaderLines', headerlines);
%    RAW = textscan(fid, '%*s %*d %d - %d - %d %d %*c', 'HeaderLines',
headerlines);
fclose(fid);

year = double(RAW{1,dateform(1)});
month = double(RAW{1,dateform(2)});
day = double(RAW{1,dateform(3)});
```

```
flow = double(RAW{1,4});
count = length(flow);

%read dates into date matrix [entry month day year]
datevals = zeros(count,1);

for ii = 1:count
   datevals(ii) = datenum(year(ii), month(ii), day(ii));
end

%create blank min flow matrix [entry min_flow]
mins = [zeros(count-O,2)];

%find forward-looking N-day period minima, retain in mins (value and
%datestamp)
for i = 1:count-O
    [a,b] = min(flow(i:i+O));
    mins(i,1) = a;
    mins(i,2) = datevals(1)+i+b-2;
end

%purge minima who satisfy: (flow)*L >= neighbors
k = 0;
pivots = zeros(count-O,2);
for i = 2:count-O-1
```

```
        A=mins(i-1,1);
        B=mins(i,1)*L;
        C=mins(i+1,1);

        if and(B<A,B<C)  %not(or(B>=A,B>=C)) %%is this right?!? seems to be in the Fortran code
            k=k+1;
            pivots(k,:) = mins(i,:);
        end
    end

    %write in interpolated values (fill blanks at 1d timestep)
    alldates = (pivots(1,2):pivots(k,2))';
    IntFlow = interp1q(pivots(1:k,2),pivots(1:k,1),alldates);
    BaseFlow = IntFlow;
    BFlag = alldates(1)-datevals(1);%accounts for lag between start of flow timeseries and first pivot of BF

    for j = 1:length(BaseFlow)
        if(BaseFlow(j) > flow(j+BFlag))
            BaseFlow(j) = flow(j+BFlag);
        end
    end

    %----------plots----------
    figure
```

```
    ax(1) = subplot(2,1,1);
    plot(datevals,flow,'g',mins(:,2),mins(:,1),'r', pivots(:,2),pivots(:,1),'o')
    legend('Flow Data','5-Day Minima','Pivots')
    title(Files{filenum,1});

    ax(2) = subplot(2,1,2);
    plot(datevals,flow,'g', pivots(1:k,2),pivots(1:k,1),'o',alldates,BaseFlow,'r')
%alldates,IntFlow,'r') %
    legend('Flow Data','Pivots','Baseflow')

    zoom off; zoom xon;
    linkaxes(ax,'xy')
    axis([min(datevals)-50 max(datevals)+50 0 max(flow)])
    pan xon

    xlswrite(fout, [alldates, m2xdate(alldates), m2xdate(alldates,1), BaseFlow])
    % xlswrite(pivotout, [pivots(1:k,2),pivots(1:k,1)]) %include if pivot
    % output is desired
end
```

APPENDIX B

Daily data analysis program for MATLAB, written by E. Miles. Example provided is for streamflow, but program is also used with temperature and precipitation data.

```
%% LTER: temp record analysis

% code developed by Evan Miles, Geoscience, OSU during Fall 2010

% analysis planned byb Julia A. Jones

% some code modified from work by Christoph Thomas, COAS, OSU

clear

%% Set paths and variables

SITE = 'site code';

STATION = 'Station name';

Date = 'date';

path.home   =   'E:\Thesis data\Matlab\matlab_code\';

path.source =   'E:\Thesis data\Matlab\wavelet_inputs\';

        mkdir('E:\Thesis data\Matlab\wavelet_outputs\',[SITE,'_',STATION,'_',Date]);

path.out    =   ['E:\Thesis
data\Matlab\wavelet_outputs\',SITE,'_',STATION,'_',Date,'\'];

fileQ = 'sofomckenzie_baseday-WY-DOY.csv';

ftsz        =   10;

ytick_vect  =   [1 32 62 93 124 153 184 214 245 275 306 337 366];

month_vect  =   ['O'; 'N'; 'D'; 'J'; 'F'; 'M'; 'A'; 'M'; 'J'; 'J'; 'A'; 'S'];

output.root = regexprep(fileQ, '-WY-DOY.csv', '_wavelet');

%% Importing data

% flow

d.Q = csvread(fullfile(path.source,fileQ),0,0);
```

```
d.Q(d.Q==0)= 0.001; %0.001;  use 0.001 for streams known to freeze/thaw - 0 discharge may be a real value.

d.Q(d.Q<0)= NaN;


%Chris' method - cuts off last year regardless

d.Q(:,end)    =   [];

YearFirst = d.Q(1,2);

YearLast = d.Q(1,end);

nYears = YearLast-YearFirst+1;

%% Display histogram of data

dt.num  =   [1:1:nYears*366];

d.rawQvec= reshape(d.Q(2:end,2:end),nYears*366,1);

d.Qmin = min(d.rawQvec);

d.Qstd = nanstd(d.rawQvec);

d.Qmean = nanmean(d.rawQvec);

d.Qmax = max(d.rawQvec);

hgram = figure;

[nQ, xQ] = hist(d.rawQvec, 50);

bar(xQ,nQ);box on; hold on;

ylabel ('count','fontsize',ftsz);

xlabel('Raw Flow [cfs]','fontsize',ftsz-2);

xlim ([d.Qmin d.Qmax]);

title ([SITE,': ', STATION, '- Raw Flow, distribution'],'fontsize',ftsz+4);

for i = -4:4

   std.cur = d.Qmean + i*d.Qstd;
```

```
    line([std.cur std.cur],[0 max(nQ)],'Color',[1 0 0])
    text(std.cur, max(nQ), [int2str(i),'\sigma'])
    std.Q(i+5) = std.cur;
end

output.cur = regexprep(output.root, '_wavelet', ['_histogram_',Date]);
saveas (hgram,fullfile(path.out,output.cur),'pdf');
%% log-transform data
dlog.Q = d.Q;
dlog.Q(2:end,2:end) = log10(dlog.Q(2:end,2:end));
dlog.Qvec= reshape(dlog.Q(2:end,2:end),nYears*366,1);
dlog.Qmin = min(dlog.Qvec);
dlog.Qstd = nanstd(dlog.Qvec);
dlog.Qmean = nanmean(dlog.Qvec);
dlog.Qmax = max(dlog.Qvec);
hgramLog = figure;
[nlog, xlog] = hist(dlog.Qvec, 50);
bar(xlog,nlog);box on; hold on;
ylabel ('count','fontsize',ftsz);
xlabel('Log-Transformed Flow [powers of 10]','fontsize',ftsz-2);
xlim ([dlog.Qmin dlog.Qmax]);
title ([SITE,': ', STATION, '- log10 flow, distribution'],'fontsize',ftsz+4);
for i = -4:4
    std.cur = dlog.Qmean + i*dlog.Qstd;
    line([std.cur std.cur],[0 max(nlog)],'Color',[1 0 0])
```

```
    text(std.cur, max(nlog), [int2str(i),'\sigma'])
    std.log(i+5) = std.cur;
end

output.cur = regexprep(output.root, '_wavelet', ['_log_histogram_',Date]);
saveas (hgramLog,fullfile(path.out,output.cur),'pdf');


%% empirical cumulative distributions
[cdf.fQ,cdf.xQ] = ecdf(d.rawQvec);
cdf.xQ1p = cdf.xQ(find(cdf.fQ < 0.01, 1, 'last' ));
cdf.xQ5p = cdf.xQ(find(cdf.fQ < 0.05, 1, 'last' ));
cdf.xQ95p = cdf.xQ(find(cdf.fQ < 0.95, 1, 'last' ));
cdf.xQ99p = cdf.xQ(find(cdf.fQ < 0.99, 1, 'last' ));
[cdf.flogQ,cdf.xlogQ] = ecdf(dlog.Qvec);
cdf.xlogQ1p = cdf.xlogQ(find(cdf.flogQ < 0.01, 1, 'last' ));
cdf.xlogQ5p = cdf.xlogQ(find(cdf.flogQ < 0.05, 1, 'last' ));
cdf.xlogQ95p = cdf.xlogQ(find(cdf.flogQ < 0.95, 1, 'last' ));
cdf.xlogQ99p = cdf.xlogQ(find(cdf.flogQ < 0.99, 1, 'last' ));
for i = 1:nYears
    cdf.nQ1p(i) = numel(find(d.Q(2:end,1+i) <= cdf.xQ1p));
    cdf.nQ5p(i) = numel(find(d.Q(2:end,1+i) <= cdf.xQ5p));
    cdf.nQ95p(i) = numel(find(d.Q(2:end,1+i) > cdf.xQ95p));
    cdf.nQ99p(i) = numel(find(d.Q(2:end,1+i) > cdf.xQ99p));
```

```
    cdf.nlogQ1p(i) = numel(find(dlog.Q(2:end,1+i) <= cdf.xlogQ1p));
    cdf.nlogQ5p(i) = numel(find(dlog.Q(2:end,1+i) <= cdf.xlogQ5p));
    cdf.nlogQ95p(i) = numel(find(dlog.Q(2:end,1+i) > cdf.xlogQ95p));
    cdf.nlogQ99p(i) = numel(find(dlog.Q(2:end,1+i) > cdf.xlogQ99p));
end


cumdist = figure;
subplot(3,1,1)
line(YearFirst:YearLast,cdf.nQ1p,'Color','b')
line(YearFirst:YearLast,cdf.nQ5p,'Color','g')
line(YearFirst:YearLast,cdf.nQ95p,'Color','r')
line(YearFirst:YearLast,cdf.nQ99p,'Color','k')
xlim ([YearFirst YearLast]);
ylabel ('Number of days beyond given percentile','fontsize',ftsz);
xlabel ('Water Year','fontsize',ftsz);
title ([SITE,': ', STATION, '- Discharge Extreme Values by Water
Year'],'fontsize',ftsz+1);
subplot(3,1,2)
line(YearFirst:YearLast,cdf.nlogQ1p,'Color','b')
line(YearFirst:YearLast,cdf.nlogQ5p,'Color','g')
line(YearFirst:YearLast,cdf.nlogQ95p,'Color','r')
line(YearFirst:YearLast,cdf.nlogQ99p,'Color','k')
xlim ([YearFirst YearLast]);
ylabel ('Number of days beyond given percentile','fontsize',ftsz);
xlabel ('Water Year','fontsize',ftsz);
```

```
title ('Log-transformed Discharge Extreme Values by Water Year','fontsize',ftsz+1);

legend('Below 1st Percentile','Below 5th Percentile','Above 95th Percentile','Above
99th Percentile')

subplot(3,2,5)

plot(cdf.xQ,cdf.fQ)

title('Discharge Cumulative Distribution')

xlabel('Discharge [cfs]')

ylabel('Cumulative Probability')

subplot(3,2,6)

plot(cdf.xlogQ, cdf.flogQ)

title('Log-Transformed Discharge Cumulative Distribution')

xlabel('Log-Discharge [orders of 10]')

ylabel('Cumulative Probability')

output.cur = regexprep(output.root, '_wavelet', ['_cdf_percentiles_',Date]);

saveas (cumdist,fullfile(path.out,output.cur),'pdf');

%% Hofmiller plots

% Loading colormaps

load('lter_colormap_temp.mat');

% load('teaching_colormap_le.mat');

hof_raw = figure;

orient landscape;

subplot (1,2,1);

box on; hold on;

data_show  =  reshape(d.rawQvec,366,nYears);

image(d.Q(1,2:end),[1:1:366],data_show,'CDataMapping','scaled'); box on; hold on;
```

```
% line (days(2:end),sun_riseset','color','k','linewidth',1.0);

colormap(color_map_lter);

caxis ([0 1000]);

xlim ([YearFirst YearLast]);

set (gca,'ytick',ytick_vect,'ylim',[1
366],'xtick',[1920:10:2010],'tickdir','out','xaxislocation','top','fontsize',ftsz);

ylabel ('DOWY','fontsize',ftsz);

h_c = colorbar('vert');

set (h_c,'ylim',[0 1000],'ytick',[1 5 10 50 100 500 1000]);%500 1000 5000

set (get(h_c,'xlabel'),'string',{'raw flow [cfs]'},'fontsize',ftsz-2);

title ([SITE,': ', STATION, '- raw flow'],'fontsize',ftsz+4);

for ii = 1 : 1 : 12

   text(YearLast+2,mean(ytick_vect(ii:ii+1)),month_vect(ii),'fontsize',ftsz);

end



subplot (1,2,2);

box on; hold on;

data_show   =   reshape(dlog.Qvec,366,nYears);

image(dlog.Q(1,2:end),[1:1:366],data_show,'CDataMapping','scaled'); box on; hold
on;

% line (days(2:end),sun_riseset','color','k','linewidth',1.0);

colormap(color_map_lter);

caxis ([0 3]);

xlim ([YearFirst YearLast]);
```

```
set (gca,'ytick',ytick_vect,'ylim',[1
366],'xtick',[1920:10:2010],'tickdir','out','xaxislocation','top','fontsize',ftsz);
ylabel ('DOWY','fontsize',ftsz);
h_c = colorbar('vert');
set (h_c,'ylim',[0 3],'ytick',[-1:0.5:5]);
set (get(h_c,'xlabel'),'string',{'log-transformed flow [powers of 10]'},'fontsize',ftsz-2);
title ( [SITE,': ', STATION, ' - log Q ', Date],'fontsize',ftsz+4);
for ii = 1 : 1 : 12
   text(YearLast+2,mean(ytick_vect(ii:ii+1)),month_vect(ii),'fontsize',ftsz);
end

text (1960,-10,['Data processed on ', Date]);
output.cur = regexprep(output.root, '_wavelet', ['_hofmiller_raw_',Date]);
saveas (hof_raw,fullfile(path.out,output.cur),'pdf');
%% Normalize log data, note dates with specific criteria
dnorm.Q = d.Q;
dnorm.Q(2:end,2:end) = (d.Q(2:end,2:end) - d.Qmean)/d.Qstd;
dnorm.logQ = dlog.Q;
dnorm.logQ(2:end,2:end) = (dlog.Q(2:end,2:end) - dlog.Qmean)/dlog.Qstd;

variance = figure;
load('normCmap.mat');
subplot (1,2,1);
box on; hold on;
data_show   =   dnorm.Q;
```

```
image(dnorm.Q(1,2:end),[1:1:366],data_show,'CDataMapping','scaled'); box on; hold on;

colormap(normCmap);

caxis ([-5 5]);

xlim ([YearFirst YearLast]);

set (gca,'ytick',ytick_vect,'ylim',[1 366],'xtick',[1920:10:2010],'tickdir','out','xaxislocation','top','fontsize',ftsz);

ylabel ('DOWY','fontsize',ftsz);

h_c = colorbar('vert');

set (h_c,'ylim',[-5 5],'ytick',-5:5);

set (get(h_c,'xlabel'),'string',{'[\sigma]'},'fontsize',ftsz-2);

title ([SITE,': ', STATION, '- raw Q variance'],'fontsize',ftsz+4);

for ii = 1 : 1 : 12

   text(YearLast+2,mean(ytick_vect(ii:ii+1)),month_vect(ii),'fontsize',ftsz);

end


subplot (1,2,2);

box on; hold on;

data_show  =  dnorm.logQ;

image(dnorm.logQ(1,2:end),[1:1:366],data_show,'CDataMapping','scaled'); box on; hold on;

colormap(normCmap);

caxis ([-5 5]);

xlim ([YearFirst YearLast]);

set (gca,'ytick',ytick_vect,'ylim',[1 366],'xtick',[1920:10:2010],'tickdir','out','xaxislocation','top','fontsize',ftsz);

ylabel ('DOWY','fontsize',ftsz);
```

```
h_c = colorbar('vert');
set (h_c,'ylim',[-5 5],'ytick',-5:5);
set (get(h_c,'xlabel'),'string',{'[\sigma]'},'fontsize',ftsz-2);
title ([SITE,': ', STATION, '- log Q variance'],'fontsize',ftsz+4);
for ii = 1 : 1 : 12
   text(YearLast+2,mean(ytick_vect(ii:ii+1)),month_vect(ii),'fontsize',ftsz);
end

output.cur = regexprep(output.root, '_wavelet', ['_hofmiller_norm_',Date]);
saveas (variance,fullfile(path.out,output.cur),'pdf');
%% extract outliers > 3.5 std from mean of entire dataset
crit = 3.5;
[dnorm.rlogQoutl dnorm.clogQoutl] = find(abs(dnorm.logQ(2:end,2:end))>crit);
[dnorm.rQoutl dnorm.cQoutl] = find(abs(dnorm.Q(2:end,2:end))>crit);
if(~isempty(dnorm.rQoutl))
   for i = 1:length(dnorm.rQoutl)
      dnorm.Qoutl(i) = dnorm.Q(dnorm.rQoutl(i),dnorm.cQoutl(i));
   end
end
if(~isempty(dnorm.rlogQoutl))
   for i = 1:length(dnorm.rlogQoutl)
      dnorm.logQoutl(i) = dnorm.logQ(dnorm.rlogQoutl(i),dnorm.clogQoutl(i));
   end
end
```

```
%% Apply continuous wavelet transform to raw data; create CWT plot
load('cwtCmap.mat');
scales1 = 1:366;
cwtrawQ = figure;
subplot(211)
plot(d.rawQvec)
title('Q')
subplot(212)
dw.Q_coeff = cwt(d.rawQvec, scales1,'sym2' ,'plot');
colormap(cwtCmap);
output.cur = regexprep(output.root, '_wavelet', ['_cwt_',Date]);
saveas (cwtrawQ,fullfile(path.out,output.cur),'pdf');
cwtlogQ = figure;
subplot(211)
plot(dlog.Qvec)
title('log Q')
subplot(212)
dw.logQ_coeff = cwt(dlog.Qvec, scales1,'sym2' ,'plot');
colormap(cwtCmap);
output.cur = regexprep(output.root, '_wavelet', ['_log_cwt_',Date]);
saveas (cwtlogQ,fullfile(path.out,output.cur),'pdf');
%% Compute distribution stats for period of record
d.Q_climavg   =   [];
for ii = 2 : 1 : size(d.Q,1)
   d.Q_climavg(ii-1,1) =   nanmean(d.Q(ii,2:end));
```

```
    dlog.Q_climavg(ii-1,1) =    nanmean(dlog.Q(ii,2:end));
    d.Q_climstd(ii-1,1) =    nanstd(d.Q(ii,2:end));
    dlog.Q_climstd(ii-1,1) =    nanstd(dlog.Q(ii,2:end));
    d.Q_climmed(ii-1,1) =    nanmedian(d.Q(ii,2:end));
    dlog.Q_climmed(ii-1,1) =    nanmedian(dlog.Q(ii,2:end));
    d.Q_count(ii-1,1) = sum(~isnan(d.Q(ii,2:end)));
    dlog.Q_count(ii-1,1) = sum(~isnan(dlog.Q(ii,2:end)));
    d.Q_SE(ii-1) = d.Q_climstd(ii-1,1)/sqrt(d.Q_count(ii-1,1));
    dlog.Q_SE(ii-1) = dlog.Q_climstd(ii-1,1)/sqrt(dlog.Q_count(ii-1,1));
end

%% Fill NaN of the original matrix with the climatologic average of the that
%DOY; fill gaps with daily ensemble avgs; get rid of Feb 29 (25% data)
d.Q_fill = d.Q;
for ii = 2 : 1 : size(d.Q,1) % all days
    for iii = 2 : 1 : size(d.Q,2) % all years
        if isnan(d.Q(ii,iii))
            d.Q_fill(ii,iii)   =   d.Q_climavg(ii-1,1);
        end
    end
end
d.Q_fill(153,:) = [];
dlog.Q_fill = dlog.Q;
for ii = 2 : 1 : size(dlog.Q,1)
    for iii = 2 : 1 : size(dlog.Q,2)
```

```
        if isnan(dlog.Q(ii,iii))
            dlog.Q_fill(ii,iii)   =   dlog.Q_climavg(ii-1,1);
        end
    end
end
dlog.Q_fill(153,:) = [];
d.Qfillvec =   reshape(d.Q_fill(2:end,2:end),nYears*365,1);
dlog.Qfillvec =   reshape(dlog.Q_fill(2:end,2:end),nYears*365,1);
%% Apply continuous wavelet transform to filled data; create CWT plot
scales2 = unique(floor(exp(0:0.01:9)));
filled_cwt = figure;
subplot(211)
dw.Qfill_coeff = cwt(d.Qfillvec, scales2,'sym2' ,'plot');
title('flow, filled with climate averages, Feb29 removed')
colormap(cwtCmap);
colorbar
subplot(212)
dwlog.Qfill_coeff = cwt(dlog.Qfillvec, scales2,'sym2' ,'plot');
title('log-transformed flow, filled with climate averages, Feb29 removed')
colormap(cwtCmap);
colorbar
output.cur = regexprep(output.root, '_wavelet', ['_filled_cwt_',Date]);
saveas (filled_cwt,fullfile(path.out,output.cur),'pdf');
%% Calculate linear trends and significance for each DOWY
alpha = 0.025;
```

```
for ii = 1:1:366

   [b bint r rint stats] =
regress(d.Q(ii+1,2:end)',[ones(1,length(d.Q(1,2:end)));d.Q(1,2:end)]',alpha);

   rQb{ii} = b(2);

   rQbint{ii,1} =bint(2,:);

   rQr{ii} =r;

   rQrint{ii} =rint;

   rQstats{ii,1} =stats;



   [b2 bint2 r2 rint2 stats2] =
regress(dlog.Q(ii+1,2:end)',[ones(1,length(dlog.Q(1,2:end)));dlog.Q(1,2:end)]',alpha);

   rlogQb{ii} = b2(2);

   rlogQbint{ii,1} =bint2(2,:);

   rlogQr{ii} =r2;

   rlogQrint{ii} =rint2;

   rlogQstats{ii,1} =stats2;

end


regQB = cell2mat(rQb);

regQBint = cell2mat(rQbint);

regQstats = cell2mat(rQstats);

reglogQB = cell2mat(rlogQb);

reglogQBint = cell2mat(rlogQbint);
```

```
reglogQstats = cell2mat(rlogQstats);

%% basic stats plots

Q_reg = figure;

h(1) = subplot(5,1,1);

plot([1 366],[0 0],'k',1:366,regQB,'g', 1:366,
regQBint,'k',find(regQBint(:,2)<0),regQB(regQBint(:,2)<0),'.b',find(regQBint(:,1)>0),
regQB(regQBint(:,1)>0),'.r','MarkerSize',10)

title('Q Daily Regressions')

ylabel('Slope')

h(2) = subplot(5,1,2);

plot(1:366,regQstats(:,1))

ylabel('R-squared value')

h(3) = subplot(5,1,3);

plot(1:366,regQstats(:,2))

ylabel('F Statistic')

h(4) = subplot(5,1,4);

plot(1:366,regQstats(:,3))

ylabel('p-value')

h(5) = subplot(5,1,5);

plot(1:366,regQstats(:,4))

xlabel('DOWY')

ylabel('error variance')

set(h(1:5),'xlim', [1,366])

output.cur = regexprep(output.root, '_wavelet', ['_trend_',Date]);

saveas (Q_reg,fullfile(path.out,output.cur),'pdf');

logQ_reg = figure;
```

```
h(1) = subplot(5,1,1);

plot([1 366],[0 0],'k',1:366,reglogQB,'g', 1:366,
reglogQBint,'k',find(reglogQBint(:,2)<0),reglogQB(reglogQBint(:,2)<0),'.b',find(reglo
gQBint(:,1)>0),reglogQB(reglogQBint(:,1)>0),'.r','MarkerSize',10)

title('log Q Daily Regressions')

ylabel('Slope')

h(2) = subplot(5,1,2);

plot(1:366,reglogQstats(:,1))

ylabel('R-squared value')

h(3) = subplot(5,1,3);

plot(1:366,reglogQstats(:,2))

ylabel('F Statistic')

h(4) = subplot(5,1,4);

plot(1:366,reglogQstats(:,3))

ylabel('p-value')

h(5) = subplot(5,1,5);

plot(1:366,reglogQstats(:,4))

xlabel('DOWY')

ylabel('error variance')

set(h(1:5),'xlim', [1,366])

output.cur = regexprep(output.root, '_wavelet', ['_log_trend_',Date]);

saveas (logQ_reg,fullfile(path.out,output.cur),'pdf');

%% plots 1,2: Tmin, Tmax stats

Q_sum = figure;

h(1) = subplot(2,1,1);
```

```
%plot([1 366],[0 0],'k',1:366,regminB,'Color',[0 0.5 0], 1:366,
regminBint,'k',find(regminBint(:,2)<0),regminB(regminBint(:,2)<0),'.b',find(regminBi
nt(:,1)>0),regminB(regminBint(:,1)>0),'.r','MarkerSize',15)

line([1 366],[0 0],'Color','k')

line(1:366,regQB,'Color',[0 0.75 0])

line(1:366, regQBint,'Color','k')

line(find(regQBint(:,2)<0),regQB(regQBint(:,2)<0),'LineStyle','none','Color','b','Marke
r','.','MarkerSize',15)

line(find(regQBint(:,1)>0),regQB(regQBint(:,1)>0),'LineStyle','none','Color','r','Marke
r','.','MarkerSize',15)

title('Q Daily Regressions and 0.025 Confidence Interval')

ylabel('Slope [lps/yr]');xlabel('Day of Water Year')

set(gca,'XTick',ytick_vect,'XTickLabel',month_vect)

for ii = 1 : 1 : 12

   text(mean(ytick_vect(ii:ii+1)),-6,month_vect(ii),'fontsize',ftsz);

end


h(2) = subplot(2,1,2);

%plot(1:366, d.min_climavg,'Color',[0 0.5
0],1:366,[d.min_climavg'+d.min_SE;d.min_climavg'-d.min_SE],'k')

line(1:366, d.Q_climavg,'Color',[0 0.5 0])

line(1:366,[d.Q_climavg'+d.Q_SE;d.Q_climavg'-d.Q_SE],'Color','k')

title('Q Daily Means and Error')

ylabel('Flow [lps]');xlabel('Day of Water Year')

set(h(1:2),'xlim', [1,366])

set(gca,'XTick',ytick_vect,'XTickLabel',month_vect)

%ypos = get(gca,'Ylim');
```

```
output.cur = regexprep(output.root, '_wavelet', ['_stats_',Date]);

saveas (Q_sum,fullfile(path.out,output.cur),'pdf');

logQ_sum = figure;

h(1) = subplot(2,1,1);

line([1 366],[0 0],'Color','k')

line(1:366,reglogQB,'Color',[0 0.75 0])

line(1:366, reglogQBint,'Color','k')

line(find(reglogQBint(:,2)<0),reglogQB(reglogQBint(:,2)<0),'LineStyle','none','Color',
'b','Marker','.','MarkerSize',15)

line(find(reglogQBint(:,1)>0),reglogQB(reglogQBint(:,1)>0),'LineStyle','none','Color',
'r','Marker','.','MarkerSize',15)

title('Log Q Daily Regressions and 0.025 Confidence Interval')

ylabel('Exponential Decay [%/yr]');xlabel('Day of Water Year')

set(gca,'XTick',ytick_vect,'XTickLabel',month_vect)

for ii = 1 : 1 : 12

   text(mean(ytick_vect(ii:ii+1)),-6,month_vect(ii),'fontsize',ftsz);

end


h(2) = subplot(2,1,2);

line(1:366, dlog.Q_climavg,'Color',[0 0.75 0])

line(1:366,[dlog.Q_climavg'+dlog.Q_SE;dlog.Q_climavg'-dlog.Q_SE],'Color','k')

title('Log Q Daily Means and Error')

ylabel('Log-Transformed Flow [powers of 10]');xlabel('Day of Water Year')

set(h(1:2),'xlim', [1,366])

set(gca,'XTick',ytick_vect,'XTickLabel',month_vect)

output.cur = regexprep(output.root, '_wavelet', ['_log_stats_',Date]);
```

```
saveas (logQ_sum,fullfile(path.out,output.cur),'pdf');

%% plot 3: all trends

Q_regs = figure;

h(1) = subplot(2,1,1);

line([1 366],[0 0],'Color','k')

line(1:366,regQB,'Color',[0 0.75 0])

line(1:366, regQBint,'Color','k')

line(find(regQBint(:,2)<0),regQB(regQBint(:,2)<0),'LineStyle','none','Color','b','Marke
r','.','MarkerSize',15)

line(find(regQBint(:,1)>0),regQB(regQBint(:,1)>0),'LineStyle','none','Color','r','Marke
r','.','MarkerSize',15)

title('Q Daily Regressions and 0.025 Confidence Interval')

ylabel('Slope [cfs/yr]');xlabel('Day of Water Year')

set(gca,'XTick',ytick_vect,'XTickLabel',month_vect)

for ii = 1 : 1 : 12

   text(mean(ytick_vect(ii:ii+1)),-6,month_vect(ii),'fontsize',ftsz);

end



h(2) = subplot(2,1,2);

line([1 366],[0 0],'Color','k')

line(1:366,reglogQB,'Color',[0 0.75 0])

line(1:366, reglogQBint,'Color','k')

line(find(reglogQBint(:,2)<0),reglogQB(reglogQBint(:,2)<0),'LineStyle','none','Color',
'b','Marker','.','MarkerSize',15)

line(find(reglogQBint(:,1)>0),reglogQB(reglogQBint(:,1)>0),'LineStyle','none','Color',
'r','Marker','.','MarkerSize',15)
```

```
title('Log Q Daily Regressions and 0.025 Confidence Interval')
ylabel('Exponential Decay [%/yr]');xlabel('Day of Water Year')
set(gca,'XTick',ytick_vect,'XTickLabel',month_vect)
for ii = 1 : 1 : 12
   text(mean(ytick_vect(ii:ii+1)),-6,month_vect(ii),'fontsize',ftsz);
end

set(h(1:2),'xlim', [1,366])
output.cur = regexprep(output.root, '_wavelet', ['_regs_',Date]);
saveas (Q_regs,fullfile(path.out,output.cur),'pdf');
%% output spreadsheet
[m,n] = size(d.Q);
Real.Q = NaN(367, 9);
Real.Q(2:end,2) = d.Q_count;
Real.Q(2:end,3) = d.Q_climavg;
Real.Q(2:end,4) = d.Q_climstd;
Real.Q(2:end,5) = d.Q_SE;
Real.Q(2:end,6) = regQB';
Real.Q(2:end,7:8) = regQBint;
Real.Q(2:end,9) = regQstats(:,3);
Real.Q = [d.Q Real.Q];
Real.Q2 = [cdf.nQ1p;cdf.nQ5p;cdf.nQ95p;cdf.nQ99p];
Real.Q2 = [NaN(4,1), Real.Q2, NaN(4,9)];
Real.Q = [Real.Q; NaN(1,n+9); Real.Q2];
XLS.Q = num2cell(Real.Q);
```

```
[XLS.Q{1,n+2:n+9}] =
deal('Count','Mean','StDev','StdErr','Slope','ConfIntMin','ConfIntMax','p-value');

[XLS.Q{m+2:m+5}] = deal('Number of days in WY below 1st percentile','Number of
days in WY below 5th percentile','Number of days in WY above 95th
percentile','Number of days in WY above 99th percentile');

XLS.Q{1,1} = 'Flow [cfs] by WY and DOWY';

output.cur = regexprep(output.root, '_Q_wavelet', ['_Q_data_',Date]);

xlswrite(fullfile(path.out,output.cur),XLS.Q);

[m,n] = size(dlog.Q);

Log.Q = NaN(367, 9);

Log.Q(2:end,2) = dlog.Q_count;

Log.Q(2:end,3) = dlog.Q_climavg;

Log.Q(2:end,4) = dlog.Q_climstd;

Log.Q(2:end,5) = dlog.Q_SE;

Log.Q(2:end,6) = reglogQB';

Log.Q(2:end,7:8) = reglogQBint;

Log.Q(2:end,9) = reglogQstats(:,3);

Log.Q = [dlog.Q Log.Q];

Log.Q2 = [cdf.nlogQ1p;cdf.nlogQ5p;cdf.nlogQ95p;cdf.nlogQ99p];

Log.Q2 = [NaN(4,1), Log.Q2, NaN(4,9)];

Log.Q = [Log.Q; NaN(1,n+9); Log.Q2];

XLS.logQ = num2cell(Log.Q);

[XLS.logQ{1,n+2:n+9}] =
deal('Count','Mean','StDev','StdErr','Slope','ConfIntMin','ConfIntMax','p-value');

[XLS.logQ{m+2:m+5}] = deal('Number of days in WY below 1st percentile','Number
of days in WY below 5th percentile','Number of days in WY above 95th
percentile','Number of days in WY above 99th percentile');

XLS.logQ{1,1} = 'Log-Transformed Flow by WY and DOWY';
```

```
output.cur = regexprep(output.root, '_Q_wavelet', ['_logQ_data_',Date]);
xlswrite(fullfile(path.out,output.cur),XLS.logQ);
```

APPENDIX C

Output from MATLAB daily analysis-Willamette Basin daily discharge

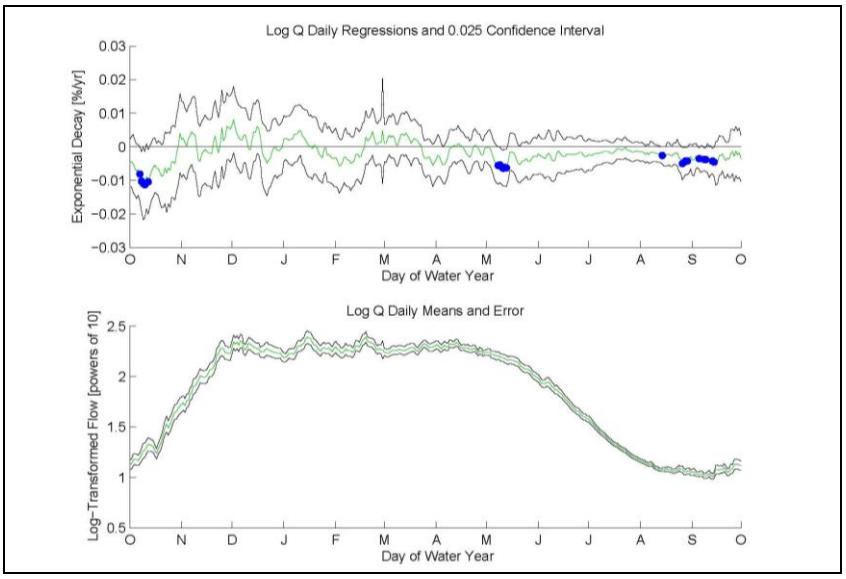

Figure C.1 Blue River total flow

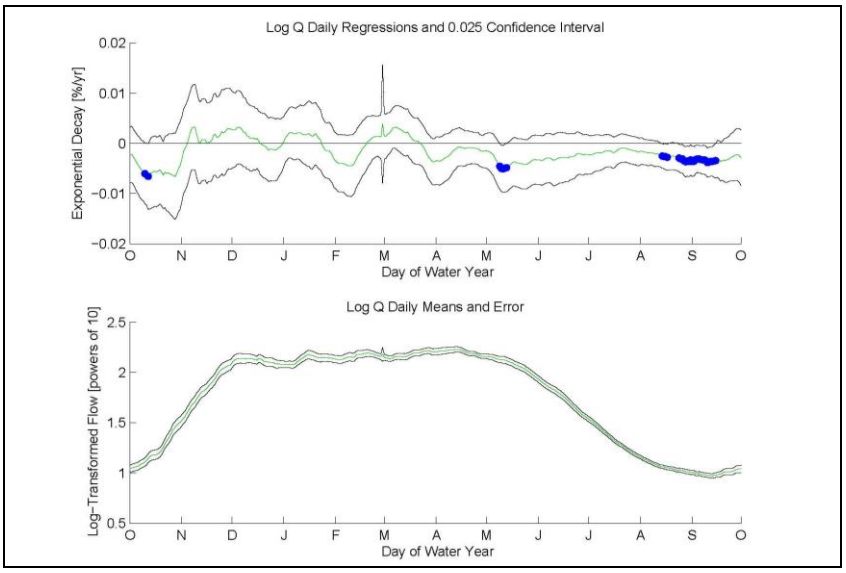

Figure C.2 Blue River baseflow

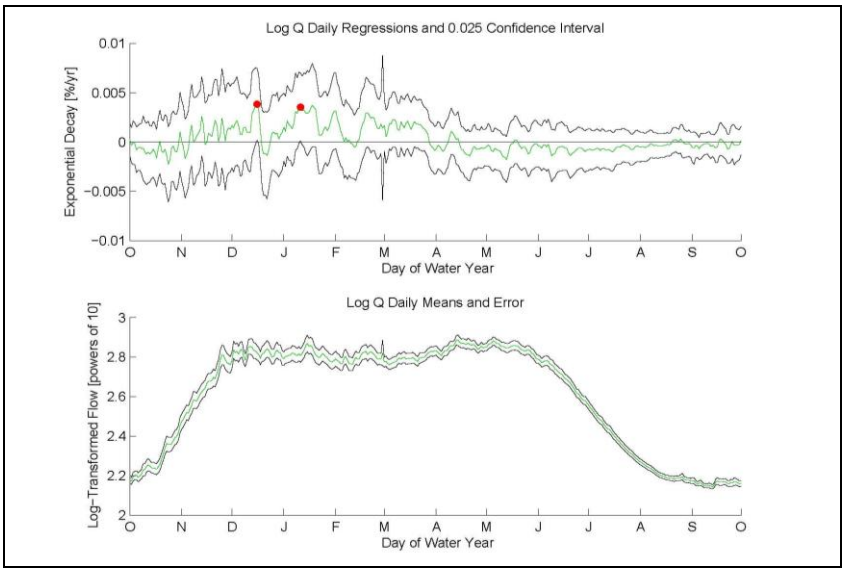

Figure C.3 Breitenbush River total flow

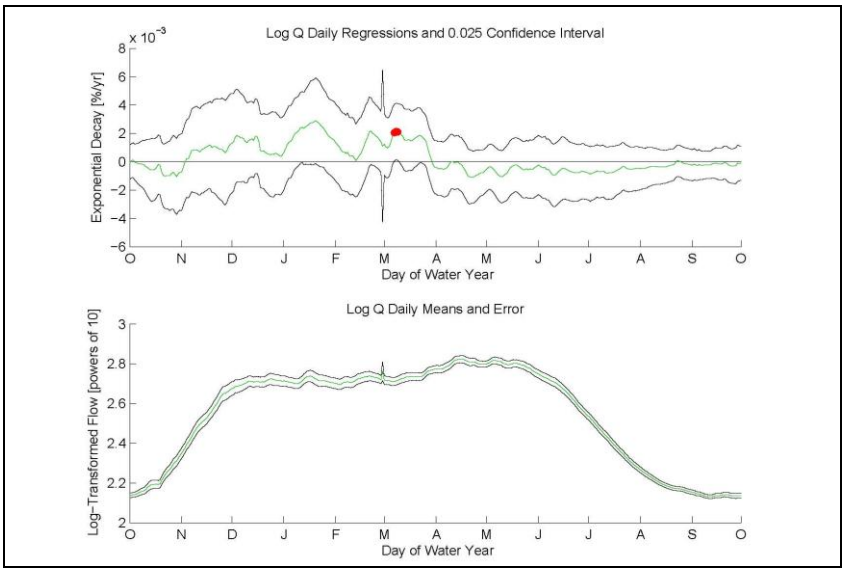

Figure C.4 Breitenbush River baseflow

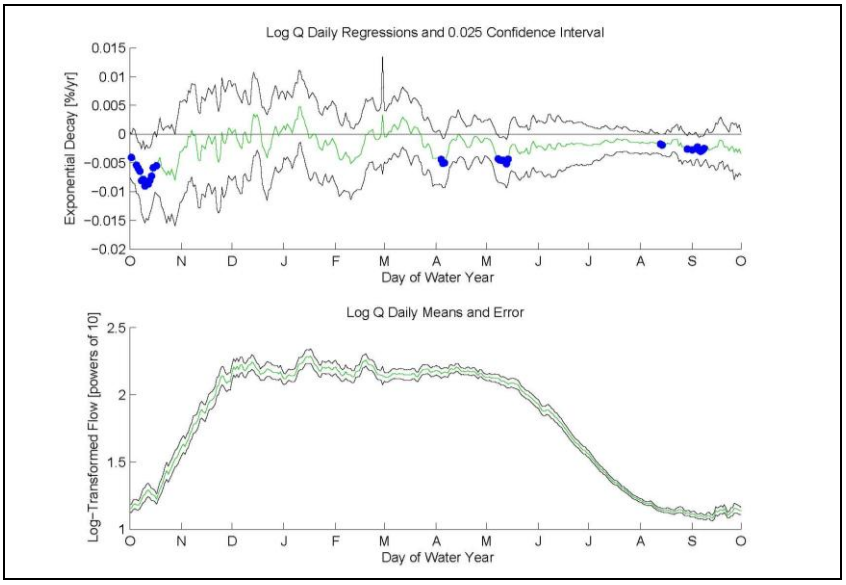

Figure C.5 Lookout Creek total flow

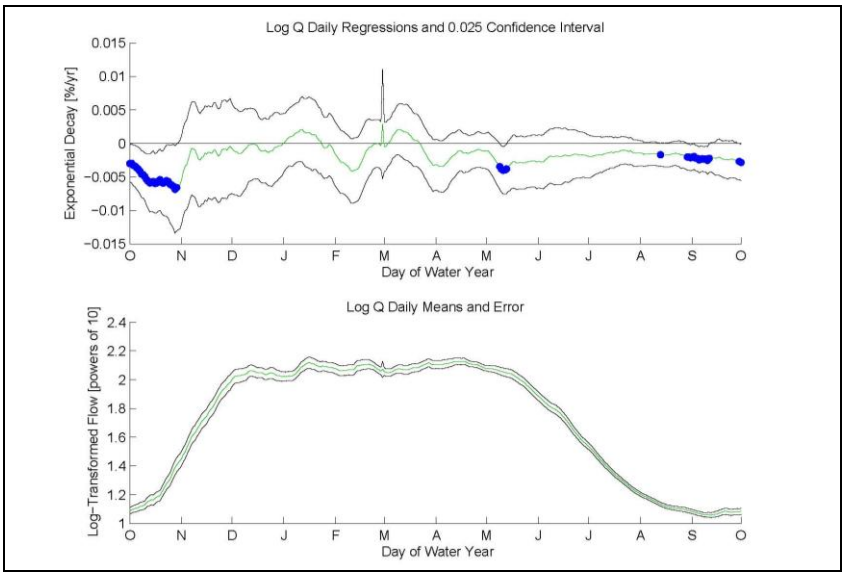

Figure C.6 Lookout Creek baseflow

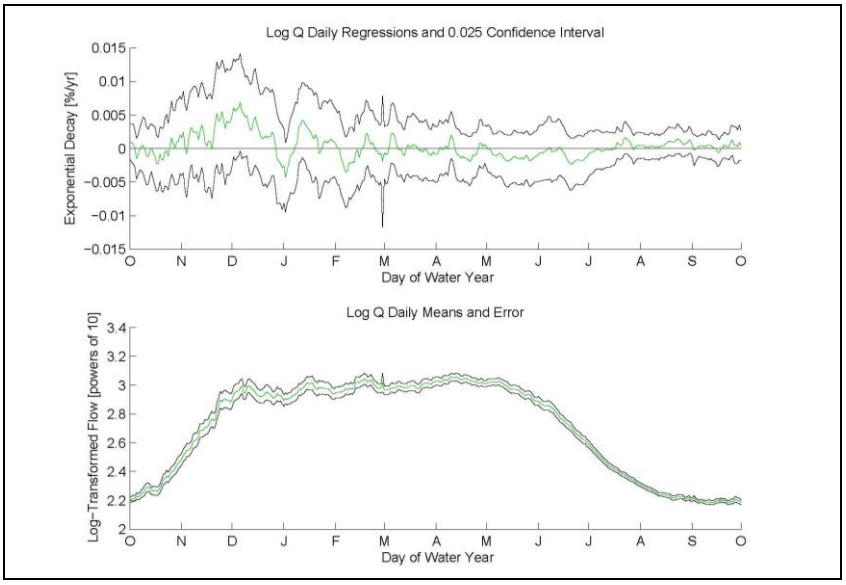

Figure C.7 North Fork Middle Fork Willamette total flow

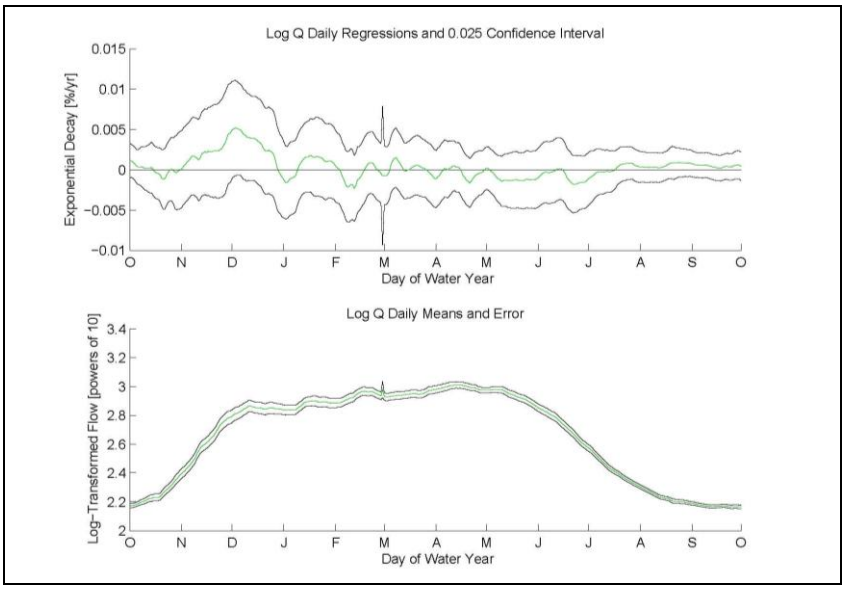

Figure C.8 North Fork Middle Fork Willamette baseflow

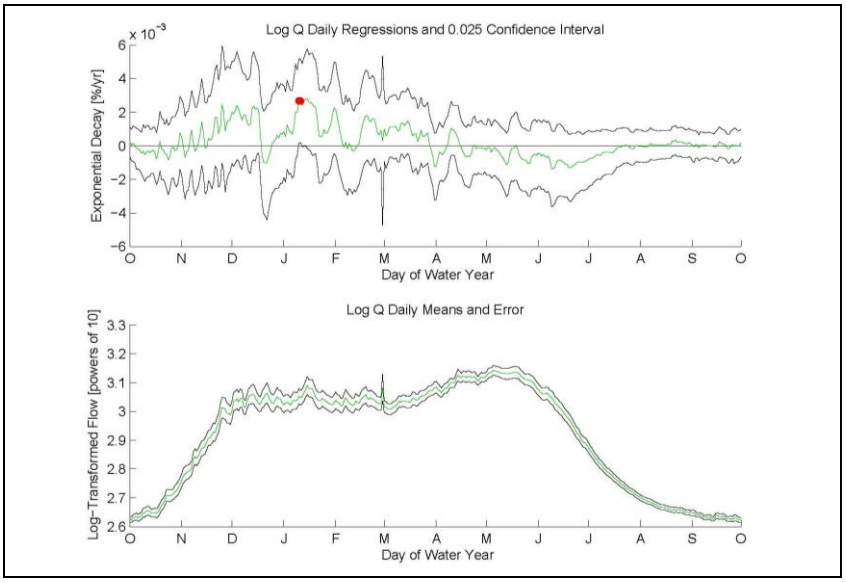

Figure C.9 North Santiam River total flow

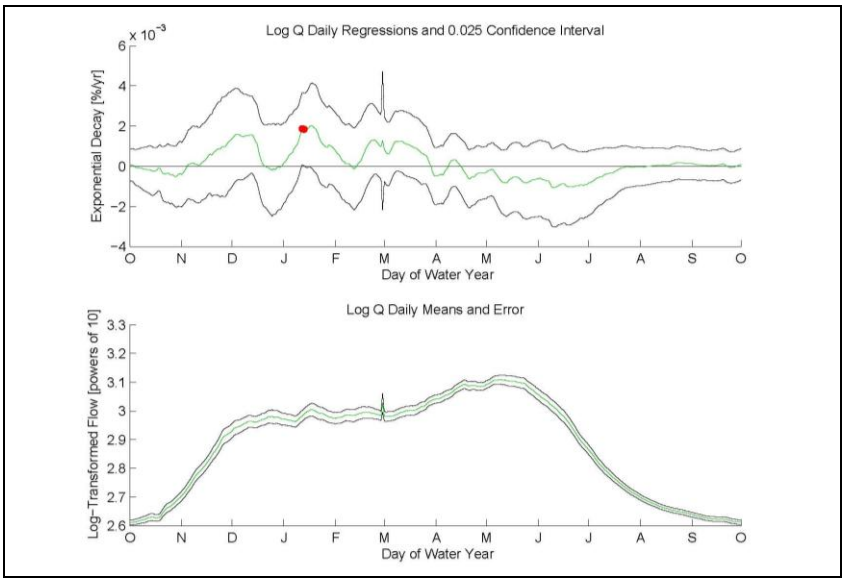

Figure C.10 North Santiam River total flow

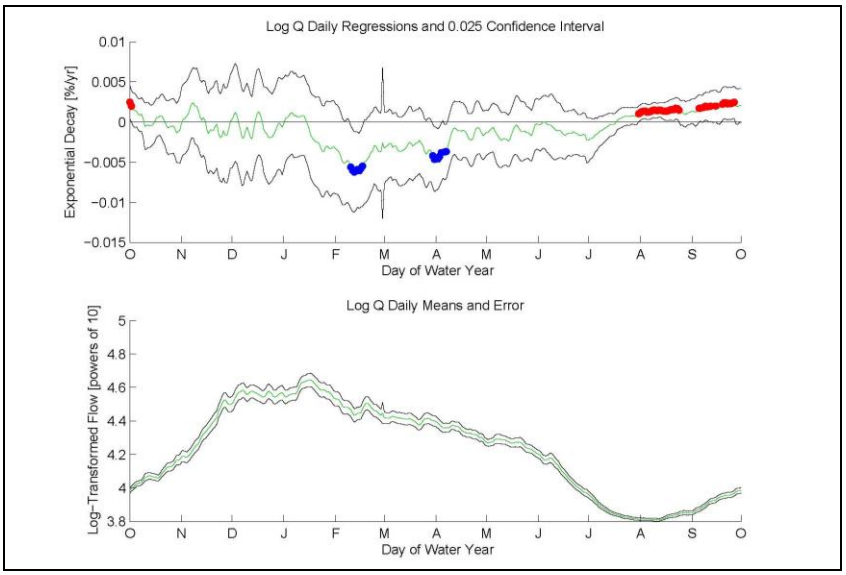

Figure C.11 Salmon Creek total flow

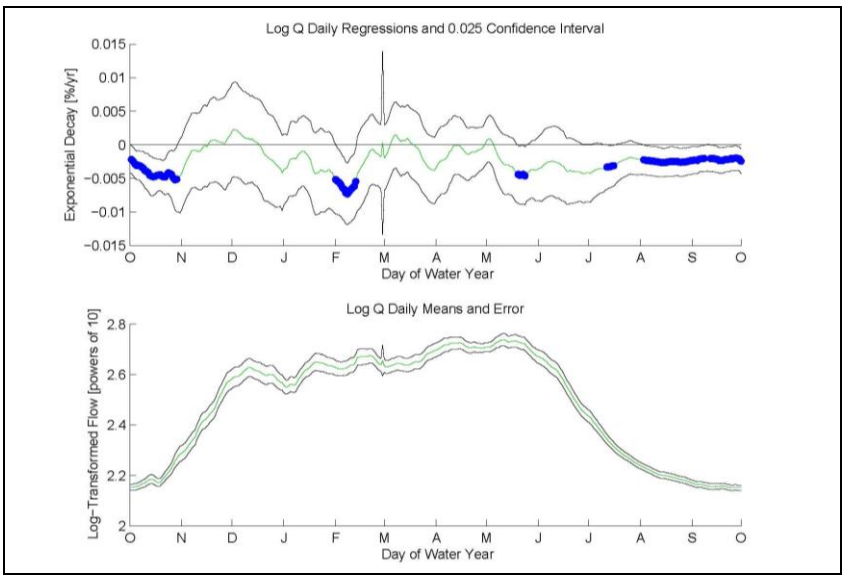

Figure C.12 Salmon Creek baseflow

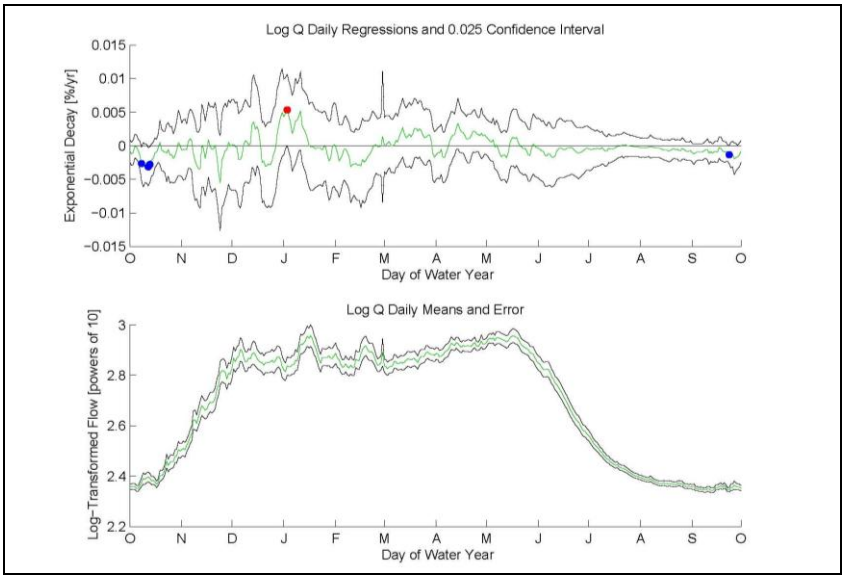

Figure C.13 South Fork McKenzie River total flow

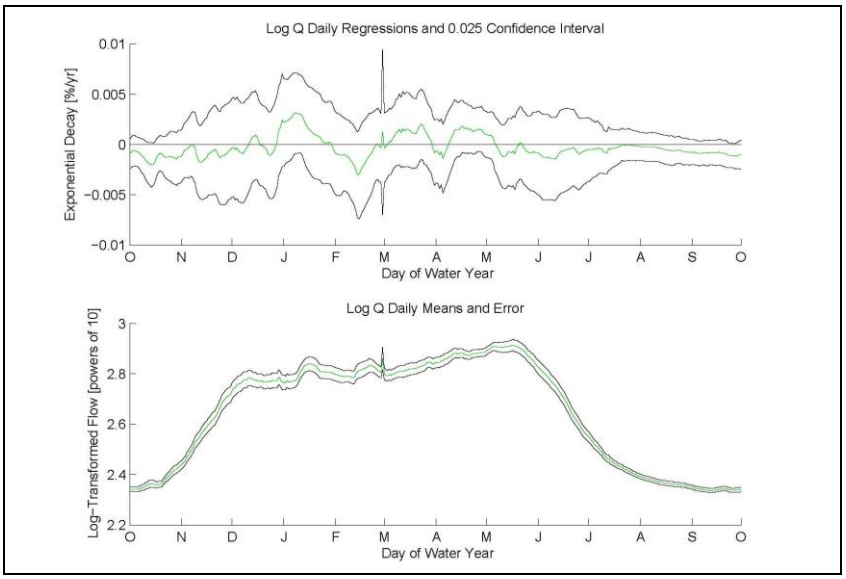

Figure C.14 South Fork McKenzie River baseflow

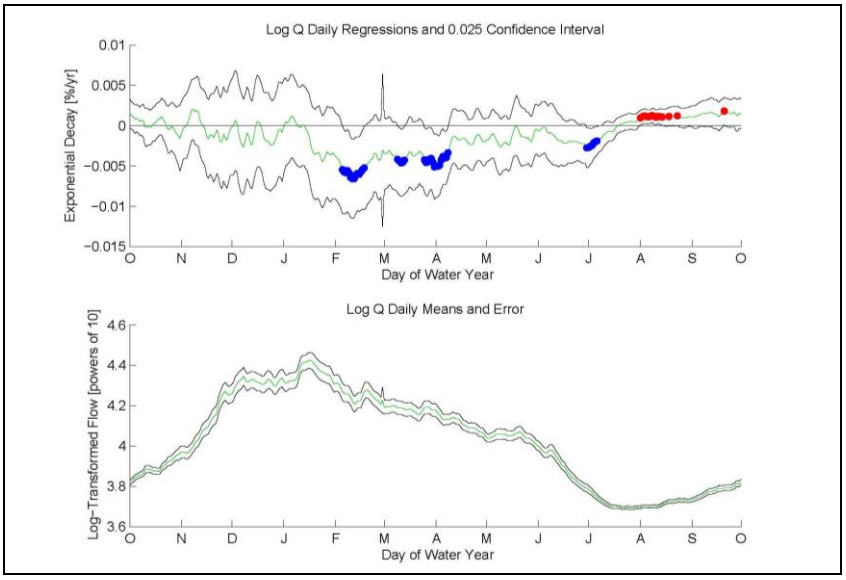

Figure C.15 Willamette at Albany total flow

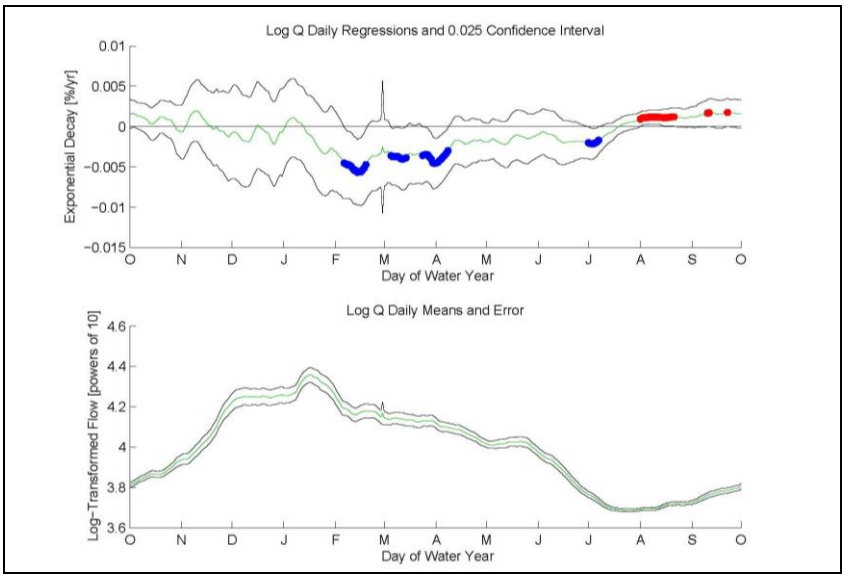

Figure C.16 Willamette at Albany baseflow

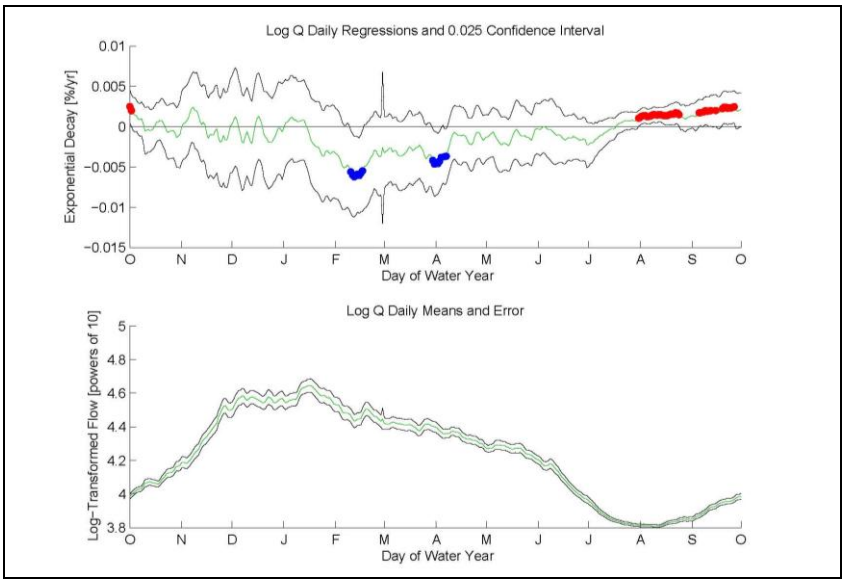

Figure C.17 Willamette at Salem total flow

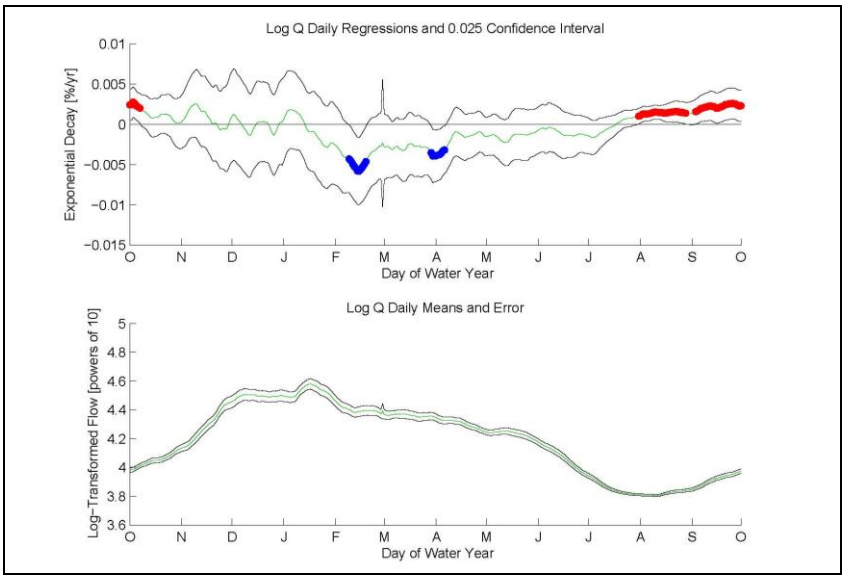

Figure C.18 Willamette at Salem baseflow

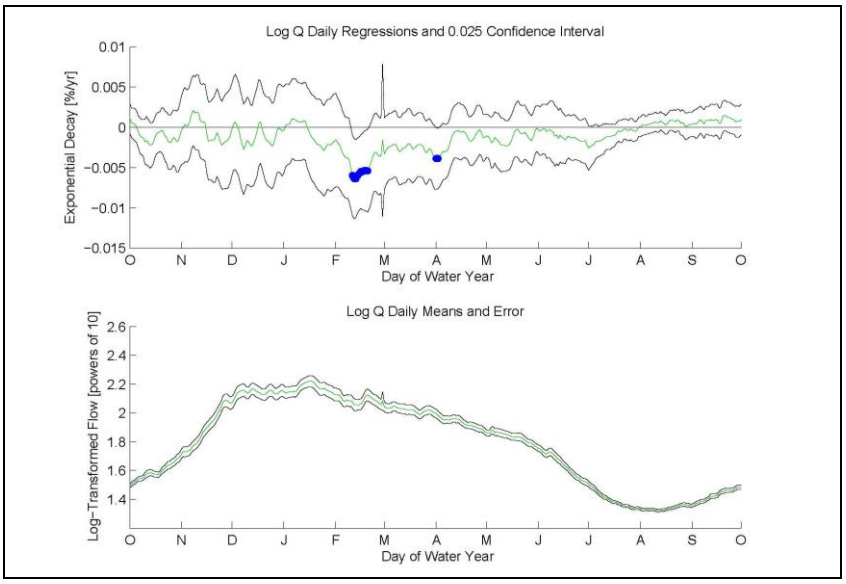

Figure C.19 Willamette at Portland total flow

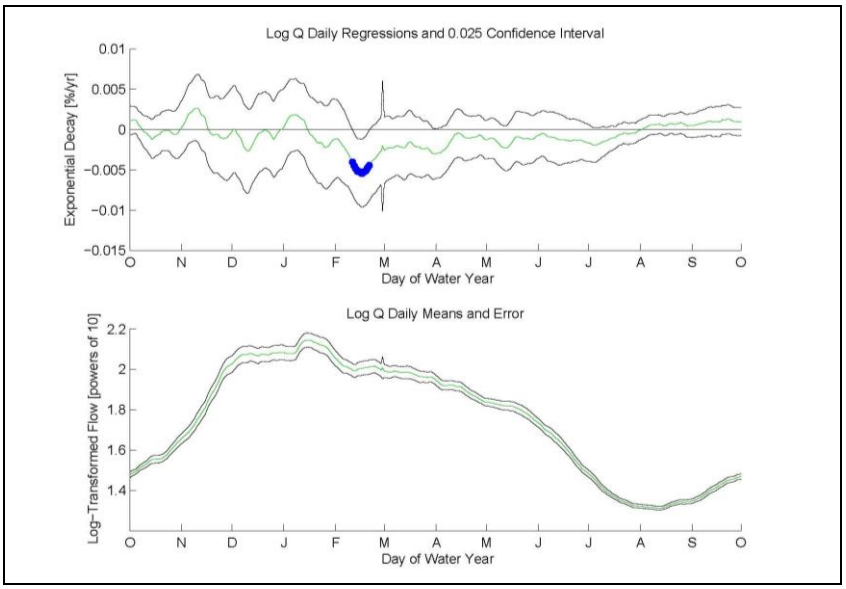

Figure C.20 Willamette at Portland baseflow

APPENDIX D

Output from MATLAB daily analysis-LTER site precipitation

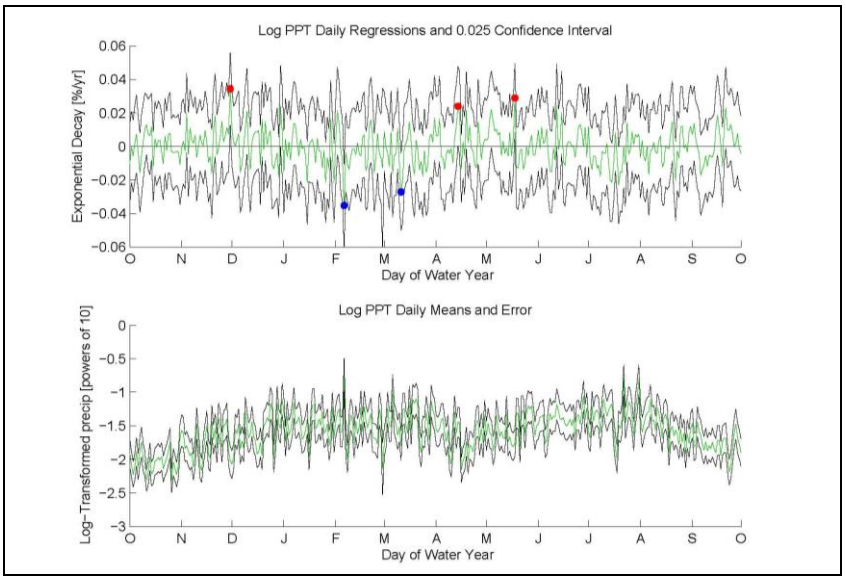

Figure D.1 Daily precipitation from Coweeta

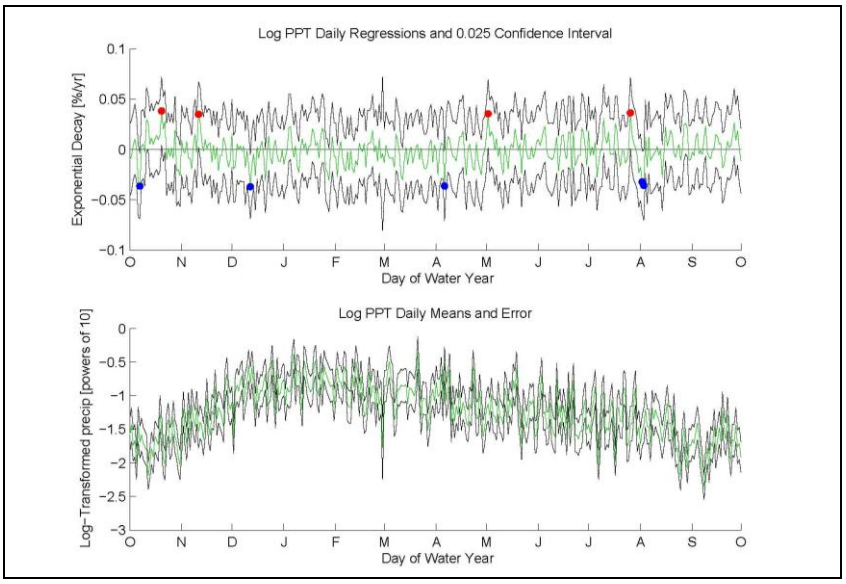

Figure D.2 Daily precipitation from Fernow

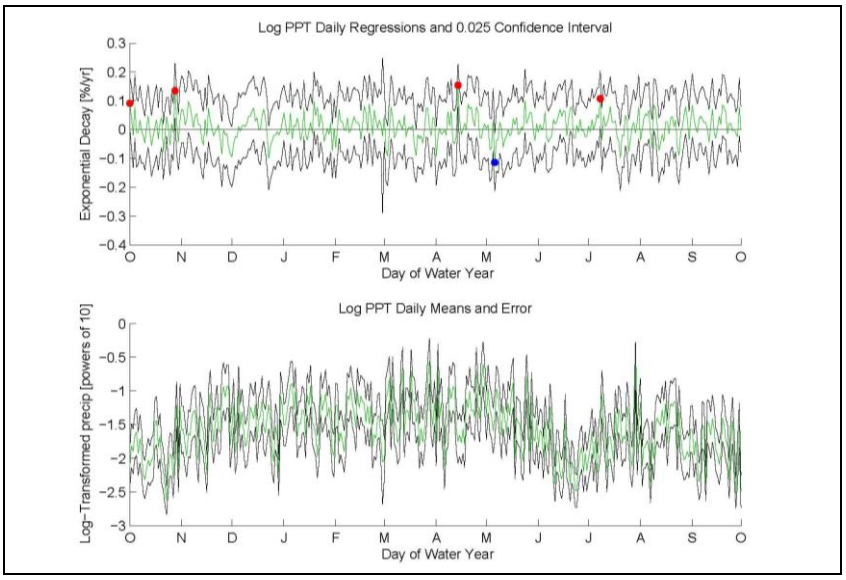

Figure D.3 Daily precipitation data from Fraser

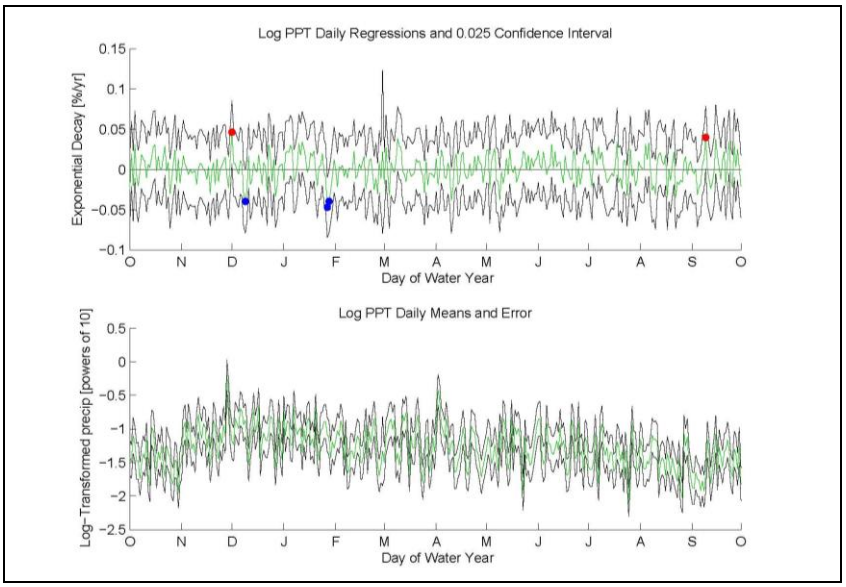

Figure D.4 Daily precipitation data from Hubbard Brook

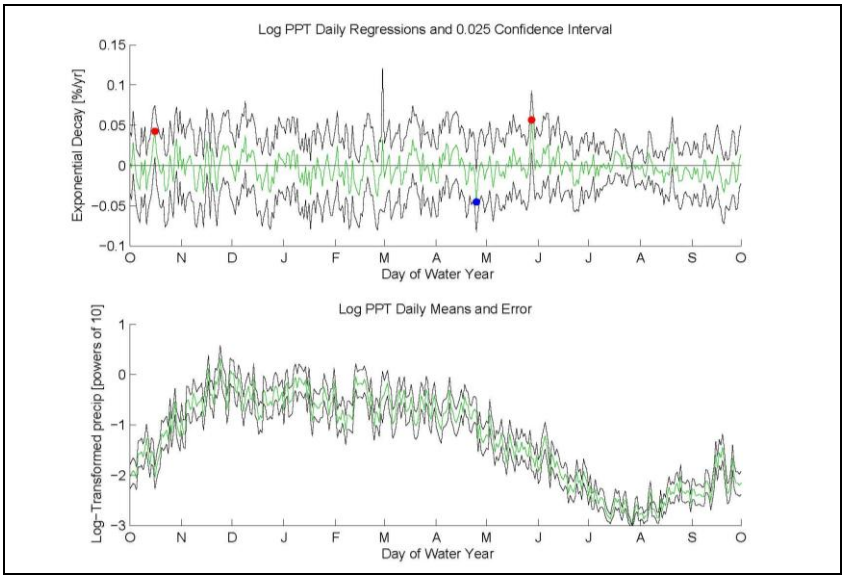

Figure D.5 Daily precipitation data from HJ Andrews

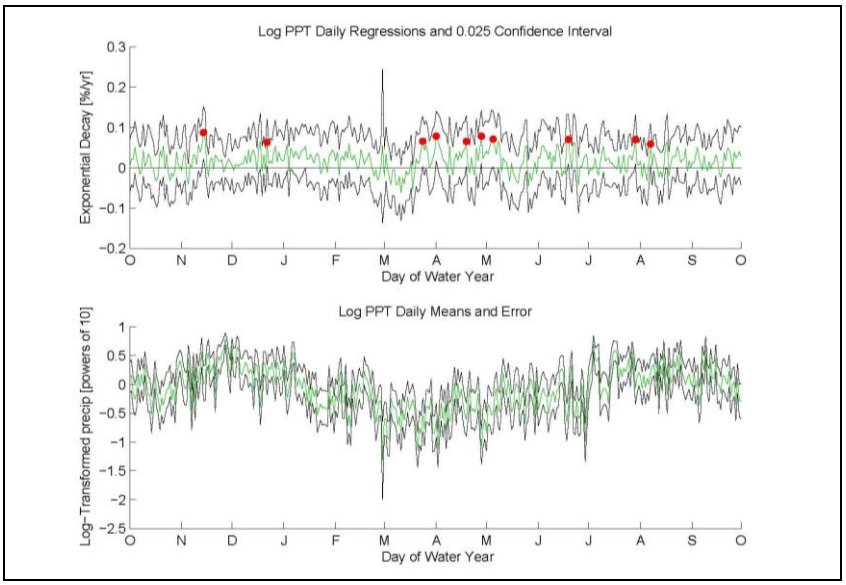

Figure D.6 Daily precipitation data from Luquillo

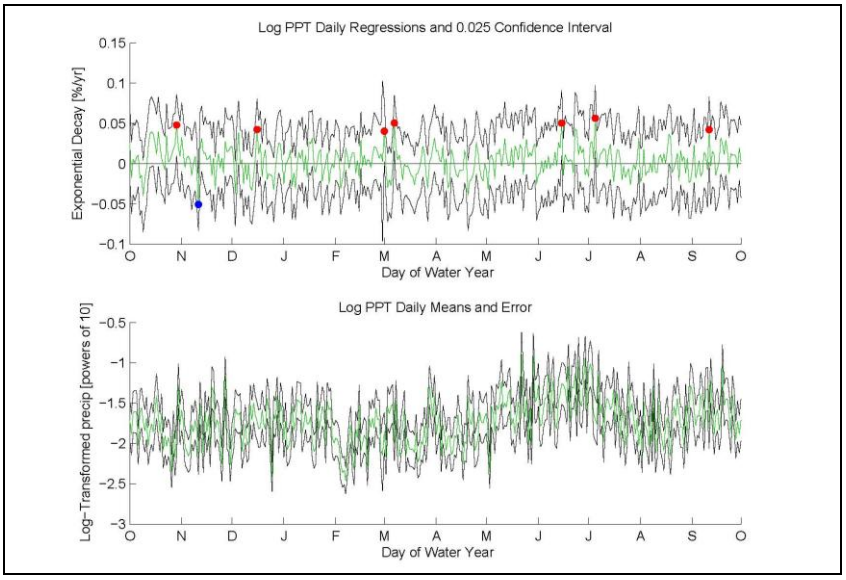

Figure D. 7 Daily precipitation data from Marcell

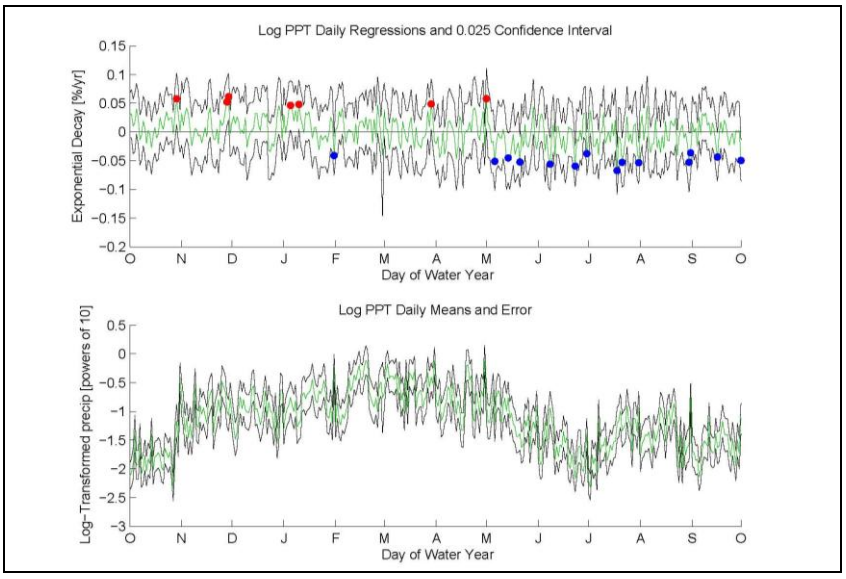

Figure D.8 Daily precipitation data from Niwot Ridge

APPENDIX E

Output from MATLAB daily analysis-LTER temperature data

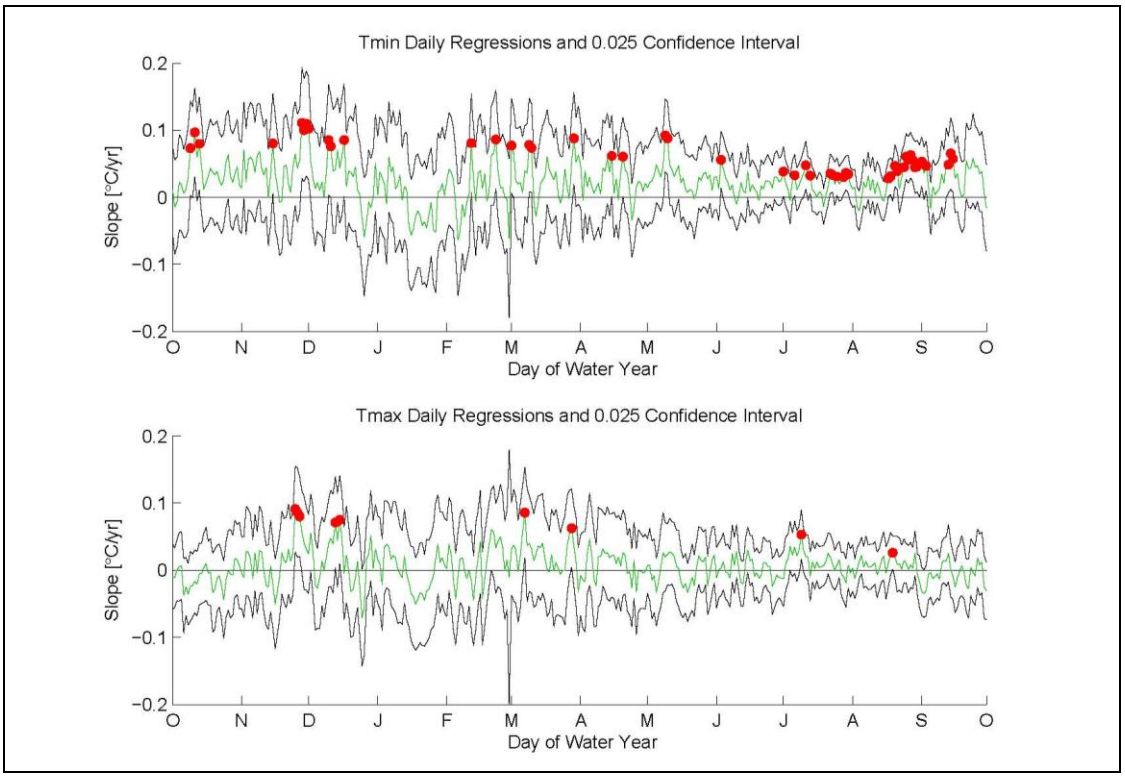

Figure E.1 Daily temperature data from Coweeta

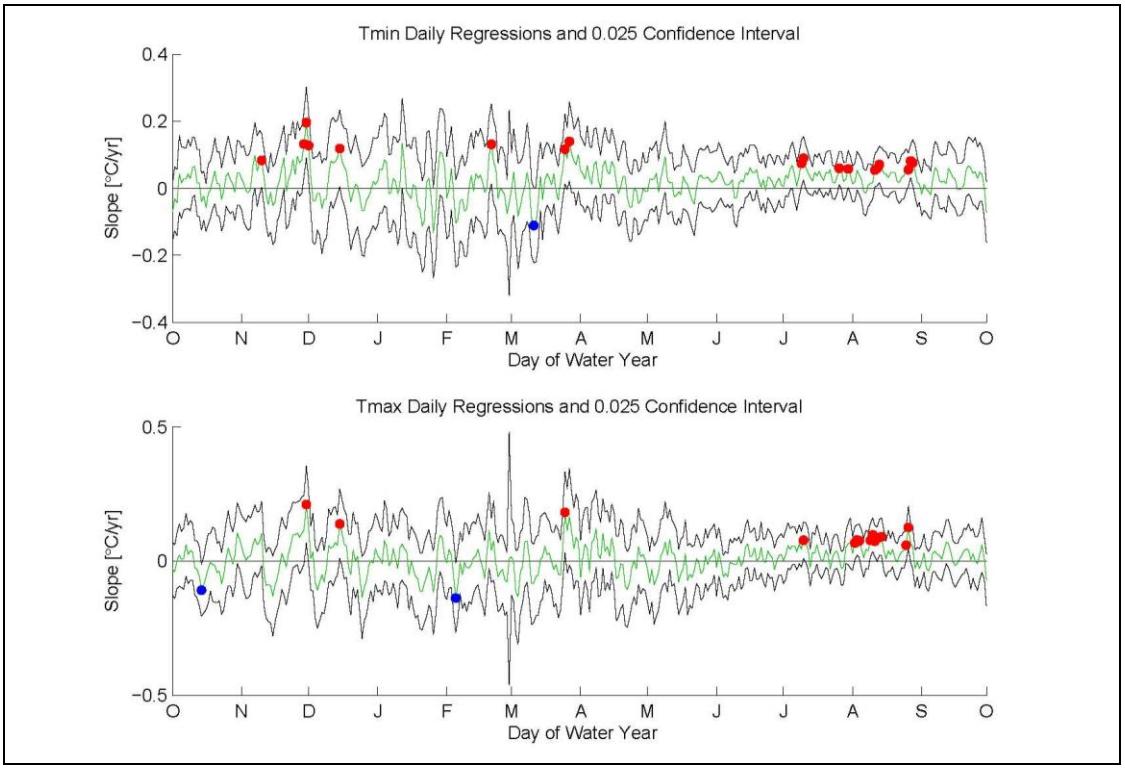

Figure E.2 Daily temperature from Fernow

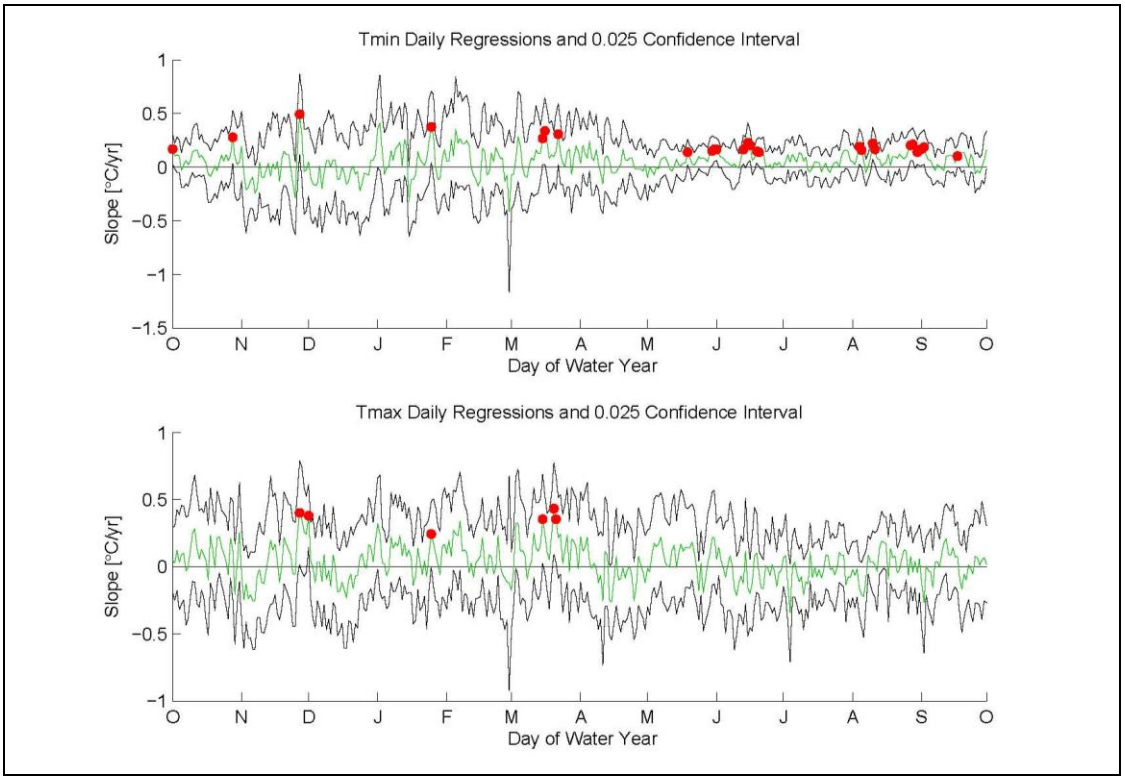

Figure E.3 Daily temperature data from Fraser

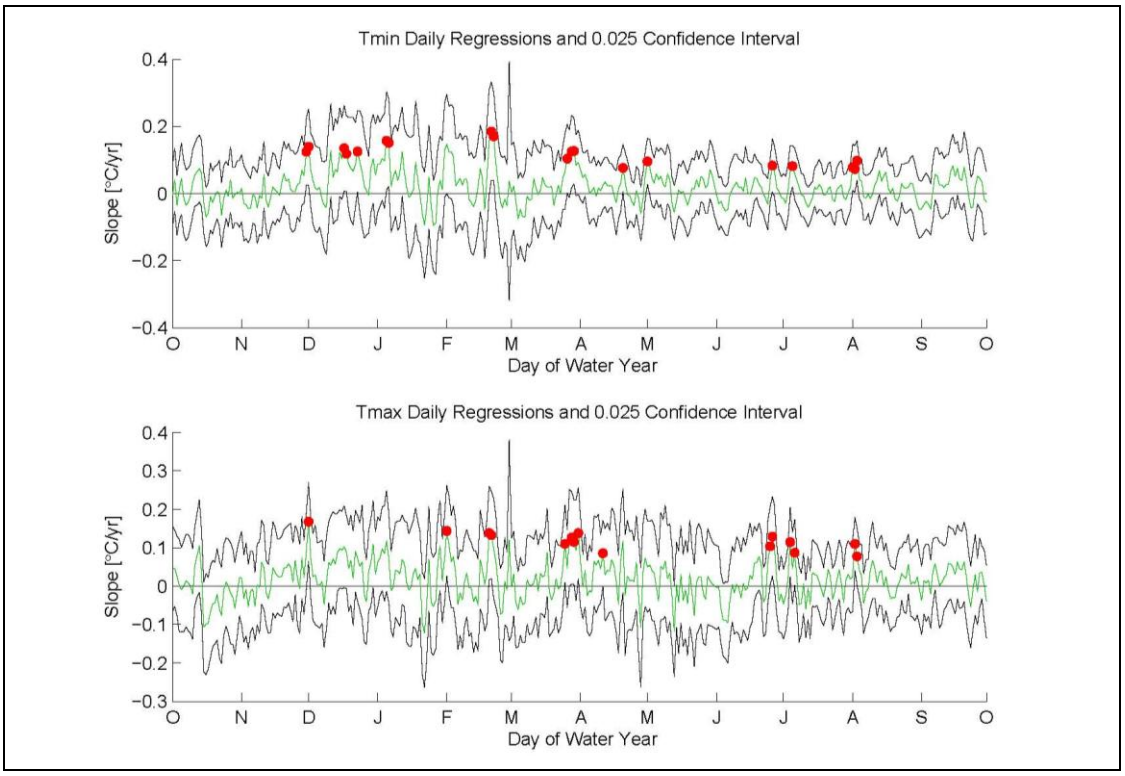

Figure E.4 Daily temperature data from Hubbard Brook

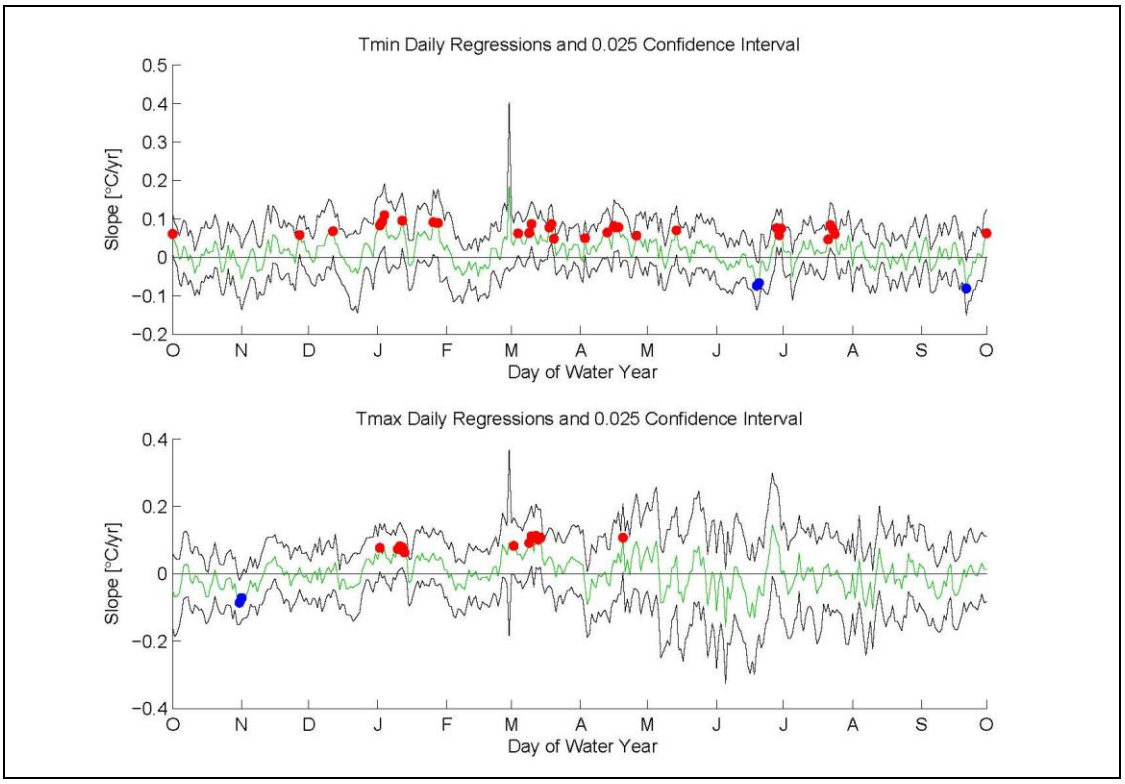

Figure E.5 Daily temperature data from HJ Andrews

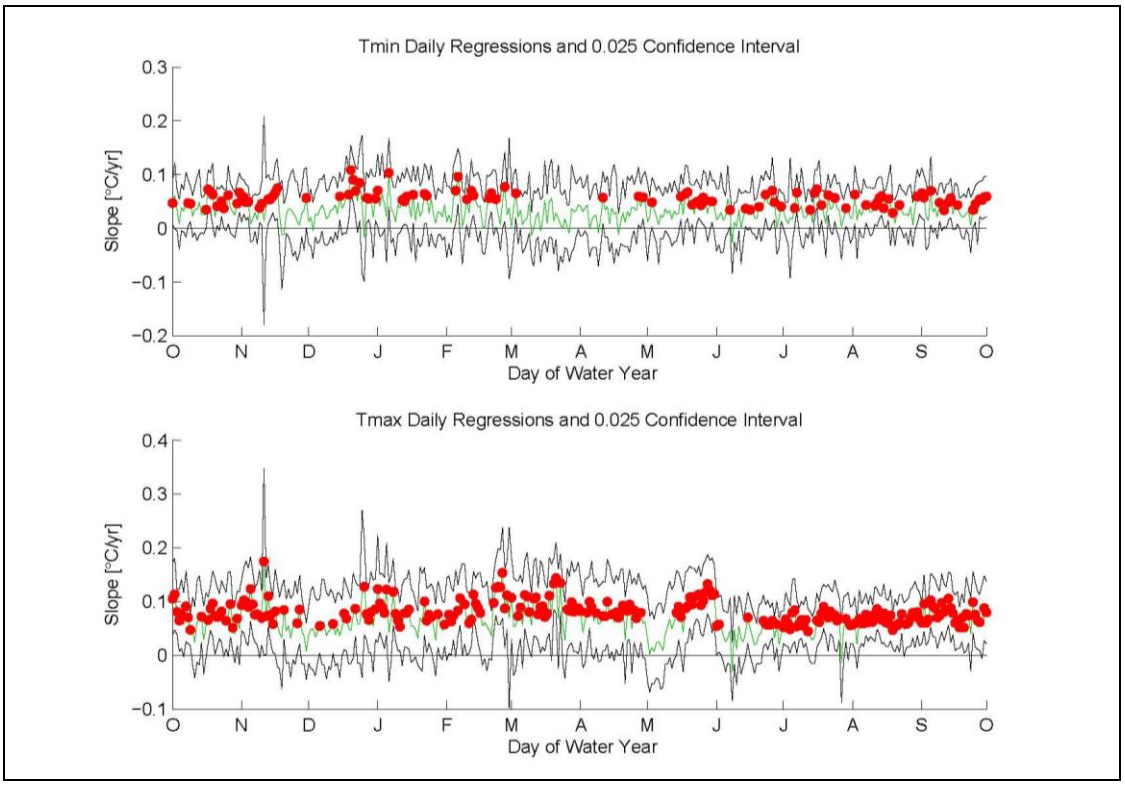

Figure E.6 Daily temperature data from Luquillo

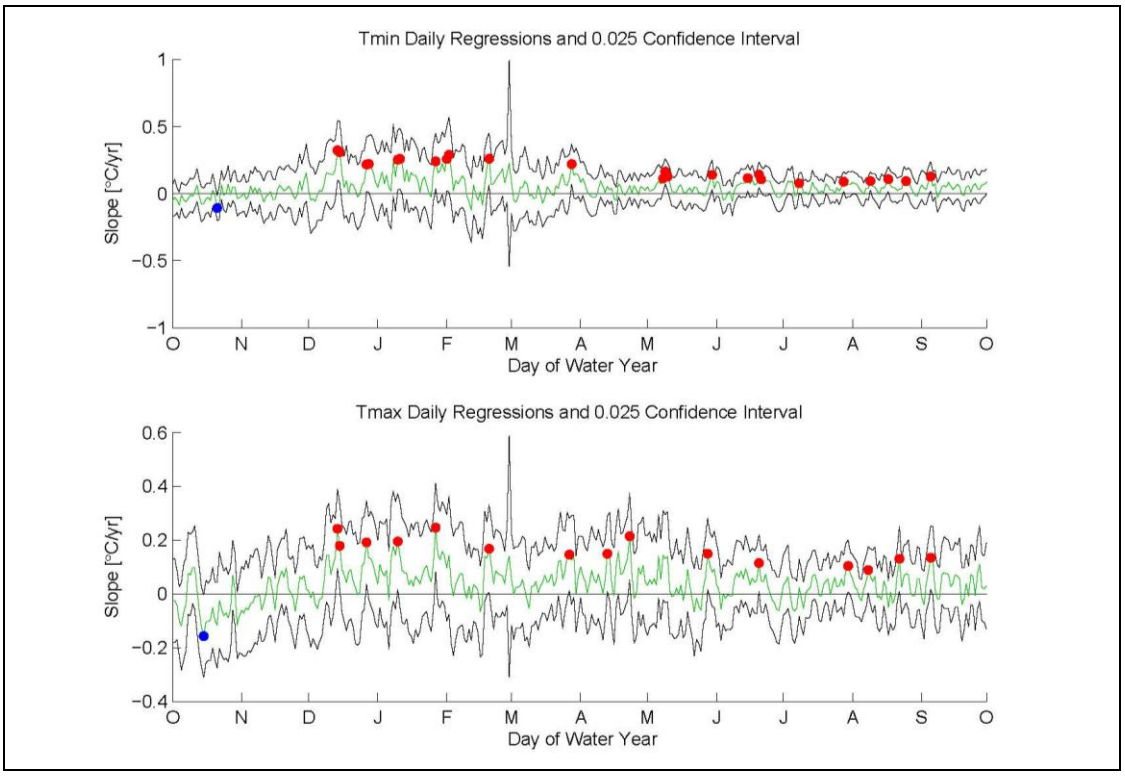

Figure E.7 Daily temperature data from Marcell

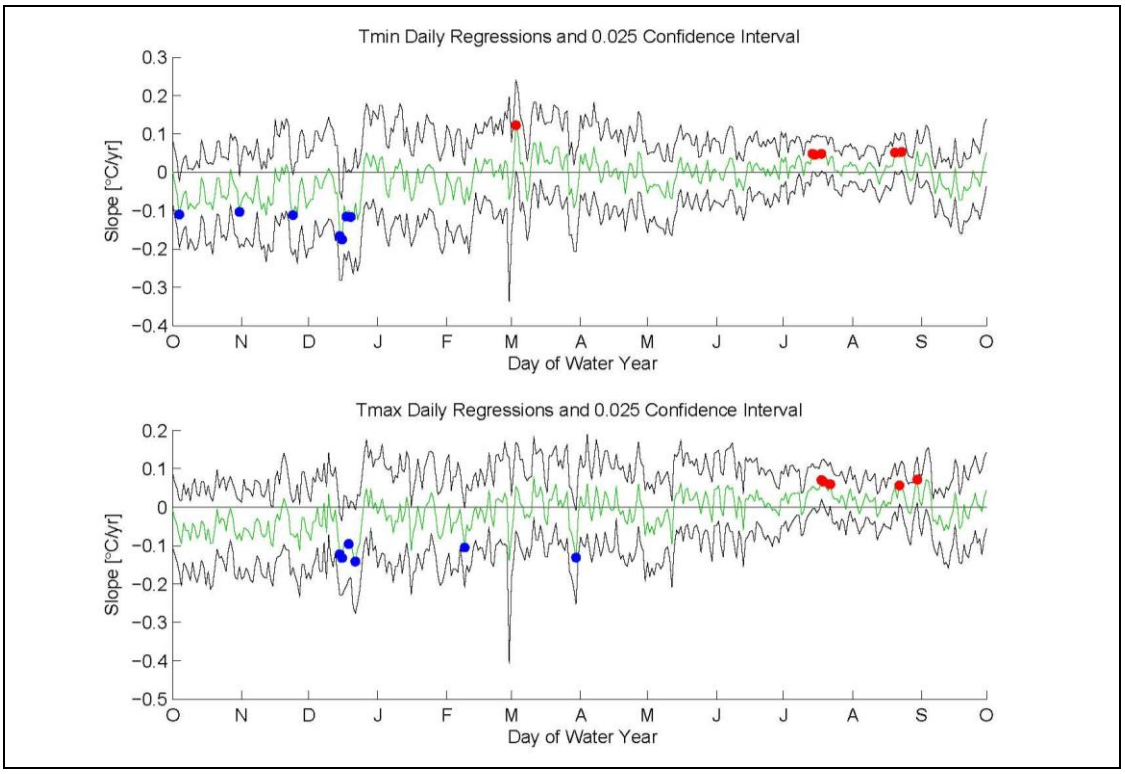

Figure E.8 Daily temperature data from Niwot Ridge

APPENDIX F

Output from MATLAB daily analysis-LTER discharge data

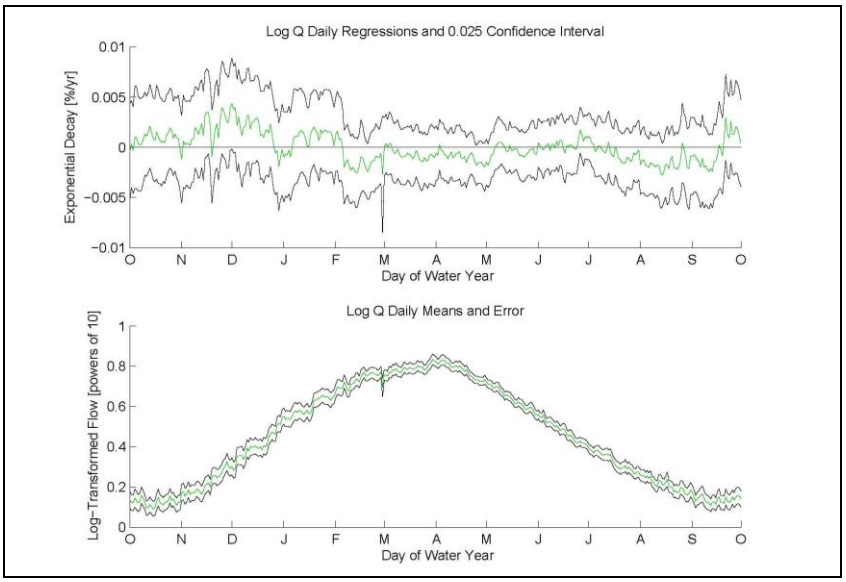

Figure F.1 Coweeta WS18 total flow

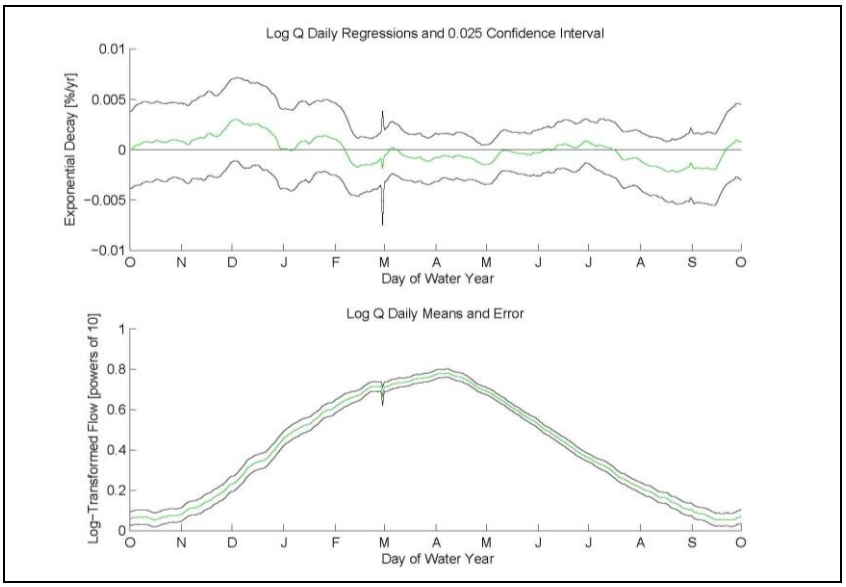

Figure F.2 Coweeta WS18 baseflow

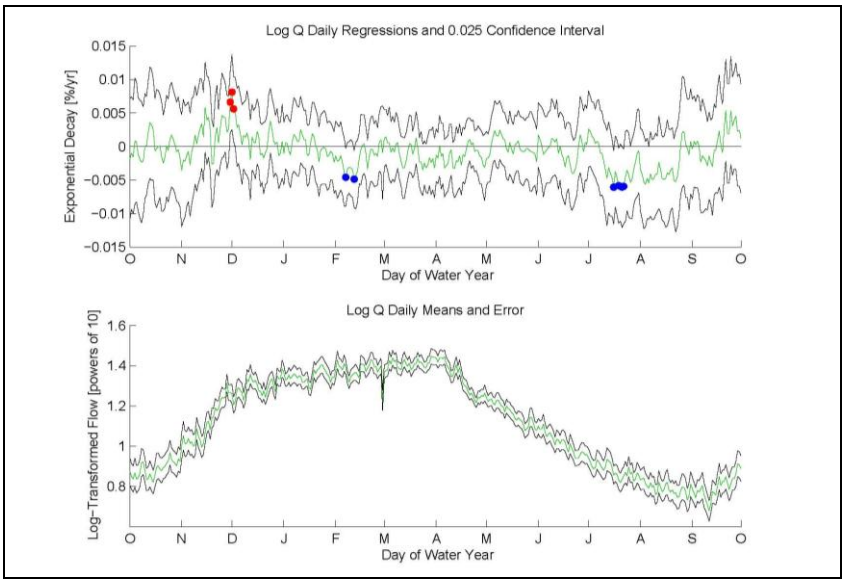

Figure F.3 Coweeta WS27 total flow

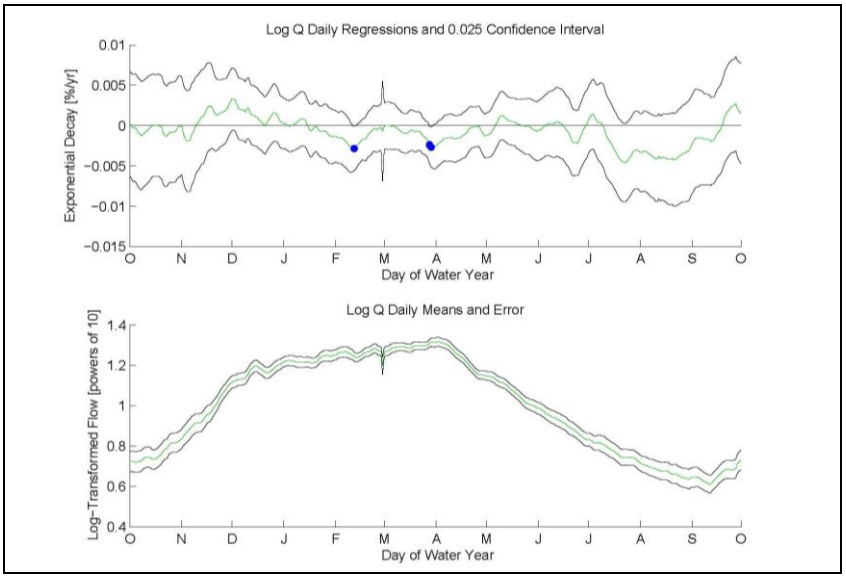

Figure F.4 Coweeta WS27 baseflow

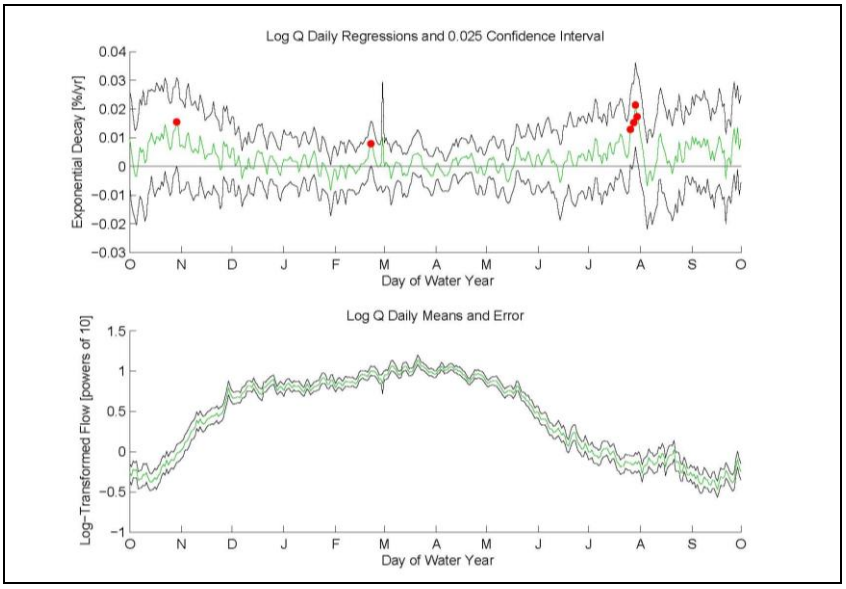

Figure F.5 Fernow total flow

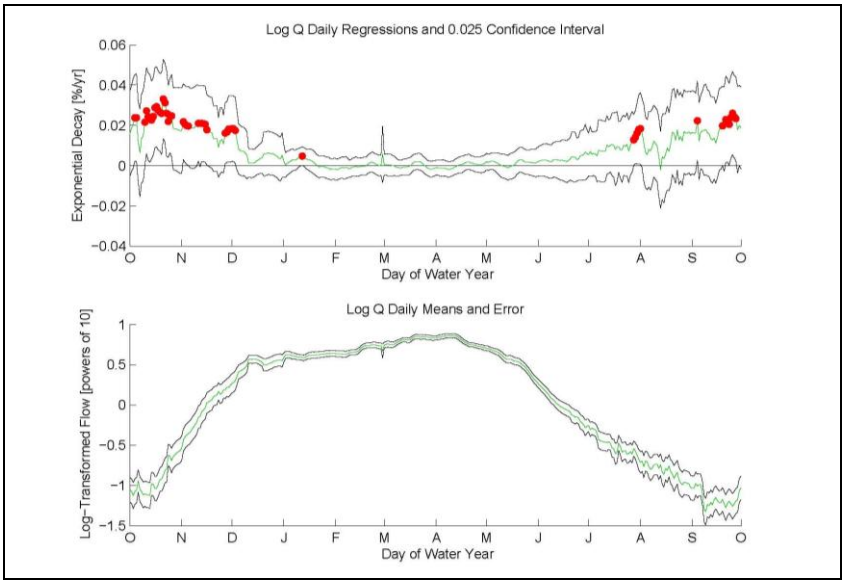

Figure F.6 Fernow baseflow

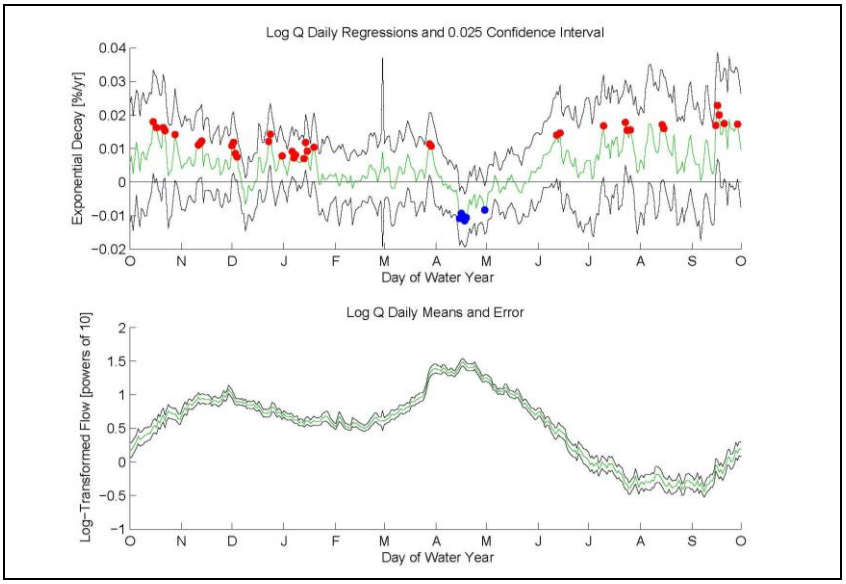

Figure F.7 Hubbard Brook total flow

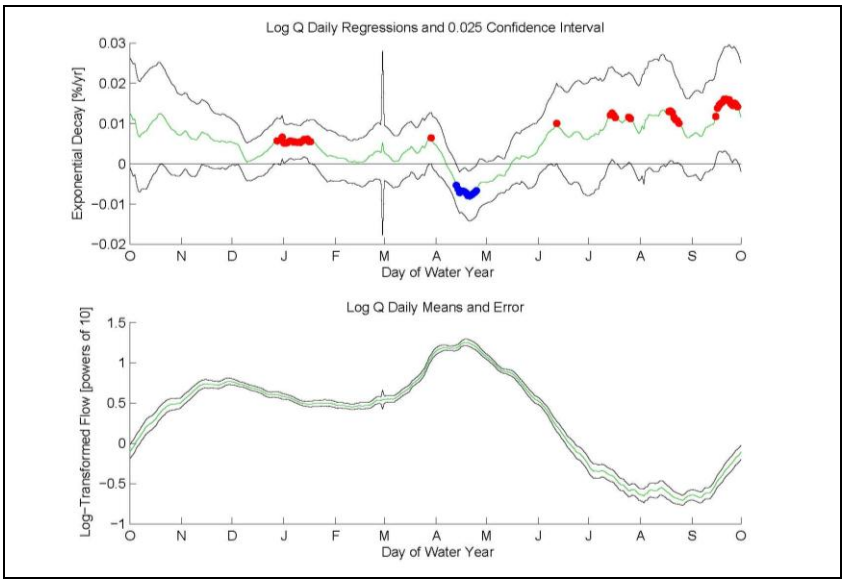

Figure F.8 Hubbard Brook baseflow

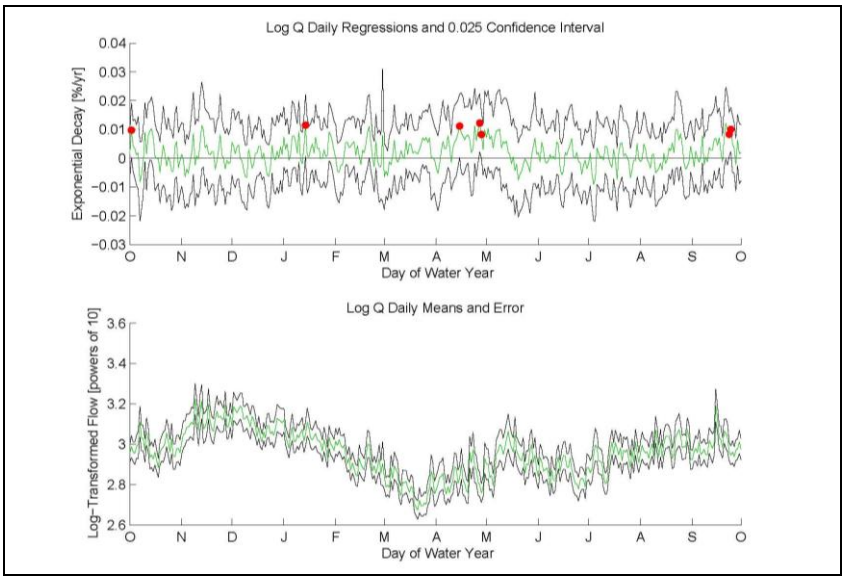

Figure F.9 Luquillo total flow

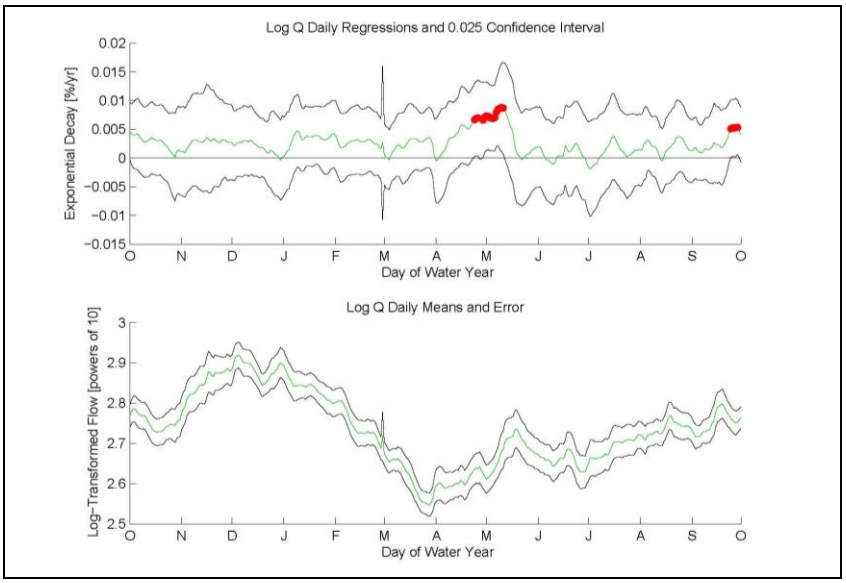

Figure F.10 Luquillo baseflow

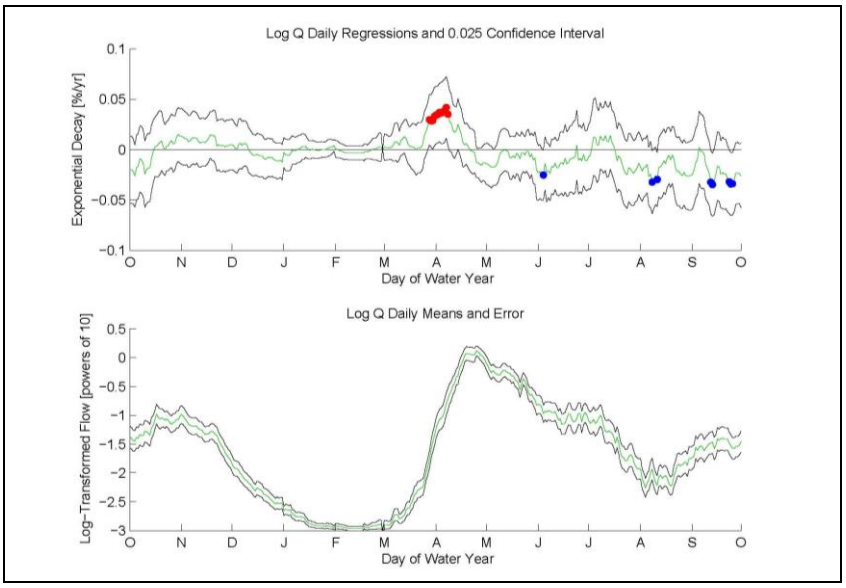

Figure F.11 Marcell S2 total flow

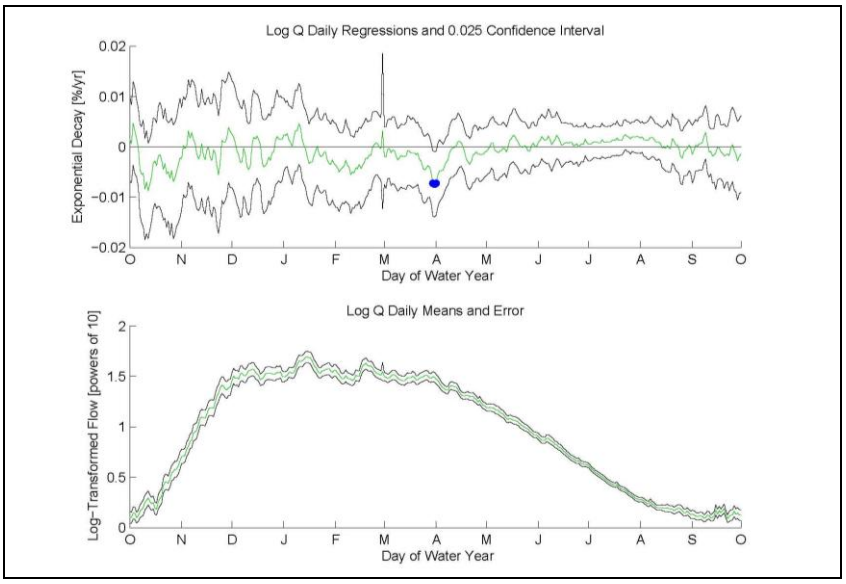

Figure F.12 HJ Andrews WS2 total flow

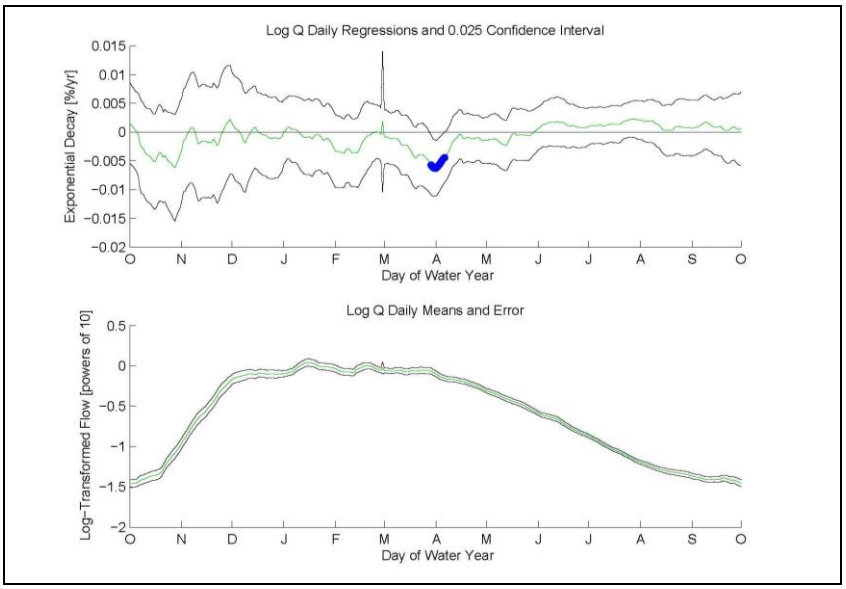

Figure F.13 HJ Andrews WS2 baseflow

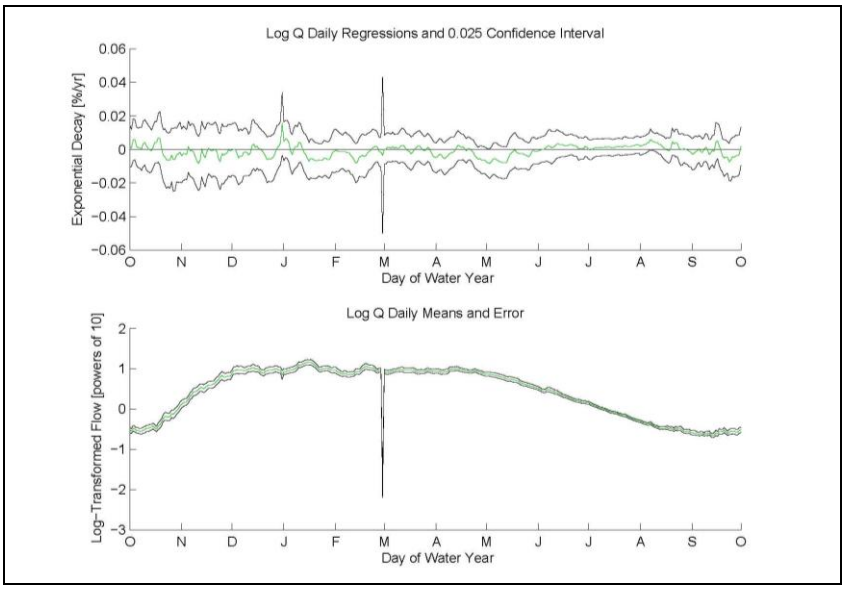

Figure F.14 HJ Andrews WS8 total flow

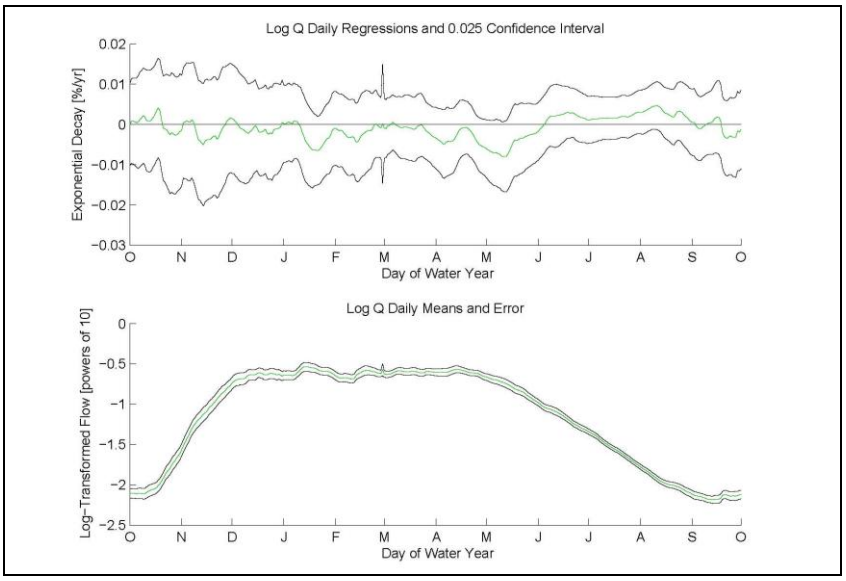

Figure F.15 HJ Andrews WS8 baseflow

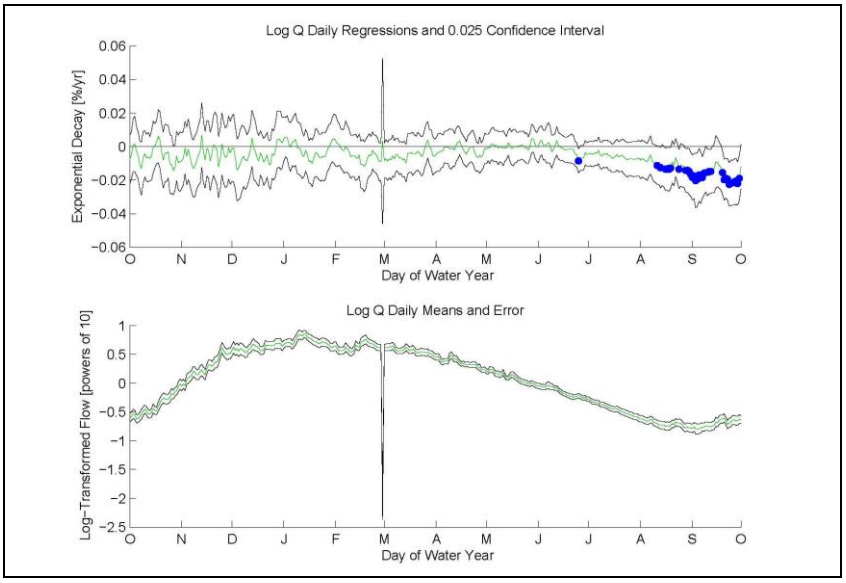

Figure F.16 HJ Andrews WS9 total flow

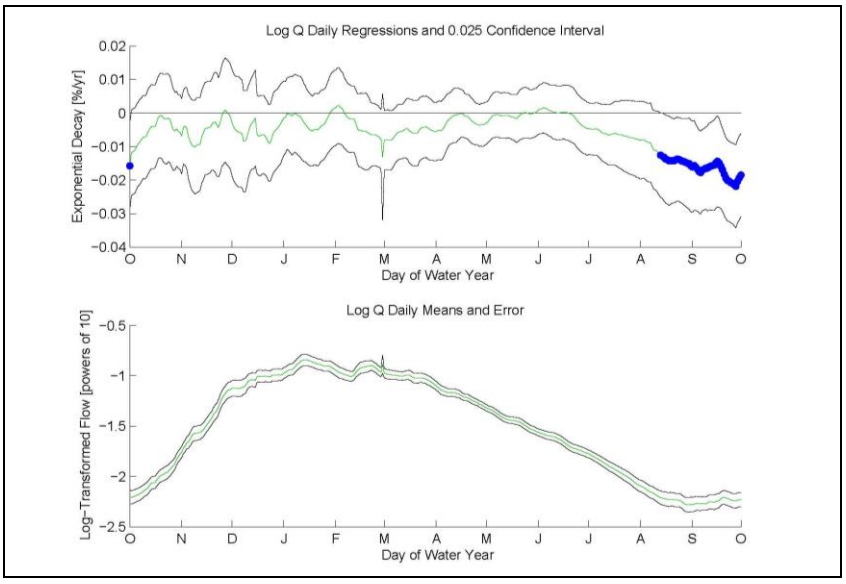

F.17 HJ Andrews WS9 baseflow